

AD-A031948

THEORETICAL STUDIES OF MATERIALS FOR HIGH-POWER INFRARED COATINGS

M. SPARKS, PRINCIPAL INVESTIGATOR, 213 / 787-7380

XONICS, INCORPORATED
VAN NUYS, CALIFORNIA 91406

SIXTH TECHNICAL REPORT 31 DECEMBER 1975

CONTRACT NO. DAHC 15-73-C-0127

EFFECTIVE DATE OF CONTRACT: 7 DECEMBER 1972

CONTRACT EXPIRATION DATE: 30 SEPTEMBER 1976

DISTRIBUTION STATEMENT A

Approved for public release
Distribution Unlimited

PREPARED FOR

DEFENSE SUPPLY SERVICE – WASHINGTON, D.C.

SPONSORED BY ADVANCED RESEARCH PROJECTS AGENCY

ARPA ORDER NO. 1969, AMENDMENT NO. 7; PROGRAM CODE NO. 6D10

Unclassified

SECURITY CLASSIFICATION OF THIS PAGE (When Data Entered)

REPORT DOCUMENTATION PAGE		READ INSTRUCTIONS BEFORE COMPLETING FORM
1 REPORT NUMBER	2 GOVT ACCESSION NO.	3 RECIPIENT'S CATALOG NUMBER
(6) 4 TITLE (and Subtitle) THEORETICAL STUDIES OF MATERIALS FOR HIGH-POWER INFRARED COATINGS.		5 TYPE OF REPORT & PERIOD COVERED Sixth Technical Report, 1 July 1975 through 31 December 1975
(10) 7 AUTHOR(s) M. Sparks		6 PERFORMING ORG. REPORT NUMBER DAHC15-73-C-6127, ARPA Order-1969
9 PERFORMING ORGANIZATION NAME AND ADDRESS Xonics, Incorporated 6840 Hayvenhurst Avenue Van Nuys, California 91406		10 PROGRAM ELEMENT, PROJECT, TASK AREA & WORK UNIT NUMBERS (12) 345 P
11 CONTROLLING OFFICE NAME AND ADDRESS Defense Supply Service Room 1D245 - The Pentagon Washington, D.C. 20310		12 REPORT DATE (11) 31 Dec 1975
14 MONITORING AGENCY NAME & ADDRESS (if different from Controlling Office) Defense Advanced Research Projects Agency 1400 Wilson Boulevard Arlington, Virginia 22209		15 SECURITY CLASS (of this report) Unclassified
		15a DECLASSIFICATION/DOWNGRADING SCHEDULE
16 DISTRIBUTION STATEMENT (of this Report) Distribution statement may be found in the abstract. Defense Supply Service, Washington, D.C.		
17 DISTRIBUTION STATEMENT (of the abstract entered in Block 20, if different from Report) (9) Technical rep't. 1 Jul - 31 Dec 75, no. 6		
18 SUPPLEMENTARY NOTES Research sponsored by Defense Advanced Research Projects Agency under ARPA Order No. 1969, No. 7, Program Code 6D10		
19 KEY WORDS (Continue on reverse side if necessary and identify by block number) coatings, antireflection, reflection enhancing, thin film, vapor deposition, absorptance, contamination, packing density, attenuated total reflection, calorimetric measurement, inclusion damage, electron-avalanche breakdown, detached film segment, ultraclean deposition		
20 ABSTRACT (Continue on reverse side if necessary and identify by block number) Results and recommendations based on a survey of the coatings literature, on discussions with a number of investigators in the field, and on very simple analyses include the following. High-packing-density films should be vapor deposited using ultraclean deposition conditions including thorough baking of the entire system before deposition, high-purity single-crystal starting materials, special care in evaporation, state-of-the-art substrate preparation, and ultrahigh vacuum. Values of film absorptance A_f per surface of $A_f = 10^{-4}$, or absorption coefficient $\beta_f = 0.5 \text{ cm}^{-1}$ roughly, are desired. A major $\beta_f = 0.5 \text{ cm}^{-1}$		

Unclassified

SECURITY CLASSIFICATION OF THIS PAGE(When Data Entered)

20. Abstract (Continued)

Beta {

problem is that the values of β_f usually are much greater than the corresponding bulk values β_b . The most likely source of this extra film absorptance is contamination of the film. The numerous contaminants include water and such other molecules or molecular ions as O_3 , HCO_3 , ClO_3 , etc. Contamination, particularly by water, occurs both during deposition and upon exposure of the films to the atmosphere (where absorption by porous films and surface adsorption are important). At $10.6 \mu m$ only two molecular layers of water or a packing density of 99.95% are required to give $A_f = 10^{-4}$. Spectroscopic and calorimetric measurements of $A_f(\omega)$ on very thick films and on normal-thickness films, both on attenuated-total-reflection plates, should be made. Material-selection guidelines, including a bulk absorption coefficient less than 0.5 cm^{-1} and a value of the index of refraction in the required range, are developed and used to select the following $10.6 \mu m$ candidate materials: ThF_4 , NaF , BaF_2 , SrF_2 , $NaCl$, KCl , $KGaF_4$, As_2S_3 , As_2Se_3 , ZnS , $ZnSe$, and Tl . A method of distinguishing between surface and bulk absorption in coatings by utilizing the fact that the electric field is zero on the surfaces of certain types of coatings and nonzero on others is proposed. Inclusion damage of coatings is expected to be similar to inclusion damage of bulk materials, with the damage threshold being $1-10 J/cm^2$ for nanosecond pulses or 10 to several hundred J/cm^2 for microsecond pulses. Intrinsic damage is expected to occur at $\sim 100 J/cm^2$ for a $10 \mu s$ pulse as a result of linear heating of the coating for the case of $A_f = 10^{-3}$ or at $\sim 10 J/cm^2$ (i.e. $I \approx 10 \text{ GW per cm}^2$) for a 10 ns pulse of 1 to $10 \mu m$ radiation as a result of electron-avalanche breakdown or perhaps another nonlinear process. The linear absorption (below the damage threshold) by strongly absorbing 1- μm -radius inclusions spaced $175 \mu m$ apart in the coating gives rise to absorptance $A_f \approx 10^{-4}$. The calculated value of 25 K temperature rise ($\sim D^2$) for a typical detached film segment of diameter $D = 2 \text{ mm}$ is surprisingly small. The thermally induced stress corresponding to 25 K has a typical value of 20 MPa ($3 \times 10^3 \text{ psi}$), which may be sufficient to cause additional detachment and a runaway process.

*0.5/cm

** 10.6 micrometers

Unclassified

SECURITY CLASSIFICATION OF THIS PAGE(When Data Entered)

TABLE OF CONTENTS

<u>Section</u>		<u>Page</u>
	Contents of Previous Reports.....	vi
	Preface	ix
I	Summary of Results.....	1
II	Near-Term Recommendations.....	10
III	Background Information	17
IV	Possible Sources of Additional Absorption in Coatings	30
V	Suggested Measurements	51
VI	Other Problems.....	73
VII	Laser Heating of Coatings	101
VIII	Laser Damage of Coatings	108
IX	Laser Damage of Detached Coatings.....	120
X	Guidelines for Selecting New Materials.....	128
XI	Candidate 10.6 μm Coating Materials	135
XII	Candidate 2-6 μm Coating Materials	165
XIII	Excerpts and Results from Literature, with Comments	169

✓
Letter on file
A

LIST OF ILLUSTRATIONS

<u>Figure</u>		<u>Page</u>
4.1	Transmittance of 5 μm of distilled water	36
4.2	Absorption bands of atmospheric contaminants	41
4.3	Positions of absorption peaks of some contaminants	43
5.1	ATR spectra of zinc selenide films on barium fluoride	60
5.2	ATR spectra of thorium tetrafluoride films on barium fluoride...	62
6.1	Spectral transmittance of: (a) polyethylene, 0.1 mm thick, and (b) plexiglas, 0.2 mm thick	88
9.1	Model heat-flow problems used in the argument that $T \geq 0$ at the edge of a detached coating	123
11.1	Reciprocal dispersion of some infrared optical materials	146

LIST OF TABLES

<u>Table</u>		<u>Page</u>
3.1	Summary of the current status of film materials and coatings	25
4.1	Values of the absorption coefficient of water at the maximum values of β , at prominent laser wavelengths, and at longer wavelengths	37
4.2	Experimentally observed absorption frequencies of several impurity ions in KCl crystals and the estimated impurity concentration to produce $\beta = 10^{-4} \text{ cm}^{-1}$ at the CO ₂ laser frequency	40
4.3	Absorption wavelengths of characteristic groups.....	42
6.1	Linear coefficient of thermal expansion and Young's modulus ...	93
6.2	Intrinsic stresses in dielectric films approximately 5000 Å thick	98
11.1	Properties of infrared coating materials	137
11.2	Film materials and thin film properties	143
11.3	Transmission regions of optical materials, 2 mm thickness.....	144
11.4	Properties of high-power infrared coatings.....	145

CONTENTS OF PREVIOUS REPORTS

1. March 1972

1. Introduction
2. Calculation of Multiphonon Absorption Coefficients
3. Calculation of Extrinsic Absorption Coefficient
4. Effects of Pressure on Operation of Windows
5. Recommendations for an Experimental Program
6. Experimental Data from the Literature
7. Nonlinear Processes

App. A Elementary Introduction to the Theory of Infrared Absorption Spectra

2. June 1972

1. Introduction
2. Calculation of Multiphonon Absorption Coefficient
3. Green's Function Analysis and Sjolander-Type Approximations
4. Rigid-Ion, Next-Near-Neighbor Model for the Scattering Hamiltonian
5. Pressure-Induced Optical Distortion in Laser Windows
6. Plans for Continued Research

App. A Tabulation of Pressure-Induced Optical-Distortion Results

App. B Eigenvectors for the Rigid-Ion, Next-Near-Neighbor Model

3. December 1972

- A. Introduction
- B. Theory of Multiphonon Infrared Absorption
- C. Theory of Infrared Absorption and Material Failure in Crystals Containing Inclusions
- D. Collection of Experimental Results for $\beta(\omega)$
- E. References to Previous Multiphonon Calculations

4. June 1973

- A. Introduction
- B. Theory of Infrared Absorption and Material Failure in Crystals Containing Inclusions
- C. Theory of Multiphonon Absorption in Insulating Crystals
- D. Temperature Dependence of Multiphonon Infrared Absorption
- E. Theory of Infrared Absorption by Crystals in the High Frequency Wing of Their Fundamental Lattice Absorption
- F. Temperature Dependence of the Absorption Coefficient of Alkali Halides in the Multiphonon Regime
- G. Temperature and Frequency Dependence of Infrared Absorption as a Diagnostic Tool
- H. Short-Pulse Operation of Infrared Windows without Thermal Defocusing

5. December 1973

- A. Introduction
- B. Extrinsic Absorption
- C. Extrinsic Absorption in $10.6 \mu\text{m}$ Laser Window Materials Due to Molecular-Ion Impurities
- D. Very High-Intensity Effects
- E. Explanation of Laser-Damage Cone-Shaped Surface Pits
- F. Nonlinear Infrared Absorption from Parametric Instabilities of Phonons
- G. High-Power $2\text{-}6 \mu\text{m}$ Window-Material Figures of Merit with Edge Cooling and Surface Absorption Included
- H. High-Power $10.6 \mu\text{m}$ Window-Material Figures of Merit with Edge Cooling and Surface Absorption Included
- I. Explicit Exponential Frequency Dependence of Multiphonon Infrared Absorption
- J. Quasiselection Rule for Infrared Absorption by NaCl-Structure Crystals
- K. The Absorption Coefficient of Alkali Halides in the Multiphonon Regime: Effects
- L. Vertex Corrections for Multiphonon Absorption
- M. Negligible Intrinsic-Absorption Processes
- N. Summary of Publications and Results
- App. Simple Pendulum Instability

6. June 1974

- A. Introduction and Summary
- B. Intensity Limits of High-Intensity Vacuum Ultraviolet Materials
- C. Multiphoton Absorption
- D. Calculated Reflectance of Aluminum in the Vacuum Ultraviolet
- E. Total-Internal-Reflection Devices
- F. The Scattering and Absorption of Electromagnetic Radiation by a Semi-Infinite Crystal in the Presence of Surface Roughness
- G. Infrared Absorption by the Higher-Order-Dipole-Moment Mechanism
- H. Stimulated Raman and Brillouin Scattering: Parametric Instability Explanation of Anomalies
- I. Extrinsic Absorption in $10.6 \mu\text{m}$ Laser Window Materials
- J. Erratum, High-Power $2\text{-}6 \mu\text{m}$ Window-Material Figures of Merit with Edge Cooling and Surface Absorption Included
- K. List of Recent Publications

7. December 1974

- A. Introduction and Summary
- B. Stimulated Raman Scattering: Enhanced Stokes Gain and Effects of Anti-Stokes and Parametric Phonon Processes
- C. Enhanced Stimulated Raman Scattering and General Three-Boson Parametric Instabilities
- D. Theory of Laser-Materials Damage by Enhanced Stimulated Raman Scattering
- E. Surface Roughness and the Optical Properties of a Semi-Infinite Material; The Effect of a Dielectric Overlayer
- E. App. Construction of the Green's Functions for the Electromagnetic Wave Equation

7. December 1974 (Cont'd)

- F. Theory of Laser Heating of Solids: I. Metals
- G. Current States of High-Intensity Vacuum Ultraviolet Materials
- H. Impurity Absorption in Halide Window Materials
- i. List of Recent Publications

8. June 1975

- A. Introduction and Summary
- B. Current Status of Electron-Avalanche-Breakdown Theory
- C. Preliminary Theory of Electron-Avalanche Breakdown in Dielectric by Laser and dc Fields
- D. VUV Window Failure by Multiphoton Absorption and Electron Defocusing, Avalanche, and Absorption
- E. Optical Distortion from the Nonlinear Refractive Index
- F. Studies of Optical Properties of Alkali Halide Crystals
- G. A Possible Mechanism for Extrinsic Absorption in Insulators below the Fundamental Absorption Edge
- H. Multiphonon Absorption of Alkali Halides and Quasiselection Rules
- I. Enhanced Stimulated Raman Scattering and General Three-Boson Parametric Instabilities
- J. List of Publications

PREFACE

This Sixth Technical Report describes the work performed on Contract Number DAHC15-73-C-0127 on Theoretical Studies of High-Power Ultraviolet and Infrared Window Materials during the nominal period from July 1, 1975 through December 31, 1975. The work on the current contract is a continuation of that of the previous Contract Number DAHC15-72-C-0129.

In view of the urgency of the problem of obtaining coatings for high-power infrared windows, a theoretical program was initiated during the report period. This program was given top priority, and the report period was extended approximately three months in order that the present report could be devoted to coatings.

Results of our other ongoing programs will be presented in subsequent reports. These programs include studies of impurity absorption in the vacuum ultraviolet; multiphoton absorption; electron-avalanche breakdown; source of the long, strong, post-Urbach absorption tails in the vacuum ultraviolet; the sources of current difficulties in explaining the optical absorption (even the position of the absorption edges) in alkali halides; and surface-state and related absorption in wide-bandgap insulators.

I. SUMMARY OF RESULTS

The results summarized below and the recommendations for future coatings programs given in Sec. II afford an overview of the present report.

The most important result is that film contamination must be avoided by obtaining high-packing-density films and using ultraclean-deposition conditions, including thorough baking of the entire system before deposition, high-purity single-crystal starting materials, special care in evaporation, special substrate preparation, and ultrahigh vacuum.

•• Absorptance

- The major current problem with high-power infrared coatings is obtaining a sufficiently low optical absorptance.
- Values of film absorptance A_f per surface of $A_f = 10^{-4}$, or absorption coefficient $\beta_f = 0.5 \text{ cm}^{-1}$ for film thickness $t_f = 2 \mu\text{m}$, are desired in order to avoid greater film absorptance than bulk absorptance.
- As a result of the coating absorptance usually being orders of magnitude greater than the value corresponding to the absorption coefficient of the bulk material, the problem of obtaining low optical absorptance has been even more difficult than the severe problems of obtaining stable coatings with ultralow reflectance plus the usual requirements for field operation.
- The most likely source of the great infrared absorption in coatings is contamination, which can occur during deposition, after deposition as surface adsorption or pore contamination, or before deposition as contamination of the starting material.

- Important contaminants include water, such other molecules or corresponding molecular ions as O_3 , HCO_3 , ClO_3 , NO_2 , CO_2 , N_2O , CO_2 , HDO, SO_4 , CH_4 , and various other hydrocarbons, and other less likely contaminants discussed in the text.
- There is ample evidence in the literature for such contamination both during deposition and upon exposure of the films to the atmosphere after deposition and for further contamination from longer exposure to the atmosphere, from cleaning solvents, and from plastic packing materials.
- High-packing-density films are expected to be necessary to avoid excessive absorptance from contamination of the pores.
- Additional possible sources of the greater film absorptance are deviations from stoichiometry and other less likely sources discussed in the text.
- The ultraclean deposition conditions mentioned above are required in order to avoid film contamination during deposition and substrate contamination before deposition and to obtain stable films in some cases.
- Substrate-surface preparation is important since the substrate condition affects the coating quality, and the substrate-surface absorptance can be much greater than 10^{-4} even before the coating is applied. In addition to infrared absorption by adsorbed layers on the surface, a damaged surface layer (resulting from polishing, for example) could absorb water or other contaminants that increase the absorptance.
- Assuming that the contamination of the substrate can be reduced sufficiently by baking, that the contamination of the film during deposition can be reduced sufficiently by the methods suggested, and that the contamination of

pores on exposure to the atmosphere can be reduced sufficiently by obtaining high-density films, there still remains the problem of adsorption of contaminants on the surface of the coating.

- As a result of this surface adsorption of contaminants, it may be difficult to reduce the total optical absorptance of field-operated, $10.6 \mu\text{m}$ optical elements below $\sim 4 \times 10^{-4}$. Two molecular layers of adsorbed water formally give absorptance $A_f = 10^{-4}$ per surface. A 99.95 percent dense, two-micrometer thick coating with the remaining 0.05 percent occupied by water gives $A_f = 10^{-4}$ per surface.

• Limitations set by the surface adsorption of contaminants conceivably could be avoided in some systems by using such precautions as cleaning the window before use, possibly even by increasing the laser intensity slowly, or maintaining the window environment at an elevated temperature.

- Concerning the greater film than bulk absorptance, the only material known to be depositable with film absorptance as low as bulk absorptance at $10.6 \mu\text{m}$ is As_2S_3 , with film and bulk absorption coefficients $\beta_f = \beta_b = 0.8 \text{ cm}^{-1}$, which would correspond to a film absorptance $A_f = 1.8 \times 10^{-4}$ for a quarter-wave optical thickness of $2.2 \mu\text{m}$.

The emphasis on the current importance of great film absorptance should not be taken to imply that there are no other problems with high-power infrared coatings. Indeed there are other problems as discussed in the following sections. These other problems, which do not appear to be as serious as the absorption problems, will of course have to be considered if they are not solved automatically in the process of lowering the absorption.

•• Measurements

Spectroscopic measurements of film absorptance A_f as a function of frequency ω on very thick films and on coated attenuated-total-reflection plates, and calorimetric measurements of A_f at specific laser frequencies conceivably could be the only absorptance measurements necessary if the high-density films deposited under the ultraclean conditions are satisfactory. However, the films surely will have to be carefully characterized, and since it is the rule rather than the exception that some difficulties will be encountered in research programs, additional measurements probably will be desirable. Measurement results are as follows:

- Attenuated-total-reflection (ATR) measurements of film absorptance at the level $A_f \approx 10^{-4}$ are difficult to perform and to relate to the calorimeter value (normally incident transmission, as opposed to oblique incidence, with total internal reflection at either the film surface or film-substrate interface). Nevertheless, even measured values of A_f greater than 10^{-4} , with the interpretation difficulties, are useful, especially in showing characteristic absorption bands of impurities.
- Previous use of 45° ATR plates for all substrates and films is known to cause difficulties in interpreting data as a result of non-total internal reflection. Appropriate ATR-plate angles should be used in the future.
- Spectroscopic measurements of $A_f(\omega)$ on very thick films, both at normal incidence and on ATR plates, should be useful for materials which can be deposited as thick films.
- It may be possible to distinguish between absorption at the surfaces of coatings, in the bulk of the coating, and at the coating-substrate interface by calorimetric studies of three films evaporated simultaneously, one with half-wave

optical thickness on a metal substrate (electric field $\tilde{E} \approx 0$ at surface and interface), one with quarter-wave optical thickness on the metal substrate ($\tilde{E} \neq 0$ at surface and $\tilde{E} \approx 0$ at interface), and one with half-wave optical thickness on a transparent substrate ($\tilde{E} \neq 0$ at surface or interface).

- Self-film growth and characterization, including film-thickness and single-deposition-vs-multiple-deposition effects, would be useful.
- In situ measurements of A_f are needed to distinguish the sources of absorption generated during and before the deposition from those generated by exposure to the atmosphere.
- Measurement of absorptance at the water-absorption peaks at $\sim 3\mu\text{m}$ and $\sim 6\mu\text{m}$ for polycrystalline films that have been exposed to high humidity and to water, possibly at elevated temperatures, are needed to rule out the remote possibility that it may be necessary to use a glassy or perhaps an amorphous or polymer film as the outside film of coatings to avoid high absorptance from water contamination of pores.
- Film-packing-density measurements are important since high-density films are required for low absorptance and for stability. Substrate temperature is important in obtaining high packing densities, at least in fluorides.

● ● Guidelines for Selecting New Materials

Figure-of-merit-type analyses, which were useful for window materials, are not appropriate for selecting coating-material candidates since the coatings must satisfy a number of independent requirements. Thus, the following guidelines for selecting candidates are given in place of the figures of merit:

- The value of the bulk absorption coefficient β_b must be less than a required value such as 0.5 cm^{-1} .
- If the recommendations of Sec. II fail to produce values of the film absorption coefficient β_f less than 0.5 cm^{-1} (for materials with $\beta_b < 0.5 \text{ cm}^{-1}$), a guideline for obtaining $\beta_f < 0.5 \text{ cm}^{-1}$ will be sought.
- The value of the index of refraction n_r must be within the required range.
In multilayer coatings, at least one low-index and one high-index material is required.
- The stress in a film is determined by the thermal-expansion-coefficient mismatch, by contamination, and by an intrinsic contribution. The former should be calculated for all new films to verify that it is sufficiently small to prevent failure. Other available information on film stress should be used as discussed in Sec. VI.
- Nonhygroscopic materials are desirable, although it is presently believed that hygroscopic materials possibly can be used as an inside layer of a multilayer stack.
- High-purity, single-crystal starting materials must be obtainable. The single-crystal requirement may be relaxed later in the program.
- Materials must be nonradioactive and nontoxic for some applications.
- The hardness of the outside materials should be great for coatings that must pass abrasion standards.
- Previous experience with the materials in question should be considered, but caution is required to avoid misleading negative results.

- The following properties are desirable, but are difficult to predict for materials that have not been prepared previously in thin-film form:

film packing density

stability (water or other chemical attack, thermal or photo decomposition)

deposition compatibility in multilayer coatings

adhesion to substrate

stoichiometric in thin-film form

no adverse diffusion effects at interface.

• • Candidate 10.6 μm Coating Materials

Materials for 10.6 μm coatings are discussed in Sec. XI, and a list of materials selected as the most promising for immediate study is given at the end of Sec. II.

• • Candidate 2-6 μm Coating Materials

Materials for coatings in the 2-6 μm region will be considered in subsequent reports. Some general comments about 2-6 μm materials are given in Sec. XII.

• • Humidity Protection

- Glassy films such as As_2S_3 offer the greatest potential for protecting underlying materials from moisture attack.

- In a subsequent report, the possibilities of using polymer films for protecting substrates or antireflection layers from moisture attack and of reducing adsorption of water on the surface of antireflection coatings will be considered. In addition to the technical problem of obtaining pin-hole-free films, there are potential basic problems of high moisture-vapor transmission through the films and of high infrared absorptance by the films.

- It is not likely that polycrystalline films can protect large areas of alkali halides from moisture attack.
 - It is probable, though not yet certain, that polycrystalline films can be sufficiently dense and sufficiently hygroscopic to allow $A_f = 10^{-4}$ to be attained in carefully prepared films.
 - Priority of future research on amorphous semiconductor films is low since the likelihood of obtaining β_f less than 0.5 cm^{-1} is small.
- Laser Heating
- For equal film (two surfaces) and bulk absorptances, $2 A_f = A_b = 2 \times 10^{-4}$, the film and bulk contributions to the spatial average of the window temperature, which determines the thermally induced optical distortion, are equal and have the total value $T_{\text{tot}} = 1.0 \text{ K}$, which is sufficient to cause thermally induced optical-distortion failure in some cases.
 - In a typical system with repeated short pulses, only the time-average heating need be considered (apart from inclusion damage, nonlinear effects and possible more stringent conditions of future systems -- see Sec. VIII).
 - The linear absorption (below the damage threshold) by strongly absorbing ($\sigma_{\text{abs}} = \pi a^2$) one-micron-radius inclusions spaced $175 \mu\text{m}$ apart in the coating gives rise to absorptance $A_f = 10^{-4}$.
- Laser Damage
- Inclusion damage is expected to occur at energy density $I_t p \approx 1-10 \text{ J/cm}^2$ for nanosecond pulses or at values of $I_t p$ ranging from approximately 10 to several hundred joules per square centimeter for microsecond pulses. In principle, values of $I_t p < 1 \text{ J/cm}^2$ are possible for nanosecond through microsecond pulses.

Sec. 1

- Intrinsic damage of coatings is expected to occur at $It_p \geq 10^3 \text{ J/cm}^2$ for a pulse of duration $t_p = 10 \mu\text{s}$ and $A_f = 10^{-3}$ as a result of linear heating of the coating, or a. $It_p \geq 100 \text{ J/cm}^2$ (or $I \geq 10 \text{ GW/cm}^2$) for a 10 ns pulse of ~ 1 to $10 \mu\text{m}$ radiation as a result of electron avalanche breakdown or perhaps another nonlinear process.

- Intuitively it appears unlikely that all inclusions could be removed from a large window. Thus the lower-threshold inclusion-damage process, rather than an intrinsic process, is expected to determine the damage threshold.

•• Damage of Detached Areas of Film

Large areas of coatings that are thermally isolated from the substrate could cause coating failure:

- The calculated value of 25 K temperature rise for a typical detached film segment of diameter $D = 2 \text{ mm}$ is surprisingly small.
- The temperature is proportional to D^2 .
- The thermally induced stress corresponding to $T = 25 \text{ K}$ has a typical value of 20 MPa ($3 \times 10^3 \text{ psi}$) which may be sufficient to cause further detachment, then further temperature increase since $T \sim D^2$, and possibly a runaway condition resulting in damage.

II. NEAR-TERM RECOMMENDATIONS

The following recommendations are based on conversations with investigators having experience in deposition of thin films, on information obtained from the literature, and on the simple analyses in the following sections. The recommendations are for a near-term program having the goal of obtaining satisfactory high-power infrared coatings. Studies of such longer-range problems as developing additional film deposition methods, developing improved methods of measuring the frequency dependence of optical absorption at low absorptance levels, or studying basic phenomena are not considered. Only the preparation of films under research-laboratory conditions, which is the first step in obtaining usable coatings, are considered directly. The ultimate applications and the problems of production of field-use coatings should of course be kept in mind throughout the near-term program to avoid obtaining a brilliant solution to an uninteresting problem.

It is hoped that once the problems of obtaining low-absorptance stable coatings with the desired properties have been solved, the stringent deposition conditions can be relaxed. Indeed, the engineering problems of carrying out a successful laboratory film to the production stage could be more difficult than the problems considered here of obtaining successful laboratory films. Concerning scale-up to large deposition areas, several laboratories already have large-deposition-area capabilities. The question of whether or not these facilities can be used to deposit low-absorptance films cannot be answered at present of course since even the near-term laboratory-film results are not yet available.

Substrate preparation, film deposition, and film measurements should be carried out at a single location. Such a program will be larger than the individual coatings programs supported in the past. The need for such a large single program is dictated by the severity of the high-power coatings problems.

• • Film Deposition

- The substrate and the entire vacuum chamber should be baked at a high temperature for a long time in order to remove adsorbed material, to prevent readsorption and contamination during deposition, and in some cases to obtain stable films.

The required temperature and time of bake vary from one film-substrate combination to another. In one case, 600°C for one day was required to prevent a film from leaving the substrate on removal from the vacuum system. The baking temperature will in general be different from the substrate temperature at deposition.

In other numerous cases films will adhere to substrates without special precautions. However, in order to obtain low values of absorptance, and in view of the known sensitivity of absorptance to trace amounts of impurities, extreme care must be exercised in deposition, substrate preparation, and selection and purification of starting materials. Such precautions are especially important in the near-term program¹ when the sources of the film problems are being sought and when new film materials are being tried. Films which could not be deposited successfully in original tries have been entirely satisfactory when proper deposition care was exercised.

- State-of-the-art ultrahigh-vacuum deposition systems should be used.

Even though ultrahigh-vacuum systems (less than 1.3×10^{-7} Pa, or 10^{-9} torr) are expensive to construct and to operate, they should be used since contamination of films during deposition has been identified (Sec. IV) as a major problem in high-power films. Even though there are cases in which film quality is reported to be insensitive to substantial changes in the deposition pressure, the best available vacuum system should be used in the study of low-absorptance films. First, ultrahigh vacuum alone, without all the other precautions, is not expected to be effective. Ultrahigh-vacuum deposition of contaminated starting material is not expected to give low-absorptance films in general. Second, a lowering of absorptance for values below $\sim 10^{-2}$ would not have been detected in most previous film studies. It is possible that lower vacuums may be tolerable at later stages of the program after the initial problems are solved. Indeed, it may be impractical to produce coatings on large windows under ultrahigh-vacuum conditions.

- The optimum substrate temperature must be determined and used.

Substrate temperature is critical in obtaining maximum film density (for minimum water uptake on exposure to the atmosphere) and maximum film stability. Trial and error are necessary to determine the optimum substrate temperature. Substrate-temperature requirements are known for some materials, but even these requirements could change when the strict deposition conditions are maintained.

- Only vacuum-evaporation deposition should be used in the near-term program.

Although there are a number of deposition techniques that appear to be promising, previous difficulties in depositing stable, low absorptance films

by methods other than vacuum vapor deposition strongly suggest that only vacuum deposition be used in the near-term program.¹ Unless the ultraclean, vacuum depositions fail to produce acceptable coatings, depositions by other methods should be considered as studies of advanced deposition methods, not as studies of coatings for high-power infrared optics.

- Extreme care must be exercised in the preparation of the material to be deposited. Only dense single-crystal, low-absorptance starting material should be used.

The following comments from Ritter's article^{*2} are highly relevant: "The preparation of the material to be evaporated is of considerable importance for the deposition of high quality optical coatings. Crucial properties are purity, gas content, and grain size. It is highly recommended that one uses vacuum sintered and outgassed materials or even pieces of dense single crystals to avoid gas outbursts and spattering during the evaporation process. Powders are normally not suitable, since they have too much adsorbed gas, which is desorbed during heating and leads to pressure rise and spattering of material, even to jumping out of the boat. Some fluorides tend to form oxide or carbonate layers on the surface. These layers may impede free evaporation and cause sudden spattering of the evaporants." Other precautions such as particle filters and great distances to the substrate should be exercised. Hughes Research Laboratories found^{*3} that commercially available As_2S_3 was not satisfactory for high-quality As_2S_3 films.

- Stoichiometry must be obtained.

Nonstoichiometric films are unstable and have great absorption.

• • Substrates

- Only substrates with state-of-the-art surface preparation should be used.

The importance of surface absorption at absorptance levels even as great as 10^{-2} and the importance of substrate smoothness and cleanliness on film quality are now known.

- ATR plates with one third of the plate uncoated, one third coated with a film of normal thickness, and one third coated with a very thick film should be used as substrates. The appropriate angle for the given substrate-coating combination should be used and the Raytheon-plate dimension, 2 mm thick and 5 cm long, should be used.

- The thick and thin films should be codeposited by shuttering the area of the thin film until most of the thick film has been deposited. It should be verified that the absorptance of this thin film is the same as the absorptance of a similar thin film grown in a separate deposition without the long shuttered time.

- Later in the program it may become desirable to make depositions simultaneously on substrates of fire-polished quartz, the most highly transparent material available, the coating material (self film), and the substrate material to be studied, and on a metal. The fire-polished quartz substrate is for ultimate smoothness. The highly transparent material is for attenuated-total-reflection and calorimetric studies of film absorptance. Later in the program, quarter-wave and half-wave optical thickness on highly reflecting surfaces may be useful as discussed in Secs. V and I.

• • Measurements

- The near-term program should include spectroscopic measurements of $A_f(\omega)$ on very thick films, on attenuated-total-reflection (ATR) plates coated with standard-thickness films, and on ATR plates coated with very thick films (even though difficulties in interpreting the experimental results have prevented accurate determination of the magnitude of A_f in the past).
- Laser-calorimetry measurements at specific wavelengths also should be included in the near-term program since small values of absorptance can be measured.
- Measurement of absorptance at the water absorption peaks at $3\text{ }\mu\text{m}$ and $6\text{ }\mu\text{m}$ for polycrystalline films that have been exposed to high humidity and to water, possibly at elevated temperatures, should be made to rule out the remote possibility that it may be necessary to use a glassy film, or perhaps an amorphous or polymer film, as the outside film of coatings to avoid high absorptance from water contamination of pores.
- Military-specification tests for adhesion, abrasion, and humidity resistance already are routinely used and should be continued. Accelerated humidity-resistance tests should be added.
- Improved methods of measuring small values of absorptance in the range of 10^{-4} as a function of wavelength from 2 through $14\text{ }\mu\text{m}$ are badly needed and should be supported. However, previous attempts to make such measurements using a variety of different techniques have all encountered serious technical difficulties. Thus it is strongly recommended that the near-term coatings program should proceed independently of any measurement-development program and should not await the results of these measurement-development programs.

The requirements for additional measurements, discussed in Sec. V, will depend on the outcome of the first phases of the recommended program.

• • Film Materials

- Studies of new materials should not be undertaken for conditions other than those specified above.

Even though new coating materials are urgently needed, it would be economical to first obtain the state-of-the-art vacuum-deposition systems and the methods of measuring low values of $\beta(\omega)$. Any failures of coatings of new materials deposited under nonoptimum conditions would be of limited value and could be misleading since it is known that good films have been deposited with sufficient care after failures under nonoptimum conditions.⁴

- The following 10.6 μm candidate film materials are selected as the most promising:

Low-index materials	High-index materials
ThF_4	ZnS
NaF	ZnSe
BaF_2	As_2S_3
SrF_2	As_2Se_3
NaCl	TlI
KCl	
KGaF_4 + other Cryolite-type materials	

The Cryolite-type materials are mixtures of $(\text{Na}, \text{K}, \text{Rb})\text{F}$ and $(\text{Al}, \text{Ga}, \text{In})\text{F}_3$.

- The material-selection guidelines of Sec. X and the information in Secs. X, XI, XII, and XIII should be used in selecting coating materials for the near-term program.

III. BACKGROUND INFORMATION

In this section coating requirements and problems are discussed in general terms, and some useful background information is given. Results of this section include:

- Coating requirements and coating problems, listed below with heavy dots, illustrate the severity of the high-power coating problem.
- Problems of surface absorptance and substrate preparation are as important as problems of coating materials.
- A reasonable current required value of absorptance per coated surface of $A_f = 10^{-4}$, which corresponds to absorption coefficient $\beta_f = 0.5 \text{ cm}^{-1}$ for film thickness $\ell_f = 2 \mu\text{m}$, is obtained by requiring the film absorptance to be no greater than a typical bulk absorptance.
- The following typical values of parameters are chosen for use in examples throughout the report unless specified otherwise: irradiance $I = 10^3 \text{ W/cm}^2$, film and bulk thermal conductivity $K_f = K_b = 5 \times 10^{-2} \text{ W/cm K}$, film absorption coefficient $\beta_f = 0.5 \text{ cm}^{-1}$, bulk absorption coefficient $\beta_b = 10^{-4} \text{ cm}^{-1}$, film thickness $\ell_f = 2 \mu\text{m}$, window thickness $\ell_b = 2 \text{ cm}$, film absorptance per surface $A_f \cong \beta_f \ell_f = 10^{-4}$, bulk absorptance $A_b \cong \beta_b \ell_b = 2 \times 10^{-4}$, wavelength $\lambda = 10.6 \mu\text{m}$, and laser pulse duration $t_p = 10 \text{ sec}$.

Excerpts from the literature are included in Sec. XIII, which is an important part of the report. Most of the results from Sec. XIII are not repeated in the other sections. Our comments interjected in brackets are intended to inter-relate the references and to relate the results of this report to those of the references.

Sec. III

Throughout the report, asterisks denote references that are excerpted. Sec. I, Summary of Results, and Sec. II, Near-Term Recommendations, together serve as a summary of the results of the report. Short section summaries are included at the beginning of each section.

The overall objective of current Department of Defense high-power infrared-material coatings programs is to obtain antireflection coatings that can withstand high powers as well as having the usual properties required for low-power use. The specific objective of the Xonics program is to provide theoretical studies for use in current and future coatings programs. The potential impact of the programs is great in view of the importance to high-power laser programs of obtaining satisfactory coatings and the current difficulties in obtaining such coatings.

The motivation for the study is as follows: The success of the recent high-power infrared-laser-development programs created an urgent need for highly transparent window materials, and the subsequent successful developments in the window-materials programs have now created an immediate need for antireflection coatings. There is a vast history of antireflection-coating research and directly related research. However, only a small fraction of this research has been concerned with coatings that can withstand high infrared intensities. Some of the relevant literature is excerpted in Sec. XIII for the convenience of the reader as mentioned above.

At the beginning of the Xonics program, it appeared that the coatings problems were so severe that the current experimental programs were not likely to yield completely satisfactory results. Thus, there was an immediate need for a program to provide theoretical studies to support current experimental coating programs and perhaps suggest additional programs. The present program was designed specifically to meet this need.

Sec. III

The preliminary results are extremely encouraging: (a) The most important coatings problems have been identified. This is significant since investigators in the field currently do not agree on which problems are important. Opinions range from stress in the films, to obtaining more materials to afford a wider choice of values of index of refraction, to absorption by surface phonon modes. (b) Sufficient evidence has been found in the literature to afford a good case for film contamination being a major source of high absorptance in films. (c) Suggestions have been made for measurements that are needed. (d) Recommendations for a program to obtain satisfactory coatings have been made. (e) Guidelines for selecting candidate materials have been developed and used to select a set of materials to investigate experimentally. Other results are summarized in Secs. I and II and discussed in the following sections. The immediate needs of the coatings program are now clear. Specific ultraclean deposition conditions are required, and high-density, stoichiometric films are necessary.

The emphasis of this report is on 10.6 μm systems, although most of the results are general and apply to other infrared systems as well. The problem of obtaining coatings for 2-6 μm systems is expected to be less difficult than for 10.6 μm systems, as discussed briefly in Sec. XII.

The problem of obtaining satisfactory antireflection and/or protective coatings for high-power infrared windows is difficult, particularly at 10.6 μm . The coatings must satisfy a number of independent requirements, each of which may put severe restrictions on the coating. (Thus, figure-of-merit analyses, such as those used for window materials,⁵⁻⁸ are not useful at the present stage of coatings studies.) The resulting overall requirements are so stringent that there are no completely

Sec. III

satisfactory coatings, and there are only a few candidate coating materials for use at $10.6 \mu\text{m}$ at present. In very general terms, the requirements include:

- low reflectance
- low optical absorptance ($A < 10^{-4}$, for example)
- low optical scattering
- good adhesion to the substrate
- ability to be prepared as thin films
- homogeneous and flat over large areas
- great hardness
- low radioactivity and toxicity
- high damage thresholds for short, high-intensity pulses in some applications
- withstand humidity, temperature changes, abrasion, radiation, and chemical attack in some applications
- acceptably low cost.

At present no specific requirements, such as the values of absorptance, hardness, etc., have been established.

It is important to realize from the beginning that the coating problem is strongly related to the surface problem. Problems of surface absorption and substrate preparation in general are as important as problems of the coating materials. There are measured values of absorptance of surfaces, before a coating is deposited, that are greater than currently acceptable values. Even a monolayer of some materials adsorbed on a surface can cause unacceptably great optical absorption.

Since applying a coating to an absorbing surface is not expected to reduce the

absorptance, the surface absorptance problem must be solved before the coatings problem is solved. It is also known that substrate preparation changes the properties of a coating in general.^{*2}

As was the case in the window-materials programs, one of the cardinal problems is the paucity of materials with low absorption at 10.6 μm . This particular problem appears at first to be less severe for coatings than for window materials since the much smaller thickness of the films allows the use of materials with greater values of optical absorption coefficient β . For example, a value of $\beta = 10^{-4} \text{ cm}^{-1}$ is currently desirable for a window material. It will be shown below that a film material for 10.6 μm use can have a value $\beta_f = 0.5 \text{ cm}^{-1}$ and still be compatible with a two-centimeter-thick window with $\beta = 10^{-4} \text{ cm}^{-1}$, roughly speaking. The advantage of being able to use materials with greater values of β in films is partially offset by the fact that the value β_f of the absorption coefficient of a material in the form of a film usually is greater, by two to four orders of magnitude in some cases, than the corresponding value β_b of the bulk material. The severity of the absorption requirement for 10.6 μm coatings is illustrated by the fact that the value $\beta_f = 10 \text{ cm}^{-1}$ for the popular and currently important infrared coating material Th₄ is a factor of 20 greater than the compatibility value $\beta_f = 0.5 \text{ cm}^{-1}$ from above. Also, materials with a range of values of the index of refraction n_r are required for coatings.

These and other specific problems with coatings are:

- difficulty in obtaining low absorption, $\beta_f \gg \beta_b$ for most coatings
- only a few candidate materials
- need materials with a range of values of index of refraction n_r

Sec. III

- need method of measuring frequency dependence $\beta_f(\omega)$ of β_f in order to identify source of absorption
- some materials craze or detach from substrate, especially for thick coatings
- some materials lack stability, especially resistance to moisture
- compatibility of layers in multilayer coatings
- good thermal contact with substrate is required
- some important film materials are radioactive (ThF_4) or toxic (TlI)
- atmospheric contamination, including water, of surfaces and pores of films may be difficult to eliminate
- substrate preparation often is difficult
- interface contamination
- diffusion of ions at interfaces
- stress in coatings
- optical scattering.

The most pressing of these problems are discussed in the sections to follow.

It will now be shown that a reasonable current required value of absorptance per coated surface is $A_f = 10^{-4}$, which corresponds roughly to $\beta_f = 0.5 \text{ cm}^{-1}$ or extinction coefficient $K = 4.2 \times 10^{-5}$ at $10.6 \mu\text{m}$. The goal of recent Department of Defense programs was an order of magnitude smaller, $A_f = 10^{-3}$. The lowest value of A_f for a $10.6 \mu\text{m}$ coating reported to date is^{*9} $A_f = 3 \times 10^{-4}$ for a two-layer ThF_4/ZnSe coating on ZnSe. The lowest value of A_f reported for a stable coating on KC1 is $A_f = 1.9 \times 10^{-3}$ per surface.^{*10} This current desired value of $A_f = 10^{-4}$ is based on compatibility with the bulk absorption in window materials, for which $\beta_b = 10^{-4} \text{ cm}^{-1}$ is now a commonly mentioned value. All of these

Sec. III

numbers are to be taken as typical values. Even smaller values of β for both films and bulk materials already would be highly desirable and may be a necessity for future systems. Finally, it should be mentioned that $\beta = 0.5 \text{ cm}^{-1}$ is only a typical value, and that the value $A_f = 10^{-4}$ can be achieved with a coating material having β_f somewhat greater than 0.5 cm^{-1} . An example is a multilayer coating in which a layer can be both thin and located at a position of low electric field, as has been shown at the Hughes Research Laboratory.^{*9}

In Sec. VII it will be shown that since thermally induced optical distortion, rather than melting or fracture, often limits the values of β_f and β_b , a convenient measure of compatibility of the coating and bulk absorption is equal absorptance by the two coated surfaces and the bulk,

$$2A_f = A_b ,$$

(rather than equal values of the maximum temperature rise from bulk and coating absorption). For $\beta_b l_b \ll 1$, where l_b is the window thickness, the absorptance of the bulk is $\beta_b l_b$, and for $\beta_f l_f \ll 1$, the absorptance of the film is $\beta_f l_f$.

Equating $2\beta_f l_f$ to $\beta_b l_b$ gives

$$\begin{aligned} \beta_f &= (l_b / 2l_f)\beta_b , & \kappa_f &= (l_b / 2l_f)\kappa_b , \\ \beta_f &= (10^4 \beta_b) 0.5 \text{ cm}^{-1} , & \text{for } l_b = 2 \text{ cm and } l_f = 2 \mu\text{m} . \end{aligned} \quad (3.1)$$

Thus, for $\beta_b = 10^{-4} \text{ cm}^{-1}$, the value of β_f from (3.1) is $\beta_f = 0.5 \text{ cm}^{-1}$ and the corresponding value of A_f is 10^{-4} , as stated above. The corresponding value of κ_f at $\lambda = 10.6 \mu\text{m}$ is $\kappa_f = 4.2 \times 10^{-5}$, which follows from the general relation

$$\begin{aligned} \kappa &= \lambda\beta / 4\pi \\ &= 8.44 \times 10^{-5} \beta \quad \text{at } 10.6 \mu\text{m} \end{aligned} \quad (3.2)$$

Sec. III

with β in units of cm^{-1} . The extinction coefficient κ is of course the negative of the imaginary part of the index of refraction, $n = n_r - i\kappa$.

High-power infrared coatings to date have consisted of at least two layers. Harold Posen¹¹ and coworkers at Air Force Cambridge Research Laboratories state that three-layer coatings are current state of the art at $10.6 \mu\text{m}$. There are so few candidate materials that a coating material with $n_{r\text{coat}} = (n_{r\text{window}})^{1/2}$ cannot be found in general. In this regard it should be kept in mind that for other applications mixtures of materials have been used to obtain specific values of n_r . The necessity for multilayer coatings puts such restrictions on the coatings problem as the requirement for materials with both high and low values of the index of refraction and limitations on the "substrate" temperature and possibly other deposition conditions for the various layers of the coating.

The current status of $10.6 \mu\text{m}$ film materials and of $10.6 \mu\text{m}$ antireflection coatings is summarized in Table 3.1. Notable features of the table are as follows. The best antireflection coating that passed the adherence, humidity, stability, and abrasion tests was a ThF_4/ZnS coating on ZnS from the Hughes Research Laboratories. The value of $A_f = 6 \times 10^{-4}$ is a factor of six greater than the currently desired value of 10^{-4} . (The value of A_f was less than the goal of 10^{-3} for that program.) The lowest value of A_f obtained to date for a $10.6 \mu\text{m}$ antireflection coating was 3×10^{-4} for a ThF_4/ZnSe coating deposited on a ZnSe substrate at the Hughes Research Laboratory. This coating passed the adherence, humidity, and stability tests, but failed the abrasion test. There are seven materials that have values of β_f that are within a factor of three of the required value of 0.5 cm^{-1} . In addition to the current low-index material thorium tetrafluoride, the

Table 3.1. Summary of the Current Status of Film Materials and Coatings.

● Lowest values film absorptance at $10.6 \mu\text{m}$						
material	KCl	As_2S_3	ThF_4	CdTe	ZnSe	TlI
$\beta_f (\text{cm}^{-1})$	<0.6	0.77	10, <1.2	<1.2	1.2	<1
$\beta_b (\text{cm}^{-1})$	7×10^{-5}	0.77	unknown	6×10^{-4}	4×10^{-4}	$> 10^{-4}$
n_r	1.46	2.38	1.35	2.57	2.42	2.16
form	poly	glass	glass	poly	poly	poly
● Best current $10.6 \mu\text{m}$ antireflection coatings:						
coating	substrate	laboratory	A_f	R_f	adherence, humidity, & stability	abrasion
ThF_4/ZnSe	ZnSe	Hughes	3×10^{-4}	3×10^{-4}	pass	fail
ThF_4/ZnS	ZnSe	Hughes	6×10^{-4}	2×10^{-4}	pass	pass

only other of these six materials that has a low value of the index of refraction is KCl. It is not yet clear if coatings containing KCl, even as inside layers, can withstand high humidity for extended periods of time.

The only material for which the film absorption coefficient β_f is equal to the bulk absorption coefficient β_b is arsenic trisulfide, with $\beta_f = \beta_b = 0.77 \text{ cm}^{-1}$. Potassium chloride, cadmium telluride, and zinc selenide have values of β_f that are three to four orders of magnitude greater than the corresponding values of β_b . The value of β_f for thorium tetrafluoride usually is quoted in the literature as $\beta_f = 10 \text{ cm}^{-1}$; however, a value of $\beta_f < 1.2 \text{ cm}^{-1}$ has been observed in one case.

The following values of parameters will be used throughout the coating study unless specified otherwise:

$$\begin{array}{ll}
 I = 10^3 \text{ W/cm}^2 & K_f = K_b = 5 \times 10^{-2} \text{ W/cmK} \\
 \beta_f = 0.5 \text{ cm}^{-1} & \beta_b = 10^{-4} \text{ cm}^{-1} \\
 \ell_f = 2 \mu\text{m} & \ell_b = 2 \text{ cm} \\
 A_f \approx \beta_f \ell_f = 10^{-4} & A_b \approx \beta_b \ell = 2 \times 10^{-4} \\
 \lambda = 10.6 \mu\text{m} & t_p = 10 \text{ s} . \\
 \end{array} \tag{3.3}$$

Here the subscripts f and b denote film (coating) and bulk values, respectively. I is the incident irradiance (intensity), K is the thermal conductivity, β is the absorption coefficient, ℓ is the coating or window thickness, A is the absorbance, t_p is the duration of time the laser is on, and λ is the laser wavelength.

The value of C is near $2 \text{ J/cm}^3 \text{ K}$ for most materials, and the value of K typically ranges from $3 \times 10^{-3} \text{ W/cmK}$ for Ti1173 chalcogenide glass to 0.13

for zinc selenide. Since the value of I can vary considerably from system to system and there is no typical value of I , the value of $I = 10^3 \text{ W/cm}^2$ is chosen as representative; the resulting typical temperature rise $T = 1 \text{ K}$, from Sec. VII also is a representative value. The choice of $t_p = 10 \text{ s}$ also is arbitrary. For $t \gg 10 \text{ s}$, the cooling of the sample must be considered. This introduces a whole new phase of engineering considerations that would obscure the central results of interest here. The other values in (3.3), which are typical values for systems of interest, are discussed as they arise.

The following conversion factors and relations are listed for convenience:

$$\beta = \frac{4\pi\kappa}{\lambda} = \left(\frac{\kappa}{10^{-4}} \right) \left(\frac{10.6 \mu\text{m}}{\lambda} \right) 1.19 \text{ cm}^{-1}$$

$$1 \text{ Pa} = 1.450 \times 10^{-4} \text{ psi} = 10.00 \text{ dyne/cm}^2 = 9.869 \times 10^{-6} \text{ normal atmosphere (760 torr)}$$

$$= 10^{-5} \text{ bar} = 7.502 \times 10^{-3} \text{ torr (mm Hg @ 0 C)}$$

$$= 1.020 \times 10^{-7} \text{ kg force/mm}^2 \text{ (Knoop units)} = 1.020 \times 10^{-5} \text{ kg force/cm}^2$$

$$1 \text{ normal atmosphere} = 760 \text{ torr} = 1.013 \text{ bar} = 1.013 \text{ M dyne/cm}^2$$

$$10 \text{ normal atmospheres} = 1.013 \text{ MPa}$$

$$100 \text{ normal atmospheres} = 1.033 \text{ Knoop} \equiv 1.033 \text{ kg force/mm}^2$$

$$1 \text{ eV/A} = 1.6 \times 10^{-4} \text{ dynes} = 1.6 \times 10^{-11} \text{ N}$$

$$\frac{1 \text{ eV/A}}{(2.8A)^2} = 2.0 \times 10^{11} \text{ dynes/cm}^2 = 20 \text{ GPa} = 3.0 \times 10^6 \text{ psi}$$

where $2.8A = 0.28 \text{ nm}$ is the near-neighbor spacing in NaCl

$$1 \text{ eV/molecule} = 24 \text{ k cal/mole}$$

$$1 \text{ g mil/(100 in}^2) 24 \text{ hr} = 4.56 \times 10^{-11} \text{ g/cm sec} .$$

The following glossary of terms is included for the convenience of the reader:

Macroscopic porosity. This term is used to indicate that the pores in the film material are sufficiently large to absorb water or perhaps other contaminants. The ordinary density, that is the mass per unit volume, can be less than the theoretical value for a perfect crystal as a result of such imperfections as vacancies that are different from the large pores involved in water absorption. Harold Posen¹¹ suggested that this distinction be clearly made.

Mechanical stability. In this report, mechanical stability will mean the resistance to crazing, cracking, clouding, and removal from the substrate resulting from stresses and/or weak adhesion to the substrate.

Near-term program. The emphasis in this report is on obtaining satisfactory high-power coatings in the shortest possible time for a reasonable commitment of funds. The near-term program recommended in Sec. II was designed for this purpose. Many studies, including investigations of new methods of measuring absorptance and methods of deposition other than vacuum evaporation, which are of basic interest or are of interest in longer-term programs are not included in the near-term program.

Packing density. The term packing density, which is often used in the thin-film literature, should not be confused with the packing density of spheres in the elementary model of a solid, as a system of packed spheres. In the present report, high packing density and low macroscopic porosity have the same connotation.

Sec. III

Low vacuum. $10^5 - 3.3 \times 10^3$ Pa , (760-25 torr)

Medium vacuum. $3.3 \times 10^3 - 0.13$ Pa , ($25 - 10^{-3}$ torr)

High vacuum. $0.13 - 1.3 \times 10^{-4}$ Pa , ($10^{-3} - 10^{-6}$ torr)

Very high vacuum. $1.3 \times 10^{-4} - 1.3 \times 10^{-7}$ Pa , ($10^{-6} - 10^{-9}$ torr)

Ultrahigh vacuum. less than 1.3×10^{-7} Pa , (less than 10^{-9} torr)

Very thin coatings. Unless specified otherwise, this term will denote coatings that are approximately 50-100 nm thick, which are used for protective coatings to reduce water adsorption and/or increase abrasion resistance.

IV. POSSIBLE SOURCES OF ADDITIONAL ABSORPTION IN COATINGS

The most important result of this section is that the most likely source of the extrinsic absorption in coatings is contamination, which can occur after deposition by surface adsorption or by pore contamination of porous films, or it can occur during evaporation. Contaminants include water and other atmospheric contaminants and many others listed below. Specific results include the following:

- One of the major current problems of high-power infrared coatings is that infrared absorption in a coating usually is much greater than in the bulk materials.
- The only material known to be depositable with film absorption coefficient as low as the bulk absorption coefficient at $10.6 \mu\text{m}$ is As_2S_3 , with film and bulk absorption coefficients $\beta_f = \beta_b = 0.8 \text{ cm}^{-1}$, which would correspond to a film absorptance $A_f = 1.8 \times 10^{-4}$ for a $10.6 \mu\text{m}$ half-wave optical thickness of $\ell_f = 2.2 \mu\text{m}$.
- Film contamination by water, by such molecules or corresponding molecular ions as O_3 , HCO_3 , ClO_3 , NO_2 , CO_2 , CO , N_2O , HDO , SO_4 , and CH_4 , or by other contaminants is the most likely source of the greater film absorption. Contamination includes surface adsorption and absorption by porous films during and/or after deposition, adsorption on substrates prior to deposition, and contamination of the bulk film during deposition. Compounds containing O_3 are especially important at $10.6 \mu\text{m}$.
- Surface optical absorption is a major problem, even on uncoated surfaces.
- Other possible sources of the greater film absorptance are deviation from stoichiometry and other less likely sources discussed below.

- It is possible that an overall absorptance of 10^{-4} may not be achievable for 10.6 μm field-operated windows. Two monolayers of adsorbed water give absorptance $A_f = 10^{-4}$ per surface. A 99.95 percent dense, two-micrometer-thick coating with the remaining 0.05 percent occupied by water gives $A_f = 10^{-4}$ per surface.

Film absorptance. One of the most serious problems with coating is the greater optical absorption in films than in the bulk materials. The absorption coefficient is two to four orders of magnitude greater in films than in the bulk materials in some cases. In fact, it is the rule rather than the exception that the value of the absorption coefficient β is greater in a film, β_f , than in the bulk, β_b , of the same material. We would like to know if the additional absorption can be eliminated and, if so, how to best accomplish the reduction.

In order to design the most effective experiments to determine the source of increased optical absorption in films, it is useful to consider possible sources of the greater absorption. Possible absorption mechanisms include the following:

- film contamination (contaminants are listed below)
- deviations from stoichiometry
- interface effects such as ionic diffusion across interfaces, contaminated interfaces, or absorbing interface layers
- free-carrier absorption
- electronic states, especially in amorphous films
- phonon or electronic surface, interface, or film modes
- strain effects.

Contamination. It is proposed that film contamination is the most likely source of the extra optical absorption in films. There are many possible contaminants, including the following:

- water contamination
- contamination by such other molecules or corresponding molecular ions as those listed in the section summary above
- macroscopic absorbing inclusions in the film or on the substrate, including polishing compounds
- precipitants
- diffused ions or molecules
- dirt
- dust
- pollen
- residues from plastic containers
- fingerprints
- particles spattered from the starting material
- residual-gas contaminants
- cleaning materials
- rinses .

In general these contaminants can be adsorbed on the surfaces of the coatings, they could be on the substrate before the film is deposited, they could be incorporated into the film material from the residual gas during deposition, they could be incorporated into the film from the starting material from which the film is deposited, they could be absorbed in the pores of the film after deposition, or they could diffuse from the substrate to the film or from the film to the substrate.

Vacuum vapor deposition and other thin-film deposition methods are after all simply methods of growing crystals. R. R. Austin¹² pointed out that the Raytheon chemical-vapor-deposition zinc selenide and zinc sulfide samples are just ultra-thick films. The difficulty with vacuum evaporation and other thin-film deposition techniques is that these techniques produce films that are extremely dirty by the standards of high-quality crystal growth methods.

The problem of greater absorption in films than in bulk materials brings to mind the problem from the early phase of the high-power window materials investigations in which hot-pressed and sintered materials had greater absorption than did single crystals. There was even the question if polycrystalline materials could have as low absorption as single crystals. It is now accepted that greater absorption results from contamination of grain boundaries. Clean grain boundaries themselves are not a source of absorption, at least at the level of $\beta_b = 10^{-4} \text{ cm}^{-1}$. Indeed, the bulk absorption coefficient of polycrystalline KCl with internally formed grain boundaries is as low as that of single-crystal KCl. Thus, contamination of any openings in coatings by water, absorbing molecules, dirt, or other absorbing materials is a plausible possible source of absorption. The great variation from film to film in reported values of β_f leaves little doubt that most reported values of β_f are extrinsic values.

Water contamination. Water absorption in coatings and water adsorption on coating and substrate surfaces are important possible sources of the extra optical absorption. Water is a strong absorber of infrared radiation at wavelengths greater than $\sim 2.7 \mu\text{m}$, and is known to be absorbed in many coatings.^{*2} In particular, films with low packing densities can absorb so much water that the value of the index of refraction changes considerably. The pores apparently are essentially filled with

water. The water absorption can occur on exposing the deposited film to the atmosphere. Water vapor in the residual gas also can contaminate the film. The packing density of a film is not only important from the point of view of its optical behavior but also of its mechanical and chemical stability.¹³

The literature abounds with evidence of absorption from water in films, as is seen from skimming the excerpts in Sec. XIII. All 18 attenuated-total-reflection spectra of coatings recently measured at Raytheon^{*14} showed evidence of water absorption, as discussed in Secs. V and XIII. In fact, most film-porosity measurement techniques involve detecting the absorbed water.^{*2} A striking example of film porosity is discussed below, in this section, in the discussion of amorphous materials.

It will be shown that at $10.6 \mu\text{m}$ a 99.95 percent dense, two-micrometer-thick coating with the remaining 5×10^{-4} fraction occupied by water has a theoretical value of absorptance $A_f = 10^{-4}$. Alternatively, two monolayers of water (formally 1 nm thick) gives rise to $A_f = 10^{-4}$. The corresponding values of A_f from two monolayers of water for $2.8 \mu\text{m}$ ($\beta = 2.2 \times 10^3 \text{ cm}^{-1}$), $3.8 \mu\text{m}$ ($\beta = 197 \text{ cm}^{-1}$), and $5.3 \mu\text{m}$ ($\beta = 340 \text{ cm}^{-1}$) are $A_f = 2 \times 10^{-4}$, 2×10^{-5} , and 4×10^{-5} , respectively.

These important results indicate that high densities of the coatings surely will be required. In fact, it may be difficult to reduce the coating absorptance of field-operated, $10.6 \mu\text{m}$ optical elements below $A = 10^{-4}$ per surface since it is believed that surfaces will have at least two monolayers of water or other absorbing molecules, dirt, or other contaminants. The following surface-adsorptance (A_s) measurements by Deutsch^{*15, 16} offer some encouragement that $A_f = 10^{-4}$ may be obtainable. At $10.6 \mu\text{m}$, for CdTe, the value $A_s = 7.7 \times 10^{-5}$ is at the double-layer-water value of $\sim 10^{-4}$, and for KBr the value 1.8×10^{-3} is well above 10^{-4} .

Sec. IV

At $5.25 \mu\text{m}$, for CdTe, the value $10^{-6} \pm 2 \times 10^{-5}$ is below the double-layer-water value of 4×10^{-5} , and for KCl the value 9×10^{-5} is above 4×10^{-5} . It is encouraging that such low values for CdTe have already been achieved. However, at some point in the coatings program it will be necessary to consider the absorptance of windows with low total absorptance (near 10^{-4}) after exposure to various contaminants and environments and after field use.

The transmittance T_r of water is shown in Fig. 4.1, and values of the absorption coefficient β at absorption maxima and at some prominent laser frequencies are listed in Table 4.1. There are strong absorption peaks at $2.95 \mu\text{m}$ ($\beta = 2.9 \times 10^3 \text{ cm}^{-1}$) and $6.04 \mu\text{m}$ ($\beta = 2.9 \times 10^3 \text{ cm}^{-1}$) and a peak at $4.70 \mu\text{m}$ ($\beta = 540 \text{ cm}^{-1}$) that is a factor of five weaker than the 2.95 and $6.04 \mu\text{m}$ peaks. (There are slight discrepancies between positions of the maxima and between relative values of β in Fig. 4.1 and Table 4.1, which are from different references.) For $\beta l_f \ll 1$, the expansion $T_r = \exp(-\beta l_f) \approx 1 - \beta l_f$ is valid for the transmittance T_r ; then

$$A_f \approx 1 - T_r \approx \beta l_f . \quad (4.1)$$

For 0.0526 percent water in a two-micron-thick coating, the average value of A_f at $10.6 \mu\text{m}$ is

$$A_f \approx (950 \text{ cm}^{-1})(2 \times 10^{-4} \text{ cm})(5.26 \times 10^{-4}) = 10^{-4} ,$$

as stated above.

Since the absorption coefficient $\beta = 2.9 \times 10^3 \text{ cm}^{-1}$ at the strong absorption peaks at 2.95 and $6.04 \mu\text{m}$ is only a factor of three greater than the value of $\beta = 950 \text{ cm}^{-1}$ at $10.6 \mu\text{m}$, a value of $A_f = 10^{-4}$ at $10.6 \mu\text{m}$ from water absorption

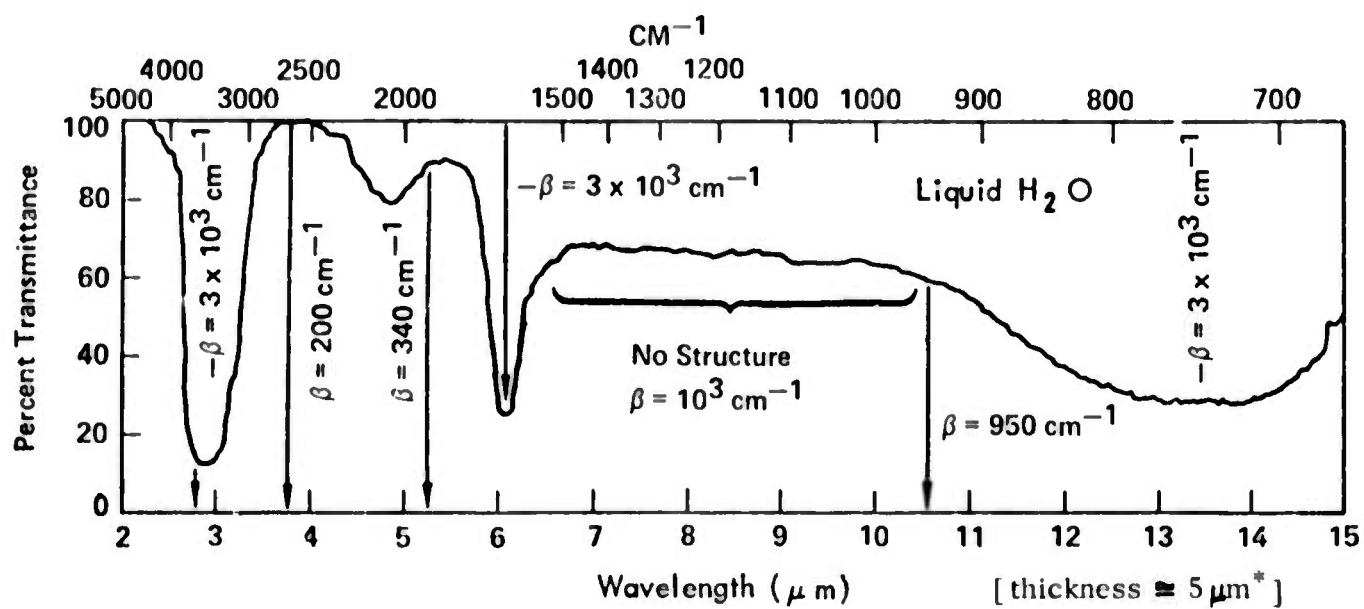


Fig. 4.1. Transmittance of $5 \mu\text{m}^*$ of distilled water.²⁹ [*The thickness was calculated from the average value $\ell = -\beta^{-1} \ln T$ at $2.9, 4.9, 6.1, 10.6$, and $13 \mu\text{m}$, using the values of β from Table 4.1. Notice the strong absorption from $7-10 \mu\text{m}$ ($\beta = 10^3 \text{ cm}^{-1}$) even though there are no absorption peaks.]

Table 4.1. Values of the absorption coefficient of water at the maximum values of β , at prominent laser wavelengths, and at longer wavelengths. Here E3 denotes " $\times 10^3$ ".

$\lambda (\mu\text{m})$	2.95	4.70	6.04	1.06 (Nd)	2.8 (HF)	3.8 (DF)	5.3 (CO)	10.6 (CO ₂)	11	12	13	18
$\beta (\text{cm}^{-1})$	2.9 E3 (max)	540 (max)	2.9 E3 (max)	0.37	2.2E3	197	340	950	1.3E3	2.2E3	2.8E3	3.2E3

would correspond to only 3×10^{-4} absorptance at the peaks. Thus, transmission measurements at the absorptance peaks would not detect the values of A_f of interest. However, assuming that attenuated-total-reflection plates can give a detectability enhancement factor of 50, the resulting effective absorptance of 1.5×10^{-2} at the water-absorption peak should be just at the limit of detectability.

Other possible sources of optical absorption and scattering resulting from water are chemical attack of surfaces (of alkali halides, for example) and recrystallization of the surface region with upward-growing crystallites.^{*3} In addition to the increase in the film absorptance, water or other contamination of pores could cause inclusion damage, as discussed in Sec. VIII.

Molecular impurities. Another important possible mechanism that could give rise to $\beta_f \gg \beta_b$ is that of optical absorption by molecular-type impurities. Such molecules could be adsorbed on the surface of the coating; they could be distributed throughout the bulk of the coating materials; they could appear as grain-boundary contaminants; or they could be concentrated, as a layer for example, at the coating-substrate interface. There is experimental evidence that each of these cases may have been observed. Contamination of the interface layer has been postulated independently to explain the thickness dependence of absorption and of the index of refraction.^{*2} For example, a ZnO layer could exist between a ZnS or ZnSe coating and a substrate. The observation^{*17} that the film absorptance A_f of sputtered ZnSe films on KCl showed very little increase as the film thickness was increased from 0.4 to 2 μm is consistent with the assumption that the major part of the absorptance arises from the interface region. Other similar results have been reported in the literature as seen in Sec. XIII.

There are many known molecules that are strongly absorbing in the infrared. Deutsch^{*15, 16} observed molecular absorption on sample surfaces in attenuated-total-reflection studies. Duthler¹⁸ showed that molecular-ion absorption was an important source of bulk absorption, pointed out the relation to matrix-isolation spectroscopy studies, and catalogued strongly absorbing molecular ions. Duthler's list of absorbing molecular ions is included as Table 4.2. Positions of absorption lines of atmospheric contaminants are shown in Fig. 4.2, which is reproduced from the Handbook of Military Infrared Technology. Table 4.3 lists characteristic absorption frequencies for several molecular groups. Fig. 4.3 is a summary of the position of the absorption peaks of some of the important molecules and molecular ions. The contaminants have absorption bands extending essentially throughout the 2-12 μm range.

Compounds containing oxygen and carbon are particularly important. Oxygen-containing compounds found in the atmosphere include O_3 , H_2O , CO, N_2O , CO_2 , and HDO. Compounds containing O_3 usually have absorption bands near 10.6 μm . Coupled with the reactivity of ozone, this makes O_3 a potentially important contaminant. Carbon-containing compounds found in the atmosphere include CH_4 , CO, and CO_2 . Many polishes, rinses, and cleaning compounds contain carbon. Scanning Auger micrographs by Bernal and Coworkers^{*19} showed a carbon-containing residue about 5 nm thick uniformly distributed over the surfaces of chemically polished KCl samples.

Formation of such molecular cations as SO_4^{2-} on the surface, with subsequent diffusion in a NaCl substrate (to a depth of 13 nm in two weeks), has been suggested to explain strong absorption bands at $\sim 9 \mu\text{m}$ and $\sim 16 \mu\text{m}$ in NaCl windows that had

Table 4.2. Experimentally observed absorption frequencies of several impurity ions in KCl crystals and the estimated impurity concentration to produce $\beta = 10^{-4} \text{ cm}^{-1}$ at the CO₂ laser frequency. From Ref. 18.

<u>Ion</u>	<u>Frequencies (cm⁻¹)</u>	<u>Conc. (ppm) for $\beta(943 \text{ cm}^{-1}) = 10^{-4} \text{ cm}^{-1}$</u>
H ⁻	500	> 10
OH ⁻	3640	> 100
SH ⁻	2590	> 100
CN ⁻	2089	100
BO ₂ ⁻	590, 1972	10 - 100
CO ₂ ⁻	1696	10 - 100
N ₃ ⁻	642, 2049	100
NCO ⁻	629, 1232, 2169	10
NO ₂ ⁻	805, 1290, 1329	0.1
NO ₃ ⁻	842, 1062, 1396	10
CO ₃ ²⁻ ^a	680-720, 883, 886, 1058, 1064, 1378, 1416, 1488, 1518	10
BO ₃ ³⁻	736, 949(w), 1222	1-10
SeO ₃ ³⁻	broad 738-850	1-10
HCO ₃ ⁻	589, 672, 713, 840, 971, 1218, 1346, 1701, 3339	0.01
BH ₄ ⁻	1142, 2321	10
SO ₄ ²⁻ ^a	630, 978, 1083, 1149, 1188	0.03
CrO ₄ ²⁻ ^a	862, 890, 930, 941	< 0.1
SeO ₄ ²⁻ ^a	834, 860, 909, 923	< 0.1
MnO ₄ ²⁻ ^a	899, 909, 914, 925	< 0.1
NH ₄ ²⁺	1405, 3100	10

a. Exact frequencies and intensities very dependent on presence of compensating M²⁺

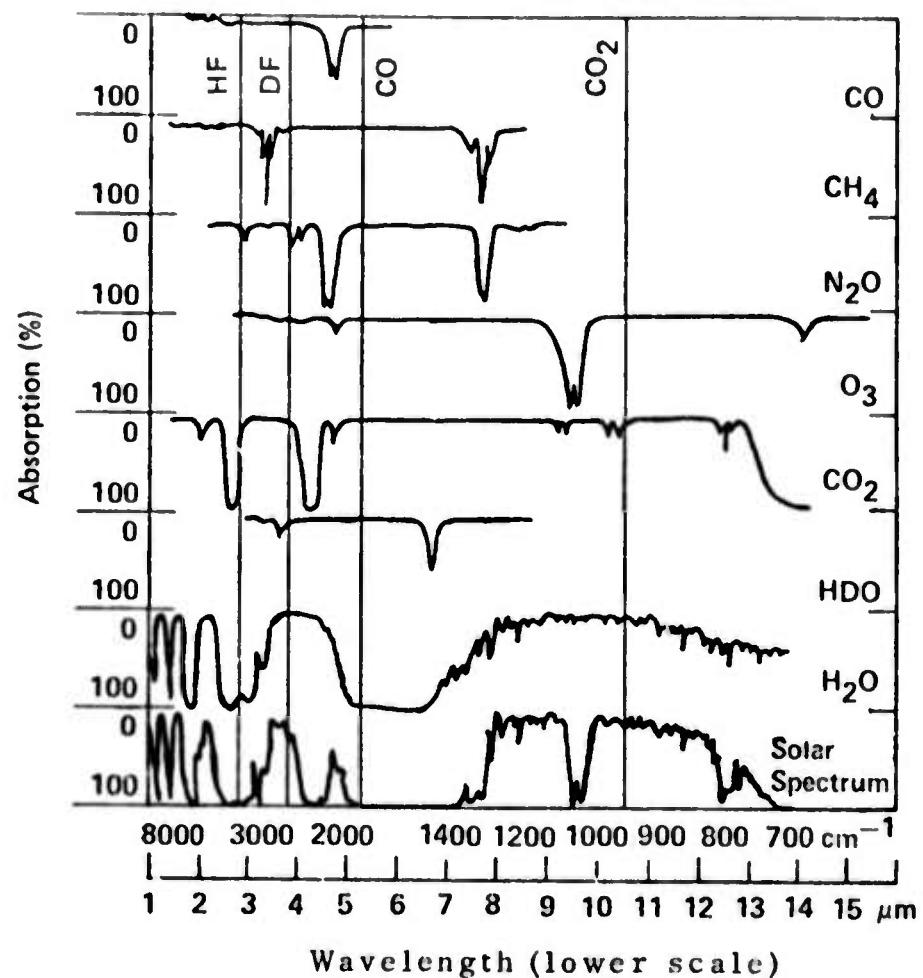


Fig. 4.2. Absorption bands of atmospheric contaminants.
From Ref. 30.

Sec. IV

Table 4.3. Absorption wavelengths of characteristic groups.
See Ref. 30.

<u>Molecular Group</u>	<u>Wavelengths of Absorption (μm)</u>
O - H	2.8
N - H	3.03, 6.12, 6.46
C - H	3.4, 6.81
C - F ₂	8.38, 8.85
Carbonyl	5.75
Methyl	7.26, 7.71
Ester	8, 9.74
C - O	9 (broad), 13.47-14.20
C - Cl	14-15
Si - O	4.5, 9.5
Al - O	~6.5
Ge - O	~5.5, 11.6

Sec. IV

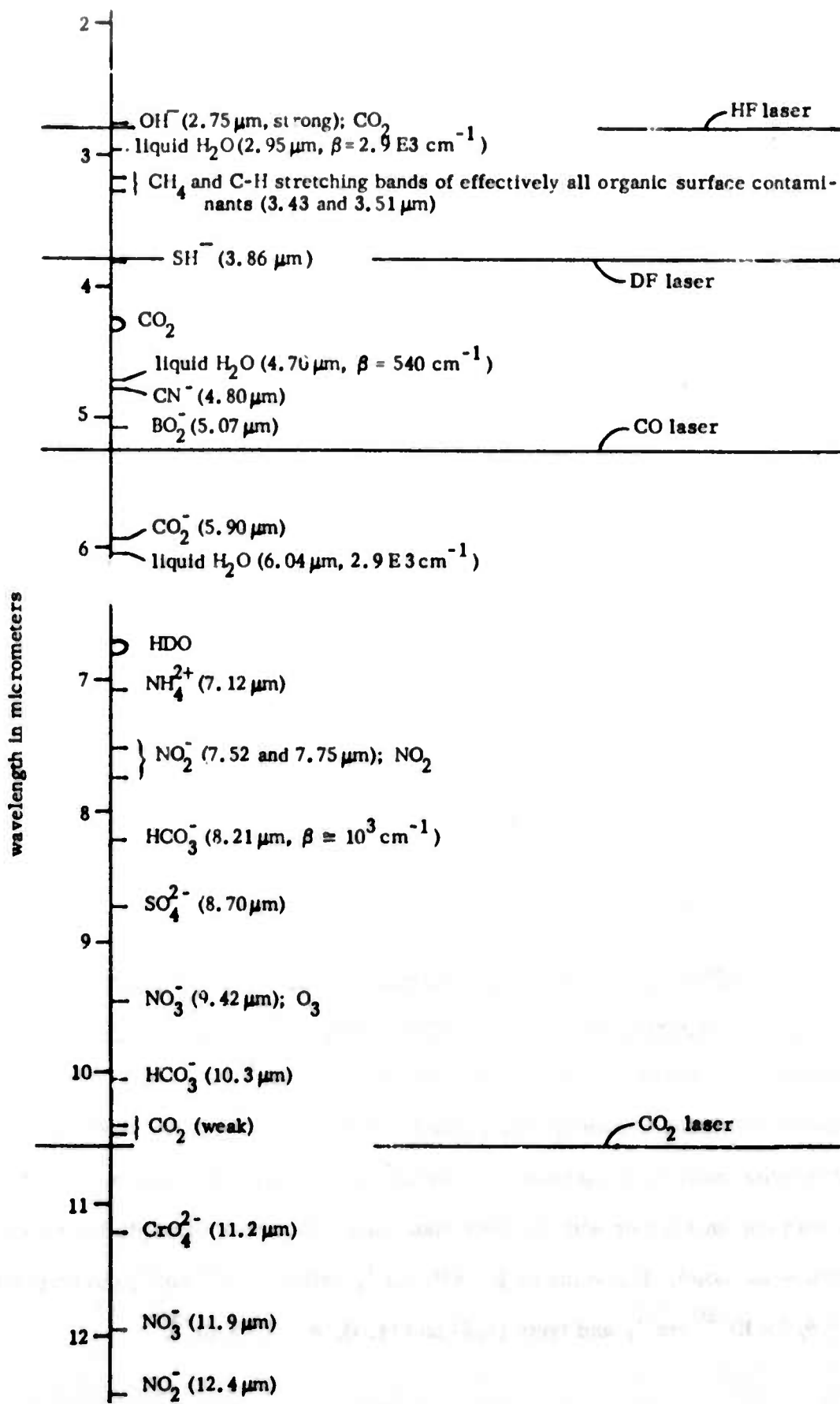


Fig. 4.3. Positions of absorption peaks of some contaminants.

been used in chemical lasers employing mixtures of CS_s and O_2 with transient active species including O , S , SO , CS , S_2O , and many others.

Consider the strength of the optical absorption of molecular contaminants.

The absorption cross section of a molecule at the peak of an absorption band has a typical value of $\sigma = \beta_m / N_m = 10^5 \text{ cm}^{-1} / 10^{22} \text{ cm}^{-3} = 10^{-17} \text{ cm}^2$. The corresponding value of β in general is, of course

$$\beta_m = N_m \sigma \quad (4.2)$$

where N_m is the number of molecules per cubic centimeter. In the limit of small absorptance $A_m \ll 1$, the expansion $\exp(-\beta_m \ell_m) \approx 1 - \beta_m \ell_m$ is valid, and the absorptance is given by the relation

$$A_m = \beta_m \ell_m . \quad (4.3)$$

For a monolayer of molecules, with $\ell_m = 0.5 \text{ nm}$ formally, and a typical density of 10^{22} cm^{-3} , (4.2) and (4.3) give

$$A_m = N_m \sigma \ell_m = 10^{22} 10^{-17} 5 \times 10^{-8} = 5 \times 10^{-3} .$$

Thus, even a monolayer of strongly absorbing material could give rise to fifty times more absorptance than the compatibility goal of $A = 10^{-4}$ per surface. The absorption cross section could be much smaller than 10^{-17} cm^{-2} , with a corresponding reduction in absorption, if the laser frequency were not at the peak of the absorption band or if the band were broadened by, say, interaction of the molecules with one another or with the host materials. The above example for water illustrates the point. The value of $\beta = 950 \text{ cm}^{-1}$, with $N = 10^{22} \text{ cm}^{-3}$, corresponds to $\sigma = 9.5 \times 10^{-20} \text{ cm}^{-1}$, and from (4.2) and (4.3), $A_m = 5 \times 10^{-5}$.

Sec. IV

Other sources of absorption. Deviations from stoichiometry can cause optical absorption that is greater than that of the stoichiometric material. Since deposited films often are not stoichiometric, this source of extra absorption should be kept in mind.

Free carriers, that is free electrons or free holes, are strong absorbers of infrared radiation. Unless special precautions are taken in the deposition of films of semiconductor materials, the resulting material can have a sufficiently great conductance to cause great absorption. Conductivity measurements of films would be useful. Also, the frequency dependence of β should show the near- λ^2 dependence that is characteristic of free-carrier absorption. (By contrast, scattering causes a reduction, rather than an increase, in transmittance with decreasing wavelength.)

Optical absorption at $10.6 \mu\text{m}$ and even at 2.8 , 3.8 , and $5.25 \mu\text{m}$ usually is related to ionic vibrations, rather than to electronic transitions. One case in which electronic transitions are believed to be the source of infrared absorption is in amorphous semiconductors. Although the absorption mechanism is not well understood, it is believed that transitions involving states in the pseudo gap are involved. The resulting absorptance normally is much greater than $A = 10^{-4}$; thus, the (non-glassy) amorphous materials studied to date are not acceptable coating materials. The lowest value of β obtained in attempts to lower the absorption of amorphous germanium films was $\beta_f = 10 \text{ cm}^{-1}$, which is to be compared with the value $\beta_b \approx 2 \times 10^{-2} \text{ cm}^{-1}$ for bulk germanium. Electronic transitions involving surface states are conceivable and will be considered if elimination of the more likely sources does reduce the absorption sufficiently. It is conceivable that the $10.6 \mu\text{m}$ absorption induced by radiation damage to KCl and NaCl samples²⁰⁻²³ could involve electronic transitions. The $10.6 \mu\text{m}$ absorption could be the absorption in the

far wing of the M-center line (or possibly another F-aggregate or the F-center line). (The value of $\beta_{10.6}$ can be as great as 10^{-2} cm for heavily damaged crystals, with $\beta_{M\text{-center}} \approx 10 \text{ cm}^{-1}$ and $\beta_{F\text{-center}} \approx 80 \text{ cm}^{-1}$.) However, Duthler's explanation¹⁸ of the radiation-induced $10.6 \mu\text{m}$ absorption as the activation (lowering symmetry to allow transitions that are not allowed by symmetry in perfect crystals) of normally non-allowed transitions such as those known to exist in impurity molecules is the most likely explanation at present.

Macroscopic absorbing inclusions in bulk window materials can severely limit the power that a window can transmit.²⁴ Both local damage and an increase in the average value of the absorption coefficient are important.²⁴ In studies of laser damage to materials, distinguishing between the inclusion damage and the damage to inclusion-free regions is important. At present it is unlikely that large laser windows which are completely inclusion free could be manufactured. Thus, inclusion damage is expected to remain as one of the severe performance limitations in short-pulse systems. The problem of inclusion damage in the coatings may not be as serious as it first appears since some inclusions in the coatings may be tolerable in view of the fact that the bulk material itself is expected to contain inclusions. However, excessive inclusions in the coatings and problems associated with the local heating of the coating and the coating-substrate interface could cause further performance limitations. Polishing compounds of various materials have been one important source of inclusions in window materials. Other sources include such macroscopic absorbing regions as Zn-rich regions in ZnSe.

Macroscopic inclusions could contribute to the absorptance, especially at the low levels of interest. In Sec. VII it is shown that one-micrometer-radius, very strongly absorbing inclusions (with absorption cross section equal to the geometrical cross section) spaced $175 \mu\text{m}$ apart gave rise to $A_f = 10^{-4}$.

Strain effects possibly could cause increases in absorption coefficients, perhaps by factors of order two greater than the intrinsic values. However, strain effects are not expected to be sufficiently strong to explain the observed increase in β_f over β_b , by factors of $10-10^3$. Sievers²⁵ has shown that even by grossly overestimating the effects of strain, only a factor of five increase over the intrinsic values of β could be obtained.

The Winsor mechanism²⁶ of scattering plus subsequent absorption of the scattered radiation with possible enhancement by total internal reflection is a possible source of increased absorption. However, there should be some sign of the characteristic increase in scattering with decreasing wavelength, and we have found no absorption data that could be related to this mechanism.

M. Hass independently suggested²⁷ that it is possible that the Winsor scattering mechanism could be operative in thin films. "If one ever looks at a thin-film coating with a visible laser it really seems to light up. A well polished single crystal does not seem to do this." In commenting on the preliminary draft of the manuscript for this report, Harold Posen stated, "We have seen damage thresholds of multilayer coatings decrease when compared to single-layer coatings. We ascribe this phenomena in part to the scattering from interlayer topography."

In the final stages of the coatings program, where the last factors of two reduction in the film absorptance are important, there are a number of other effects that become important. In this case, accurately calculating the film absorptance and in designing multilayer coatings requires consideration of the distribution of the electric field across the coating.^{*10} As an example of designing coatings, it is possible to reduce the electric field in the most strongly absorbing coating layer

by properly designing a two-layer coating or by going to coating with more than three layers.

The remaining mechanisms, which are related to surface, interface, or film modes, are less likely sources of the additional absorption. As such, they will be studied later if the more likely sources are ruled out.

Many investigators must share Harold Posen's¹¹ feelings that "---- the optimization of a coating is dependent not only on the material but also on a matrix of deposition techniques, surface preparations, and sometimes - we are convinced - the appropriate phases of the moon." Perhaps this comment could even be taken as support of the possible importance of contamination of coating since the resulting irreproducibility of results could suggest moon-phase correlation.

M. Hass suggested²⁷ that it might be useful to distinguish between resonant and nonresonant absorption. "The resonant type is a result of such processes as molecular impurity absorption which we think might be removed by means of proper vacuum deposition technique. The nonresonant type appears to be one whose wavelength dependence is slowly varying. In some cases it is well understood as for multiphonon absorption and free-carrier absorption. For dielectric coatings one is often well removed from the intrinsic bulk limit."

"How does one go about investigation in a systematic way? The present approach tends to focus attention on the operating wavelength, and problems due to oxygen containing impurities seem to occur at $10.6 \mu\text{m}$ in the chemical laser wavelength. My approach would be to ascertain the nature of the absorption away from these resonant impurities first, as this localizes the nature of the problem. In some cases the Nd:YAG wavelength of $1.06 \mu\text{m}$ can be employed. In other cases, $5.3 \mu\text{m}$

can be used. In a number of cases studies at $5.3\text{ }\mu\text{m}$ have been carried out primarily because this is a CO operating wavelength. However, it also provides an indication of the lower limit at other wavelengths."

The separation of absorption into resonant and nonresonant components would be useful if there were some basic wavelength-independent process and if the extrinsic absorption gave rise to bands. Unfortunately, neither situation is this simple. In most materials the intrinsic absorption from single-photon excitation across the gap and from multiphonon absorption is so small that it will surely be masked by extrinsic absorption. Almost all of the known extrinsic absorption mechanisms are strongly wavelength dependent. Thus the absorption at a particular wavelength such as $1.06\text{ }\mu\text{m}$ or $5.3\text{ }\mu\text{m}$ simply gives information about the extrinsic process that is dominant at that wavelength and is not extremely useful in estimating lower bounds for absorption at other wavelengths.

The statement sometimes seen in the literature that the extrinsic absorption is expected to be small because there are no observed absorption bands in the frequency region of interest is not true in general. A striking example is seen in Fig. 4.1 where the transmittance of water is extremely flat from approximately $7\text{ }\mu\text{m}$ to approximately $11\text{ }\mu\text{m}$. The complete lack of absorption bands in this region would imply that the absorption coefficient should be extremely small. However, the measured absorption coefficient has the extremely large value of 10^3 cm^{-1} .

In passing, it is mentioned that there is some discussion in the literature that the bonding strength of a film to a substrate may be increased by a thin

Sec. IV

intermediate layer of a third material at the interface. Strong adhesion of metal films to glass results from an intermediate oxide layer.²⁸ Even a monolayer of oxygen could cause too much optical absorption. If experimental results should point to investigation of this effect at a later time, layers of S and perhaps Se or Te could be considered.

V. SUGGESTED MEASUREMENTS

Recommendations from this section are as follows:

- The near-term program¹ should include spectroscopic measurements of $A_f(\omega)$ on very thick films, on attenuated-total-reflection (ATR) plates coated with standard-thickness films, and on ATR plates coated with very thick films even though difficulties in interpreting the experimental results have prevented accurate determination of the magnitude of A_f in the past.
- Laser-calorimetry measurements at specific wavelengths also should be included in the near-term program since small values of absorptance can be measured.
- ATR plates with one third of the plate uncoated, one third coated with a film of normal thickness, and one third coated with a very thick film should be used as substrates. The appropriate angle for the given substrate-coating combination should be used and the Raytheon-plate dimension, 2 mm thick and 5 cm long, should be used. The thick and thin films should be codeposited by shuttering the area of the thin film until most of the thick film has been deposited. It should be verified that the absorptance of this thin film is the same as the absorptance of a similar thin film grown in a separate deposition without the long shuttered time.
- Measurement of absorptance at the water absorption peaks at 3 μm and 6 μm for polycrystalline films that have been exposed to high humidity and to water, possibly at elevated temperatures, should be made to rule out the remote possibility that it may be necessary to use a glassy film, or perhaps an amorphous or polymer film, as the outside film of coatings to avoid high absorptance from water contamination of pores.

- Military-specification tests for adhesion, abrasion, and humidity resistance already are routinely used and should be continued. Accelerated-humidity resistance tests should be added.

Other results of this section include the following:

- A method of measuring the frequency dependence $A_f(\omega)$ of absorptance A_f at the low level of $A_f \leq 10^{-4}$ and of distinguishing between coating and bulk absorptance is badly needed and should be supported. However, in view of the great technical difficulties experienced in previous attempts to make such measurements, the near-term coatings program should proceed independently of any measurement-development program and should not await the results of these measurement-development programs.
- It may be possible to distinguish between absorption at the surfaces of coatings, in the bulk of the coating, and at the coating-substrate interface by laser-calorimeter measurements of three films evaporated simultaneously, one with half-wave optical thickness on a metal substrate ($E \approx 0$ at surface and interface), one with quarter-wave optical thickness on the metal substrate ($E \neq 0$ at surface and $E \approx 0$ at interface), and one with half-wave optical thickness on a transparent substrate ($E \neq 0$ at surface or interface).
- Self-film growth and characterization, including film-thickness and single-deposition-vs-multiple-deposition effects, would be useful.
- In situ measurements of β may be needed.
- Other experiments are discussed and listed below.

Absorptance measurements. The main purpose of the experiments considered is to determine the source of the additional absorption in coatings. However, methods of characterizing candidate coatings also are important.

Methods of measuring the absorptance of coatings include the following:

- laser calorimetry
- spectroscopic transmission
- attenuated-total-reflection spectroscopy
- emissivity
- ellipsometry
- surface acoustic-wave velocity measurements
- optical waveguide measurements
- Perkin-Elmer alpha-phone measurements (measuring the pressure change in a cavity that is mechanically, but not optically connected to the laser irradiated sample.)

Techniques of increasing the sensitivity of the measurements, of distinguishing between surface, bulk, and interface absorption, and of studying the additional absorption in films include the following:

- spectroscopic measurements on extremely thick films
- Sievers²⁵ low-temperature calorimetry to obtain large temperature rise from small heat capacity
- thermal-diffusion-time method of M. Hass and coworkers³¹ of distinguishing between surface and bulk absorption
- China Lake wedge-angle method^{*32,*32a} of distinguishing between surface and bulk absorption
- utilization of the near-zero electric field on certain surfaces of films deposited on reflectors to separate surface and bulk absorption in films as discussed below

- studies of self films (such as zinc selenide films deposited on zinc selenide substrates)
- variable film-thickness measurements of β and other variables on a series of coatings codeposited with various thicknesses and on coatings with thickness increased by successive additional deposition or decreased by, say, sputtering, etching, or polishing
- studies of films deposited on such other substrates as fire-polished quartz
- in situ measurements of β in the deposition chamber
- measurement of A_f for various film thicknesses has been used to determine the value of β_f .

Measurements other than absorptance. In addition to these measurements of the optical absorptance in films, the following measurements would be useful in characterizing films:

- electrical conductivity
- packing density
- residual gas analysis in the deposition chamber
- such surface measurements as Auger analysis, especially in conjunction with removal of surface layers by sputtering or possibly other methods
- electron microscopy
- X-ray analysis
- Rutherford back scattering.

Absorptance measurements from 2-15 μm . The most useful measurement for determining the source of the additional film absorption is the frequency dependence of the absorption coefficient, $\beta(\omega)$. (The relation between the absorption coefficient β_f and the absorptance A_f for the cases of interest in which $A_f \ll 1$ is, of course,

$A_f \cong \beta_f l_f$, where l_f is the film thickness. Absorbing molecules show their characteristic absorption bands, electronic absorption tends to increase with increasing frequency, free-carrier absorption increases with increasing wavelength λ (as λ^n with $n \cong 2$ typically), and scattering typically decreases with increasing wavelength (as λ^{-4} for Rayleigh scattering).

The measurement of $\beta(\omega)$ is not trivial in general. The detectable absorptance limit of spectrometers, which is typically ~ 0.01 , is not sufficient to measure the values of $\sim 10^{-4}$ of current interest. There are not enough high-power laser frequencies available for calorimetry measurements.

$A(\omega)$ for very thick films. For materials that can be deposited as very thick films, spectroscopic measurements on the thick films should be made. For $50\text{ }\mu\text{m}$ -thick films on both sides of a substrate and a detectable absorptance of 0.01, the minimum detectable absorption coefficient is $\beta = 0.01/(2)(5 \times 10^{-3}) = 1\text{ cm}^{-1}$, which is only a factor of two greater than the desired value of 0.5 cm^{-1} . Difficulties with the thick-film method are that not all materials can be deposited as thick films, that the ratio of surface and interface absorptance to the absorptance in the bulk of the film will be difficult in general for the thick test films and the thinner antireflection coatings, and that changes in the deposition conditions can make the absorption in the bulk of the two films different. Thick films afford the important advantage that the greater film absorptance A_f makes the measurements less sensitive to the value of the substrate absorptance.

It would be interesting to grow extremely thick self films. The substrate could even be removed from the film. If these very thick self films have the same high absorption coefficient as the thin films, the implication is that the crystal-growth

process (rather than the thin-film geometry of the sample, interface effects, substrate effects, or film-surface effects) is responsible for the additional absorption. The Raytheon chemical-vapor-deposition ZnS and ZnSe crystals are in fact grown as films (though not by vacuum-evaporation deposition) and the crystals do not exhibit the anomalously large absorption coefficients.

In future programs it could be of interest to deposit four films simultaneously, one on the substrate of interest, one on the lowest absorptance substrate obtainable, one on fire-polished quartz, and one self film.

A(ω) from attenuated-total-reflectance spectroscopy. Attenuated-total-reflection (ATR) spectroscopy has already been used to obtain useful information about surface^{*15, 16} and coating^{*14} absorption in high-power infrared-laser-window materials. The experiments require the technical ability to deposit the films and the analytical ability to carry out the ATR-plate spectroscopic measurements, and there are difficulties in interpreting the results, as discussed below. In spite of the difficulties, ATR spectroscopy and thick-film spectroscopy are the best currently available methods of observing surface and coating absorbance as a function of wavelength.

The minimum detectable film absorptance in ATR measurements can be estimated very roughly. For a spectrometer that can detect $A = 0.01$, an ATR plate with 50 reflections could measure $A_f \approx 0.01/50 = 2 \times 10^{-4}$, very roughly. For normal-thickness films, this value of $A_f = 2 \times 10^{-4}$ corresponds to $\beta_f \approx 1 \text{ cm}^{-1}$ very roughly. By using very thick films, values of β_f considerably smaller than the goal of $\beta_f = 0.5 \text{ cm}^{-1}$ can be measured in principle. For example, for $t_f = 50 \mu\text{m}$, the minimum measurable value of β_f is $\beta_f \approx 2 \times 10^{-4}/5 \times 10^{-3} = 4.0 \times 10^{-2} \text{ cm}^{-1}$, very roughly.

The minimum detectable film absorptance could be limited by the bulk absorptance of the ATR plate. For a 45-degree ATR plate 2 mm thick, the beam travels 2.8 nm between internal reflections. The absorptance in this distance is equal to the above film absorptance $A_f = 2 \times 10^{-4}$ for a plate with bulk absorption coefficient $\beta_b = 2 \times 10^{-4} / 0.28 = 7.2 \times 10^{-4} \text{ cm}^{-1}$. Thus, in a plate with a large absorption coefficient, say $\beta_b = 10^{-2} \text{ cm}^{-1}$, the bulk absorptance of the plate could mask the coating absorptance. For 2 mm-thick plates of state-of-the-art materials, with say $\beta_b = 10^{-4} \text{ cm}^{-1}$, the bulk absorptance of the plate does not limit the measurements of the coating absorptance. Some difficulties with previous ATR measurements could be related to large values of the ATR-plate absorptance.

In previous coatings programs the best available substrates were not always used. In the future, only the best substrate materials obtainable should be used. In exact ATR-plate calculations, the reflectance R at the substrate-film interface must be taken into account. The value of R lies on the range $|(n_s - n_r)/(n_s + n_r)| \leq R \leq 1$, depending on the angle of incidence.

For normal-thickness films, measurements of film absorptance lower than the above estimated ATR-plate value of 2×10^{-4} are of interest. However, even measurements at this level would be extremely valuable. In the first place the current coatings that suffer from the additional absorptance often have values of A that are greater than 2×10^{-4} , thus this detectable limit would be sufficient to determine the source of gross problems. Even if the value of A were 5×10^{-5} at the operating wavelength, say $10.6 \mu\text{m}$, it is possible that there would be greater absorption at other wavelengths that could be extrapolated to the operating wavelength in order to estimate the value of β there. If characteristic absorption bands

from specific impurities are present, the frequency dependence of absorptance of the impurity can be used to extrapolate from values of β at the absorption peaks to values at other wavelengths. Finally, for very thick films the value of $\Lambda_f = 2 \times 10^{-4}$ corresponds to small values of β_f . For example, for film thickness $l_f = 50 \mu\text{m}$, $\beta_f = 2 \times 10^{-4} / 5 \times 10^{-3} = 4 \times 10^{-2}$, which is over ten times smaller than the desired value 0.5 cm^{-1} . In the case of total internal reflection at the substrate-film interface discussed below, the electric field may not penetrate far enough into a thick film to give such small values of β_f .

At Deutsch's suggestion, coatings were deposited on half of an ATR plate in order that a direct comparison could be made of coated and uncoated surfaces.^{*14} In the near-term program one third of the ATR plates should be coated with the standard-thickness film, one third should be coated with a very thick film, and one third should be uncoated. Spectroscopic measurements on the uncoated third of the film are useful for measuring surface absorptance and for comparison with the two coated sections. Calorimetric measurements can be made on these same ATR plate samples. In the calorimetry measurements the laser beam could either pass through the coating at normal incidence or could follow the ATR beam path in order to emphasize the coating absorptance. If the ATR plate is made of a material that is different from that of the substrate to be used in the application it must be kept in mind that the value of β_f depends on the substrate material (and condition) in general. The Raytheon ATR plates were 2 mm thick, 5 cm long, and were cut at 45° . It would be convenient to maintain these dimensions in future experiments except that the angle should be different for every film-substrate pair as discussed below. Problems arising from using 45° plates are discussed below in connection with barium-fluoride plates.

The thick and thin films should be codeposited by shuttering the area of the thin film until most of the thick film has been deposited. It should be verified that the absorptance of this thin film is the same as the absorptance of a similar thin film grown in a separate deposition without the long shuttered time.

Eighteen half-coated ATR plates from three vendors were measured on the coated and uncoated halves.^{*14} Coatings of ThF_4 , ZnS , and As_2S_3 on ZnSe substrates and coatings of ThF_4 , ZnSe , and As_2S_3 on BaF_2 substrates were included. All 18 coatings spectra showed evidence of the water absorption bands, ranging from barely detectable in two cases to zero transmittance from $2.8 \mu\text{m}$ to $3.2 \mu\text{m}$ in the worst case.

Difficulties in interpreting the ATR spectra severely limit the usefulness of the method. Ideally the aperture of the spectrometer could be adjusted to give a reading of 100 percent transmittance for the uncoated ATR plate at some wavelength at which the absorptance is negligible for the uncoated half of the ATR plate. Deviations from 100 percent would then give the surface absorptance, assuming that the bulk absorptance is negligible. Then the aperture would be readjusted to give 100 percent transmittance for some wavelengths at which the absorptance of the coated ATR plate is zero. The difference between the two traces should give the coating absorptance. The first obvious difficulty with this method is that there may not be a region of negligible absorptance at which the maximum transmittance can be set. There are other difficulties. In one case^{*14} of a ZnSe coating on BaF_2 the two traces were nearly identical from 2.5 to $\sim 5.6 \mu\text{m}$, and for longer wavelengths the transmittance of the coating plus substrate was greater than that of the substrate alone, as seen in Fig. 5.1. Greater values of transmittance for the coating plus substrate were observed in a number of other cases. Another difficulty is that of verifying that the bulk absorptance is negligible for all wavelengths of interest.

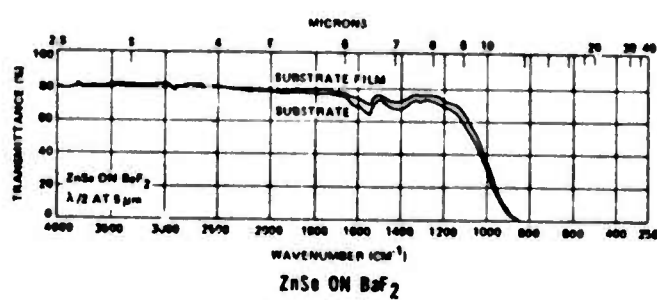


Fig. 5.1. ATR spectra of zinc selenide films on barium fluoride. From Ref. *14.

Even if the net film absorptance could be obtained, the relation to the value of A_f for normally incident transmission would have to be calculated for each coating-substrate pair at each wavelength. If total internal reflection occurs at the substrate-coating interface ($n_{\text{sub}}/n_{\text{coat}} > \sqrt{2}$ for the 45 degree ATR plates), as in the case of ThF_4 on ZnSe at $10.6 \mu\text{m}$ ($n_{\text{ZnSe}}/n_{\text{ThF}_4} = 1.79 > \sqrt{2}$), the electric field decays exponentially in the coating. On the other hand, if total internal reflection occurs at the coating-air interface, as in the cases of ZnS or As_2S_3 on ZnSe , the effective path length through the coating is not equal to the coating thickness ℓ_f . If $n_{\text{sub}} < \sqrt{2}$, then there will not be total internal reflection at either the interface or the surface, and the measured transmission through the ATR plate will be reduced as a result of transmission across the film-air interface (lack of total reflection). For example, the values of n_r for BaF_2 at 5.3 and $10.6 \mu\text{m}$ are $n_r = 1.45 > \sqrt{2}$ and $n_r = 1.395 < \sqrt{2}$, respectively. Thus, the lack of total internal reflection in 45 degree ATR plates of BaF_2 theoretically should cause a reduction in the observed transmittance beginning at some wavelength between 5.3 and $10.6 \mu\text{m}$. The effect has not been analyzed, but all nine spectra for BaF_2 samples in the Raytheon measurements^{*14} do show evidence of such reduction (Fig. 5.1), while the ZnSe -ATR-plate spectra do not show such reduction, as illustrated in Fig. 5.2. Increasing the internal-reflection angle from 45 to 50 degrees should eliminate the reduction resulting from nontotal reflection since all wavelengths for which $n_s > (\sin 50)^{-1} = 1.31$ are then totally reflected.

The difficulties in interpreting the ATR spectra possibly may be reduced by the suggested addition of the very thick film. Calibrating the coated ATR trace against the calorimetric result at one wavelength and verifying the trace value at other wavelengths also would be of interest.

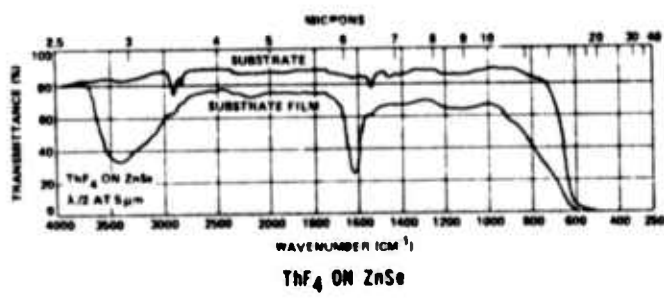


Fig. 5.2. ATR spectra of thorium tetrafluoride films on zinc selenide. From Ref. *14.

Consider the ATR-plate angle θ . The value of θ should be adjusted to give total internal reflectance at the outside surface of the coating (called the f-a interface) with "f" for film, "a" for air, and "s" for substrate). The required value of β can be determined by using the reflection-angle formula

$$n_1 \sin \theta_1 = n_2 \sin \theta_2 \quad (5.1)$$

and the total-internal-reflection equation

$$\sin \theta_{12} = n_2/n_1 \quad (5.2)$$

successively at the air-film and film-substrate interfaces. The ATR plate angle θ is equal to the angle of incidence of the ray in the substrate measured with respect to the normal of the film surface.

Using (5.1) and (5.2) it is easy to show that when the inequality

$$\theta > \theta_{sa} \equiv \sin^{-1}(1/n_s) \quad (5.3)$$

is satisfied, there will be total internal reflection either at the film-air interface or at the substrate-film interface. In other words, there is no wave transmitted into the air. The symbol θ_{sa} denotes the total internal reflection angle that would exist for a substrate-air interface.

For the case of $n_f > n_s$, total internal reflection is possible only at the film-air interface. For the case of $n_f < n_s$, total internal reflection is possible at either the film-air interface or the substrate-film interface. In order to have the maximum absorptance in the film the internal reflection should occur at the film-air interface. It will now be shown that this is the case when the inequality

$$\theta_{sa} < \theta < \theta_{sf} \equiv \sin^{-1}(n_f/n_s) , \quad \text{for } n_f < n_s \quad (5.4)$$

is satisfied. The condition for no internal reflection at the substrate-film interface is $\theta < \theta_{sf}$, which is the second part of the inequality in (5.4).

The other inequality $\theta_{sa} < \theta$ in (5.4) is the condition for overall total internal reflection, as already stated. This follows from $\sin\theta_{fa} = 1/n_f$ and $\sin\theta = (n_f/n_s) \sin\theta_{fa} = 1/n_s = \sin\theta_{sa}$.

As an example of the required value of θ consider a ZnSe ($n_f = 2.4$) coating on a KCl ($n_s = 1.46$) substrate. Since $n_s < n_f$, total internal reflection can occur only at the film-air interface, and the condition (5.3) for total internal reflection is $\theta > \theta_{sa} = \sin^{-1}(1/n_s) = 43.23^\circ$.

As a second example, for a KCl ($n_f = 1.46$) coating on a ZnSe ($n_s = 2.4$) substrate, the values of θ_{sa} and θ_{sf} are $\theta_{sa} = \sin^{-1}(1/n_s) = 25^\circ$ and $\theta_{sf} = \sin^{-1}(1.46/2.4) = 37^\circ$. Thus (5.4) gives $25^\circ \leq \theta \leq 37^\circ$. For a 45° ATR plate, the total internal reflection would occur at the substrate-film interface.

For the case of $n_f < n_s$, it is possible in principle to use an ATR plate with $\theta > \theta_{sf}$ and a relatively thick coating (so that $E \approx 0$ at the coating surface) in conjunction with other measurements to distinguish between absorption at the surface of the coating and at other positions in the structure.

The opinion has been expressed that ATR plate measurements are expensive. However, M. Hass²⁷ pointed out that this apparently is not true: "The major cost is in obtaining an ATR plate. We paid \$300.00 for a calcium fluoride ATR plate although one might be obtained for approximately \$50.00. The coating is something one will have to do anyway and a custom evaporation should run at least \$100.00. The special spectroscopic instrumentation for ATR is less than \$1,000.00

as it fits on a standard infrared spectrometer. As far as interpretation goes, you have a point that there are difficulties." At present (March 1976) Hass pointed out that he paid \$250 for the ATR attachment and is now paying \$85 each for ATR plates.

Laser-calorimeter measurements. Even a method of measuring the coating absorption at one wavelength or at several wavelengths would be useful in the absence of the frequency dependence of β_f , especially in characterizing available materials. It is known from bulk-sample measurements that much smaller values of β can be detected by laser calorimetry than by spectrometer measurements. Thus, laser-calorimeter measurements of A_f should be made. As already mentioned above in the discussion of attenuated-total-reflection plates, two calorimetric measurements, with the laser beam normally incident on the plate and with the laser beam following the ATR beam path, are desirable.

Measurement techniques. There are a number of calorimetric methods that could be useful at wavelengths at which sufficient power is available (typically of order of five watts or greater). Hass and coworkers³¹ have proposed and developed a thermal-diffusion-time method of distinguishing between surface and bulk absorption. A radiation-shielded thermocouple is placed sufficiently far from the illuminated surfaces that there is a significant delay between the time at which the laser is turned on and the heat that is generated at the surface diffuses to the thermocouple. The bulk-generated heat reaches the thermocouple much sooner since it has a shorter distance to diffuse. The ability to distinguish between bulk absorption and coating absorption (including the surface of the coating) makes this method attractive.

It may be possible to distinguish between absorption at the surface of a coating, absorption in the bulk of the film, and absorption at the film-substrate interface by comparing the absorption in films deposited simultaneously on highly transparent substrates and on highly reflecting metallic substrates. The electric field \underline{E} of normally incident radiation is very small at the surface of the metal and at the surfaces of a half-wavelength optical thickness of transparent dielectric deposited on a metallic substrate. But the electric field is great at the surfaces of coatings deposited on a transparent substrate and at the outside surface of a quarter-wavelength optical thickness of a transparent dielectric deposited on a metallic substrate. For the reflector, there is only the very small power flow corresponding to the small absorptance in the reflector. Thus $\text{Re } \underline{E} \times \underline{H}^* \approx 0$, and the traveling-wave component of field has $\underline{E} \approx 0$. The boundary condition for a perfect conductor is $\underline{E} = 0$, and the electric field outside of the conductor is a standing wave, with nodes at integral half wavelengths and maxima at quarter wavelengths from the nodes. The fact that the electric field is not zero at the surface of a half wave dielectric on a reflector for non-normal incidence could be used in measurement techniques.

Surface absorption is expected to be great for the film on the transparent substrate and for the quarter-wave film and less for the half-wave film. Interface absorption is expected to be great for the film on the transparent substrate and less for the films on the metallic substrate. Pore contamination or other absorption that extends throughout the films or well into the films should increase the absorptance of all three films.

This three-film technique could be especially useful in studying the increase in absorptance on exposure to the atmosphere, to humidity, or to other contaminants.

It may be possible to distinguish between adsorbed contaminants and those absorbed deeper in films.

The surface-electric-field effect could explain the following "anomalous" results: The value of $\beta_f < 1.2 \text{ cm}^{-1}$ for a ThF_4 film on molybdenum is lower than the bulk value of $\beta_b = 3.6 \text{ cm}^{-1}$. Also, the consistently obtainable values of $3-4 \text{ cm}^{-1}$ for ThF_4 on molybdenum are lower than the consistently obtainable values³³ of $7-10 \text{ cm}^{-1}$ for ThF_4 on KCl and ZnSe. This explanation on the basis of so little information is of course highly speculative.

Concerning these ThF_4 measurements, it is significant that the lowest value of $\beta_f < 1.2 \text{ cm}^{-1}$ measured for ThF_4 is well below the value $\beta_f = 10 \text{ cm}^{-1}$ which can be obtained consistently.³³ It would be of great significance if the conditions required to obtain $\beta_f < 1.2 \text{ cm}^{-1}$ were discovered and if such low values, or perhaps even lower values, could be obtained consistently. It appears that this approach of obtaining consistently low values of the absorption coefficient of ThF_4 is one of the most promising solutions to the coatings problem. An important reservation is that the low value of $\beta_f < 1.2 \text{ cm}^{-1}$, obtained for reflection-enhancing coatings on metallic substrates, may not be obtainable for coatings on window materials as a result of zero-electric-field surface effects. Thus, measurements of absorptance of ThF_4 films codeposited on metals and transparent substrates are among the more urgent present needs.

There are a number of other experiments that would be useful in determining the source of increased film absorption: The growth and study of self films should yield useful information about various film materials. Self films are such films as ZnSe films grown on ZnSe substrates. Measured values of $\beta_f = 1-2 \text{ cm}^{-1}$ for ZnSe

films are much greater than the bulk values $\beta_b \approx 10^{-4} \text{ cm}^{-1}$. Eliminating the material difference between the coating and substrate eliminated the mismatches between the thermal expansion coefficients and lattice constants, assuming that there is no difference between the film and bulk values. It should be possible to deposit thicker coating than for heterofilms (films grown on a substrate of material different from that of the film) since the increase in strain with increasing thickness in the latter often limits their thickness. The measurement of $\beta(\omega)$ is simpler in general for thick films, and the variable-film-thickness measurements discussed below may be possible for some self films which could not be grown sufficiently thick as heterofilms. Some sources of contamination, such as foreign molecules deposited along with film material, will be the same for self films and heterofilms, while other sources, such as diffusion of substrate ions into the film, will be different. Strain-dependent absorption should be different for the two film types. Comparison of self-film and heterofilm results can yield information on the effects of film morphology on absorption. It should be possible in some cases to deposit self films as epitaxial, polycrystalline, or amorphous films.

Studies of films deposited on substrates other than those of the final application could be useful. Such supersmooth substrates as fire-polished quartz would be useful, but the great absorptance of the substrate at $10.6 \mu\text{m}$ limits the studies to properties other than optical absorption at $10.6 \mu\text{m}$ and to values of β at shorter wavelengths. As pointed out above in the discussion of ATR plates, the value of β_f depends on the substrate material and condition in general. Harold Posen and coworkers¹¹ also emphasized that the results of deposits on substrates other than the desired design are often not transferable. There are implications in the literature that the intrinsic stress in films may tend to be independent of substrate

material. The point is that deposits on various substrates could be useful, but extreme care is required in interpreting the results.

Variable-film-thickness measurements should provide extremely useful information about coatings, including information about the region of the interface between the coating and the substrate. In some cases it may be possible to grow such thick films, say even 100 μm thick, that a significant increase in absorption would be obtained, thus making the measurement of absorptance easier. The substrate and interface region could be removed from thick films.

Absorption at the region of the interface between the coating and the substrate also could possibly be detected by comparing the absorptance of codeposited films of various thicknesses. Also, the relative values of the absorptance of two equally thick films, one of which is deposited continuously and the other which is deposited as a series of thin layers (of the same material) could give useful information on interface absorption.

Depth profiling by removing successive layers of material, which has been useful in such other fields as ion implantation of semiconductors, also has been used in antireflection-coating studies. Auger and other surface analyses can be made after the removal of each layer. Ion sputtering has been used in conjunction with surface measurements.

It is well known that films often deteriorate on removal from the vacuum-deposition chamber and that absorptance sometimes increases after exposure to the atmosphere. Since it is possible that the absorptance could increase on removal of the film from the deposition chamber, in situ measurements of absorptance would be useful. Such in situ measurements are planned at China Lake.³⁴

M. Hass²⁷ commented that "--- making calorimetric measurement in situ at 10.6 μm doesn't hit me as too big of a problem. Here one could use windows to go into the evaporator and the vacuum chamber should make an ideal adiabatic vacuum calorimeter. A small CO₂ laser should be ideal. Again this is not something to be done lightly, but might be expected of research problems on coatings."

Since in situ measurements of $\beta(\omega)$ are not simple, an alternative would be useful. One possibility would be to heat the sample prior to removal from the deposition chamber and maintain the sample at the elevated temperature until the measurements are completed. There are several disadvantages to this method. First, there may be some contamination even at an elevated temperature. Second, absorptances usually are temperature dependent; thus, comparison of absorptance on removal (at the elevated temperature) with that after exposure to the atmosphere (at room temperature) is complicated by the temperature difference.

Sievers suggested²⁵ laser calorimeter measurements at low temperature, where the heat capacity of the sample is small and temperature rise is correspondingly large. The temperature dependence of the absorption coefficient must be taken into account of course.

Sparks suggested³⁵ measuring the temperature rise in calorimeter experiments by observing the optical distortion of second low-power laser beam.

The wedge-angle technique of Burdick and Rehn³² distinguishes between surface and bulk absorption by using the fact that light traversing the thick part of a wedge encounters more of the bulk material than does light traversing the thin part of the wedge. Steady-state ac methods of measuring thermal conductivity could be adapted to the measurement of coating absorptance.

Other methods of measuring absorptance. The method of measuring $\beta(\omega)$ that has the greatest potential is emissivity spectroscopy. However, the measurements are difficult, and the potential of this method has not been achieved in measurements of bulk absorption. The Xonics emissivity cavity should make the measurements much easier. The difficulty from the point of view of the coatings program is that an emissivity spectrometer development program would be required before the method could be applied to coatings with confidence.

Like emissivity measurements, ellipsometry measurements show promise of high sensitivity, but have been of limited use as a result of experimental difficulties. Other methods of measuring absorptance include surface acoustic-wave velocity measurements,³⁶ optical-wave-guide measurements, Perkin-Elmer alpha-phone measurements (measuring the pressure change in a cavity that is in mechanical and thermal contact with, but is optically insulated from, the laser-irradiated sample). All of these methods have experienced great technical problems.

Other measurements. Humidity tests are important since the stability and the absorptance of films are sensitive to moisture. Recall from Sec. IV that there is a possibility that it may be necessary to use a glassy film, or perhaps an amorphous or a polymer film as the outside film of coatings in order to avoid high infrared absorption from water contamination of film pores. An often used humidity test is storage at 48°C, relative humidity 95 percent, 24 or 48 hr. Immersion in water, often salt water, is a test frequently applied. Well prepared films of MgF₂, many oxide films, and combinations of these films withstand the humidity and immersion tests.

The military-specification tests that are usually performed should be performed routinely in the near-term¹ program. These tests include adhesion and abrasion in addition to humidity.

Since film contamination is a major possible problem, a residual-gas analyzer, which can detect partial pressures of 10^{-10} torr ($\sim 10^{-8}$ Pa) would be useful. Residual-gas analyzers already are in use in high-power infrared coatings programs. Atmospheric contamination of surfaces has been studied by measuring the partial pressures of contaminants on surfaces that had been exposed to the atmosphere. Film density measurements^{*2} would be extremely useful in view of the great absorption by porous films. Electrical-conductivity measurements would give information on free-carrier absorption. Other measurements, including those listed at the beginning of this section, will be discussed in future reports as the need arises.

VI. OTHER PROBLEMS

Problems other than optical absorption in films, measurements, laser heating, laser damage, and material selection are considered in the present section. Recommendations for the near-term program¹ from this section are as follows:

- Only vacuum evaporation deposition should be used in the near-term program.
- The entire vacuum system should be baked at high temperature for a long time in order to reduce the desorption and diffusion contributions to the residual gas, to clean the substrates and starting materials, and to obtain stable films.
- The purity and preparation of the starting materials is one of the most important aspects of the near-term program. Only dense single-crystal low-absorptance starting materials should be used. Impurity concentrations in the range of parts per million can cause difficulty.
- Only state-of-the-art substrates should be used since the surface absorptance of the substrate can give rise to A_f greater than 10^{-4} and the substrate can strongly affect the film properties.
- Only ultrahigh-vacuum deposition should be used in the near-term program, even though it is hoped that this requirement will be relaxed in the production of large field-use units.

Other results of this section include the following:

- Glassy films such as arsenic trisulfide offer the greatest potential for protecting underlying materials from moisture attack.
- In a subsequent report, the possibility of using polymer film for protecting substrates and antireflection layers from moisture attack and of reducing adsorption of water on the surface of antireflection layers will be considered. In addition to the technical problem of obtaining pin-hole-free films, there are potential basic problems of high moisture-vapor transmission through the films and of high infrared absorptance by the films.
- It is not likely that polycrystalline films can protect large areas of alkali halides from moisture attack.
- It is probable, though not yet certain, that polycrystalline films can be sufficiently dense and sufficiently hygroscopic to allow $A_f = 10^{-4}$ to be attained in carefully prepared films.
- Priority of future research on amorphous semiconductor films is low since the likelihood of obtaining β_f less than 0.5 cm^{-1} is small.
- The stress in a film is determined by the thermal-expansion-coefficient mismatch, by contamination, and by an intrinsic contribution. The former should be calculated for all new films.
- Radioactivity and toxicity should be considered in selecting film materials.

The problems considered in this section include the following:

- deposition method
- baking requirements
- starting-material preparation
- substrate preparation
- ultrahigh vacuum requirement
- thin protective coating
- adhesion and stress.

Deposition method. Although there are a number of deposition techniques that are promising, previous difficulties in obtaining stable, low absorptance films by methods other than vacuum evaporation deposition strongly suggest that only vacuum evaporation deposition be used in the near-term program.¹ Unless the ultraclean, vacuum evaporation depositions fail to produce acceptable coatings, depositions by other methods should be considered as studies of advanced deposition methods, not as part of the near-term program. Development of other deposition methods would be of interest in other, longer-term programs.

Vacuum evaporation deposition has been the most successful method of preparing films in general. Ritter^{*2} states that, "among the various production methods vacuum evaporation has especially shown remarkable progress with respect to size and efficiency of coating unit, reliability of the process, and the control of film thickness and uniformity. Despite the enormous progress that has taken place in reactive and rf sputtering, only very few optical applications of sputtered films are known. This may be due to the small area to be coated in sputtering systems (except some special arrangements), to the relatively low sputter rates, and to the

difficulties in thickness monitoring if very accurate monitoring is required." Such accurate monitoring is of course required in the multi-layer antireflection coatings.

All high-quality low-absorptance high-power infrared coatings to date have been deposited by the vacuum evaporation process. It is suggested that vacuum evaporation deposition be used in the near-term program. There are of course many other deposition methods including reactive and rf sputtering, chemical vapor deposition, deposition from organic solution, ion plating (a combination of sputtering and evaporation process), and gas discharge deposition.

There have been some successes in using other deposition methods. Harold Posen¹¹ pointed out that his group demonstrated that sputtered coatings can have a higher laser damage threshold than evaporated coatings. Other film growth methods would be of interest in programs other than the near-term program.

Baking requirements. Baking of the system including the substrate, the starting material, and the entire vacuum system in high temperature and high vacuum is required in order to reduce the desorption and diffusion contributions to the residual gas and to clean the substrates and starting materials. Baking may be required also to obtain stable films.

The required temperature and time of the bake varies from one film substrate combination to another. In one case, 600°C for one day was required to prevent a film from leaving the substrate on removal from the vacuum system.⁴ The baking temperature will in general be different from the substrate temperature during the deposition.

In other numerous cases films will adhere to substrates without these special precautions. However, in order to obtain low values of absorptance and in view of

the known sensitivity of absorptance to trace amounts of impurities, extreme care must be exercised in deposition, substrate preparation, and selection and purification of starting materials. Such precautions are especially important in the near-term program when the sources of the film problems are being sought and when new film materials are being tried. In some cases the precautions are necessary in order to obtain stable films. Films which could not be deposited successfully in original tries have been entirely satisfactory when proper deposition care was exercised.

H. Posen¹¹ pointed out important restrictions on baking substrates: "We cannot arbitrarily bake substrates either before, during, or after deposition unless one carefully considers the problems of thermally activated grain growth in the substrate, decomposition of the depositing layer, etc." These potential problems must be carefully considered when determining the baking conditions.

Stierwalt and Hass^{*37} found that baking KCl at 250°C for 60 hours at atmospheric pressure reduced the surface absorptance as discussed below in the present section.

Starting materials. The purity and preparation of the starting materials is one of the most important aspects of the near-term program. Only dense, single-crystal, low-absorptance starting materials should be used. The following quotation from Ritter^{*2} describes the problem well. "The preparation of the material to be evaporated is of considerable importance for the deposition of high quality optical coatings. Crucial properties are purity, gas content, and grain size. It is highly recommended that one uses vacuum sintered and outgassed materials or even pieces of dense single crystals to avoid gas outbursts and spattering during the

evaporation process. Powders are normally not suitable since they have too much adsorbed gas which is desorbed during heating and leads to pressure rise and spattering of materials, even to jumping out of the boat. Some fluorides tend to form oxide or carbonate layers on the surface. These layers may impede the free evaporation and cause sudden spattering of the evaporant." Other precautions such as particle filters and great distances to the substrate also may be required.

Braunstein and coworkers^{*10} found that increasing the purity of thorium tetrafluoride and cadmium telluride used in multilayer coatings reduced the absorptance of their coatings from 5×10^{-3} to 1.2×10^{-3} . The authors anticipated that further improving the starting material purity would result in further reductions of the film absorptance. They found that rigorous control of starting materials used for the coatings and the deposition techniques were essential for the preparation of low-absorptance coatings. Commercially available arsenic trisulfide was not satisfactory for high-quality films.

Concerning the purity of the starting materials, H. Posen states: "I am not convinced that a major source of film absorptance are molecular contaminants other than the OH radical. We find that deposition under clean systems ensures radical free deposits. When we observe the OH bands by careful spectroscopy we find that the contaminant is an integral part of the deposited material rather than occluded water pickup. A part of the problem is the purification of the coating material. Both our laboratory and the Hughes groups using residual gas analyzers during the deposition process have monitored this phenomena."

Impurity concentrations in the range of parts per million can cause difficulty. For a strongly absorbing impurity with $\beta = 10^5 \text{ cm}^{-1}$ at an impurity peak, five parts per million of the impurity in the film gives $\beta = 0.5 \text{ cm}^{-1}$. For water at $10.6 \mu\text{m}$,

250 parts per million in the film gives $\beta = 0.5 \text{ cm}^{-1}$. The impurity level in the starting material can of course be quite different from that in the film.

Substrate preparation. Only substrates with state-of-the-art surface preparation should be used. Surface preparation is important because surface absorptance as great as 10^{-2} is possible and the substrate can greatly affect the film quality. The problems of substrate preparation have received considerable attention in the last four years. There are many prescriptions for preparing various substrates and new techniques are still being developed. The excerpts in Sec. XIII contain several examples. Before preparing a given substrate the recent literature should be checked.

In view of the importance of the substrate surface absorptance a method of avoiding contamination (in contrast to removing contaminants) until the film is applied would be extremely useful. Unfortunately, avoiding contamination would be extremely difficult. The freshly grown crystal could be maintained at an elevated temperature until it is cut and polished in a clean-room environment at near zero relative humidity. The sample could then be maintained at an elevated temperature in a low humidity environment until the coating is applied. Even with these precautions it would be surprising if the film were not contaminated, especially during the cutting and polishing processes.

The process of baking in the ultrahigh vacuum will hopefully remove some of the substrate contaminants. Stierwalt and Hass^{*37} found that baking a KCl sample at 250 C for 60 hours reduced the absorption coefficient at an absorption line at $9.5 \mu\text{m}$ from approximately $2.5 \times 10^{-4} \text{ cm}^{-1}$ to approximately $1.4 \times 10^{-4} \text{ cm}^{-1}$. This experiment is significant first because it shows that baking can reduce surface

absorption and second because it showed that the surface absorption was not entirely removed. It is not clear whether extending the baking time and reducing the pressure would be effective in removing the remaining absorption. (The experiment further illustrated that after exposure to air for 30 hours the absorption coefficient increased to its original value of approximately $2.5 \times 10^{-4} \text{ cm}^{-1}$.)

Ultrahigh vacuum. According to the "Glossary of Terms Used in Vacuum Technology" issued by the American Vacuum Society Committee on Standards, Pergamon Press, New York, 1958, various degrees of vacuum are:

low vacuum	$10^5 - 3.3 \times 10^3 \text{ Pa}$	(760-25 torr)
medium vacuum	$3.3 \times 10^3 - 0.13 \text{ Pa}$	(25- 10^{-3} torr)
high vacuum	$0.13 - 1.3 \times 10^{-4} \text{ Pa}$	($10^{-3} - 10^{-6}$ torr)
very high vacuum	$1.3 \times 10^{-4} - 1.3 \times 10^{-7} \text{ Pa}$	($10^{-6} - 10^{-9}$ torr)
ultrahigh vacuum	less than $1.3 \times 10^{-7} \text{ Pa}$	(less than 10^{-9} torr).

"High vacuum" also is used in the broader sense to denote pressure less than 10^{-3} torr. Recall that 1 MPa is approximately equal to 10 atm, or, precisely, one normal atmosphere is equal to 760 torr or $1.01325 \times 10^5 \text{ Pa}$.

It is recommended that ultrahigh-vacuum deposition be used in the near-term program.¹ Even though ultrahigh vacuum systems are expensive to construct and operate they should be used since contamination of films has been identified (Sec. V) as a major problem in high-power films. Even though there are cases in which the film quality is reported to be insensitive to substantial changes in the deposition pressure, ultrahigh vacuum systems should be used in the near-term program.¹ A lowering of the absorptance below 10^{-2} would not have been detected in most previous film studies. The reason for using ultrahigh vacuum systems is that the

absorptance in coatings currently is the factor that limits the performance of some high-power laser systems, and every effort must be made to reduce the absorptance. The relaxation of the ultrahigh-vacuum requirement after satisfactory laboratory films have been obtained is discussed below.

Self cleaning. Since there is evidence in the literature that the deposition process itself can clean the system, it would be worthwhile to run the deposition process with the sample shuttered for a period of time at the beginning of the deposition. There are also a number of indications in the literature that film quality tends to increase on successive depositions of the same film material.

Production of coatings for large windows. The recommendations for the ultraclean deposition conditions are intended for the near-term program in which the source of the additional film absorption is being studied and eliminated. It is hoped and anticipated that once satisfactory laboratory films are prepared the ultraclean deposition requirements can be relaxed. Indeed, the difficulty in manufacturing large components under the ultraclean deposition conditions is illustrated by the following comments by Leonard P. Mott of the Optical Coating Laboratory, Inc.^{37a} in response to the preliminary version of this report: "I agree with your conclusion that the use of an ultrahigh vacuum system for coating experiments will remove many of the sources of film contamination that operate during the deposition process; however, I believe that experiments should be carried out on a dual basis using both conventional and ultrahigh vacuum chambers because I anticipate that the coating of full sized flight hardware will have to be done in a conventional type of chamber employing diffusion pumps. With the dual approach, all developments in the ultrahigh vacuum chamber could be immediately related to production

capabilities in conventional chambers. This approach may also uncover techniques for achieving acceptable coating properties in currently available coating equipment. Adequate chamber bake out, for example, can vastly improve the residual gas content of conventional as well as ultrahigh vacuum systems. Obviously, these dual experiments must be performed at the same facility and by the same investigators so that the results can be meaningfully compared."

"It is important to consider the type of coating apparatus that will be required for the application of the research developments. Our experience at OCLI with the coating of the APT window illustrates my concern. Although a 25 inch window can be coated in a chamber with interior dimensions that are just large enough to accommodate it, we found that in order to achieve the uniformity in thickness and optical properties that were required, we had to use coating equipment with interior dimensions nearly three times the size of the window. Availability of suitable ultrahigh vacuum equipment of this size may not occur for quite some time."

The point to be made is the difficulty of large ultrahigh vacuum systems. Concerning the dual depositions, one possibility is to use dual depositions from the beginning of the program. Another possibility would be to first develop the laboratory films in the ultraclean deposition system and then use dual depositions in developing the production process. The latter approach may save time and money.

Thin protective coatings: glassy, polymer, and amorphous films. Protective coatings for such hygroscopic window materials as alkali halides have been discussed in the literature for some time. It still is not known if moisture protection and low infrared absorptance can be obtained. At the present time glassy films such as arsenic trisulfide offer the greatest promise of affording moisture protection. However, polymer films have not been ruled out and will be considered further in a subsequent report.

In view of the importance of the adsorption and pore contamination even in nonhygroscopic materials, it may become extremely important to develop a thin protective layer to seal the surface and reduce adsorption. Since water adsorption is a major contaminant, a hydrophobic coating would be desirable. The hydrophobic coating could be very thin, which will mean approximately 50 to 100 nm in the following discussion. The coating could be applied over an antireflection coating, or it could be the outside layer of an antireflection coating.

It will be shown that information in the literature suggests the following results: (a) It is not likely that polycrystalline films can protect large areas of alkali halides from moisture attack. (b) It is possible though not certain that polycrystalline films can be sufficiently dense and sufficiently hydrophobic to allow $A_f = 10^{-4}$ to be attained in carefully prepared films. (c) Very thin glassy films¹ were found not to protect alkali halides. (d) Thick glassy films, say 1 μm thick on well polished substrates, did protect alkali halides. However, on long exposure to humidity, moisture attack that started at the edges of the sample eventually covered the entire substrate under the coating. (e) Polymer films will be considered further in a subsequent report to determine the possibility of their providing sufficient moisture protection in spite of the known great moisture-vapor transmission rates and to determine the possibility of reducing their normally great optical absorption to acceptably low values. (f) The possibility of using very thin¹ polymer films as hydrophobic outside layers over antireflection coatings to reduce adsorption on the surface will also be investigated. (g) Priority of future research on amorphous semiconductors is low since the likelihood of obtaining β_f less than 0.5 cm^{-1} is small. (h) The abrasion resistance of protective films will be considered in subsequent reports.

First consider polycrystalline coatings. Young's observation^{*38} which has been confirmed by other investigators, that polycrystalline coatings could not prevent moisture attack of alkali halides has the obvious important consequence that other types of coating materials will be required to afford moisture protection. In addition, this observation implies that the polycrystalline films probably contain openings and that water goes through the openings. Thus even for the case of substrates that are not attacked by water the observation raises the question of whether or not polycrystalline films can be made sufficiently dense to keep the absorbed contaminants from raising A_f above 10^{-4} , since this value of A_f corresponds to only 5×10^{-4} fractional content of openings. Fortunately there is some evidence that suggests that polycrystalline films may have $A_f \approx 10^{-4}$. Raytheon measurements^{*14} on ZnS films deposited on a ZnSe attenuated-total-reflection (ATR) plate by Optical Coating Laboratories and by Spectra Physics gave $\beta_f = 1.00 \pm 0.85 \text{ cm}^{-1}$ for one film and $\beta_f < 1.39 \text{ cm}^{-1}$ (detectable limit) for another. For film thickness $z_f = 5.25 \times 10^{-4}/(2)(2.16) = 1.2 \mu\text{m}$, the corresponding values of absorptance are $A_f = 1.2 \times 10^{-4}$ and $A_f < 1.7 \times 10^{-4}$. The point is that values of A_f near 10^{-4} have been measured for polycrystalline films. It is still conceivable that exposure to humidity or other contaminants could cause an increase in these values of A_f .

An additional point of interest on the measurement of A_f for these ZnS films is that ATR plate measurements for a film with $A_f = 1.2 \times 10^{-4} \pm 1.0 \times 10^{-4}$ are consistent with the calorimetric value, but the accuracy of the comparison is only a factor of approximately two to ten. The value of A_f is obtained from the ATR trace as follows. It is assumed that there are 25 reflections from the coating (only one surface coated and an estimated 50 reflections^{*15}) and that the absorptance for an internal reflection at approximately 45 degrees ($n_{\text{ZnS}} \approx n_{\text{ZnSe}}$, roughly) with

two passes through the film is $2\sqrt{2}$ times that for normally incident absorptance. These gross approximations could easily give a factor of two to four error. The reduction in transmittance (of the coated half of the plate with respect to the uncoated half) at 750, 800, and 900 cm^{-1} are approximately four, three, and one percent, respectively. At 943 cm^{-1} ($10.6 \mu\text{m}$), the value, which is too small to be read from the traces, is assumed to be 0.5 percent based on these neighboring values. Thus it is estimated that the ATR-plate spectra should correspond to a calorimetric value of $A_f \approx 5 \times 10^{-3} / 2\sqrt{T} 25 = 7.1 \times 10^{-5}$. The agreement with the calorimetric value $A_f = 1.2 \times 10^{-4} \pm 1.0 \times 10^{-4}$ is well within the expected accuracy of the ATR-value estimate.

Next consider glassy films. Young^{*38} found that very thin glassy films did not protect alkali halides from moisture attack. Thick films, typically $1 \mu\text{m}$ thick, on well polished substrates did protect the alkali halides. The film thickness had to be somewhat greater than the size of the largest polishing scratches on the substrate. For example, Young^{*38} found that on NaCl surfaces with $0.5 \mu\text{m}$ scratches, $0.92 \mu\text{m}$ of As_2S_3 was required, and for $1.5 \mu\text{m}$ scratches, $1.85 \mu\text{m}$ of As_2S_3 was required. Even for the films that were protected from humidity, on long exposure, moisture attack that started at the edges of the sample eventually covered the entire substrate under the coating. In spite of this difficulty it appears that glassy films offer the greatest promise for protection of coatings and substrates from moisture attack.

It is of interest that the only $10.6 \mu\text{m}$ coating material for which $\beta_f \approx \beta_b$ is the glassy material As_2S_3 , for which $\beta_f \approx \beta_b \approx 0.8 \text{ cm}^{-1}$. (It is conceivable that ThF_4 , which is X-ray amorphous and has the appearance of glass when broken, may be another example of a material with $\beta_f \approx \beta_b$. However, a reliable value

of the intrinsic value of D is not known.) It is possible that the relatively pore-free glassy structure of As_2S_3 does not absorb water or other contaminants.

Our study of polymer coatings is not yet completed, and even additional literature search is required. The results to date are as follows: There are two potential uses of polymer films that could be extremely important. First, in view of the importance of water adsorption it would be useful to determine if satisfactory hydrophobic polymer films could be obtained. A number of polymers are known to be hydrophobic, but it is not known if polymer coatings would prevent such small adsorption as two molecular layers of water. The hydrophobic films could be extremely thin, possibly only 10-100 nm thick. They could be applied as a protective coating over an antireflection coating stack. The hydrophobic film possibly need not be pin-hole free since it only prevents adsorption, not penetration.

The second use of polymer films would be to prevent moisture penetration of substrates or underlying layers of antireflection coatings. In this case the polymer film could be one of the antireflection coating layers or possibly it could be a thin overcoating of an antireflection stack.

The main concern about polymer coatings in the past was that of obtaining pin-hole-free coatings in order to prevent moisture attack of the underlying antireflection coating or substrate. This is indeed important since it is known that moisture will attack underlying substrates through pin holes in polymer films. Unfortunately, in addition to this technical problem there are two fundamental properties of polymer films that possibly could prevent their use as moisture protection films.

First, the rate at which moisture vapor permeates through a polymer is one of the routinely measured properties of polymers. Formally using the measured

values of this moisture vapor transmission rate through unsupported (i.e., not deposited on substrates) polymer films suggests that pin-hole free polymer films would not be useful in preventing water from penetrating through the polymer to a substrate or an antireflection coating. However, the moisture vapor transmission rate could be drastically different for a polymer deposited on a solid from that of an unsupported polymer film. The results from the literature and from workers in the field are conflicting, in some cases suggesting that moisture vapor protection is possible and in other cases not. We suspect that inhibition of the moisture vapor transmission at the interface of the polymer and the substrate is important if polymers do indeed provide sufficient moisture vapor protection. In considering the problem of moisture vapor transmission through polymer coatings, it must be recalled that these coatings are extremely thin and that only two monolayers of water transmitted through the film could cause unacceptably great optical absorption. In addition to addressing these problems in a subsequent report, it will be shown that according to available data absorption of water by plastic films (as opposed to water vapor transmission through the films) probably will be tolerable at 2.8, 3.9, 5.3, and 10.6 μm .

The second fundamental problem with polymer coatings is that the published infrared spectra of all polymers that we have found to date show values of absorptance that are too great to allow $A_f = 10^{-4}$ for either antireflection coatings or very thin protective coatings. Two typical spectra are shown in Fig. 6.1. The possibility of obtaining sufficiently low values of absorptance at the various laser frequencies of interest by selecting the proper polymer and by eliminating contamination in the polymer coatings will be considered in subsequent reports.

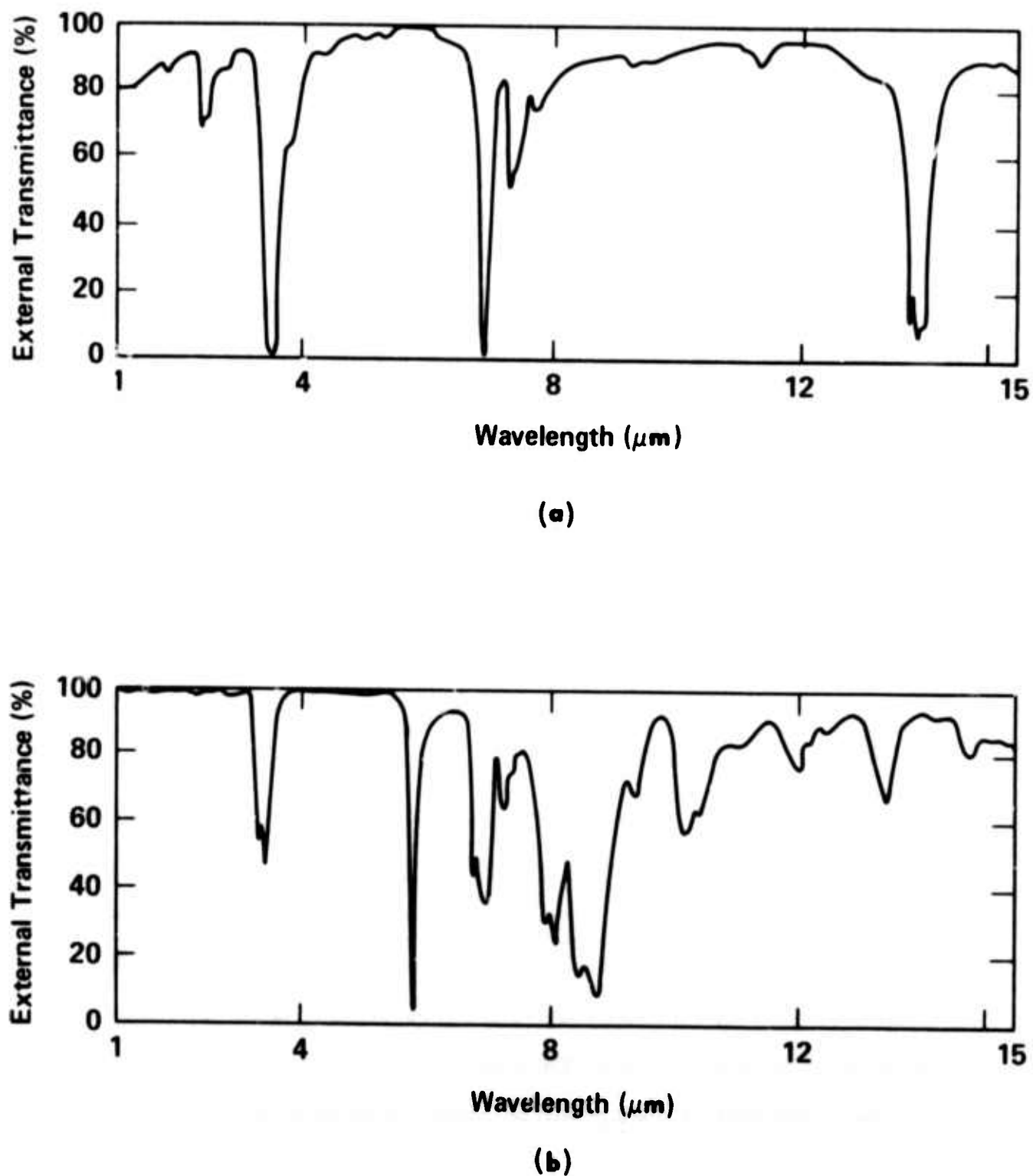


Fig. 6.1. Spectral transmittance of: (a) polyethylene, 0.1 mm thick, and (b) plexiglas, 0.2 mm thick. From Ref. 30.

Next consider amorphous semiconductors. These materials were tried in the past since it was believed that the amorphous structure was less penetrable to moisture than crystalline structures. Priority of future research on amorphous semiconductors is low since the likelihood of obtaining $\beta_f < 0.5 \text{ cm}^{-1}$ is small. Even large bandgap materials exhibit too great an absorption when deposited as amorphous films. In the context of coatings, a distinction will be drawn between amorphous and glassy materials, the latter of which have shown sufficiently small values of β_b . In an amorphous solid such as amorphous germanium, the arrangement of nearest-neighbor ions is subject to several constraints and departs only slightly from the disposition in a perfect lattice. This is a direct consequence of the fact that chemical bonds especially covalent ones are relatively rigid both in direction and length and their distortion beyond certain limits requires excessive energy. On the other hand, glasses have a multiplicity of flexible bonds and as a result remain vitreous over a wide range of temperature. Glasses have the ability to form more than one type of bond. Both glasses and amorphous solids lack long range order in the position of the ions. It should be mentioned that there are a number of materials with well known crystalline structures in the bulk form that can be deposited as amorphous or glassy films. Examples from Table I of Ritter^{*2} (included in Sec. XIII) are ThF_4 , Al_2O_3 , As_2S_3 , As_2Se_3 , TiO_2 , Si, and Ge.

Other protection considerations. Adsorption of contaminants on the surface of a coating conceivably may not limit the operation of some systems since it may be possible to remove surface contamination prior to use. There is some evidence in the literature that surfaces may be cleaned by the laser beam itself at intensities below the intrinsic damage threshold.³⁹ In some cases it may be possible to maintain the window at an elevated temperature to reduce surface adsorptance, as is a common practice in spectrometers.

Another possibility of avoiding pore contamination is intentionally filling the pores with a nonabsorbing material. Anticipated difficulties are finding a non-absorbing material that would fill and remain in the pores and avoiding contamination before the nonabsorbing material is applied. If absorptance measurements made before removal of the films from deposition chambers do not show sufficiently low absorptance then pore filling would not be expected to be effective.

Film stability; stress and adhesion. Chemical stability and good mechanical stability of a film, that is the resistance to crazing, cracking, clouding, and removal from the substrate, are obviously important requirements of a coating. From the practical point of view of obtaining stable films, the most important result from the literature is that the recommended ultraclean deposition conditions should improve the film stability as well as reducing the optical absorptance.

Specific results from the literature include the following: The packing density of a film is not only important from the point of view of its optical behavior but also of its mechanical and chemical stability.^{*2} This is an important fact since there may be temptation to first obtain stable films, then reduce the absorptance. The stress in a film and its adhesion to the substrate are important factors that determine mechanical stability. Substrate preparation is extremely important in obtaining good adhesion of a film to a substrate. Ritter states that, "Adhesion of zinc selenide and cryolite was found to be 2.9×10^6 psi and 6.4×10^6 psi without a glow discharge cleaning. In the case of zinc selenide the adhesion could be improved to 5.3×10^6 psi by a 20-minute glow discharge whereas in the case of cryolite the adhesion increased only to 6.8×10^6 psi. Adhesion depends strongly on the preparation and cleanliness of the surface and the chemical composition of the surface and electrostatic charging effects have to be taken into consideration."

Sec. Vi

The stress in a thin film is believed to consist of three components, one from the mismatch of the thermal expansion coefficient of the film and the substrate, one from contaminants in the film, and one from an intrinsic contribution. The contribution from the mismatch of the thermal expansion coefficient is well understood, and very simple calculations give the observed values of this component of stress. For any new proposed film-substrate combination this thermal-expansion mismatch component of stress should be calculated in order to determine if the film can withstand this stress. Examples are given below.

Film contamination typically leads to compressive stresses. Campbell^{39a} states that, "in impure films in which oxygen and other materials are incorporated into the structure during growth, the resultant stresses are usually sufficiently high to overshadow any of the "pure film" effects. The stresses are then usually compressive, at least in the initial stages of growth and provided that the reacting species migrate through growing film to the interface. Compressive stresses are observed in thermally grown, anodized, and certain sputtered and evaporated films. If the ion migration takes place from the interface to the film surface tensile stresses will be observed." Of great importance for the power of stress are the packing density and the water vapor absorption. During exposure to atmosphere very often a stress relief takes place.^{*2}

The intrinsic contribution to the stress in a film is not well understood. It is not possible to predict in advance what the stress will be in a new film material on a given substrate. However, for film materials that have been previously deposited it is possible to predict with a fair degree of success what the stress will be for a given film-substrate combination or for a particular multilayer coating on a given substrate.

In spite of the fact that either the intrinsic or the "impurity" contributions to the stress usually dominates the expansion-coefficient-mismatch contribution, the latter can cause mechanical failure of films of current interest. Thus, the thermal stress should be calculated before depositing any new coatings. The strain ϵ is determined by the relation $\epsilon = (\alpha_f - \alpha_s) \Delta T$, where α_f and α_s are the linear thermal expansion coefficients of the film and substrate, respectively, and ΔT is the difference between the deposition temperature and the temperature at which the measurement is made. For simplicity it is assumed that the stress σ is related to the strain ϵ by the Young's modulus E , that is, $\sigma = E\epsilon$. This is an approximation since the Young's modulus is appropriate for a tensile stress acting in one direction on a sample with free sides. This is in contrast to the film case in which the stress is exerted by the substrate. Combining these two relations gives

$$\sigma = (\alpha_f - \alpha_s) E \Delta T \quad . \quad (6.1)$$

Values of the linear thermal expansion coefficient α and the Young's modulus E are listed in Table 6.1. Notable features of the table are first that the values of the Young's modulus do not vary greatly from material to material, with the greatest value of 50×10^6 psi for sapphire being a factor of 12 greater than the least value of 4.3×10^6 psi for KC1. Second, the ranges of values of the linear thermal expansion coefficient α for various classes of materials in the table are as follows:

Semiconductors, including IV, III-V, and II-V: $\alpha = 4-8 \times 10^{-6} \text{ K}^{-1}$

Oxides: $\alpha = 5-25 \times 10^{-6} \text{ K}^{-1}$

Alkaline earth fluorides: $\alpha = 13-20 \times 10^{-6} \text{ K}^{-1}$

Sec. VI

Table 6.1. Linear Coefficient of Thermal Expansion and Young's Modulus

Material	Coefficient of Thermal Expansion α $10^{-6}/\text{C}^\circ$	Average Temperature or Temperature Range ($^\circ\text{C}$)	Young's Modulus E 10^6 psi
SiO_2	0.5	20 to 900	
Invar	0.9	20	
Si	4.2	25	19.0
CdS	4.2	27 to 70	
InSb	4.9	20 to 60	
InAs	5.3	-	
Ge	5.5 to 6.1	25	14.9
GaAs	5.7	-	12.3
CdTe	5.9	50	5.3
$\text{MgO} \cdot 3.5 \text{Al}_2\text{O}_3$	5.9	40	
Al_2O_3	6.7 ^d 5.0 ^e	50 50	50
ZnSe	7.0		10.3
SiO_2	7.97 ^d 13.37 ^e	0 to 80 0 to 80	
Borosilicate crown glass	9	22 to 498	
TiO_2	9.19 ^d 7.14 ^e	40 40	
SrTiO_3	9.4	-	
NaNO_3	12 ^d 11 ^e	50 50	
MgF_2	13.7		24.5
MgO	13.8	20 to 1000	36.1

Table 6.1. Linear Coefficient of Thermal Expansion and Young's Modulus (Cont'd)

Material	Coefficient of Thermal Expansion α $10^{-6}/\text{C}^\circ$	Average Temperature or Temperature Range ($^\circ\text{C}$)	Young's Modulus 10^6 psi
Cu	14.09	-191 to 16	
Tl 1173 glass	15.0		3.1
SrF ₂	15.8		14.7
Te	16.75	40	
BaTiO ₃	19 ^a 6.2 ^{b,d} 15.7 ^{b,e}	10 to 70 ^a 4 to 20 ^b 4 to 20 ^b	
CaF ₂	19.7	20 to 60	11.0
BaF ₂	20.3		7.7
As ₂ S ₃	24.6	33 to 165	
CaCO ₃	25 ^d -5.8 ^e	0 0	
AgCl	30	20 to 60	
Se	34 ^c	-	
NaF	36	Room	
KCl	36	20 to 60	4.3
LiF	37	0 to 100	
KI	42.6	40	
KBr	43	20 to 60	
NaCl	44	-50 to 200	5.8
CsBr	47.9	20 to 50	

Sec. VI

Table 6.1. Linear Coefficient of Thermal Expansion and Young's Modulus (Cont'd)

Material	Coefficient of Thermal Expansion α $10^{-6}/\text{C}^\circ$	Average Temperature or Temperature Range ($^\circ\text{C}$)	Young's Modulus 10^6 psi
KRS-6	50	20 to 100	
CsI	50	25 to 50	
TlBr	51	20 to 60	
TlCl	53	20 to 60	
KRS-5	58	20 to 100	

- a Ceramic
- b Single crystal
- c Estimated
- d Thermal expansion measured parallel to c axis
- e Thermal expansion measured perpendicular to c axis
- Value not indicated

Chalcogenide glasses: $\alpha = 15-25 \times 10^{-6} \text{ K}^{-1}$

Alkali halides: $\alpha = 30-60 \times 10^{-6} \text{ K}^{-1}$.

Fused silica (SiO_2) has a very small value of $\alpha = 0.5 \times 10^{-6} \text{ K}^{-1}$. Van Uitert and coworkers⁴⁰ recently found that a single crystal of ThF_4 had $|\alpha| \approx 2 \times 10^{-6} \text{ K}^{-1}$ for temperatures between 25 C and 400 C, and the total expansion $\alpha\Delta T$ for $\Delta T = 25 \text{ C}-600 \text{ C}$ was zero (with α negative on part of this interval). The crystal was not cracked by application of a blowtorch. The great differences between the values of α for the semiconductor materials and the alkali halides indicates that great thermal stresses are a potential problem for this combination of film and substrate materials.

An important practical example of thermal stress is the failure in compression of zinc selenide films on potassium chloride substrates for $\Delta T = 200 \text{ K}$.

From (6.1),

$$\begin{aligned}\sigma &= (\alpha_{\text{ZnSe}} - \alpha_{\text{KCl}}) E_{\text{ZnSe}} \Delta T \\ &= (7 - 36) 10^{-6} (10.3 \times 10^6) 200 \\ &= -6.0 \times 10^4 \text{ psi} = -0.41 \text{ GPa}.\end{aligned}$$

Using the rule of thumb that the compressive strength σ_c is approximately eight times the tensile strength gives $\sigma_c \approx 8(7 \times 10^3) = 5.6 \times 10^4 \text{ psi}$ for ZnSe. Thus failure is expected since the compressive stress exceeds the compressive strength, $|\sigma| > \sigma_c$. A similar calculation for GaAs on NaCl with $\Delta T = 270 \text{ K}$ shows that the GaAs film should fail in compression, in agreement with experimental observations.

In addition to these primary practical results, the following results also are of interest. Stress-induced optical absorption should be negligible, especially at the level of $\beta_f = 0.5 \text{ cm}^{-1}$. Thin-film adhesion and stress are reviewed briefly in the Handbook of Thin Film Technology⁴¹ and in Ritter's article,^{*2} and the subjects are surveyed in detail by Chapman⁴² and by Hoffman.^{*43} Hoffman's review and a key paper by Ennos^{*44} are excerpted in Sec. XIII.

In Table 6.2 from Hoffman's article stresses are listed for a number of films. The values measured by Ennos^{*44} are not included in the table. Hoffman points out two notable features of the results in the table. First there are a relatively large number of dielectric films that exhibit compressive stress. Second, there are many instances where the magnitude of the stress is small.

The following quotations from Ennos^{*44} are of interest: "Most materials investigated develop a tensile stress. This is what is to be expected for a film material which when it is first condensed must be considerably hotter than the substrate. On cooling thermal contraction will cause a tensile stress. The compressive stress of the cadmium telluride reported here is probably due to dissociation of the material and partial recombination on the surface. The reduction in tensile stress of thorium oxyfluoride films exposed to damp air is also due to the same effect."

"Some remarks can be made regarding the failure of films by cracking, peeling, etc. It is obvious from these measurements that the fact that a high stress exists in a film does not necessarily mean that it will break. Compressive stresses can be borne more easily than tensile ones for instance since a large area of the film will have to become detached if it fails in compression.

Sec. VI

Table 6.2. Intrinsic Stresses in Dielectric Films Approximately 5000 Å Thick

Material	Substrate Temperature °C ^a	Substrate Material	Stress, 10^9 dyne/cm ² ^b	Sign ^c	Method ^d	Ref.
ZnS	110	Glass	1.0	C	C	30
	A	Glass	(0.022)	C	C	28
	A	Mica		C	C	60
SiO	110	Glass	1.2	C	C	30
	A	Nickel	4	T	C	33
MgF_2	110	Glass	2.0	T	C	30
	75	Mica	2.2	T	B	38
	A	Glass	(0.11)	T	C	28
	A	Mica	(0.11)	T	C	60
	A	Glass	1	T		57
LiF	110	Glass	0.4	T	C	30
	A	Cellulose	2.0	T	ED	47
	A	Glass	0.28	T		57
	A	Mica	(0.023)	T	C	60
	A	Glass	(0.023)	T	C	28
CaF_2	110	Glass	0.2	T	C	30
	A	Mica	(<0.0003)	T	C	60
	A	Glass	(none)		C	28
Cryolite	A	Glass	(0.061)	T	C	28
	A	Glass	(0.06)	T	C	60
	A	Glass	0.5	T		57
$PbCl_2$	50	Glass	0.18	T	C	30
	A	Glass	(0.014)	T	C	28
PbF_2	110	Glass	0.8	T	C	30
$AgCl$	A	Glass	(none)		C	28
AgF	A	Glass	(none)		C	28
AgI	A	Glass	(none)		C	28
BaF_2	A	Glass	(0.006)	T	C	28
BaO	50	Glass	0.15	C	C	30
Sb_2O_3	A	Glass	(0.004)	C	C	28
Sb_2S_3	A	Glass	(0.007)	T	C	28

Table 6.2. Intrinsic Stresses in Dielectric Films Approximately 5000 Å Thick (Cont'd)

Material	Substrate Temperature °C ^a	Substrate Material	Stress, 10^9 dyn/cm ² ^b	Sign ^c	Method ^d	Ref.
Ce ₂ O ₃	50	Glass	1.6	C	C	30
CeF ₃	40	Glass	2.8	T	C	30
CdS	110	Glass	0.8	C	C	30
SnO ₂	A	Glass	(0.008)	T	C	28
C	A	Glass	4.0	C	C	31
NaF	A	Glass	0.1	T		57
B ₂ O ₃	90	Glass	0.1	T	C	30
Chiolite	A	Glass	(0.029)	T	C	28
AlPh ^e	40	Glass	0.6	C	C	30
MgPh ^e	40	Glass	0.6	C	C	30
MoO ₃	A	Glass	(0.013)	T	C	28
CuI	A	Glass	(none)		C	28
AlF ₃	A	Glass	(none)		C	28
SrSO ₄	A	Glass	(none)		C	28

^a A, thermally floating at ambient temperature^b Values in parentheses are relative^c C and T, compression or tension^d B, end-supported beam; C, cantilever beam; and ED, electron-diffraction technique^e Al and Mg thalocyanine

"In fact, three factors are involved in the process of failure: (a) The stress in the film and its direction, (b) the rupture strength of the film material alone, and (c) the bond strength between the film and the substrate. The latter can exert great influence. For example, a film having great rupture strength will break only when the shearing force between the substrate and the film becomes greater than the adhesive force. On the other hand, a film having weak rupture strength will break internally before the adhesive forces are overcome. This can manifest itself as a clouding of the film rather than a complete break."

Turner⁴⁵ was able to increase the total thickness of a coating which could be deposited from 6 to 40 μm by measuring the stress in films of various materials and by using alternate layers with compressive and tensile stress. Campbell^{39a} makes a broad distinction between weak physical adhesion by Van der Waal's forces ($\sim 0.1 \text{ eV}$ adsorption energy per bond) of a film to a substrate and strong chemical adhesion ($\sim 1 \text{ eV}$ per bond) by chemical bonds. Values of the adsorption energy per ion for the weak physical adhesion and the strong chemical adhesion are, very roughly, 0.1 eV and 1 eV, respectively. The chemical behavior of the films is of importance with respect to the substrate and to neighboring layers. Between glass constituents like PbO and film materials like La₂O₃ chemical reactions can take place and lead to the formation of absorbing metallic lead. Reactions among film materials are also possible, especially at higher substrate temperatures.

Radioactivity and toxicity. There is disagreement on the importance of the radioactivity of ThF₄. One comment on the preliminary draft was that the radioactivity of ThF₄ was blown out of proportion to its real importance, while another investigator stated that the ThF₄ coatings could not be used on large high-power laser windows. There are similar disagreements on the importance of toxicity.

VII. LASER HEATING OF COATINGS

The results of this section are as follows:

- For $2 A_f = A_b = 2 \times 10^{-4}$, the film and bulk contributions to the spatial average of the window temperature, which determines the thermally induced optical distortion, are equal and have a typical value $T_{\text{tot}} = 1.0 \text{ K}$, which is sufficient to cause thermally induced optical-distortion failure in some cases.
- In a typical system with repeated short pulses, only the time-average heating need be considered (apart from inclusion damage, nonlinear effects and possible more stringent conditions of future systems -- see Sec. VIII).
- The linear absorption (below the damage threshold) by strongly absorbing ($\sigma_{\text{abs}} = \pi a^2$) one-micron-radius inclusions with an average spacing of $175 \mu\text{m}$ gives rise to absorptance $A_f = 10^{-4}$.

There are three damage or failure regimes of interest in general. The first is damage or optical distortion resulting from heating by ordinary linear absorption in the coating. The second is the absorption by macroscopic imperfections such as inclusions. This absorption can be linear or nonlinear. The third is the intrinsic nonlinear damage mechanism. The first is considered in the present section, and the third is considered in Sec. VIII. The effect of inclusions on ordinary heating is considered in the present section, and the effect of inclusions on the damage threshold is considered in Sec. VIII.

As in the case of laser heating of bulk materials, thermally induced optical distortion⁶ often limits the average temperature rise to values (typically ranging

from a fraction of a degree to several tens of degrees Kelvin) below the melting temperature or the temperature at which fracture occurs. (Small-diameter windows can fail by fracture, however.⁸)

Spatial-average temperature, for thermally induced optical distortion. For this case of thermally induced optical distortion, the problem of determining the effect of the temperature rise is simple. The average temperature along a ray, i.e., the average temperature across the thickness ℓ ,

$$\langle T \rangle_{\ell} = \ell^{-1} \int_0^{\ell} dx \ T \quad (7.1)$$

determines the optical distortion since the system remains linear for the small temperature changes that can be tolerated. For the nearly constant absorption in the bulk for the case of $\exp(\beta_b \ell) \approx 1 - \beta_b \ell$, or $A_b = \beta_b \ell \ll 1$, the temperature rise is obtained simply from the heat-capacity relation that the temperature rise is equal to the energy added $I A_b \Delta t$ to the volume $\Delta \ell$ divided by the heat capacity $C \Delta \ell$ of the volume. This gives⁴⁶

$$T_b = I \beta_b t / C = I A_b t / C \ell = 0.50 K \quad . \quad (7.2)$$

For no radial diffusion (discussed below) it is obvious from the heat capacity argument that the average value $\langle T \rangle_{\ell}$ of the temperature rise resulting from absorption in the coating will be equal to that, T_b , from bulk absorption if the total energies absorbed are equal in the two cases. That is,

$$2 A_f = A_b \quad , \quad (7.3)$$

where the factor of two accounts for the coating absorption at the two surfaces, as in Sec. III. When (7.3) is satisfied, the average value T_{tot} of T from the bulk and coating absorption is twice the value in (7.2).⁴⁶

$$T_{\text{tot}} = 2 I \beta_b t / C = 1 \text{ K} , \quad (7.4)$$

which is sufficient to cause failure by thermally induced optical distortion in some systems.⁴⁷

Spatial temperature distribution. This spatial-average temperature in (7.4) is all that is usually needed. However, in some cases the actual temperature distribution will be needed. Also, it must be verified that abnormal temperatures are not present so that the assumed linearity is valid and thermal fracture from the temperature gradients resulting from the coating heating do not occur. Thus, the temperature distribution is considered briefly.

The temperature rise resulting from the absorption of energy from the laser beam by the coating has been calculated previously^{48,49} as part of a general study of laser heating of materials. The results of interest for the present case of absorption by a coating are as follows. The absorption coefficient in the coating is β_f , which has a desired value of $\beta_f = 0.5 \text{ cm}^{-1}$ as found in Sec. III. The window material itself is assumed to have $\beta_b = 0$ since the interest is not in the bulk window absorption. For systems with no intentional cooling of the window, the small cooling by radiation and radial heat diffusion will be neglected.

As an example of radial diffusion, consider the thermal-diffusion distance ℓ_{th}^{46}

$$\ell_{\text{th}} = (4 K t / C)^{1/2} = 1.0 \text{ cm} . \quad (7.5)$$

For the large windows of current interest ($D > 10\text{ cm}$ in some cases), the inequality $\ell_{\text{th}} \ll D$ is well satisfied, and radial diffusion can be neglected in the simple estimate used here. There are of course some cases in which radial diffusion is important. For example, the case of continuous operation of edge-cooled windows for long periods of time has been considered previously.^{49, 50}

First it will be shown that in a typical system with repeated short pulses, only the time-average heating need be considered (apart from the inclusion damage and nonlinear effects, Sec. VIII). Thus, the continuous-operation results discussed below can be applied to the typical repeated pulse system by using the time averaged power for the latter. The time constant τ_{ℓ_f} associated with the diffusion of heat for a distance ℓ_f , the coating thickness is⁴⁶

$$\tau_{\ell_f} = C \ell_f^2 / 4K = 4 \times 10^{-7} \text{ s} . \quad (7.6)$$

For a short pulse duration $t_p < \tau_{\ell_f}$, the heat generated in the coating does not have time to diffuse far into the substrate. Then, equating the energy absorbed $I \beta_f \ell_f \Delta t_p$ by the volume $\Delta \ell_f$ of the film to the heat-capacity result $T_p C \Delta \ell_f$ gives⁴⁶

$$T_p = I t_p / \beta_f C = 2.5 \text{ K} , \quad (7.7)$$

for

$$t_p \ll \tau_{\ell_f} \quad (7.8)$$

where the numerical value is for the case of $I t_p = 10 \text{ J/cm}^2/\text{pulse}$, which corresponds to a typical case of 100 pulses per second and a time average intensity of 10^3 W/cm^2 .

This small temperature rise 2.5 K in (7.7) is expected to be negligible.

First, the average temperature (which determines the thermally induced optical distortion) is $\langle T \rangle_{\ell} = 2.5 \text{ K} (2 \times 2 \mu\text{m}) / 2 \text{ cm} = 5 \times 10^{-4} \text{ K}$, which is negligible.

Second, the small value of 2.5 K is not expected to cause damage. For example, the value of the thermal expansion coefficient α_f of the film, in the present case, is not greatly different from a typical value of the difference $\alpha_f - \alpha_b$ between the film and bulk values, in the case of cooling of the film and substrate from the deposition temperature of $\sim 100 \text{ C}$ typically.

If (7.8) is not satisfied, that is, if the pulse duration is greater than the order of a microsecond for the example in (7.6), then the heat diffusion into substrate reduces the value of T_p below that of (7.7). Since the temperature rise during the pulse duration, $T_p = 2.5 \text{ K}$ from (7.7), already is negligibly small and the heat generated during the pulse diffuses into the substrate during the time between pulses, the temperature rise is well approximated by replacing the repeated pulses by a continuous beam of the same average power.

Next consider this case of continuous operation for a time $t \gg \tau_{lf}$, with $\tau_{lf} \approx 0.4 \mu\text{s}$ according to (7.6). The temperature rise depends on the relative magnitudes of t_p and⁴⁶

$$\tau_{lb} = C l_b^2 / 4K = 40 \text{ s} , \quad (7.9)$$

which is the time required for heat to diffuse across the window thickness l_b , roughly speaking.

For $\tau_{lf} < t < \tau_{lb}$, the volume of material heated is $\sim A l_{th}$, where l_{th} is the thermal diffusion distance in (7.5). The heat deposited in this volume is

$I A_f \alpha t_p$, which corresponds to the temperature rise of $\sim (I A_f \alpha t) / C \alpha \ell_{th}$. The resulting maximum temperature rise (at the surface) is, with the correct numerical factor $(4/\pi)^{1/2}$ included,⁴⁶

$$T = I A_f (4 t_p / \pi C K)^{1/2} = 1.1 K , \quad (7.10)$$

which is negligible.

For the case of $\ell_b \ll \ell_{th} < D_b$, where D_b is the characteristic distance over which the laser-intensity distribution changes appreciably, the temperature rise is again easily obtained. The energy absorbed $2 I A_f \ell t_p$ at the two faces of the window heats the whole volume $V = \alpha \ell_b$, rather than the volume $2 \alpha \ell_{th}$ as in the case of $\ell_{th} \ll \frac{1}{2} \ell_b$. The heat capacity result then gives⁴⁶

$$T = 2 I A_f t_p / C \ell_b = 50 K \quad (7.11)$$

for this case of $\ell_f \ll \ell_b \ll \ell_{th} < D_b$. This result (7.11) also follows directly from (7.2) and (7.3). The large numerical value $T = 50 K$ is for $t = 10^3$ sec (and $I t_p = 10^6 J/cm^2$) and values of other parameters from (3.3). The corresponding value of ℓ_{th} is 5 cm. Thus, this value of $T = 50 K$ is only a rough estimate since $\ell \ll \ell_{th} \ll D_b$ is not well satisfied.

Finally, it is mentioned that the temperature difference through the thickness of the coating is negligibly small, a result that is obvious since the coatings are so thin. This result can be checked by examining the previous result for the temperature distribution.^{48, 49} The following check is even simpler. Since all of the heat generated in the film flows into the substrate (across the boundary $x = \ell_f$) in the steady state, the heat flow J_δ at $x = \ell_f$ is simply

$$J_{\ell f} = I A_f .$$

Sec. VII

Equating this expression for $J_{\ell f}$ to $-KT'$, where $T' \equiv (dT/dx)_{x=\ell_f}$, gives $T' = IA_f/K$. Since the gradient decreases to zero at $x = 0$ (no heat flow out of the sample), an upper bound to the temperature difference $(T)_{x=0} - (T)_{x=\ell_f}$ is $-T'\ell_f = 4 \times 10^{-4}$, which shows that the temperature difference across the coating is negligibly small as expected.

Coating absorptance from inclusions. In bulk materials, linear heating of inclusions at intensities too low to cause damage (at a given value of t_p) can increase the overall absorption coefficient β of the material.²⁴ In the same way, inclusions in the vicinity of the coating or of a surface could increase the overall value of A_f or of A_s . For example, consider the damage in (ZnSe/ThF₄)-enhanced reflectors observed by Wang, Giuliano, and Garcia.³⁹ If the damage (at 70 J/cm²) were a result of inclusions having radius $a = 1 \mu\text{m}$, cross section $\sigma_{\text{abs}} = \pi a^2$, and a mean spacing of 30 μm between inclusions, the value of film absorptance would be

$$A_f = \pi a^2 / (30 \mu\text{m})^2 = 3.5 \times 10^{-3} .$$

Since the measured absorptance $A_f = 3 \times 10^{-3}$ was believed to result from absorbing in bulk of the coating materials, the fact that $A_f^{\text{theory}} = 3.5 \times 10^{-3} > A_f^{\text{meas}} = 3 \times 10^{-3}$ for $a = 1 \mu\text{m}$ suggests that $a < 1 \mu\text{m}$. Alternate explanations are that $\sigma_{\text{abs}} \ll \pi a^2$ or that the inclusion spacing is much greater than 30 μm . For $a = 1 \mu\text{m}$ and a spacing of 175 μm , the corresponding value of A_f is 10^{-4} .

VIII. LASER DAMAGE OF COATINGS

In this section it will be shown that:

- Inclusion damage is expected to occur at energy density $It_p \cong 1 - 10 \text{ J/cm}^2$ for nanosecond pulses or at $It_p \cong 10$ to several hundred joules per square centimeter for microsecond pulses. In principle, values of $It_p < 1 \text{ J/cm}^2$ are possible for nanosecond through microsecond pulses.
- Intrinsic damage of coatings is expected to occur at $It_p \cong 10^3 \text{ J/cm}^2$ for a pulse of duration $t_p = 10 \mu\text{s}$ and $A_f = 10^{-3}$ as a result of linear heating of the coating, or at $It_p \cong 100 \text{ J/cm}^2$ (or $I \cong 10 \text{ GW/cm}^2$) for a 10 ns pulse of ~ 1 to $10 \mu\text{m}$ radiation as a result of electron-avalanche breakdown or perhaps another nonlinear process.
- Intuitively it appears unlikely that all inclusions could be removed from a large window. Thus the lower-threshold inclusion-damage process, rather than an intrinsic process, is expected to determine the damage threshold.

The failure of high-power window materials can occur as a result of ordinary linear heating of the bulk material. This laser heating causes distortion of the optical beam or fracture or melting of the material. For lasers that are continuously operated, laser heating is the usual failure mechanism that limits the useful transmittance of window materials. In short-pulse systems and in repeated pulse systems, as the pulse duration is decreased the irradiance (intensity) increases if the energy density is maintained constant. For sufficiently short pulses, material damage can result from absorption by macroscopic inclusions or from such intrinsic nonlinear damage mechanisms as electron-avalanche breakdown, two-photon

absorption, or enhanced-stimulated-Raman scattering (each of which possibly could be initiated by self focusing. In this report, "laser damage" will denote inclusion damage and intrinsic nonlinear damage. For coated materials, damage of the coating as well as inclusions can occur at short-pulse durations. This short-pulse coating damage, which has been observed already in laser-damage studies of coatings,^{39,51} will be included in the laser-damage category.

Absorption by macroscopic inclusions. Damage of bulk materials resulting from absorption by inclusions has been considered in great detail, both for inclusions deep in the material²⁴ and for inclusions near the surface of the material.⁵² The previous results should apply directly to the case of inclusions in the region of the coating and the interface of the coating and the substrate. There are also at least two additional effects that could occur in coatings. First, the number and size distribution of inclusions may be different in the vicinity of the coating. Of particular interest is damage from absorption by water, or possibly other contaminants, in pores in the coating or at a surface. The effect of pore contamination on absorptance was discussed in Sec. IV. In addition to causing failure, inclusions also can contribute to the average heating of the window, as already mentioned in Sec. VII.

Second, the stresses in the coating and the differences in strengths of the coating and interface region from that of the bulk could affect the damage threshold. For example, it is conceivable that the stress in the region of the inclusion could cause or initiate film detachment. The film-detachment damage mechanism discussed in Sec. IX could then be involved in the last stage of such a damage mechanism. The net effect could be a somewhat lower damage threshold for coated materials than for uncoated ones.

The analyses of these two effects is low on the list of priorities since the results will depend on details of the coatings and inclusions which are not known, and in fact would be difficult to measure. The lack of a complete theory of inclusion damage in coatings is not serious at present, since the damage threshold for inclusion damage of uncoated surfaces and of the bulk window material already is very low, and the other problems with coatings are great. In any case, a zeroth-order approximation to the damage threshold could be obtained simply by lowering the value of the temperature rise (10^3 K has been assumed²⁴ to be a reasonable value for inclusion in the bulk) at which damage is assumed to occur.

There is a vast literature on laser damage of materials. It is believed that intrinsic damage thresholds of materials can be measured by focusing laser pulses into small volumes of bulk material. The damage threshold varies greatly from pulse to pulse. If the small focal volume contains an absorbing inclusion, damage occurs at a low energy density. If the focal volume is free of imperfections, the much greater energy density is believed to be the intrinsic value for the material.

It is expected that it will be difficult to avoid the inclusion-induced low-damage thresholds in large windows for use in the $2-11\mu\text{m}$ region since it may be extremely difficult to remove inclusions and only a few inclusions in the whole window may be sufficient to cause failure in some cases. However, history does afford the encouraging story of the removal of platinum inclusions from $1.06\mu\text{m}$ -laser glass. The resulting glass damage is limited by self focusing, rather than by inclusions, for picosecond pulses. For this particular case of laser glass, a threshold of 10 GW/cm^2 in a 100 psec pulse still corresponds to only 1 J/cm^2 . But values of

energy density It_p (where I is the irradiance, i.e. intensity, and t_p is the laser pulse duration) possibly as great as $60-100 \text{ J/cm}^2$ over large areas for 30 ns pulses of $1.06 \mu\text{m}$ radiation have been reported⁵³ for an inclusion-'purified' glass. Such a great value $It_p = 60-100 \text{ J/cm}^2$ is two orders of magnitude greater than the value $It_p = 1 \text{ J/cm}^2$ for damage by $1 \mu\text{m}$ -radius inclusion in the example below. This strongly suggests, but does not prove conclusively, that the purified glass does not contain inclusions of approximately one micrometer radius.

Recall that inclusions near the surface of a bulk material can give rise to cone-shaped craters on the surface.^{54,52} For coated samples it is possible that either these cone-shaped damage sites or the detachment discussed in Sec. IX could result. In any studies of inclusion damage, the important result of Boling and Dube⁵⁴ that the inclusions may be difficult to detect by methods other than actual laser damage should be kept in mind. Careful electron microprobe searches failed to detect inclusions in samples that subsequently showed the cone-shaped surface damage. It might be expected that this anomalous result could be explained as absorption by pores filled with water or other contaminants that are transparent in the visible region of the spectrum. However, the absorption coefficient of water at $1.06 \mu\text{m}$ is small ($\beta = 0.4 \text{ cm}^{-1}$), and this mechanism is unlikely. At $1.06 \mu\text{m}$ for inclusions in sapphire ($n_r = 1.7$), $ka = 1.7(2\pi)a/\lambda$ is equal to unity for $a = 0.1 \mu\text{m}$. Since inclusions that are even somewhat smaller than this value of $0.1 \mu\text{m}$ could still absorb strongly, and the inclusions could be widely spaced, their detection could be difficult.

Inclusion damage threshold. Assuming that inclusions will determine the damage threshold, recall that inclusion-damage thresholds vary greatly, with typical values for $1-10 \mu\text{m}$ radiation of $1-10 \text{ J/cm}^2$ for nanosecond pulses and

10 to several hundred joules per square centimeter for microsecond pulses. It is difficult to make an accurate calculation of the inclusion-damage threshold even for inclusions in the bulk because such details of the inclusions as their size, absorption coefficient, and shape are not known and the exact damage process is not known. The inclusion-damage-threshold value of the energy density It_p depends on the pulse duration. In the absence of specific values of It_p , the typical values of $1-10 \text{ J/cm}^2$ and 10 to several hundred joules per square centimeter just mentioned will suffice as estimates of values to be expected in coated or uncoated materials. It is emphasized that values of energy density (J/cm^2) alone have little significance.^{54a}

Current theories²⁴ are sufficient to demonstrate that these values of It_p are reasonable. The general theory is somewhat complicated and the results are quite uncertain for the usual case in which the nature of the inclusions is unknown. However, simple cases of the theory serve to illustrate central features of inclusion damage. A major factor in determining damage by an inclusion is the relative size of the duration t_p of the laser pulse and the thermal-diffusion time⁴⁶

$$\tau_H = C_H a^2 / 4K_H = 0.1 \mu\text{s} \quad (8.1)$$

where C_H and K_H are the heat capacity per unit volume and the thermal conductivity of the host material and a is the radius of the inclusion, assumed to be spherical and to have thermal conductivity much greater than K_H for simplicity.

The numerical value $0.1 \mu\text{s}$ in (8.1) is for the case of $a = 1 \mu\text{m}$. For $t_p \ll \tau_H$, the heat generated in the inclusion does not have time to diffuse into the host material, and the temperature rise T is determined by equating the energy absorbed to the product of the heat capacity and T :

Sec. VIII

$$T \cong (3It_p / 4aC_I)(\sigma_{abs}/\pi a^2) , \quad \text{for } t_p \ll \tau_H \quad (8.2)$$

where σ_{abs} and C_I are the absorption cross section and heat capacity per unit volume of the inclusion and I is the irradiance (intensity) incident on the inclusion. For the other extreme of $t_p \gg \tau_H$, which is satisfied for a $1\mu s$ pulse with $1\mu m$ -radius inclusions according to (8.1), the steady-state result for T is valid:²⁴

$$T \cong (Ia/4K_H)(\sigma_{abs}/\pi a^2) , \quad \text{for } t_p \gg \tau_H . \quad (8.3)$$

It has been argued²⁴ that failure occurs when T reaches a value $T_f \cong 1000$ K, as a rough estimate. Setting $T = T_f$ in (8.2) and (8.3) and solving for It_p gives

$$It_p = \frac{4}{3} a C_I T_f (\pi a^2 / \sigma_{abs}) , \quad \text{for } t_p \ll \tau_H \quad (8.4)$$

$$It_p = (4K_H t_p T_f / a) (\pi a^2 / \sigma_{abs}) , \quad \text{for } t_p \gg \tau_H . \quad (8.5)$$

For the moment it is assumed that $\sigma_{abs} = 0.1 \pi a^2$, and that all inclusions have the same radius $a = 1\mu m$. Then, for a 10 ns pulse, $t_p \ll \tau_H$ is well satisfied according to (8.1), and (8.4) gives

$$It_p = 2.7 \text{ J/cm}^2 , \quad \text{for } t_p = 10 \text{ ns} . \quad (8.6)$$

For a $1\mu s$ pulse, $t_p \gg \tau_H$ is satisfied, and (8.5) gives

$$It_p = 20 \text{ J/cm}^2 \quad (8.7)$$

thus illustrating values of It_p on the range $1-10 \text{ J/cm}^2$ for 10 ns pulses and 10 to a few hundred joules per square centimeter for microsecond pulses.

Sec. VIII

Next consider the ratio $(It_p)_{1\mu s}/(It_p)_{10 ns}$. From (8.4) and (8.5),

$$\frac{(It_p)_{1\mu s}}{(It_p)_{10 ns}} = \frac{3K_H(1\mu s)}{C_I a^2} = 7.5 \quad (8.8)$$

where the numerical value 7.5 is for the case of $a = 1\mu m$.⁴⁶ For $a = 0.1\mu m$, the ratio has the value 750, and the values of It_p are $0.27 J/cm^2$ and $200 J/cm^2$ for 10 ns and $1\mu m$ pulses, respectively.

The temperature rise depends strongly on the inclusion radius a , as seen in (8.4) and (8.5). If a sample contains inclusions having a wide range of values of a , then inclusions of a certain value (that depends on the values of t_p , K_H , and other parameters) will determine the damage threshold since their temperature rise will be the greatest.²⁴ The value of $a = 1\mu m$ used in the examples gives rise to large values of T , but the value of a was not optimized²⁴ in the interest of simplicity of the examples.

Minimum inclusion-damage threshold. It will be shown that values of energy density less than $1 J/cm^2$ are possible in principle for nanosecond to microsecond pulses. The value of the power density at which inclusion damage occurs becomes great for both very small values of a and for very large values of a . First, for sufficiently small values of a the inequality $t_p \ll \tau_H$ will be satisfied, and the value of It_p will be given by Eq. (8.4). Thus the value of It_p becomes extremely large for large values of a . Next for small a , such that $ka \ll 1$ is satisfied, where $k = 2\pi n_r/\lambda$, the absorption cross section is small, $\sigma_{abs} \ll \pi a^2$, and It_p is great according to (8.4) or (8.5).

The value of $\sigma_{abs}/\pi a^2 = 0.1$ used above is a reasonable approximation for a typical case. For example, for $ka \gtrsim 1$, the value of $\sigma_{abs}/\pi a^2$ for a metal is

Sec. VIII

$(1 - R)$, where R is the average value of the reflectivity over the various angles of incidence on the spherical inclusions. A typical numerical value of this factor $1 - R$ is 0.1 in agreement with the approximation. For dielectric inclusions the value of $\sigma_{\text{abs}}/\pi a^2$ is less than 1 if either $ka \ll 1$ or $\beta_I a \ll 1$ is satisfied, where β_I is the absorption coefficient of the inclusion.

Finally consider the minimum value of energy density It_p for a sample containing the worst type of absorbing inclusions. The problem of minimizing the value of It_p as a function of the inclusion radius and other parameters of the inclusion is difficult in general. However, the following simple analysis should suffice for a rough estimate of the minimum value of It_p . The maximum heating for a given energy density and a given value of the inclusion radius occurs for the case of $t_p \ll \tau_H$ since in this case the heat does not have time to diffuse out of the inclusion. In this case the value of the energy density is given by (8.4). If a is formally taken as an arbitrarily small number, then the value of It_p is arbitrarily small. However, the value of a must be greater than

$$l_{\text{th}} = (4K_H t_p / C_H)^{1/2} = (t_p / 1 \mu s)^{1/2} 3.2 \mu m , \quad (8.9)$$

which is equivalent to $t_p \ll \tau_H$, in order for (8.4) to be valid. Furthermore, a must be greater than

$$k^{-1} = \lambda / 2 \pi n_I = \left(\frac{\lambda}{10.6 \mu m} \right) \left(\frac{2}{n_I} \right) 0.84 \mu m , \quad (8.10)$$

otherwise the value of $\pi a^2 / \sigma_{\text{abs}}$ in (8.4) becomes very large.

For a 10 ns pulse at $10.6 \mu m$, the value of k^{-1} is greater than the value of l_{th} . Thus the value of a is limited by the value of k^{-1} . Substituting $a = k^{-1} = 0.84 \mu m$ from (8.10) into (8.4) with $\pi a^2 / \sigma_{\text{abs}} = 1$ gives $It_p = 0.2 \text{ J/cm}^2$. For a $1 \mu s$ pulse

the value of $\ell_{th} = 3.2 \mu\text{m}$ is greater than the value of $k^{-1} = 0.84 \mu\text{m}$ for $10.6 \mu\text{m}$ radiation. Substituting this value of $a = \ell_{th} = 3.2 \mu\text{m}$ into (8.4) gives $i_{tp} = 0.83 \text{ J/cm}^2$. Thus inclusion-damage values of energy density less than 1 J/cm^2 are possible in principle for nanosecond to microsecond pulses.

In using the value $\pi a^2 / \sigma_{abs} = 1$, it is tacitly assumed that the inclusions are not metallic since the factor $1 - R$ for metallic inclusions is considerably less than 1. In order to have $\pi a^2 / \sigma_{abs} \approx 1$ for the dielectric inclusions, the value of the absorption coefficient β_I must be sufficiently great that $\beta_I a > 1$ is satisfied, but that the value of β_I must not be so great that the reflectance of the inclusion becomes sufficiently great to reduce the absorption cross section.

Braunstein and coworkers^{*10} at the Hughes Research Laboratories measured a damage threshold of multilayer antireflection coatings for metals of 65 J/cm^2 for their nominal $0.6 \mu\text{s}$ pulse, which consists of a $0.23 \mu\text{m}$ pulse followed by a $3 \mu\text{s}$ tail roughly. The size of the laser spot on the target was not reported; however, the damage was reported to be at localized damage sites. This result, 65 J/cm^2 , is in the range of 10 to several hundred joules per square centimeter given above.

Laser damage from heating of the coating. The intrinsic damage threshold of antireflection coatings is of interest in interpreting experimental results and in determining the ultimate possible performance. Consider a $10.6 \mu\text{m}$ coating of thickness $\ell_f = 2 \mu\text{m}$ and absorptance $A_f = 10^{-3}$. The diffusion time τ_ℓ for distance ℓ_f is⁴⁸

$$\tau_\ell = C \ell_f^2 / 4K . \quad (8.11)$$

For $C = 2 \text{ J/cm}^3 \text{ K}$, $K = 5 \times 10^{-2} \text{ W/cm K}$, and $\ell_f = 2 \mu\text{m}$, this gives $\tau_\ell = 0.4 \mu\text{s}$.

Sec. VIII

For $t_p \gg \tau_\ell$, which is valid for a $6\mu s$ pulse for example, diffusion into the substrate must be considered, and the temperature rise is⁴⁸

$$T = 2IA_f(t/\pi CK)^{1/2} . \quad (8.12)$$

For $T = 10^3 K$ and $A_f = 10^{-3}$, (8.12) gives $I = 0.11 \text{ GW/cm}^2$, or

$$It_p = 700 \text{ J/cm}^2 . \quad (8.13)$$

Since such nonlinear effects as electron-avalanche breakdown and multiphoton absorption do not usually occur for $I \gtrsim 10 \text{ GW/cm}^2$, which is less than the value of 0.11 GW/cm^2 in the example, the intrinsic damage threshold is expected to be 700 J/cm^2 , as given in (8.13) for ordinary linear heating.

For $t_p \ll \tau_\ell$, as for nanosecond pulses, the heat generated in the coating does not have time to diffuse into the substrate, and the temperature rise is

$$T = IA_f t_p / C \ell_f . \quad (8.14)$$

The value of It_p corresponding to $T = 10^3 K$ is

$$It_p = 400 \text{ J/cm}^2 \quad \text{for } A_f = 10^{-3} \quad (8.15)$$

and the corresponding value of I is 40 MW/cm^2 . Since values of I for electron-avalanche breakdown can be smaller than 40 MW/cm^2 , the electron-avalanche-breakdown mechanism could cause breakdown at values lower than the thermal-breakdown value of 400 J/cm^2 from (8.15). For example for 10 ns pulses, the observed value of $I = 16 \text{ GW/cm}^2$ for NaCl corresponds to

$$It_p = 160 \text{ W/cm}^2 . \quad (8.16)$$

Finally, it is mentioned that the intensity $2 \times 10^8 \text{ W/cm}^2$ corresponding to $I t_p = 2 \text{ J/cm}^2$ and $t_p = 10^{-8} \text{ s}$ is much greater than the cw intensities I_{cw} at which failure occurs. Values of I_{cw} vary greatly depending on the material and operating conditions. A representative value is $I_{\text{cw}} = 10^3 \text{ W/cm}^2$. In a repeated pulse system, for example a laser with a long train of microsecond or nanosecond pulses, either the single pulse threshold such as $1-100 \text{ J/cm}^2$ or the average heating threshold such as 10^3 W/cm^2 could be the limiting factor, and both effects must be considered.

It should be kept in mind that it is known that dirty surfaces damage easily. In large Atomic Energy Commission lasers, the high powers of the flash lamps are used to clean the optical-component surfaces.^{54b} In addition to removing such particles as dust, it is believed that adsorbed layers (which are a less serious problem at $1.06 \mu\text{m}$) also are removed.

Intrinsic nonlinear damage. Nonlinear damage mechanisms include electron-avalanche breakdown, two-photon absorption, enhanced-stimulated-Raman scattering, and self focusing. Recent experiments have provided a wealth of information on intrinsic damage thresholds in bulk materials. The intensity I_f at which damage occurs in NaCl for 10 ns pulses of $10.6 \mu\text{m}$ radiation is $\sim 15 \text{ GW/cm}^2$, and the values for other materials of interest typically are not drastically different from this value. The pulse-duration dependence of I_f has been studied in detail experimentally for $1.06 \mu\text{m}$ radiation.⁵⁵ There the values of I_f increase from $\sim 16 \text{ GW/cm}^2$ at $t_p = 10^{-8} \text{ s}$ to $\sim 500 \text{ GW/cm}^2$ at $t_p = 1.5 \times 10^{-11} \text{ s}$.

These values are for bulk materials. It is possible that the intrinsic failure threshold could be lower at the surface of a coating, at the surface of an uncoated

material, at the interface of the coating and the material, or in the coating itself. For example, Boling⁵³ suggested that electronic surface effects such as modifications of the band structure or states in the gap could lower the damage threshold.

At the present time we simply want to keep in mind the possibility of a lower surface threshold. Calculation of this lower intrinsic value of I_f has low priority at present since the intrinsic damage mechanism in even the bulk damage is not well understood. A recent theory⁵⁶ of breakdown does contain sufficient details to allow estimates of surface effects to be made. Since the validity of the theory has not been well tested, we shall not extend it to the surface damage case at present.

IX. LASER DAMAGE OF DETACHED COATINGS

The following results are obtained in the present section:

- The calculated value of 25 K temperature rise for a detached film segment of diameter $D = 2 \text{ mm}$ is surprisingly small.
- The temperature is proportional to D^2 .
- The thermally induced stress corresponding to $T = 25 \text{ K}$ has a typical value of $20 \text{ MPa} (3 \times 10^3 \text{ psi})$, which may be sufficient to cause further detachment, then further temperature increase since $T \sim D^2$, and possibly a runaway condition resulting in damage.

The absorption in coating is much greater than in the window material itself in most cases of interest, and the impedance to heat flow is much greater along the long path through a film than through the direct path from the film into the bulk window material. Thus, it was originally expected that even very small detached areas of the coating would be easily damaged. The results of the sample calculation below were surprising. A detached area can be quite large without excessive temperature rise. For example, for the typical values of intensity $I = 10^3 \text{ W/cm}^2$, film absorptance $A_f = 10^{-4}$, and film thermal conductivity $K = 5 \times 10^{-2} \text{ W/cm K}$, the temperature rise T in a detached area of diameter $D = 2 \text{ mm}$ is only 25 K.

This result is encouraging. However, the corresponding thermally induced stress has a typical value of $20 \text{ MPa} (3 \times 10^3 \text{ psi})$. Even though greater stresses have been measured in films (70 MPa , or 10^4 psi , is a fairly large value), this

value may cause further detachment of the already detached area. The larger detached area would have greater temperature. Thus a runaway condition resulting in damage could occur.

The detached area is assumed to be circular and thermally insulated from the substrate. A noninfinite thermal impedance could be included easily, but is not justified at this early state of investigation. Radiation and all other mechanisms of heat loss in the detached area other than the heat flow along the detached film into the substrate in the adjoining attached area are neglected. The temperature is measured with respect to the initial constant temperature of the coating and substrate; i.e. $T = 0$ at time $t = 0$. The film is assumed to absorb only a small fraction of the incident radiation. Thus, $\exp(-\beta_f l_f) \approx 1 - \beta_f l_f$, and the absorptance is $A_f \approx \beta_f l_f$ as before.

It will be argued below that in cases of interest the heat flow from the edge of the detached film into the substrate is sufficiently rapid to maintain $T \approx 0$ at the edge of the detached area, at $\rho = \frac{1}{2}D$, where ρ is the cylindrical radial variable. This reduces the problem to the trivial one of heat generated at the constant rate $I\beta_f$ throughout a cylinder whose surface at $\rho = \frac{1}{2}D$ is held at temperature $T = 0$. With this boundary condition, the steady-state heat-flow equation

$$-K\nabla^2 T = -\frac{K}{\rho} \frac{\partial}{\partial \rho} \rho \frac{\partial}{\partial \rho} T = I\beta_f$$

has the solution

$$T = \frac{I\beta_f}{4K} \left[\left(\frac{1}{2}D \right)^2 - \rho^2 \right] , \quad (9.1)$$

which is easily verified by substitution. The maximum temperature, at $\rho = 0$, is

$$T_{mx} = I\beta_f D^2 / 16 K . \quad (9.2)$$

Notice the linear dependence of the maximum temperature on the detached area, $T_{mx} \sim D^2$. The proportionality of T_{mx} to β_f , rather than to $A_f = \beta_f \ell_f$, is a result of the fact that T_{mx} must be independent of ℓ_f since the heat flow in the detached coating is radial, thus making the problem equivalent to that of radial heat flow in an infinitely long cylinder.

With the values of the parameters in (3.3) and $D = 2$ mm, the result (9.2) gives

$$T_{mx} = 25 K \quad (9.3)$$

as previously stated.

We must now check the assumption that the boundary condition $T \cong 0$ at $\rho = \frac{1}{2}D$ is valid. There are several simple models that give this result. The following is the most satisfactory. The heat flow out of the detached area, at $\rho = \frac{1}{2}D$, is

$$J = -K(dT/d\rho)_{\rho=D/2} .$$

With (9.1) this gives

$$J = \frac{1}{4} I\beta_f D . \quad (9.4)$$

This is the heat flow out of the area $\pi D \ell_f$.

The temperature rise at $\rho = \frac{1}{2}D$ is the same order of magnitude as that at the surface S in Fig. 9.1a for a semi-infinite medium with a heat flowing in at

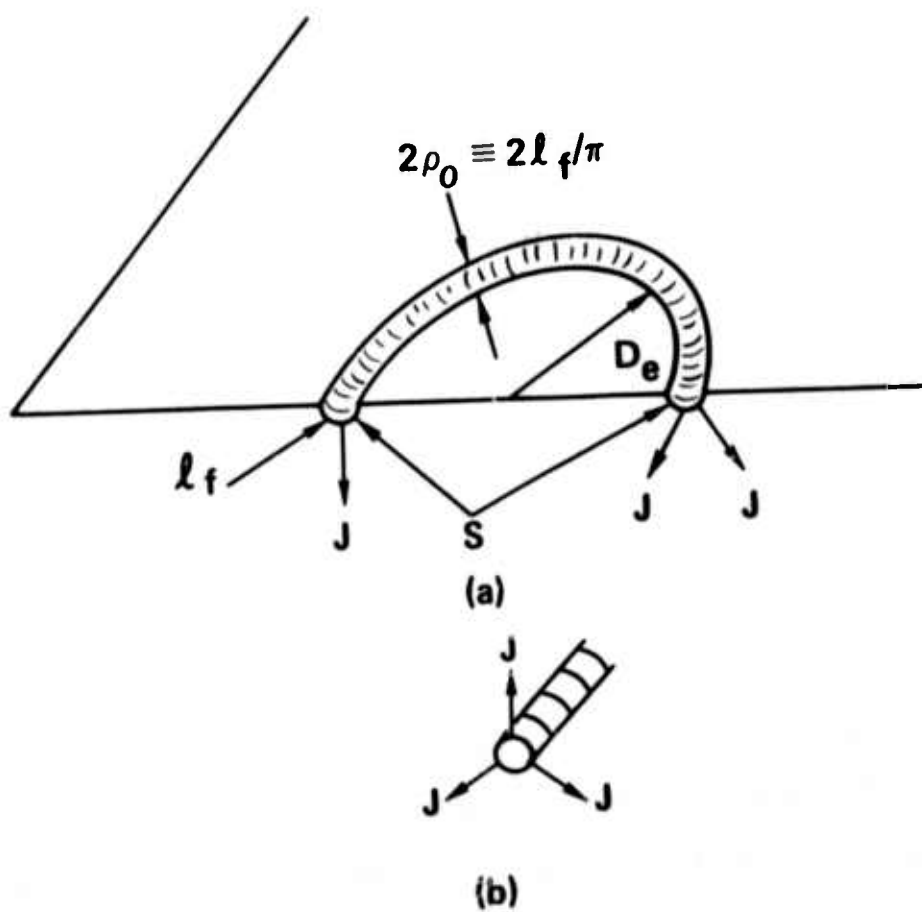


Fig. 9.1. Model heat-flow problems used in the argument
that $T \approx 0$ at the edge of a detached coating.

the hemitoroidal surface S . If the thermal diffusion distance

$$\ell_{th} = (4Kt/C)^{1/2}$$

is less than $\sim D_e$, it makes little difference if the circular source in Fig. 9.1a is replaced by an infinitely long straight-line source, and by symmetry this source in a semi-infinite medium can be replaced by a cylindrical source in an infinite medium, as shown in Fig. 9.1b.

It can be shown by direct substitution that

$$T = -C_1 Ei(-u) \quad . \quad u = Cp^2 / 4Kt \quad , \quad (9.5)$$

where the exponential integral is defined as

$$-Ei(-u) \equiv \int_u^\infty e^{-s} (e^{-s}/s) \quad ,$$

is a solution to the source-free thermal-diffusion equation

$$- \frac{K}{\rho} \frac{\partial}{\partial \rho} \rho \frac{\partial T}{\partial \rho} + C \frac{\partial T}{\partial t} = 0 \quad .$$

We are interested in large times ($t > Cp_0^2 / 4K \sim 10^{-7}$ sec), for which the approximation⁴⁸ $-Ei(-u) \approx \ln(\gamma u)^{-1}$, with $\gamma = 1.781$, is valid. Then, choosing the value of $C_1 = \rho_0 J / 2K$, where $\rho_0 = \ell_f / \pi$ (see Fig. (9.1a), with J given by (9.4) in order to give the same value of the heat flow in model problem and the real problem, roughly speaking, reduces (9.5) to

$$\frac{T_1}{2D} \approx \frac{I \beta_f D \ell_f}{8\pi K} \ln \frac{4\pi^2 K t}{\gamma C \ell_f^2} \quad . \quad (9.6)$$

With the values of the parameters from (3.3), the value of $T_{\frac{1}{2}D}$ from (9.6) is

$$T_{\frac{1}{2}D} = 0.30 \text{ K} . \quad (9.7)$$

This value of $T_{\frac{1}{2}D} = 0.30 \text{ K}$ is negligible with respect to $T_{mx} = 25 \text{ K}$ from (9.3), as we intended to show. If the time is increased from ten seconds to ten hours, the value of $T_{\frac{1}{2}D}$ is increased by a factor of only 1.6. The approximation $\ell_{th} \ll D_e$ is not satisfied for some cases of interest. For the case of $\ell_{th} \gg D_e$, other models could be used. However, this is not necessary since it is clear from the present model in Fig. 9.1a and the result (9.7) that $T_{\frac{1}{2}D} \ll T_{mx}$ is still satisfied when $\ell_{th} < D_e$ is not satisfied. Specifically, a great increase in the value of $T_{\frac{1}{2}D}$ over the value in (9.7) is not expected. There should be a very slight increase in the value of $T_{\frac{1}{2}D}$ as a result of the heat flow arriving from across the diameter in Fig. 9.1a. But there is a decrease in the value of $T_{\frac{1}{2}D}$ since the diffusion is in three dimensions (spherically) for $\ell_{th} \gg D_e$, whereas the heat diffuses in only two dimensions (cylindrically) for $\ell_{th} \ll D_e$.

Next consider the thermally induced stress resulting from the temperature rise of the detached area. A rough estimate will suffice. The stresses σ are related to the strains e by the elastic constant C_{el} . For the simple estimate, the usual sum⁷ is replaced by a single typical term

$$\sigma = E e \quad (9.8)$$

where E is Young's modulus and the typical strain e is given by

$$e = \alpha T_{av} . \quad (9.9)$$

Here α is the linear thermal expansion coefficient and T_{av} is the average temperature

$$T_{av} = \left(\frac{\pi}{4} D^2 \right)^{-1} 2\pi \int_0^{D/2} d\rho \rho T .$$

With T given by (9.1) and (9.2), evaluating the integral gives

$$T_{av} = \frac{1}{2} T_{mx} . \quad (9.10)$$

Comparing (9.8)-(9.10) gives

$$\sigma = \frac{1}{2} E \alpha T_{mx} \quad (9.11)$$

The value of Young's modulus does not vary greatly from material to material, a factor of ten variation from one material to another being very large. For example, KC1 has a small value, $E = 29 \text{ GPa} = 4.3 \times 10^6 \text{ psi}$ at room temperature, while sapphire has a large value, $340 \text{ GPa} = 5.0 \times 10^7 \text{ psi}$. We choose the average, $E = 170 \text{ GPa} = 2 \times 10^7$ as a representative value. The thermal expansion coefficient has a representative value of $\alpha = 10^{-5} \text{ K}^{-1}$ ($\alpha = 0.7 \times 10^{-5} \text{ K}^{-1}$ for ZnSe and $\alpha = 3.6 \times 10^{-5} \text{ K}^{-1}$ for KC1). With these values of E and α , (9.11) and (9.3) give

$$\sigma = 21 \text{ MPa} = 3.1 \times 10^3 \text{ psi} . \quad (9.12)$$

It is possible that this value of stress could cause further detachment. As already mentioned, greater values of stress have been measured in films. However, since this stress is applied to the crack at the border of the detached area, further opening of the crack could result. The increased value of D causes an increase

in the value of T_{mix} according to (9.2). The stress is therefore increased, and a runaway situation should result.

It could also happen in some cases that the coating itself could fracture, thus tending to isolate the detached area thermally. For a thermally isolated area of the coating, all of the energy $I A_f \Delta t_p = I \beta_f \ell_f \Delta t_p$ absorbed in the volume $\Delta \ell_f$ appears as heat in this volume. Thus, equating this energy absorbed to $C \Delta \ell_f T$ gives⁴⁶

$$T = I \beta_f t_p / C = 2.5 \times 10^3 \text{ K} . \quad (9.13)$$

Thus, the coating materials of interest would melt if they became thermally isolated. There is a remote possibility that a melted area of the film could be self healing after the laser is turned off in some special cases, but this is unlikely in general.

In pulsed operation, for short pulse durations $t_p \ll \tau_\ell$, where $\tau_\ell \equiv C \ell_f^2 / 4K$ has a typical value of $0.4 \mu\text{s}$ according to (8.11), the detachment causes little additional temperature rise since diffusion into the substrate already was negligible. For very long pulse durations $t_p \gg \tau_D$, where $\tau_D \equiv C (\frac{1}{2} D)^2 / 4K$ has a typical value of $2.5 \times 10^{-2} \text{ s}$ for detached diameter $D = 1 \text{ mm}$, the above steady-state results are approached. For intermediate pulse durations $\tau_\ell < t_p < \tau_D$, the detachment causes a greater temperature rise

$$T \approx I A t_p / C \ell_f$$

than the corresponding value $T = I A t_p / C \ell_{z=0}$, with $\ell_{z=0} = (\pi K t_p / 4C)^{1/2}$, for unimpeded diffusion into the substrate.

X. GUIDELINES FOR SELECTING NEW MATERIALS

Figure-of-merit-type analyses, which were useful for window materials, are not appropriate for selecting coating-material candidates since the coatings must satisfy a number of independent requirements. Thus, the following guidelines for selecting candidates are given in place of the figures of merit:

- The value of the bulk absorption coefficient β_b must be less than a required value such as 0.5 cm^{-1} .
- If the recommendations of Sec. II fail to produce values of the film absorption coefficient β_f less than 0.5 cm^{-1} (for materials with $\beta_b < 0.5 \text{ cm}^{-1}$), a guideline for obtaining $\beta_f < 0.5 \text{ cm}^{-1}$ will be sought.
- The value of the index of refraction n_r must be within the required range.
In multilayer coatings, at least one low-index and one high-index material is required.
- The thermal-expansion-mismatch stress must be sufficiently small to prevent failure. Other available information on stress should be used, as discussed in the text.
- Nonhygroscopic materials are desirable, although it may be possible that hygroscopic materials can be used as an inside layer of a multilayer stack.
- High-purity, single-crystal starting materials must be available or obtainable. The single-crystal requirement may be relaxed later in the program.
- Materials must be nonradioactive and nontoxic for some applications.
- The hardness of the outside materials should be great for coatings that must withstand abrasion.

- Previous experience with the materials in question should be considered, but caution is required to avoid misleading negative results.

- The following properties are desirable, but are difficult to predict for new materials that have not been prepared previously in thin-film form:

film packing density

stability (water or other chemical attack, thermal or photo decomposition)

deposition compatibility in multilayer coatings

adhesion to substrate

stoichiometric in thin-film form

no adverse diffusion effects at interface.

Figure-of-merit and general broad-brush analyses, such as the figure-of-
merit analyses for window materials that were developed previously,⁵⁻⁸ would
be extremely useful for coatings materials. Unfortunately, figures of merit are
not useful for coatings materials at present. For window materials, values of
the total power through a window under various conditions were convenient figures
of merit.⁶⁻⁸ The dependence $P(\beta, \sigma, C, K, \dots)$ of the power P , calculated by
making simplifying assumptions, on such parameters as the absorption coeffi-
cient β , material strength σ , heat capacity C , and thermal conductivity K clearly
shows the relative importance of these parameters. For example, diamond is a
good material in some applications because its great strength and thermal con-
ductivity more than compensate for its high $10.6\mu\text{m}$ absorption coefficient.

Coatings on the other hand must satisfy a number of independent require-
ments. For example, coatings must have good adhesion to the substrate,

homogeneity, stability in the atmosphere, and low absorptance, reflectance, and scattering. Failure to achieve any one of these properties makes the coating unacceptable, no matter how good the other properties are. An absorptance of 10^{-10} would not compensate for the inability to adhere to the substrate. Thus the figures of merit must be replaced by a set of individual requirements.

At the present stage of high-power infrared coatings studies, a major problem is the extra optical absorption in films. The source of this extra absorption is not presently known. Thus it has been difficult in the past to judge the probability of success of any new coating materials, and there have been no guidelines for selecting new candidate materials. Since such guidelines would be extremely useful, a preliminary set will now be discussed. Our recommendation that no new materials be studied in nonoptimum deposition systems should be kept in mind in the current discussion of new materials.

There are no magic formulas, calculations, or results for selecting materials. Only the simple application of what is presently known can be used. Unfortunately the current state of knowledge of films is not sufficiently complete to allow a totally satisfactory set of guidelines to be developed. For example there is no way to tell in advance if a given coating material will adhere well to a given substrate. In spite of the difficulties, using the guidelines should greatly enhance the probability of selecting a satisfactory coating material.

One problem in selecting the most promising coating materials is that the values of β_f of new materials are not known, and even the values of β_b are not known for some film materials. Sufficiently accurate estimates of the values of β_b often can be made by using known tendencies of changes in β with material

and crystal-type changes in conjunction with known values of β for similar materials.⁵⁸ There is no reliable way of estimating the values of β_f since the physical source of the large observed values of β_f is not yet known. Thus, materials will be selected on the basis of their bulk absorption coefficients. Indeed, the first task of the near-term program will be to obtain low values of β_f of the chosen materials.

The first and most important guideline is that the bulk absorption coefficient must be less than the desired value, such as 0.5 cm^{-1} as discussed in Sec. III. Even though this value of $\beta_b = 0.5 \text{ cm}^{-1}$ is extremely high with respect to the typical value of 10^{-4} cm^{-1} for bulk materials, this guideline still eliminates a great number of materials that come under consideration, as will be seen in Sec. XI on candidate $10.6 \mu\text{m}$ coating materials. For example, the absorption is too great in the oxides for which the $10.6 \mu\text{m}$ absorption coefficient is known. Other oxides for which the bulk absorption coefficient at $10.6 \mu\text{m}$ is not known are considered poor candidates for this wavelength since the absorptance of a number of oxides is known to be high. As another example, the $10.6 \mu\text{m}$ bulk absorption coefficient of the fluorides is marginal. The values of $\beta_b = 50 \text{ cm}^{-1}$, 18 cm^{-1} , and 3 cm^{-1} for lithium fluoride, magnesium fluoride, and calcium fluoride, respectively, are too great. The absorption coefficient of $1-2 \text{ cm}^{-1}$ for lanthanum fluoride is marginally too great, while the values 0.17 cm^{-1} and 0.5 cm^{-1} for barium fluoride and sodium fluoride, respectively, are sufficiently small.

Depending on the outcome of the experiments to eliminate the extra film absorption, a guideline on film absorptance may be inserted at this point. If the film absorption coefficient cannot be reduced to the desired value (such as 0.5 cm^{-1}), the expected value of the film absorptance will be a major factor in

selecting the best candidates. Specific guidelines for this selection will be sought if this inability to reduce the film absorption coefficient comes to pass.

The second guideline is simply that the value of the index of refraction n_r must be in the required range. Since all serious coating candidates now contain at least two layers, materials having both high and low values of refractive index are needed. This serves as a convenient criterion for dividing coating materials into two classes. In the following section, low- and high-index materials are considered separately.

The third guideline is that the film stress resulting from the mismatch of the thermal expansion coefficient of the film and substrate should not be sufficiently great to cause the film to crack, peel or be removed from the substrate. As discussed in Sec. VI, the thermal expansion mismatch contribution to the stress can be calculated with sufficient accuracy that failure can be predicted. Thus this calculation should be made for every film-substrate combination. Unfortunately, the thermal expansion mismatch contribution to the stress usually is smaller than the intrinsic and contamination contributions to the stress. These two larger contributions to the stress cannot be calculated with the accuracy with which the thermal expansion mismatch contribution can be calculated. Nevertheless some investigators in the field believe that some estimates of the intrinsic contribution to the stress can be made based on known stresses for a large number of previously deposited coatings. Based on information in the literature and discussions with workers in the field these estimates of the values of intrinsic stress are available only in the private files of individual coatings companies.

The next few guidelines involve known bulk properties of materials. The fourth guideline is that it would be desirable to have a material that is not

hygroscopic, although this is not presently an absolute necessity. First it may be possible that hygroscopic materials can be used as inside layers in multi-layer stacks. Second, it is possible that extremely thin hygroscopic polymer layers may be used on coatings to prevent water from penetrating the coating. Third, for substrates that are water sensitive, the problem of hygroscopicity of the coatings is somewhat less important since the substrate materials themselves already must be protected from water.

The fifth guideline is that the coating material must be available as a deposition starting material in high-purity single-crystal form. The requirement for a single-crystal starting material may be relaxed in the future, but should be retained in the ultraclean deposition experiment of the near-term program,¹ as discussed in Secs. VI and II.

The sixth guideline is that the material should be nonradioactive and non-toxic. In some applications these requirements may not be necessary. Indeed, thorium tetrafluoride, which is radioactive, is one of the most popular current coating materials. At the present time there is some controversy over the importance of radioactivity, as discussed in Sec. VI. As another example, thallium iodide is a good current candidate for high-power $10.6 \mu\text{m}$ coatings, and KRS5, which also contains the toxic material thallium, has been used as an infrared transmitting material for many years.

The seventh guideline is that the material should be hard. Again, this is not an absolute necessity for all systems; however, it will be necessary for the outside layer of coatings that must withstand abrasion.

In addition to the guidelines above, the following properties of coating materials are desirable but are difficult to predict for new materials that have not been prepared previously in thin-film form:

macroscopic porosity

stability (water or other chemical attack, thermal or photo decomposition)

deposition compatibility in multilayer coatings

adhesion to the substrate

stoichiometry in thin-film form

no adverse diffusion effects at the interface.

Unfortunately this list of properties that are difficult to predict contains some of the most important properties of the film. For example, the films obviously must adhere well to the substrate and be stable. The macroscopic porosity must be extremely low in order to avoid absorptance of water, which increases the optical absorption, as discussed in Sec. IV.

XI. CANDIDATE $10.6 \mu\text{m}$ COATING MATERIALS

Since there are no coatings available with $A_f = 10^{-4}$ for any of the infrared frequencies of interest, and only a small handful of coating materials have been investigated, it is important to select new candidates with the highest probability of success. Of the materials considered to date, the following are chosen as the best candidates for $10.6 \mu\text{m}$ coatings:

- ThF_4
- $\text{Na}(\text{F}, \text{Cl})^{59}$
- KCl
- $(\text{Ba}, \text{Sr})\text{F}_2$
- KGaF_4 and other Cryolite-type materials
- $\text{As}_2(\text{S}_3, \text{Se}_3)$
- $\text{Zn}(\text{S}, \text{Se})$
- TlI

A typical goal for absorption in window materials is $\beta_b = 10^{-4} \text{ cm}^{-1}$. Fortunately, such a low value is not required in coating materials since the coatings are so much thinner than the windows themselves (and the heat generated in the coating diffuses into the window). As discussed in Sec. III, a value of absorptance $A_f = 10^{-4}$, which corresponds to $\beta = 0.5 \text{ cm}^{-1}$ for $l_f = 2 \mu\text{m}$, is desired. At the chemical-laser wavelengths, slightly greater values of β can be tolerated since smaller values of l_f can be used. For example, at $2.8 \mu\text{m}$, a value of $\beta = 2 \text{ cm}^{-1}$ may be tolerable.

This greater value of β for coating materials than for window materials means that there are many more candidate materials for coatings than for windows. As in the early days of selecting candidate materials for high-power laser windows, some gross selections must be made in order to reduce the thousands of materials to a manageable few that can be studied further in order to choose several materials to study experimentally. The guidelines of the previous section were developed to aid in this selection.

Table 11.1 contains a collection of values of refractive Indices n_r and bulk and film absorption coefficients β_b and β_f at 10.6, 5.3, 3.8, and 2.8 μm . Table 11.2, taken from Ritter's article,^{*2} contains a collection of useful information on a number of coatings. The precise meaning of the transmittance range is not known. It does appear that the upper wavelength must be greater than 15 μm in order for $\beta_f \approx 0.5 \text{ cm}^{-1}$ to be satisfied. For example, the transmittance range of ThF_4 is listed as 0.2-15 μm , and the 10.6 μm value of β_f probably is $\beta_f \approx 10 \text{ cm}^{-1}$. The range for ZnS is 0.4-14 μm , and the 10.6 μm value of β_f probably is $\beta_f \approx 2 \text{ cm}^{-1}$. There may be exceptions to this greater-than-15 μm rule. For example, ZnS, with transmission to 14 μm , has $\beta_b \approx 0.15 \text{ cm}^{-1}$, and recently $\beta_f < 1.4 \text{ cm}^{-1}$ was measured.^{*14}

Table 11.3 and Fig. 11.1, from the Handbook of Military Infrared Technology,³⁰ contain the transmission regions and the values of n_r (and dispersion) for several wavelength regions. Table 11.4 lists properties of coating stacks that have been developed for use at 10.6 μm .

Useful sources of information on values of parameters of materials include the following: "Harshaw Optical Crystals" catalog; Compendium on High-Power

Table 11.1. Properties of Infrared Coating Materials.^v

Material	10.6 μm			5.3 μm			3.8 μm			2.8 μm		
	n_r	$\beta_f(\text{cm}^{-1})$	$\beta_b(\text{cm}^{-1})$	n_r	$\beta_f(\text{cm}^{-1})$	$\beta_b(\text{cm}^{-1})$	n_r	$\beta_f(\text{cm}^{-1})$	$\beta_b(\text{cm}^{-1})$	n_r	$\beta_f(\text{cm}^{-1})$	$\beta_b(\text{cm}^{-1})$
LiF	1.222 ^d	40 ^{74, v}	0.5 ⁶²	1.299 ⁶²			1.309 ⁶²			1.314 ⁶²		
KF					1.330 ^{*75}		1.355 ^{*75}			1.365 ^{*75}		
MgF ₂			3 ⁶⁸	1.39 ^{*75}	4 E-4 ⁷⁷	1.41 ^{*75}				1.42 ^{*75}		
CaF ₂			0.46 ^{*3}	1.40 ^{*75}	4 E-5 ⁷⁷	1.41 ^{*75}				1.42 ^{*75}	5 E-4 ⁷⁷	3.7 E-4 ⁷⁷
SrF ₂							1.457			1.463	1-2 E-3 ⁷⁸	1-2 E-3 ⁷⁸
BaF ₂	1.395 ^{*9}	6 ^{10,b}	0.172 ^{*3} ±0.003	1.450 ^{*75}								
PbF ₂ ^f	1.73		10 ⁻² ₋₆ ⁷¹ $\times 10^{-2}$									
AlF ₃ ^g			≈ 250 ⁷⁹				1.17 ^{*5} ±0.03					
LaF ₃												
TlF ₃ ^j												
CeF ₃	1.63 ^{*2}		"to 14 μm ^{i,68}	1.59 ^{*75}			1.59 ^{*75}			1.59 ^{*75}		

Table 11.1. Properties of Infrared Coating Materials (Cont'd)

Material	10.6 μm			5.3 μm			3.8 μm			2.8 μm		
	n_r	$\beta_f(\text{cm}^{-1})$	$\beta_b(\text{cm}^{-1})$	n_r	$\beta_f(\text{cm}^{-1})$	$\beta_b(\text{cm}^{-1})$	n_r	$\beta_f(\text{cm}^{-1})$	$\beta_b(\text{cm}^{-1})$	n_r	$\beta_f(\text{cm}^{-1})$	$\beta_b(\text{cm}^{-1})$
PrF ₃	1.57*10	180*10,b										
YbF ₃	1.57*10		3.6*10									
ThF ₄ ^c	1.35*10	7-10 ^a	<1.2a,*9*10		0.69*14	<1*14						
			*14 & 4.1*81		on BaF ₂							
			on ZnSe		<0.36*14							
KGaF ₄												
NaAlF ₄			"to 14 μm "*68									
cryolite												
XZnF ₄ ⁿ												
LiCl												
NaCl	1.483 ⁶²		3x10 ^{-4*38}		1.518 ⁶²							
KCl	1.46*10	<0.6*10,0	7x10 ^{-5*15}									
RbCl												
CsCl												

Table 11.1. Properties of Infrared Coating Materials (Cont'd)

Material	10.6 μ m			5.3 μ m			3.8 μ m			2.8 μ m		
	n_r	$\beta_f(\text{cm}^{-1})$	$\beta_b(\text{cm}^{-1})$	n_r	$\beta_f(\text{cm}^{-1})$	$\beta_b(\text{cm}^{-1})$	n_r	$\beta_f(\text{cm}^{-1})$	$\beta_b(\text{cm}^{-1})$	n_r	$\beta_f(\text{cm}^{-1})$	$\beta_b(\text{cm}^{-1})$
CuCl	1.88-1.93	6 E-3								2.003		
AgCl ⁱ	1.978	E-2										
PbCl ₂ ^h		$\ll 3.4 \times 10^{-269}$										
KBr		$\ll 3.4 \times 10^{-269}$										
AgBr		$\ll 10^{-4}$										
TlBr		7.3 E-3										
		11.8 *81 on KCl										
CuI			$10^3 *81$									
TlF ^e	2.34	$\ll 1 *19.79 \sim 10^{-4}$										
		on KCl										
TlI-KCl graded			25 *19									
KRS-5 (TlI-TlBr)			$\ll 4.5 *66$ on KCl									
ZnS	2.1 *10	$2.4 *10^b \sim 0.15 *14$ $\ll 1.4 *14$ on ZnSe		2.20 *77 $\ll 0.1 *14$ on ZnSe						2.22 *77		2.24 *77

Table 11.1. Properties of Infrared Coating Materials (Cont'd)

Material	10.6 μm				5.3 μm				3.8 μm				2.8 μm			
	n_r	$\beta_f(\text{cm}^{-1})$	$\beta_b(\text{cm}^{-1})$	n_r	$\beta_f(\text{cm}^{-1})$	$\beta_b(\text{cm}^{-1})$	n_r	$\beta_f(\text{cm}^{-1})$	$\beta_b(\text{cm}^{-1})$	n_r	$\beta_f(\text{cm}^{-1})$	$\beta_b(\text{cm}^{-1})$	n_r	$\beta_f(\text{cm}^{-1})$	$\beta_b(\text{cm}^{-1})$	
CdS																
As ₂ S ₃	2.38 ^{*10}	0.77 ^{*10,b}	0.77 ^{*10}	≤ 2.4 on ZnSe				0.32 ^{*14}	5 $\times 10^{-3}$ ^{*14}							
Sb ₂ S ₃								<0.5 ^{*14}	3-10 $\times 10^{-4}$ ^{*14}							
ZnSe	2.42 ^{*9}	1.2 ^{*9}	4 E-77					on BaF ₂	4 E-4 ⁷⁷							
As ₂ S ₃ ^k	2.403 ⁷⁷						0.11 ⁸²									
ZnTe	3.0 ^{*10}	2.4 ^{*10,b}														
CdTe	2.57 ^{*10}	≤ 1.2 ^{*10,b}	6 E-4 ⁸³	~ 2 ^{*10,o}				on CdTe								
AlP																
GaP							0.39									
GaAs							10 ⁻² ^{*71}									

Table 11.1. Properties of Infrared Coating Materials (Cont'd)

Material	10.6 μm			5.3 μm			3.8 μm			2.8 μm		
	n_r	$\beta_f(\text{cm}^{-1})$	$\beta_b(\text{cm}^{-1})$	n_r	$\beta_f(\text{cm}^{-1})$	$\beta_b(\text{cm}^{-1})$	n_r	$\beta_f(\text{cm}^{-1})$	$\beta_b(\text{cm}^{-1})$	n_r	$\beta_f(\text{cm}^{-1})$	$\beta_b(\text{cm}^{-1})$
AISb				0.3								
Si	3.41			1-3								
Ge	4.8 *10 ¹⁰	18 *10 ^b	1.5 E-2	10								
				amorphous								
S(amorphous)m												
Se(amorphous) ^t												
Te(amorphous)												
T11173 glass					2 E-2							

a) The following information on the value of β_f at 10.6 μm was kindly furnished by Mr. A. Braunstein:⁶³ Values of $\beta_f = 7 - 10 \text{ cm}^{-1}$ can be obtained consistently for KCl and ZnSe substrates. Values of 3-4 cm^{-1} can be obtained for deposition on molybdenum. A value of $\beta_f < 1.2 \text{ cm}^{-1}$ was obtained for one film on molybdenum and a value of 3.5 cm^{-1} was obtained for one film on KCl. Extreme care in measurements is required for such low values of β_f .

- b) These values of β_f were measured for films grown on KCl and/or metallic substrates.
- c) Thorium is radioactive.

Table 11.1. Properties of Infrared Coating Materials (Cont'd)

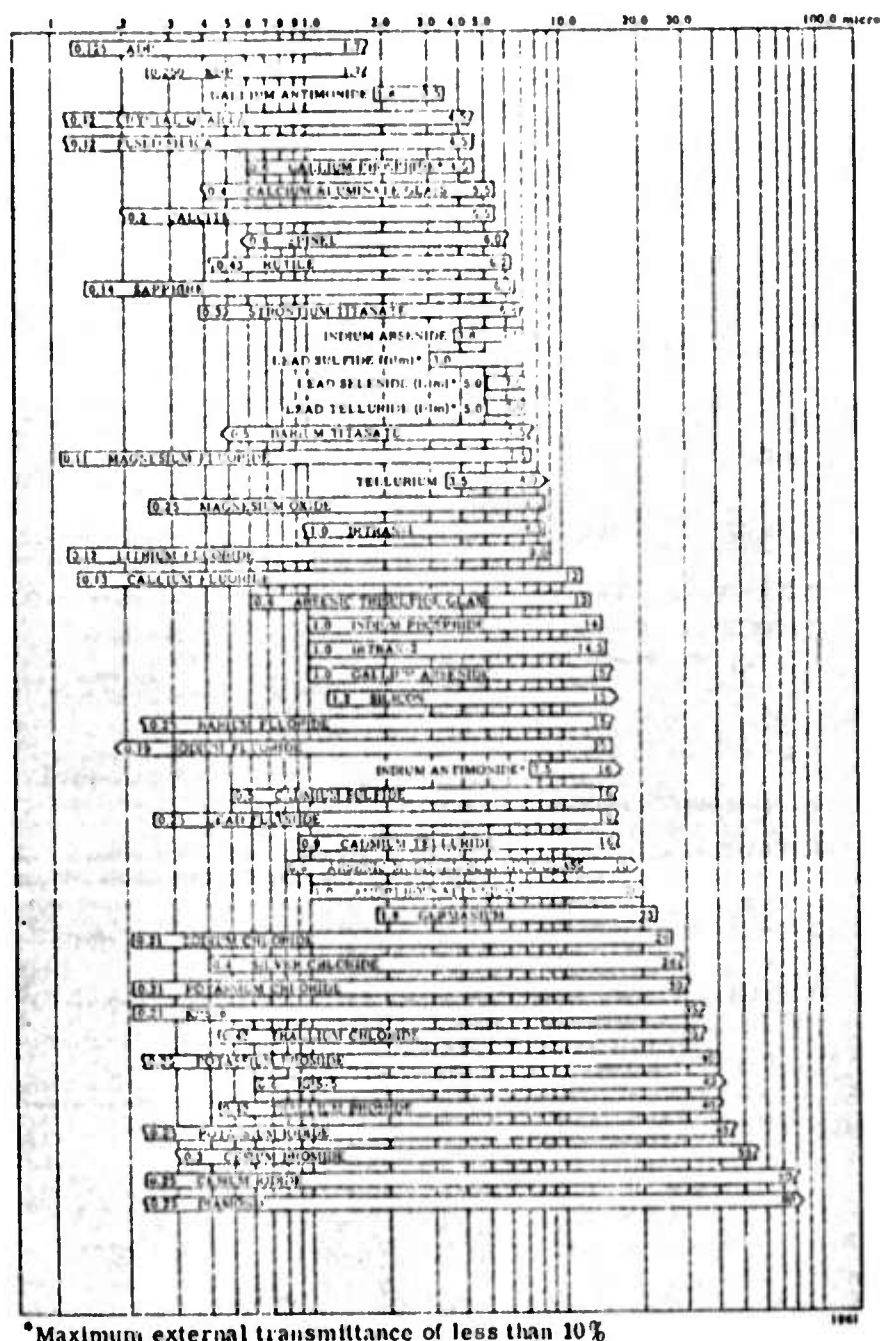
- d) AIP Handbook, p. 6-83: Thin films of sodium fluoride are easy to grow. Sodium fluoride is less soluble than potassium chloride and sodium chloride. Sodium fluoride was independently suggested by Dr. H. E. Bennett.
 - e) Thallium is toxic.^{*2}
 - f) AIP Handbook, p. 6-92: Lead fluoride was used as a coating on Ti11173 glass.
 - g) Reference *2, p. 33: Alumnum fluoride is "transparent to 10 μm ."⁶⁸
 - h) AIP Handbook, p. 6-89: Lead chloride was used as an antireflection coating for indium antimonide.
 - i) Silver chloride is insoluble in water. Its hardness lies between the values for sodium chloride and potassium chloride. Ritter^{*2} says silver chloride is a good coating material.
 - j) Thallium is toxic.^{*2}
 - k) AIP Handbook, p. 6-91: Arsenic triselenide melts at 400 C.
 - l) AIP Handbook, p. 6-80: The amorphous or vitreous form of selenium is fairly stable below 50 C but converts to trigonal form at higher temperatures; AIP Handbook, p. 6-82: Selenium films have been used successfully to protect sodium chloride from attack by moisture.
 - m) AIP Handbook, p. 6-84: Rhombic sulfur is not hygroscopic. The bulk absorption coefficient has a value of approximately 1 cm^{-1} at 10.6 μm . Films are easy to prepare.
 - n) X = Na, K, Rb, or Cs and Z = Ga, In, or Tl.
 - o) These are self films (e.g., KC1 on CdTe on CdTe).
- ▼ The superscripts on the values in this table are reference numbers.

Table 11.2. Film materials and thin film properties, from Ref. *2.

Starting material	Deposition method* and approximate evaporation temperature	Film composition	Film crystal structure and packing density ρ at substrate temperature T_s ; film stress S	Refractive index n at wavelength and substrate temperature T_s	Transmittance range (μm)
Na_3AlF_6	B (1000°C)	Depending on boat temperature	crystalline, $\rho = 0.88$ ($T_s = 30^\circ\text{C}$) $\rho = 0.93$ ($T_s = 190^\circ\text{C}$) S : low tensile	1.32-1.35 depending on film composition	0.2-14
MgF_2	B (1250°C)	MgF_2	crystalline $\rho = 0.72$ ($T_s = 30^\circ\text{C}$) $\rho = 0.96$ ($T_s = 300^\circ\text{C}$) S : high tensile	1.32-1.39 at 550 nm in vacuum, depending on T_s , 1.38-1.40 at 550 nm in air (depending on T_s)	0.11-4 (cracking)
SiO_2	E	SiO_2	amorphous $\rho = 0.9$ ($T_s = 30^\circ\text{C}$) $\rho = 0.98$ ($T_s = 150^\circ\text{C}$) S : compressive	1.45-1.46 at 550 nm	0.2-9
ThF_4 , ThOF_2	B (1100°C)	ThF_4	X-ray amorphous S : medium tensile	1.52 at 550 nm and $T_s = 35^\circ\text{C}$	0.2-15
SiO	B, R (1250-1350°C)	Si_2O_5	amorphous	1.55 at 550 nm ($T_s = 30^\circ\text{C}$)	0.4-9
Al_2O_3	E (2050°C)	Al_2O_3	amorphous	1.50 at 550 nm and $T_s = 40^\circ\text{C}$, 1.63 at $T_s = 300^\circ\text{C}$.	0.2-7
CeF_3	B (1350°C)	CeF_3	crystalline S : high tensile	1.43 at 550 nm and $T_s = 300^\circ\text{C}$	0.3-5
MgO	E (2800°C)	MgO	crystalline	1.70 at 550 nm and $T_s = 50^\circ\text{C}$, 1.74 at $T_s = 300^\circ\text{C}$	0.2-8
SiO	B (1250-1350°C)	SiO	amorphous	2.0 at 550 nm and $T_s = 30^\circ\text{C}$	0.7-9
ThO_2	E (3050°C)	ThO_2		1.95 at 300 nm	0.3
PbF_2	B (850°C)	PbF_2	β - PbF_2 , S : depending on thickness compressive or tensile	1.75 at 550 nm 1.98 at 300 nm ($T_s = 30^\circ\text{C}$)	0.3-17
ZrO_2	B or E (2700°C)	ZrO_2		1.97 at 550 nm ($T_s = 30^\circ\text{C}$) 2.05 ($T_s = 200^\circ\text{C}$)	0.34-12
CeO_2	B or E (1600°C)	CeO_2	crystalline		0.4-12
TiO	B, R (1750°C)	TiO_2	amorphous at room temperature, crystalline at higher T_s , S : high tensile	1.9 at 550 nm ($T_s = 30^\circ\text{C}$) 2.3 at 550 nm ($T_s = 220^\circ\text{C}$) 2.55 at 550 nm ($T_s = 260^\circ\text{C}$)	0.1-3 (clouding)
ZnS	B (1200°C)	ZnS	crystalline S : medium compressive	2.3 at 550 nm ($T_s = 30^\circ\text{C}$)	0.4-14
Si	B or E (1500°C)	Si	amorphous up to $T_s = 300^\circ\text{C}$	3.4 at 3 μm	1-9
Ge	B or E (1600°C)	Ge	amorphous up to $T_s = 300^\circ\text{C}$	4.4 at 2 μm ($T_s = 30^\circ\text{C}$)	2-23
PbTe	B (550°C)	PbTe		5.6 at 5 μm	3.5-20

* B, boat; E, electron beam; R, reactive.

Table 11.3. Transmission regions of optical materials, 2 mm thickness; cutoff is defined as 10 percent external transmittance, and materials marked with an asterisk never have external transmittance as high as 10 percent. A bar with a straight vertical ending indicates that the cutoff exists at the wavelength represented by the end of the bar exactly as defined above; a bar with an S-shape ending represents a material which cuts off at approximately that wavelength; a bar ending in an angle indicates that the material transmits at least to that wavelength, and probably further. From Ref. 30.



*Maximum external transmittance of less than 10%

Table 11.4. Properties of High-Power Infrared Coatings.

Coating	Substrate	Δ_f %	R %	λ μm	Ref.	Date of Report
$\text{As}_2\text{S}_3/\text{ThF}_4^{84}$	KCl	0.19	0.03	10.6	10	Feb. '75
ZnSe/ThF_4	KCl	0.24	0.02	10.6	10	Feb. '75
		0.17	--	10.6	10	Feb. '75
ZnSe/ZnS	KCl	0.05	5	10.6	11	July '73
BaF_2/ZnS	CdTe	0.06	0.15	10.6	11	July '73
ZnS/ThF_4	CdTe	0.25	0.15	10.6	11	July '73
$(\text{ZnSe}/\text{ThF}_4)^3$	KCl	<0.1	0.2	10.6	11	July '75
TlI/ThF_4	KCl	0.26	0.09 @ $9.5 \mu\text{m}$	10.6	12	July '75
ThF_4/ZnSe	ZnSe	0.03		10.6	3	July '75
$\text{ZnSe}/\text{ThF}_4^a$	KCl				8	Feb. '75
ThF_4/ZnSe	KCl	0.24 -0.40		10.6	8	Feb. '75
$\text{As}_2\text{S}_3/\text{ThF}_4$	KCl	0.19	<0.03	10.6	8	Feb. '75
BaF_2/ZnS	ZnSe	0.11	0.23	10.6	82	
ThF_4/ZnSe	ZnSe	0.03	0.03	10.6	82	
ThF_4/ZnS	ZnSe	0.06	0.02	10.6	82	
ThF_4/ZnS	ZnSe	0.07	0.2	10.6	83	
BaF_2/ZnS	ZnSe	0.12	0.1	10.6	83	
ThF_4/ZnSe	15 cm diam. ZnSe	0.08	0.06	10.6	92	

a. cracked and peeled upon removal from vacuum system ($10^{-6}-10^{-7}$ torr)

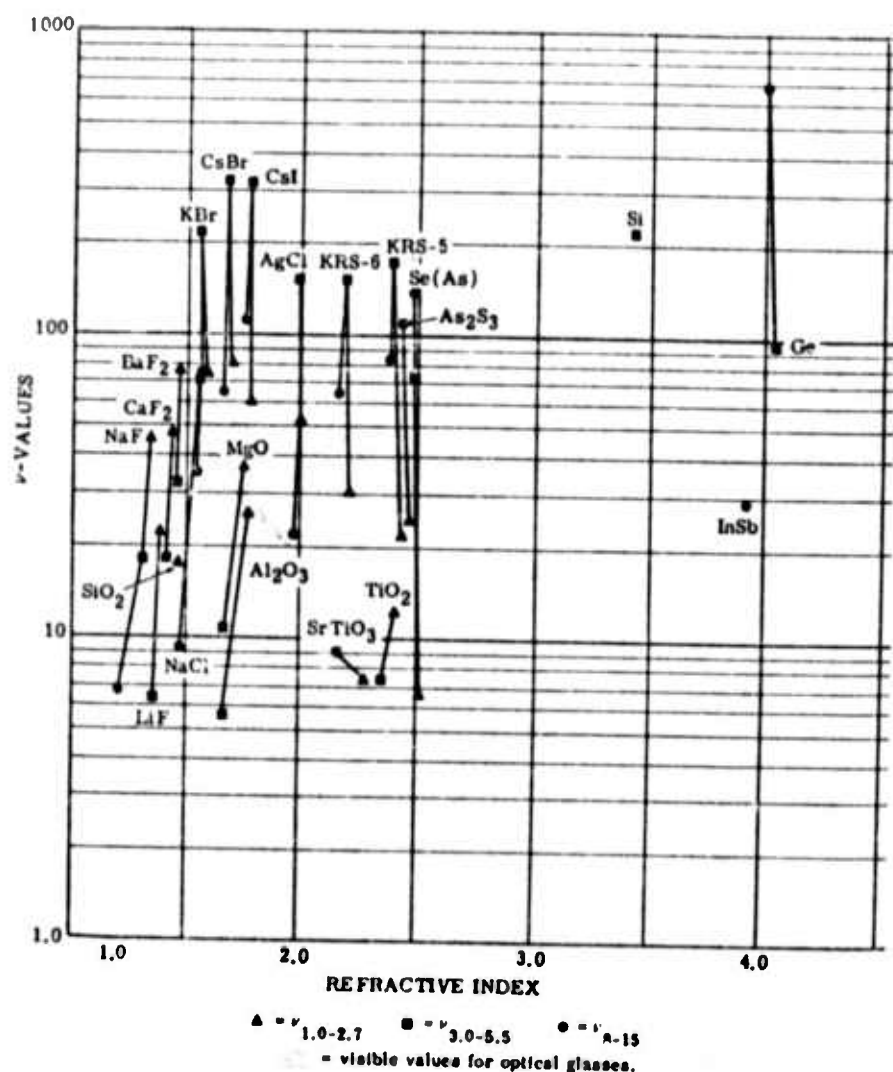


Fig. 11.1. Reciprocal dispersion of some infrared optical materials; from Ref. 30.

Infrared Laser Window Materials;⁶⁰ Infrared Laser Window Materials Property Data for ZnSe, KCl, NaCl, CaF₂, SrF₂, BaF₂, Stanley Dickinson, Air Force Cambridge Research Laboratories Report AFCRL-TR-75-0138; ^{*61} American Institute of Physics Handbook;⁶² and the Handbook of Military Infrared Technology.³⁰

Best Low-Index Candidates

A specific coatings problem is to find a low-index replacement for ThF₄, which is radioactive and whose accepted absorption coefficient $\beta_f = 10 \text{ cm}^{-1}$ (however, see note (a) of Table 11.1) is greater than the desired value of $\beta_f = 0.5 \text{ cm}^{-1}$. The most likely choice, based on the requirement of a small index of refraction, is another fluoride. The second choice would be a chloride, but the fluorides are generally physically superior to the chlorides, bromides, and iodides.

Halogenides in general and fluorides especially belong to a class of materials that can easily be evaporated and condensed stoichiometrically. One disadvantage is that some fluorides and in particular chlorides and bromides are quite soluble in water. The most important fluorides are cryolite (generally speaking the compounds of NaF and AlF₃), MgF₂, and ThF₄.

Consider the variation of the index of refraction from material to material. The index of refraction n_r of a low-loss dielectric is equal to the square root of the dielectric constant ϵ . For a crystal composed of two types of ions with polarizabilities α_+ and α_- , the Clausius-Mossotti expression⁵⁷ (in SI units)

$$\frac{\epsilon - 1}{\epsilon + 2} = \frac{N}{3\epsilon_0} (\alpha_+ + \alpha_-)$$

where N is the number of + or - ions per unit volume and $\epsilon_0 = 10^7 / 4\pi c^2$ is the permeability of free space, relates ϵ to the α 's for materials with $4\pi P/3$ local field correction. For no local field correction, the factor $\epsilon + 2$ is missing. In either case, ϵ (and n_r) decreases as the net polarizability $\alpha_+ + \alpha_-$ decreases and as the near-neighbor spacing $a_{nn} \sim N^{-1/3}$ increases. Fluorides generally have smaller refractive indices than chlorides, bromides, iodides, sulfides, selenides, tellurides, and arsenides because the polarizability of the fluorine ion is quite small. Positive ions tend to have lower polarizabilities than negative ions of the same mass, and more massive ions tend to have greater polarizabilities than lighter ions.⁵⁷ Sodium fluoride, with $\alpha_- = \alpha_F = 1.0 \times 10^{-24} \text{ cm}^3$, $\alpha_+ = \alpha_{Na} = 1.8 \times 10^{-25} \text{ cm}^3$, and $a_{nn} = 0.2317 \text{ nm}$ has the lowest known index of refraction, $n_r = 1.222$ at $10.6 \mu\text{m}$. The value of $(\alpha_+ + \alpha_-)/a_{nn}^3$ is lower for NaF than for "neighboring" compounds. With values of α and a_{nn} from Kittel,⁵⁷ we find:

$$\text{LiF: } \frac{0.652 + 0.03}{(2.014)^3} = 0.083$$

$$\text{NaF: } \frac{0.652 + 0.14}{(2.317)^3} = 0.064 \quad \leftarrow \text{min}$$

$$\text{KF: } \frac{0.652 + 1.33}{(2.674)^3} = 0.104$$

$$\text{RbF: } \frac{0.652 + 1.98}{(2.815)^3} = 0.118$$

$$\text{NaCl: } \frac{2.97 + 0.14}{(2.820)^3} = 0.139 \quad .$$

The most likely candidates for the ThF_4 replacements are NaF , KF , SrF_2 , KGaF_4 or another Cryolite-type material, NaCl , and KC1 . None of these materials are radioactive or toxic.

ThF_4 . Thorium tetrafluoride itself is one of the most promising low-index materials in spite of the fact that the commonly used value of $\beta_f = 10 \text{ cm}^{-1}$ is much greater than the desired value $\beta_f = 0.5 \text{ cm}^{-1}$. Note that $\beta_f < 1.2 \text{ cm}^{-1}$ has been measured in ThF_4 .^{*10} See note (a) on Table 11.1. The use of ThF_4 is restricted to cases in which the radioactivity can be tolerated. X-ray analyses indicate that ThF_4 films are amorphous. Cracked films look like cracked glass.^{*2}

The deposition temperature must be greater than 150°C to avoid OH absorption bands. Sputtering gives a fluorine deficiency, with grey or black color. Thick films, at least $3-4 \mu\text{m}$ thick, can be grown. Bulk samples have been grown at Bell Telephone Laboratories and at Hughes Research Laboratories. The bulk crystalline structure of ThF_4 is monoclinic. As mentioned in Sec. VI, Van Uitert and coworkers⁴⁰ recently found that a single crystal of ThF_4 had $\alpha \approx 2 \times 10^{-6} \text{ K}^{-1}$ for temperatures between 25°C and 400°C , and the total expansion $\alpha\Delta T$ for $\Delta T = 25^\circ\text{C} - 600^\circ\text{C}$ was zero. The crystal was not cracked by application of a blowtorch.

Considerable reduction of ThF_4 films on exposure to air has been reported.^{*2}

Thorium tetrafluoride films with $\beta_b < 1.2 \text{ cm}^{-1}$ have been grown on occasion, but values below $\sim 7-10 \text{ cm}^{-1}$ cannot be obtained consistently.⁶³

The following excerpt is from Ref. *10. "ThF₄ from five different sources was evaluated during the contract period. Material from British Drug House was found to contain high levels of metallic impurities (particularly iron) and yielded

highly absorbing films. ThF_4 crystallites obtained from Balzers A.G. contained carbon impurity and also yielded high absorption films. Material from American Potash was found to be acceptable if selected by lot. Certain lots produced films with absorption index of 1×10^{-4} or less, while others had a high ThO_2 content, which made deposition extremely difficult and yielded absorptions in the 1×10^{-3} region. Poly Research Corporation supplied material from several different lots that had no detectable impurities by emission spectrograph or X-ray microprobe analysis. This material melted cleanly in the Mo-box source and deposited films in the 1×10^{-4} absorption index range."

"The best and most consistent material obtained during the contract period was prepared at HRL by the reactive-atmosphere process (RAP). This process was used to purify commercial ThF_4 material, such as that obtained from British Drug House, by melting it in the presence of HF gas and subsequently to pull crystals from the melt. American Potash ThO_2 powder was also converted to ThF_4 by a wet process followed by drying of the ThF_4 powder in a gaseous HF environment and subsequent melting and crystal growth in gaseous HF. Either the processed and dried powder or the melted material was found to yield low-absorption films. The high-reflectance mirrors fabricated during the final part of the contract period contain ThF_4 from RAP melted ingots."

"Bulk absorption measurements were made on RAP-grown ThF_4 crystals for comparison with the film absorptions. An absorption index for the bulk crystals of approximately 3×10^{-4} was found. This is one of the few cases where film absorptions are less than those of the bulk, and it may be indicative of the fact that better bulk crystals can be prepared."

Ritter^{*2} states, "In recent years ThF₄ films have become important as low index material for dielectric mirrors, especially for the laser technique. Thorium fluoride as well as thorium oxifluoride can be used as a starting material. At 1000 C only thorium fluoride evaporates for either starting material. ThO₂ evaporates above 2000 C only. ThF₄ films are transparent from 0.2μm up to 15μm. The films are mechanically and chemically quite stable. The packing density seems to depend on the preparation conditions. Films with high packing density can be obtained. ThF₄ films show tensile stress on the order of 110-150 MPa (1.6×10^4 - 2.1×10^4 psi). At exposure to air an appreciable reduction occurs. ThF₄ films can be made quite thick without the formation of cracks or peeling off. This property makes them well suited for infrared applications. ThF₄ is very compatible with ZnS in multilayer coating, e.g., for laser mirrors."

"One obvious disadvantage of ThF₄ is its radioactivity. It is necessary to follow up the security measures provided for work with radioactive materials according to the regulations of the authorities."

NaF. Sodium fluoride has an acceptably low value of bulk absorption coefficient, $\beta_b = 0.5 \text{ cm}^{-1}$, but the film absorption coefficient β_f is not known. It has the lowest known index of refraction ($n_r = 1.222$ at $10.6 \mu\text{m}$). The water solubility of NaF (4.22 g/100 g water) is between that of LiF (0.27 g/100 g water) and that of KCl (34.7 g/100 g water) or of NaCl (35.7 g/100 g water). The Knoop hardness (Knoop 60, or 590 MPa) also is between that of LiF (Knoop 99, or ~970 MPa) and that of KCl (~Knoop 8, or ~80 MPa) or NaCl (~Knoop 17, or ~170 MPa). Thin films of NaF are easy to deposit.⁶² Dr. H. Bennett has suggested NaF as a replacement for ThF₄.³⁴

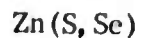
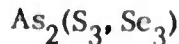
(Sr, Ba)F₂. Barium and strontium fluoride were selected as the most promising of the alkaline-earth fluorides, which have better physical and chemical properties than the alkali halides. The absorption is too great in CaF₂ ($\beta_b = 3 \text{ cm}^{-1}$). Barium fluoride, with $\beta_b = 0.17 \text{ cm}^{-1}$, would appear to be a better choice than SrF₂, with $\beta_b = 0.46 \text{ cm}^{-1}$. However, consistently fewer problems have been encountered with SrF₂ than with BaF₂. Since CaF₂ films are very porous and are not very stable, measurement of the packing density of SrF₂ films is especially important. Dr. Harold Posen and coworkers¹¹ agree that the alkaline-earth fluorides are good candidates.

KGaF₄ or other Cryolite-type materials. By Cryolite-type materials we mean materials containing⁵⁹ (Na, K, Rb, Cs)F plus (Al, Ga, In, Tl)F₃. Since the absorption of Cryolite (NaAlF₄) is expected to be too great at 10.6 μm but the films are otherwise quite good, replacing the light elements Na and Al by heavier elements K or Rb and Ga or In possibly could result in a satisfactory film material. Such materials are speculative since even the bulk materials apparently have not been studied, but we have not made a literature search of the materials.

(K, Na)Cl Potassium chloride is included in the list of low-index materials because $\beta_f < 0.6 \text{ cm}^{-1}$ already has been attained. If KCl is included, NaCl, with its lower water solubility and slightly greater Knoop hardness, should be considered also. The bulk 10.6 μm absorption coefficient of NaCl is $\beta_b \approx 3 \times 10^{-4} \text{ cm}^{-1}$. It is hoped that such hygroscopic materials can be used as inside layers in multi-layer coatings, but this has not yet been established.

Best Higher-Index Candidates

The following list of best candidates for higher-index film materials is necessarily even more arbitrary than the low-index material list since the low-index materials are limited essentially to the fluorides and chlorides:



TII.

As₂S₃. Arsenic trisulfide is the only known film for which $\beta_f = \beta_b$ ($= 0.8 \text{ cm}^{-1}$) at $10.6 \mu\text{m}$ (with the possible exception of ThF_4 , for which the intrinsic value of β_b is not well known). It was found at Hughes Research Laboratories^{*10} that purchased high-purity As_2S_3 powder was not satisfactory even after it had been melted in the presence of H_2S . Arsenic trisulfide was synthesized at the Hughes Research Laboratories under conditions designed to keep it oxygen-free. It was pointed out in China Lake reports^{*19,*32} that there is a possible problem of photodissociation of As_2S_3 and As_2Se_3 followed by oxidation of the arsenic, resulting in additional absorption and optical densification.

As₂Se₃. The $10.6 \mu\text{m}$ value of the absorption coefficient $\beta_b = 0.011 \text{ cm}^{-1}$ is 70 times smaller than the value $\beta_b = 0.77 \text{ cm}^{-1}$ for As_2S_3 .

ZnS. Zinc sulfide is a common coating material. Films are polycrystalline.^{*2} Occasionally observed inhomogeneities are attributed to a ZnO layer. The value of β_b is $\sim 0.15 \text{ cm}$. Measured values of β_f are as low as $\beta_f < 1.4 \text{ cm}^{-1}$. The following excerpt is from Ritter's article.^{*2} "ZnS films show a high packing density. The stability of ZnS films, e.g., their adhesion, depends very much on the cleaning and pretreatment of the substrate. For use as an antireflection coating on Ge, e.g., it is recommended that one use a 150°C substrate temperature and

an effective glow discharge just prior to evaporation. In this way films can be produced to withstand several hours boiling in 5% salt water, repeated washing, and exposure to moisture without damage. ZnS evaporates at approximately 1200 C. During heating ZnS dissociates into Zn and S. This was proved by mass spectrometric investigations. During condensation recombination of Zn and S to ZnS takes place. This evaporation mechanism explains the strong temperature dependence of the condensation coefficient of ZnS, even in the range 20-300 C. ZnS can be evaporated from molybdenum or tungsten boats. A source well suited for the evaporation of large amounts of ZnS at rather high deposition rates is described by Cox and Hass."

ZnS is one of the standard coating materials for optical applications in the visible and infrared region. It is often used in combination with one of the low index fluorides, like MgF_2 , ThF_4 , or cryolite. It forms thick films that do not crack or peel off. The useful transmittance range covers the visible and the infrared up to 14 μm . The refractive index in the visible ranges between 2.60 and 2.30 since it shows a strong dispersion near the absorption edge. In the infrared the refractive index is around 2.3.

ZnSe. The bulk absorption coefficient is $\beta_f = 4 \times 10^{-4} \text{ cm}^{-1}$, and $\beta_f = 1.2 \text{ cm}^{-1}$ has been reported. Zinc-selenide films crack off KCl substrates unless the ZnSe film is thin.

TlI. Thallium iodide is included in the list of best candidates because $\beta_f < 1 \text{ cm}^{-1}$ has been attained.^{*64} Films are highly textured polycrystalline. Rapid deposition is required to obtain the low values of β_f . There is a problem with film clouding of thick films ($> 0.3\text{-}0.5 \mu m$) grown on glass, cleaved KCl, and mechanically polished KCl. Scanning-electron-micrograph edge views of films showed

an abrupt switch from a pancake morphology in the thin films to a loosely packed columnar growth pattern for the thick films. Good TlI coatings were deposited at room temperature. Coatings deposited at 100°C were cloudy and had rough surfaces. The toxicity of Tl may exclude TlI from some applications.

Next-Best Candidates

Some of the materials listed here possibly could form good films and could be studied in the future. However, the best candidates just listed were chosen for first studies to keep the list manageable small.

CdTe. The following information is from Ref. *65: "Sputtered CdTe can be deposited as crystalline (cubic and/or hexagonal) or amorphous, depending on the argon pressure. Films have tellurium-rich surfaces and have small amounts of oxygen incorporated into the surface layer. For CdTe on KCl, X-ray peaks not corresponding to KCl or CdTe were found. Similar results obtained by others by electron diffraction for CdTe on NaCl and on mica were attributed to stacking faults."

The following excerpt is from Ref. *10: "Films of CdTe prepared from a new improved starting material have a cadmium deficiency of a few percent to as much as twenty percent, with absorption index values as high as 10^{-2} . Near the end of the contract period, a portion of an old ingot was found that yielded absorptions in the 1×10^{-4} range. This material was coupled with the best RAP-processed ThF_4 to produce the final high-reflectance mirrors prepared. Satisfactory explanations still are not available as to what the factors are among stoichiometry, thermal history, and doping of a CdTe ingot that control the manner in which it sublimes to form CdTe films." Dr. Harold Posen and coworkers¹¹ suggest that CdTe has merit.

(Ca, Sr, Ba)(S, Se, Te), and Mg(Se, Te). The properties of the IIA-VI compounds are not so well known as those of the IIB-VI compounds, such as ZnSe, and are more speculative. They have the sodium chloride structure and have larger electronegativity differences than the corresponding IIB-IV materials, which indicates that they have a higher degree of ionic bonding than do the IIB-VI materials. The value of E_g for barium telluride probably will not be too small since barium telluride has the sodium chloride structure.

KRS-5(TlI-TlBr). Thallium is toxic, but in applications in which the toxicity is tolerable, KRS-5 will be a good candidate. The bulk absorption coefficient is sufficiently small, $\beta_b \ll 0.5 \text{ cm}^{-1}$, and a value of $\beta_f < 4.5 \text{ cm}^{-1}$ was obtained even without the special precautions now believed necessary to obtain ultralow values of β_f . KRS-5 is much finer grained than TlI. The following excerpts are from a recent Perkin-Elmer report:^{*66} "When KRS-5 is deposited on a substrate with a low coefficient of expansion, it forms a film with a low tensile stress. It has a low value of bulk absorption coefficient and, while not as hard as zinc selenide (Knoop number 40 compared with Knoop number 100), it is harder than the component materials, thallium bromide and thallium iodide (Knoop number ~10)."

"In this investigation only single discrete films of KRS-5 were evaluated. The thickness was chosen to represent the thickness that would be employed in a six-film design. The results indicated excellent adhesion to KC1. The first two runs produced erratic absorption measurements, presumably because of the poor quality substrates, but a later run on substrates of better quality indicated that the 1.1 μm -thick film had less than 0.05% absorption." [Thus, $\beta_f < 4.5 \text{ cm}^{-1}$.] "The KRS-5 vapor would not condense on substrates held at 150°C which means that in a multilayer combination with thorium fluoride it would be necessary to cycle the

substrate temperature between alternate film depositions. Another negative factor was an index homogeneity in the film thickness direction. This took the form of a refractive index increasing with thickness, which is indicative of preferential evaporation or condensation of the iodide component at the initial stages of the evaporation."

AgCl, TlCl, TlBr, CsI. These materials produce good quality antireflection coatings.^{*2} Bulk absorption is extremely low. The thallium compounds are toxic, and CsI is hygroscopic.

GaAs. Careful growth is required to insure a steep absorption edge and the corresponding small value of β_f .^{*2}

Sb₂S₃. Films have been deposited successfully. The value of n_r at 600 nm is 2.35. Films of As₂S₃ have been studied in much greater detail, and Sb₂S₃ is expected to have lower absorption than As₂S₃.

Ge. The value of β_f for amorphous films depends on the deposition conditions. The smallest value found in the literature is $\beta_f = 10 \text{ cm}^{-1}$, which is much greater than β_b for crystalline bulk germanium. The value of β_f is much smaller on fused quartz than on NaCl.

If germanium becomes a serious candidate, it should be determined if the well known thermal runaway problem is alleviated by the restriction to small values of temperature rise dictated by thermally induced optical distortion.

The low laser-damage threshold observed by Young^{*38} was attributed to thermal runaway.

The observed increase in β with increase in frequency ω from $\hbar\omega = 0.1 \text{ eV}$ ($\beta = 30 \text{ cm}^{-1}$) to 1.3 eV ($\beta = 6 \times 10^4 \text{ cm}^{-1}$) for amorphous germanium strongly

suggests an electronic absorption mechanism related to "states in the gap" of amorphous materials.

Germanium was found tens of nanometers into a KC1 substrate. Germanium films become oxidized throughout, which increases β .

Chalcogenide glasses. In addition to As_2S_3 and As_2Se_3 discussed above, there are other chalcogenide glasses such as Texas Instruments TI 1173 (a glass containing Ge, As, and Se). Dr. A. R. Hilton⁶⁷ pointed out that the coatings will have to be rf sputtered, and that rf sputtering has been accomplished at Texas Instruments to fabricate optical wave guides.

Unacceptable and Unlikely Candidates

Most of the materials listed below are unacceptable for $10.6\mu m$ use as a result of great absorption or other known properties. A few of the materials possibly could form good films, but are considered as even less promising than the next-best candidates above.

Materials containing the light elements H, He, Li, Be, C, N, and O. The light masses are expected to give rise to a fundamental resonance too near $10.6\mu m$, thus making $\beta > 0.5\text{ cm}^{-1}$. Note that the vast number of materials containing oxygen or carbon are expected to be unsatisfactory.

Many oxides are known to have $\beta_b > 0.5\text{ cm}^{-1}$ at $10.6\mu m$. Although we cannot be sure that some oxides will not have a sufficiently low absorption coefficient, the generally high absorption at $10.6\mu m$ of oxides makes them less likely candidates. Specific oxides include the following:

MgO ($\beta_b = 7 \text{ cm}^{-1}$; to $8 \mu\text{m}$)⁶⁸

SiO (to $8 \mu\text{m}$)⁶⁸, SiO_2

Al₂O₃ (to $7 \mu\text{m}$)⁶⁸

BaTiO₃ ($\beta_b \approx 100 \text{ cm}^{-1}$)

(Si, Ti, T_x, Ce, . . .)O₂

(Ce, Zr)O₂ (to $12 \mu\text{m}$)⁶⁸ $n_r \approx 1.9-2.1$

(La₂, Nd₂, Ce₂, Y₂, . . .)O₃ $n_r = 1.9-2.1$

Pr₆O₁₁ $n_r = 1.9-2.1$

YAG (yttrium aluminum garnet), YIG (yttrium iron garnet)

borosilicate and calcium aluminate glasses

Other unacceptable and unlikely materials include the following:

(Ca, Sr, Ba, Zn, Cd, Hg)(Cl₂, Br₂, I₂). Since (Ca, Sr, Ba, La)F₂ are of interest, it might appear that replacing F₂ by Cl₂, Br₂, or I₂ to increase the masses, thereby decreasing the value of β , would result in satisfactory materials. However, the physical properties of the materials containing chlorine, bromine, or iodine are inferior even to those of the alkali halides.

(Ga, In, Tl)(Cl₃, Br₃, I₃). Such corresponding III-VII₃ materials as GaBr₃ have still poorer physical properties. Thus, these materials are unlikely candidates.

(Ge, In, Sb)(Cl₄, Br₄, I₄). It is possible that some of these materials could be acceptable. They are considered unlikely on the weak argument that they may have poor physical properties because the physical properties are progressively worse

in the series I-VII, II-VII₂, III-VII₃, and these IV-VII₄ materials are the next ones in the progression.

Sn, (In, Tl)(As, Sb, Bi), Pb, (Pb, Sn)(Se, Te), Bi₂(Se₃, Te₃), (Mg, Ca)(Si, Ge, Sn, Pb), Mg₂Sn, ZnSb, CdSb, Cd₃As₂. The energy gaps of these materials are too small for use at room temperature. Some of these materials possibly would be good candidates if lower temperatures were used.

Layered structures. The facts that the interlayer forces are small and that the structure can open up to accept even large molecules makes these materials unlikely candidates. Such materials include:

Ge (S, Se, Te)

(Zr, Hf)S₂

Hf(Se₂, Te₂)

Ti(S₂, Se₂, Te_{1.17})

ZrSe_{1.98}

ZrTe_{1.76}

HSSe

Mo(S₂, Se₂)

W(S₂, Se₂)

Cd(Br₂, I₂)

SnS₂ .

The absorption of the following fluorides is expected to be too great ($\beta > 0.5 \text{ cm}^{-1}$):

<u>CaF₂</u>	$\beta_b = 3 \text{ cm}^{-1}$
<u>LiF</u>	$\beta_b = 50 \text{ cm}^{-1}$
<u>MgF₂</u>	$\beta_b = 18 \text{ cm}^{-1}, \beta_f = 270 \text{ cm}^{-1}$

Cryolite (NaAlF₄, or, in general, NaF plus AlF₃). Transmission to 14 μm .⁶⁸

Cryolite films have low packing densities, ranging from 0.88 for 30°C substrate temperature to 0.92 for 190°C substrate temperature.^{*2}

PbF₂. Even though the bulk absorption coefficient $\beta_b = 0.01-0.06 \text{ cm}^{-1}$ of PbF₂ is below the desired value of 0.5 cm^{-1} , films are not expected to have a sufficiently low value of absorptance β_f unless the film density can be increased above the current value of 0.9.^{*2} If PbF₂ is considered, it is expected that platinum or ceramic crucibles will be essential.^{*2} Horrigan and Deutsch⁶⁹ found that they could not deposit stable films. The films absorbed moisture, were soft and milky colored, and showed OH⁻ and H₂O absorption bands. Perhaps these films were deposited from tantalum, tungsten, or molybdenum boats.^{*2}

Lead fluoride films consist of β - PbF₂. The packing density is about 0.90. [Unless the packing density can be increased, PbF₂ films probably will absorb so much water that the optical absorption will be too great for high-power use.] The stress behavior is interesting since with increasing film thickness a change from compressive to tensile stress occurs. The absolute stress values are low.

TlF₃. This material is considered as a less desirable candidate because Tl is toxic, the values of β_f and β_b are unknown, and there are a sufficient number of other fluorides without these problems.

AlF₃. The absorption is expected to be too great. The value of the film absorption coefficient $\beta_f \approx 250 \text{ cm}^{-1}$ at $10.6 \mu\text{m}$ estimated from the transmittance curve of Heitmann^{*70} probably is at or near the intrinsic bulk value. Since the AlF₃ films showed strong water absorption at ~ 3 and $\sim 6 \mu\text{m}$ and the absorptance of water begins to increase at $10 \mu\text{m}$, the cut off of AlF₃ beginning at $10 \mu\text{m}$ conceivably could be the result of the water, rather than the intrinsic cut off of AlF₃. However, the water cut off, which is seen to reduce the transmittance of $30 \mu\text{m}$ of water to a small value (<5 percent) in Fig. 4.1, is not sufficiently strong to explain the cut off observed in AlF₃. In Table 4.1 or Fig. 4.1 it is seen that values of β from $10-14 \mu\text{m}$ are less than the peak value at ~ 3 and $\sim 6 \mu\text{m}$; at $18 \mu\text{m}$, $\beta = 3.2 \times 10^3 \text{ cm}^{-1}$, compared with $\beta = 2.9 \times 10^3 \text{ cm}^{-1}$ at the $\sim 3 \mu\text{m}$ and $\sim 6 \mu\text{m}$ peaks. If the cut off were the result of the water in the films, there is a possibility of reducing the $10.6 \mu\text{m}$ absorptance since the films were deposited at ambient temperature and higher temperature deposition of fluorides often results in higher density films with less water absorption.

(Ce, La, Nd, Pr, Yb) F₃. It is questionable that these materials will have a sufficiently small absorptance ($\beta_f < 0.5 \text{ cm}^{-1}$). From transmittance values from $8-16 \mu\text{m}$ ^{*62} for two samples of thickness 0.43 and 11.7 mm, we calculate $\beta_b = 1-2 \text{ cm}^{-1}$ for the bulk absorption coefficient of LaF₃, in agreement with $\beta_b = 1.2 \text{ cm}^{-1}$ from Ref. *3. Bulk LaF₃ is thermally and chemically stable, and is insoluble in water and sodium hydroxide.⁶² The index of refraction of CeF₃ at 550 nm is $n_r = 1.63$. The stability of CeF₃ is not very satisfactory according to Ritter.^{*2} However, it was found at the Air Force Cambridge Research Laboratories^{*71} that crack-free CeF₃ coatings adhered strongly to KCl substrates and were immune to atmospheric humidity. Transmission measurements showed

"100 percent transparency in the 3-14 μm region." This probably means that $A_f \gtrsim 10^{-2}$, compared with the desired value of $A_f < 10^{-4}$. For a 1-2 μm thick film, the limit $A_f \gtrsim 10^{-2}$ corresponds to $\beta_f \gtrsim 50-100 \text{ cm}^{-1}$. Ritter's^{*2} listing "to 14 μm " implies⁶⁸ that $A_f > 10^{-4}$. Thin (100 nm) PrF_3 protective films deposited on ZnSe at 250 C did not pass the MIL-C-675A requirements for abrasion and humidity.

KF. Potassium fluoride should have a lower intrinsic bulk infrared absorptance than NaF. Compare the 10.6 μm absorptance coefficient, $\beta = 40 \text{ cm}^{-1}$, of LiF with that, $\beta = 0.5 \text{ cm}^{-1}$, of NaF. However, as M. Hass²⁷ and H. Posen and coworkers¹¹ pointed out, KF probably will not be suitable since it is more hygroscopic than KCl or KBr.

Other unlikely materials include the following:

Pb(Cl₂, Br₂). The bulk absorption coefficient surely is sufficiently low, but these chlorides and bromides normally are expected to be inferior to PbF₂. An antireflection coating of PCl₂ was used on InSb.⁶²

SiC. Transmission to 5 μm .⁶⁸

CuI. $\beta_b = 1 \text{ cm}^{-1}$ (expected extrinsic). $\beta_f = 10^3 \text{ cm}^{-1}$ on KCl substrate. A long copper diffusion tail into the KCl substrate is believed to be related to the greater value of $\beta_f = 10^3 \text{ cm}^{-1}$.^{*72} Films are stable at high humidity.^{*19}

Amorphous S, Se, or Te. The amorphous nature of these materials would appear to make them attractive candidates. However, Dr. A. R. Hilton pointed out that these materials have no strength, they have absorption bands, and the structure is very permeable. Dr. H. Posen and coworkers¹¹ pointed out that amorphous sulfur transforms readily near room temperature. Dr. T. M. Donovan⁷³ also expressed the opinion that amorphous S and Se would be poor candidates.

The following information from the Third Edition of the American Institute of Physics Handbook, page 6-84, is of interest: "Unlike sodium chloride and potassium bromide, rhombic sulfur is not hygroscopic. It is easy to prepare in virtually any rectangular size needed and it is inexpensive. It can be useful for windows in infrared equipment and in surveillance systems." From page 6.80 of the same reference, "Selenium can exist in various forms. The trigonal (or crystalline) form is the most stable. The amorphous (or vitreous) form is fairly stable below 50 C but converts to the trigonal form at higher temperatures." And from page 6.85, "Tellurium is an interesting anisotropic crystal. Single crystals of tellurium are hard to grow; a polycrystalline ingot (which is brittle and difficult to polish) usually forms from the melt. When tellurium is ground, a conducting layer tends to form on its surface; this layer can be removed by chemical etching although this does not leave an optical surface. Optical polishing can probably be accomplished without this effect; thin layers of tellurium have been made that have a good optical finish."

XII. CANDIDATE 2-6 μm COATING MATERIALS

Even though the emphasis of the present report is on 10.6 μm materials, some general information on materials for the chemical laser wavelength (2.8 μm for HF, 3.8 μm for DF, and 5.25 μm for CO) may be useful. The chemical-wavelength problems will be considered in subsequent reports.

Since the intrinsic values of β_b in the 2-12 μm region tend to be limited by ionic rather than electron absorption mechanisms, the value of β_b tends to decrease as the wavelength λ decreases. Thus, materials that are useful at 10.6 μm usually are useful at 2-6 μm . There are exceptions to this rule. First, the extrinsic absorption can be greater at wavelengths less than 10.6 μm than at 10.6 μm . A film containing water absorbs strongly at the HF wavelength 2.8 μm . Second, the electron absorption can be great for small bandgap materials. A bandgap of 0.5 eV corresponds to a wavelength of 2.5 μm . Third, scattering and scattering-related absorption increase as the wavelength decreases. Other examples include absorption related to interconduction band absorption processes.

In addition to the use of 10.6 μm material at 2-6 μm , there are materials that can be used at 2-6 μm that have too great absorption at 10.6 μm . The largest such group probably is the oxides. Aluminum oxide (Al_2O_3) has $\beta_b < 0.01 \text{ cm}^{-1}$ at 3.8 μm and $\beta_b \approx 18 \text{ cm}^{-1}$ at 5.25 μm . Magnesium fluoride, which is perhaps the most popular coating material, has acceptably small absorptance, $\beta_b < 0.1 \text{ cm}^{-1}$, on the 2-6 μm range, but $\beta_b = 18 \text{ cm}^{-1}$ at 10.6 μm is greater than the desired value of $\sim 0.5 \text{ cm}^{-1}$.

Oxides represent a very important group of coating materials because of their mechanical and chemical stability as well as because of their wide range of useful

refractive indices. The preparation of oxide films is generally not as easy as of fluoride or sulfide films since most oxides react with crucible materials or dissociate at the required high temperatures. Useful low index oxide films are SiO_2 and Si_2O_3 . Medium index films are SiO , Al_2O_3 , MgO , ThO_2 , ZrO_2 , and the rare earth oxides, whereas CeO_2 and TiO_2 represent high index materials. SiO_2 films are transparent from 200 nm up to 9 μm .

By evaporation of SiO without oxygen, films are produced which are absorbing in the visible range but transparent in the infrared up to approximately 8 μm . Al_2O_3 films are transparent from at least 200 nm up to 7 μm if they are prepared correctly. MgO films have not yet found wide application since their stability is limited. They are transparent from 220 nm to 8 μm if evaporated with an electron beam. The films are crystalline and show increasing crystal size with increasing substrate temperature. During extended exposure to air a hazy bluish scattering coating forms on the surface of MgO films. This limits their usefulness as an optical coating material if used as an outer layer.

ZrO_2 films are transparent from 340 nm up to 12 μm .⁶⁸ One difficulty encountered when using ZrO_2 is a marked tendency to form inhomogeneous films probably due to a structural effect. The mechanical and chemical behavior is excellent, and it can easily be combined with other oxides and with MgF_2 .

The rare earth oxides such as La_2O_3 , Pr_6O_{11} , Nd_2O_3 , Sc_2O_3 , and Y_2O_3 also form films with a refractive index in the range from 1.9 to 2.1.

CeO_2 films are transparent in the visible and infrared region up to 12 μm .⁶⁸ Thick films of CeO_2 exhibit high scattering losses which limits their usability already in the near infrared. The films are cubic at all substrate temperatures

and the difference in refractive index is due to a different content of grain boundaries since at higher temperature the crystal size increases and therefore the concentration of boundary layers decreases. CeO_2 films are very stable, hard, and well adherent.

TiO_2 is an important high index material. It forms hard and adherent films with good chemical stability. Thick TiO_2 films show scatter loss which limits the usefulness in the infrared to around $3 \mu\text{m}$; otherwise thin films can be used up to $10-12 \mu\text{m}$.⁶⁸ Bi_2O_3 films have been prepared by evaporation.

Mentioned in the literature, but obviously rarely used, are the oxides of antimony Sb_2O_3 , arsenic As_2O_3 , beryllium BeO , boron B_2O_3 , lead PbO , gallium Ga_2O_3 , germanium GeO_2 , and tellurium TeO_2 .

Most oxides show absorption if they are not fully stoichiometric and if oxygen vacancies have been created. Also sulfide and selenide films with an excess of the metallic constituent show increased absorption. Thick films, e.g. of CeO_2 , tend to form large crystallites which cause scattering.

Fluoride films tend to form films with lower packing density if not deposited on heated substrates. MgF_2 films, e.g., deposited on unheated substrates, have a packing density of only 74%. The corresponding refractive index, measured in vacuum, is 1.32 instead of 1.38. At approximately 300 C a high packing density and the expected index of at least 1.38 are obtained. During exposure to air, water vapor is absorbed in films with reduced packing density, filling the holes with water. As discussed in Sec. IV, this filling of the holes with water is expected to be a strong source of absorption for all wavelengths greater than $\sim 2.7 \mu\text{m}$. Thus, attaining low-porosity films is one of the most important goals

of the high-power coating programs. As a consequence of the water absorption, an increase in refractive index n_r is observed and the values of compact MgF_2 are almost achieved again. Similar effects are known for cryolite, CaF_2 , and AlF_3 and to a smaller extent for SiO_2 . The optical absorption by the water can of course be more important than the change in n_r .

The films of MgF_2 are always crystalline, but thin films and films on cold substrates shew a much finer grain size than thick films or films on heated substrates. Usually the films are formed of prismatic crystals which grow preferentially in the direction of the incident vapor beam. At thicknesses above 100 nm the films tend to be inhomogeneous and the inhomogeneity is increased with increasing thickness. MgF_2 films show extremely high tensile stress $3 \times 10^7 - 5 \times 10^7 \text{ kg/m}^2$ (4×10^4 to $7 \times 10^4 \text{ psi}$). This stress is probably responsible for the appearance of cracks at larger thicknesses, for the inhomogeneity, and for some cases of incompatibility with other film materials, e.g., TiO_2 .

The mechanical and chemical properties of MgF_2 films are predominantly dependent on the packing density. Films with high packing density, obtained at a substrate temperature of 300 C or by annealing after deposition are extremely stable, hard, and adherent. MgF_2 films are also combined very often with ZnS , although here the stability is much less since no high substrate temperature can be used during the deposition of ZnS .

XIII. EXCERPTS AND RESULTS FROM LITERATURE, WITH COMMENTS

Some of the key results from the literature on thin films are collected in the present section. Our comments in brackets inter-relate the references and relate the references to the present work. The underscoring in the excerpts is ours. It should be emphasized that no attempt at completeness has been made. There is no article or paper that gives a complete overview of the field of high-power infrared coatings. However, the article by E. Ritter^{*2} and the paper by P. A. Young^{*38} contain a wealth of information and afford a good introduction to the subject. The contents of the eight volumes of *Physics of Thin Films*, edited by Georg Hass and Rudolf E. Thun, Academic Press, are listed for the readers convenience. In these notes from the literature, the original reference numbers are enclosed in parentheses. References that are excerpted in the present section are denoted by asterisks throughout the report. Many of the excerpted papers, articles, and reports^{*85-*111} were not referenced in other sections.

Physics of Thin Films

The contents of the eight volumes that have appeared to date are listed for the convenience of the reader. Also included are the remarks of the editors in the prefaces about the contents of each volume (which started with volume 3).

Volume 1

Ultra-High Vacuum Evaporators and Residual Gas Analysis, Hollis L. Caswell

Theory and Calculations of Optical Thin Films, Peter H. Berning

Preparation and Measurement of Reflecting Coatings for the Vacuum Ultra-violet, Robert P. Madden

Structure of Thin Films, Rudolf E. Thun

Sec. XIII

Low Temperature Films, William B. Ittner, III

Magnetic Films of Nickel-Iron, Emerson W. Pugh

Volume 2

Structural Disorder Phenomena in Thin Metal Films, C. A. Neugebauer

Interaction of Electron Beams with Thin Films, C. J. Calbick

The Insulated-Gate Thin-Film Transistor, Paul K. Weimer

Measurement of Optical Constants of Thin Films, O. S. Heavens

Antireflection Coatings for Optical and Infrared Optical Materials,

J. Thomas Cox and Georg Hass

Solar Absorptance and Thermal Emittance of Evaporated Coatings, Louis F. Drummetter, Jr. and Georg Hass

Thin Film Components and Circuits, N. Schwartz and R. W. Berry

Volume 3

Film-Thickness and Deposition-Rate Monitoring Devices and Techniques for Producing Films of Uniform Thickness, Klaus H. Behrndt

The Deposition of Thin Films by Cathode Sputtering, Leon I. Maissel

Gas-Phase Deposition of Insulating Films, L. V. Gregor

Methods of Activating and Recrystallizing Thin Films of II-VI Compounds, A. Vecht

The Mechanical Properties of Thin Condensed Films, R. W. Hoffman

Lead Salt Detectors, D. E. Bode

The first article by K. H. Behrndt on thickness and rate monitoring devices and methods for preparing coatings of uniform thicknesses provides a detailed

review of those measuring and control methods which permit the accurate reproduction of thin-film properties — an art which the preface of Volume 1 claimed was mastered, but so far lacked a comprehensive review. In the second article, L. I. Maissel discusses the many aspects of film deposition by cathode sputtering. This field in particular has mushroomed during the last few years, and it has spawned such new, extremely useful deposition methods as dc bias sputtering and radio frequency ac sputtering.

The following article is L. V. Gregor's treatment of the deposition of insulating films by heterogeneous gas-solid reactions. This discussion encompasses inorganic amorphous solids and organic polymers and describes pyrolytic reactions as well as those triggered by radiation or electrical excitation. The discussion of preparative methods is concluded by A. Vecht with his description of the activation and recrystallization of II-VI compound films which find increasing interest because of their electrooptical properties.

Volume 3 is completed by two articles concerned primarily with thin-film properties. R. W. Hoffman gives a broad review of our present knowledge of the mechanical properties of thin films. Not only is this material of profound scientific interest, but it should be familiar to every development team striving for reasonably durable and stress-free films, no matter what the application might be. In the final article D. E. Bode reviews lead salt films which probably represent the most important class of infrared detectors.

Volume 4

Precision Measurements in Thin Film Optics, H. E. Bennett and Jean M. Bennett

Nucleation Processes in Thin Film Formation, J. P. Hirth and K. L. Moazed

Evaporated Single-Crystal Films, J. W. Matthews

Sec. XIII

The Growth and Structure of Electrodeposits, Kenneth R. Lawless

Thin Glass Films, W. A. Pliskin, D. R. Kerr, and J. A. Perri

Hot-Electron Transport and Electron Tunneling in Thin Film Structures,
C. R. Crowell and S. M. Sze

The first article in Volume 4, by H. E. Bennett and Jean M. Bennett, discusses precision measurements in thin film optics. This should find a wide interest beyond the boundaries of thin film optics, since it describes many convenient methods of general utility in the characterization of films. The following three articles deal with nucleation, growth, and structure of thin films, which may be considered common ground for the entire field of thin film physics. J. P. Hirth and K. L. Moazed give in their article on nucleation processes in thin film formation a review of today's theoretical models and their comparison with actual experimental findings. J. W. Matthews follows with a review article on evaporated single-crystal films, covering their growth and structure, and K. R. Lawless discusses the growth and structure of electrodeposits, giving the reader an opportunity to compare structural behavior as a function of deposition processes. The next article on thin glass films by W. A. Pliskin, D. R. Kerr, and J. A. Perri should be of great interest to those concerned with microelectronic research and development, since such glass films have gained increasing importance in this field. The last article of this volume, on hot-electron transport and electron tunneling by C. R. Crowell and S. M. Sze, discusses one of the currently most exciting fields of solid state electronics.

Volume 5

Interference Photocathodes, D. Kossel, K. Deutscher, and K. Hirschberg

Design of Multilayer Interference Filters, Alfred Thelen

Oxide Layers Deposited from Organic Solutions, H. Schroeder

The Preparation and Properties of Semiconductor Films, M. H. Francombe
and J. E. Johnson

The Preparation of Films by Chemical Vapor Deposition, W. M. Feist,
S. R. Steele, and D. W. Readey

A few years ago, vacuum deposition techniques such as evaporation and sputtering were the dominating deposition techniques. Today, new film preparation methods using predominantly chemical processes are gaining in importance and are described and discussed in various chapters of this volume.

The first article by D. Kossel, K. Deutscher, and K. Hirschberg on interference photocathodes shows that the efficiency of photoemissive materials can be increased by interference effects which improve the energy transfer from photons to electrons. This article should be of special interest to those concerned with photoemissive devices.

The article by A. Thelen describes the design of a variety of multilayer interference filters which are now widely used in the field of optics.

H. Schroeder reports on his experience of producing oxide layers from organic solutions and describes the use of such films as optical coatings and protective layers. This is followed by an extensive article by M. H. Francombe and J. E. Johnson which provides a status report on recent and current developments in the field of semiconductor films.

Sec. XIII

Volume 5 is completed by an article concerned with the preparation of films by chemical vapor deposition. In this chapter, W. M. Feist, S. R. Steele, and D. W. Readey discuss the chemical processes used in chemical vapor deposition and give examples and applications of semiconductor, dielectric, and metallic films prepared by this technique.

Volume 6

Anodic Oxide Films, C. J. Dell'Oca, D. L. Pulfrey, and L. Young

Size-Dependent Electrical Conduction in Thin Metal Films and Wires,

D. C. Larson

Optical Properties of Metallic Films, F. Abeles

Interactions in Multilayer Magnetic Films, Arthur Yelon

Diffusion in Metallic Films, C. Weaver

Volume 6 begins with an article on anodic oxide films by C. J. Dell'Oca, D. L. Pulfrey, and L. Young, which discusses progress in this field subsequent to that treated in Young's well-known standard text "Anodic Oxide Films." Of particular topical interest are the inclusion of recent work on the controversial subject of gaseous or plasma anodization and a discussion of conduction, polarization, and dielectric breakdown effects.

The present status of studies on size-dependent electrical conduction in thin metal films and wires is reviewed by D. C. Larson, who considers both classical and quantum size effects and discusses some of the more recently examined anisotropic characteristics in epitaxial metal films. The following article by F. A. Abeles presents a detailed, and mainly theoretical, treatment of the optical properties of metal films.

Sec. XIII

The final two chapters of the volume are reviews respectively on interactions in multilayer magnetic films by A. Yelon and diffusion in metal films by C. Weaver. The magnetic films article discusses some novel aspects of exchange coupling, its effect on magnetization reversal and its exploitation in memory storage applications. The discussion of recent work on diffusion should be of special interest to those concerned with aging effects in bi-metallic film systems.

Volume 7

Electron Diffraction Analysis of the Local Atomic Order in Amorphous Films,

D. B. Dove

The Preparation and Use of Unbacked Metal Films as Filters in the Extreme Ultraviolet, W. R. Hunter

Properties and Applications of III-V Compound Films Deposited by Liquid Phase Epitaxy, H. Kressel and H. Nelson

Electromigration in Thin Films, F. M. d'Heurle and R. Rosenberg

Built-Up Molecular Films and Their Applications, V. K. Srivastava

In the first article of Volume 7 the status of research on the structure of amorphous films is reviewed by D. B. Dove. This is the first of several reviews which are planned for future volumes on various aspects of the important rapidly developing field of structurally disordered films. An article dealing with the dc electrical conductivity behavior of amorphous films by A. K. Jonscher and R. M. Hill is scheduled for Volume 8.

The second chapter by W. R. Hunter deals with metal film optical filters for use in the extreme ultraviolet. In particular, the preparation, optical properties, and applications of unbacked metal filters in laboratory and space instrumentation are discussed. This article is the tenth in the area of thin film optics to be

published in the Physics of Thin Films series, and readers interested in this field will find complete discussions of related aspects in earlier volumes.

The third article by H. Kressel and H. Nelson presents a timely review of the impressive body of work that has developed in recent years in the new field of liquid phase epitaxy. This growth technique is rapidly finding application, especially in the fabrication of high-quality single-crystal layers of semiconductor and magnetic oxide materials, and the authors place special and authoritative emphasis on III-V compound layers for use in optical and microwave devices.

The fourth review covers a topic which has long been a fundamental interest to metallurgists and thin film physicists, and more recently has achieved special significance for the designers of thin film microcircuit components, i.e., electro-migration in thin films. F. M. d'Heurle and R. Rosenberg survey recent developments in this technologically important field and discuss both the effects observed in pure metal films and the inhibiting influence of alloying additives. Incidentally, newcomers to this field of metal films should find that previous articles in this series on film growth and structure (Volume 4) and mechanical properties (Volume 3) provide useful supplementary reading.

In the fifth and final chapter of this volume, a novel thin film topic not hitherto included in this series is introduced by V. K. Srivastava, covers in some detail the historical background, preparation, and structural, optical, and electrical properties of built-up molecular films, and concludes by summarizing some of the interesting and diverse applications of such layers, e.g., in thickness gauges, optical and X-ray gratings, chemical analyses, and dielectric film devices.

Sec. XIII

Volume 8

Dielectric Film Materials for Optical Applications, Elmar Ritter

Inhomogeneous and Coevaporated Homogeneous Films for Optical Applications, R. Jacobsson

Discontinuous and Cermet Films, Z. H. Meiksin

Electrical Conduction in Disordered Nonmetallic Films, A. K. Jonscher
and R. M. Hill

Topologically Structured Thin Films in Semiconductor Device Operations,
H. C. Nathanson and J. Guldberg

The present volume contains two articles on optical films. The first, by E. Ritter, deals with the preparation, physics, and application, e.g., in anti-reflection coatings and filters, of dielectric film materials. R. Jacobsson has reviewed recent novel developments in the area of inhomogeneous optical films, and discusses the method of preparation, optical properties, and utilization of films of mixed dielectrics and semiconductor-dielectric combinations in which the refractive index is varied in a controlled fashion with thickness. The interesting practical consequences of optical inhomogeneity in films used as antireflection coatings, matching layers for multilayer films and absorbing layers, e.g., in sunglasses, are discussed.

The third article, by Z. H. Meiksin, deals mainly with the electrical transport properties of discontinuous and cermet films. Such films are finding growing application as high-value thin-film resistors and sensitive strain gauges, and the present review provides useful insight not only into the background physics but also into the practical potential of some simple metal-dielectric systems. In the

Sec. XIII

next chapter A. K. Jonscher and R. M. Hill discuss electrical conduction in nonmetallic amorphous films.

In the fifth article, by H. C. Nathanson and J. Guldberg, novel ways of using thin films in specially shaped configurations suitable for imaging and microwave devices are reviewed. Numerous interesting examples of such applications are cited, and demonstrate clearly the growing need for these approaches in the rapidly developing area of solid state technology.

E. Ritter, "Dielectric Film Materials for Optical Applications," Physics of Thin Films, Vol. 8, 1 (1975)

Conclusions from the behavior of the same material as single crystals or solid plates are not always valid since in thin evaporated films additional absorption due to deviation from stoichiometry or to impurities may occur. For example, most oxides show absorption if they are not fully stoichiometric and if oxygen vacancies have been created. Also sulfide and selenide films with an excess of the metallic constituent show increased absorption. Thick films, e.g. of CeO_2 , tend to form large crystallites which cause scattering (14). A porous film structure may also be the reason for scattering, e.g., with some fluorides, as well as the incorporation of microdust or spattered material. Barr (15) has demonstrated the decrease of scatter loss by using a particle filter to separate dust and spattered particles from the vapor. [This could be important also for lowering the absorptance and the damage threshold for films.]¹¹²

The exact determination of loss figures and the distinction between scatter losses and absorption require elaborate methods. Photometric methods are usually limited to loss of about 0.1%. With calorimetric methods absorption losses of 0.02%, corresponding to a k value of 10^{-4} at $1.06 \mu\text{m}$ or a β value of 10 cm^{-1} , can be determined with an accuracy of $\pm 5\%$ (6).

Measurements of the light attenuation in wave guides allow loss measurements of 0.1 dB, corresponding to a k value of 1×10^{-7} or a β value of 0.02 cm^{-1} (633 nm) (12). By choosing proper conditions intrinsic losses can be distinguished from losses due to boundary scattering (11, 177).

The losses in tantalum oxide and organosilicone compounds at 633 nm are to a large extent due to scattering at the grain boundaries. Theoretical analyses of this effect have been carried out by P. H. Lissberger and others [listed in Lissberger (13)].

TiO₂ films show a very marked dependence of the refractive index on substrate temperature, since in the interval between 20°C and 400°C the films can be amorphous or anatase or rutile or they are mixtures of these phases (18). Therefore the refractive index at 550 nm varies between 1.9 and 2.6, depending on the substrate temperature. Even films of the same material and the same crystal structure can show varying refractive indices due to different grain size or packing density. The smaller content of less dense boundaries in the case of larger crystals leads to an increase in refractive index (14, 19, 20).

Fluoride films tend to form films with lower packing density if not deposited on heated substrates. MgF₂ films, e.g., deposited on unheated substrates, have a packing density of only 74% (21, 26). The corresponding refractive index, measured in vacuum, is 1.32 instead of 1.38. At approximately 300°C a high packing density and the expected index of at least 1.38 are obtained (23, 24). During exposure to air, water vapor is absorbed in films with reduced packing density, filling the holes with water. [As discussed in Sec. IV of this technical report, this filling of the holes with water is expected to be a strong source of absorption for all wavelengths greater than ~2.7 μm. Thus, attaining low-porosity films is one of the most important goals of the high-power coating programs.] As a consequence an increase in refractive index n_r is observed and the values of compact MgF₂ are almost achieved again (21, 23, 26). Similar effects are known for cryolite (25, 27, 28), CaF₂ (22, 28), and AlF₃ (29) and to a smaller extent for SiO₂ (30). [The optical absorption by the water can of course be more important than the change in n_r.]

The cause of a reduced packing density appears as a structural effect or a gas incorporation in the film or as multiple collisions of vapor molecules with gas molecules during the transport from the source of the substrate. Sometimes several

effects are superimposed. Increased substrate temperature normally increases the packing density. The packing density of a film is not only important from the point of view of its optical behavior but also of its mechanical and chemical stability (178). [This is an important fact since there may be temptation of contractors or agencies to first obtain stable films, then reduce the absorptance.]

The need for films with different refractive indices has stimulated a search for mixtures of dielectrics which will evaporate simultaneously and result in films with a great variety of refractive indices. The refractive index then corresponds to the ratio of the mixture. Experimental results have been reported for $\text{CeO}_2\text{-SiO}_2$, $\text{CeF}_3\text{-ZnS}$, and $\text{CeO}_2\text{-CeF}_3$ mixtures (35-37).

There are many examples of inhomogeneous films listed in the literature on MgF_2 films (25, 38, 39), on cryolite films (27, 31, 40), on CaF_2 films (41), and on ZnS films (42, 43). The inhomogeneity may be a steady variation across the film thickness causing an increase or decrease of the refractive index with increasing film thickness, or it may be a more or less abrupt change in the refractive index somewhere in the film cross section.

For so-called "hardness," the eraser test is still the test method, although other test methods have been worked out (55-57). In the "Sandstrahl test" the surface to be tested is exposed to a standard beam of sand. The light scattering produced by the impact of the sand on the surface compared with an untreated surface is used as a measure of hardness.

Adhesion is normally tested by the "Scotch Tape" test, although other tests are available. The adhesion of ZnS and cryolite was found to be 2.9×10^6 psi and 6.4×10^6 psi without a glow discharge cleaning. In the case of ZnS the adhesion could be improved to 5.3×10^6 psi by a 20-min glow discharge whereas in the case of cryolite the adhesion increased only to 6.8×10^6 psi.

The adhesion is influenced by the type of bonding between the film materials and the substrates; e.g., oxide films normally adhere very well on glass. Furthermore, it depends strongly on the preparation and cleanliness of the surface (59, 179), and the chemical composition of the surface (60) and electrostatic charging effects (61) have to be taken into consideration. High stress may cause cracking of the films and even peeling off. A detailed survey on thin-film adhesion and its measurement was very recently given by Chapman (180).

Many films are in a state of stress during and after condensation. At least two factors can be held responsible for these stress effects: (1) structure and (2) difference of the expansion coefficient of film and substrate. The consequences of stress can be: (1) fissures in the films, in extreme cases peeling off; (2) fissures in neighboring films and incompatibility of film combinations; (3) deformation of substrates.

Of great importance for the power of stress are the packing density and the water vapor absorption. During exposure to atmosphere very often a stress relief takes place. Stress in dielectric films has been investigated by several authors (62-67). The articles by Enncls (62), Hoffman (63), and Scheuermann (64, 65) are very instructive.

An often used humidity test is storage at 42°C, relative humidity 95%, 24 or 48 hr (68). Immersion in water, often salt water, is a test frequently applied. Well-prepared films of MgF_2 , many oxide films, and combinations of these films withstand the humidity and immersion tests.

Multilayer coatings of MgF_2 and ZnS show after first exposure to humidity the formation of spots or stains, differently colored. Multilayer systems of ZnS

and ThF_4 do not show such a "conversion." Only at pin holes in the film does a local saturation with water vapor occur and consequently a discoloration appears.

The chemical behavior of the films is of importance with respect to the substrate and to neighboring layers. Between glass constituents like PbO and film materials like La_2O_3 chemical reactions can take place and lead to the formation of absorbing metallic lead. Reactions among film materials are also possible, especially at higher substrate temperatures.

Among the various production methods vacuum evaporation has especially shown remarkable progress with respect to size and efficiency of coating units, reliability of the process, and the control of film thickness and uniformity. Despite the enormous progress that has taken place in reactive and rf sputtering, only very few optical applications of sputtered films are known. This may be due to the small area to be coated in sputtering systems (except some special arrangements), to the relatively low sputter rates, and to the difficulties in thickness monitoring if very accurate monitoring is required. Other methods include deposition from organic solution (87), sputtering, ion plating, and gas discharge deposition. Ion plating is a new deposition technique which combines the sputtering and evaporation processes (122).

The preparation of the material to be evaporated is of considerable importance for the deposition of high quality optical coatings. Crucial properties are purity, gas content, and grain size. It is highly recommended that one uses vacuum sintered and outgassed materials or even pieces of dense single crystals to avoid gas outbursts and spattering during the evaporation process. Powders are normally not suitable, since they have too much adsorbed gas, which is desorbed

during heating and leads to pressure rise and spattering of material, even to jumping out of the boat. Some fluorides tend to form oxide or carbonate layers on the surface. These layers may impede free evaporation and cause sudden spattering of the evaporants. [Other precautions such as particle filters and great distances to the substrate may be required.]

Electron beam evaporation has found widespread use during the past decade. Its advantages are the avoidance of reactions of the evaporant with the boat material, the possibility of achieving very high temperatures, and a relatively careful evaporation of easily dissociating compounds if carried out correctly. Possible disadvantages are the charging of substrates and ionization of the evaporated material (91-94).

Only a very limited number of compounds can be evaporated directly by means of boat evaporation, electron beam, or laser evaporation and condensed again as a stoichiometric compound without any additional measures. In the case of III-V or II-VI compounds flash evaporation techniques proved to be useful for the preparation of nearly stoichiometric films. The material to be evaporated is fed in small portions to a crucible, the temperature of which is high enough to evaporate all constituents immediately. The method has been used successfully for the preparation of AlSb, GaAs, InSb, and other III-V compounds (100, 102).

Another way of preparing III-V or II-VI compound films is the so-called "three-temperature method" of Günther (103). Here the elements are evaporated separately from two controlled sources. Reaction to form the compound takes place on the substrate. This method was used successfully for the production of films of GaAs (104), InSb, InAs, Bi_2Te_3 , CdSe (105), and others (102).

The use of rate monitors, which are now commercially available (ionization gauge and quartz crystal oscillator types), improves the film homogeneity and facilitates the control of reaction in the case of compound formation. Mass Spectrometers proved to be useful to check the residual gas constituents and their changes as well as the occurrence of gases due to dissociation and to investigate the nature and to control the rate of the gas phase species of the evaporant (24, 25, 107, 112-116, 182).

Halogenides in general and fluorides especially belong to a class of materials that can easily be evaporated and condensed stoichiometrically. One disadvantage is that some fluorides and in particular chlorides and bromides are quite soluble in water. The most important fluorides are cryolite (generally speaking the compounds of NaF and AlF₃), MgF₂, and ThF₄.

Cryolite is transparent from 200 nm up to 14 μm, and forms films with low absorption in this region. Cryolite films show inhomogeneities in the refractive index of about 0.03. The packing density ranges between 0.88 and 0.92. During and after evaporation water vapor is absorbed in the films. The stress in cryolite films is tensile and amounts to 1.5×10^3 to 3.0×10^3 psi for a thickness of 1000 Å. The films are not very resistant to high humidity since at least NaF is quite soluble in water. In spite of the above-mentioned disadvantages cryolite films are often used, especially in combination with ZnS, for multilayer systems because they have the lowest refractive index of the useful materials and therefore give a good index contrast.

MgF₂ is probably the most widely used coating material. MgF₂ films can be used from 115 nm up to about 4 μm, the upper limit being due to the appearance

of cracks in a quarter-wave film at this wavelength and not to absorption. In thinner films it can be used up to $10\mu\text{m}$. [Unfortunately, the $10.6\mu\text{m}$ absorption coefficient $\beta \approx 10\text{ cm}^{-1}$ is too great.]

The films of MgF_2 are always crystalline, but thin films and films on cold substrates show a much finer grain size than thick films or films on heated substrates. Usually the films are formed of prismatic crystals which grow preferentially in the direction of the incident vapor beam. At thicknesses above 1000 \AA the films tend to be inhomogeneous and the inhomogeneity is increased with increasing thickness (39). MgF_2 films show extremely high tensile stress $3 \times 10^7 - 5 \times 10^7 \text{ kg/m}^2$ (4×10^4 to 7×10^4 psi). This stress is probably responsible for the appearance of cracks at larger thicknesses, for the inhomogeneity, and for some cases of incompatibility with other film materials, e.g., TiO_2 (135).

The mechanical and chemical properties of MgF_2 films are predominantly dependent on the packing density. Films with high packing density, obtained at a substrate temperature of 300°C or by annealing after deposition are extremely stable, hard, and adherent. MgF_2 films are also combined very often with ZnS , although here the stability is much less since no high substrate temperature can be used during the deposition of ZnS .

In recent years ThF_4 films have become important as low index material for dielectric mirrors, especially for the laser technique. Thorium fluoride as well as thorium oxifluoride can be used as a starting material. At 1000°C only thorium fluoride evaporates for either starting material (136). ThO_2 evaporates above 2000°C only. ThF_4 films are transparent from $0.2\mu\text{m}$ up to $15\mu\text{m}$. The films are mechanically and chemically quite stable. The packing density seems to depend on the preparation conditions. Films with high packing density can be obtained (22).

ThF_4 films show tensile stress on the order of $1.1 \times 10^7 - 1.5 \times 10^7 \text{ kg/m}^2$ ($1.6 \times 10^4 - 2.1 \times 10^4 \text{ psi}$). At exposure to air an appreciable reduction occurs (62). ThF_4 films can be made quite thick without the formation of cracks or peeling off. This property makes them well suited for infrared applications. ThF_4 is very compatible with ZnS in multilayer coatings, e.g., for laser mirrors.

One obvious disadvantage of ThF_4 is its radioactivity. It is necessary to follow up the security measures provided for work with radioactive materials according to the regulations of the authorities.

Other fluorides used occasionally for optical applications are CeF_3 (eventually LaF_3 or NdF_3) (53), LiF , BaF_2 , and PbF_2 . CeF_3 with its refractive index of 1.63 at 550 nm seems to be suitable for a three-layer antireflection coating (138). The stability is, however, not very satisfying.

BaF_2 can be used in the infrared up to $15\mu\text{m}$; its refractive index is 1.45 at $5\mu\text{m}$.

AlF_3 was recently proposed and investigated as a low index material (29). The films are transparent from 0.195 up to $10\mu\text{m}$; the refractive index in air is 1.38, in vacuum only 1.23. This large difference is due to a packing density of only 0.64.

Lead fluoride films consist of $\beta\text{-PbF}_2$. The packing density is about 0.90. [Unless the packing density can be increased, PbF_2 films probably will absorb so much water that the optical absorption will be too great for high-power use.] The stress behavior is interesting since with increasing film thickness a change from compressive to tensile stress occurs. The absolute stress values are low. PbF_2 will be reduced by hot tantalum, tungsten, or molybdenum. It has to be evaporated from Pt or ceramic crucibles.

CaF₂ forms very porous films which are not very stable. Therefore it is only rarely used today, although it played an important role for antireflection coatings 35 years ago.

Other halogenides that have been investigated for their possible use in the infrared are AgCl, TlCl, TlBr, and CsI. It has been shown that vacuum-deposited layers of these materials produce good quality antireflection coatings. AgCl and TlCl are most useful for wavelengths less than 30 μm. TlBr should be most useful in the range 30-45 μm, where AgCl and TlCl exhibit high optical absorption. The usefulness of CsI is limited because it is hygroscopic. Thallium compounds are toxic, therefore when working with such material, precautions should be taken to avoid poisoning (142).

ZnS is one of the standard coating materials for optical applications in the visible and infrared region. It is often used in combination with one of the low index fluorides, like MgF₂, ThF₄, or cryolite. it forms thick films that do not crack or peel off. The useful transmittance range covers the visible and the infrared up to 14 μm. The refractive index in the visible ranges between 2.60 and 2.30 since it shows a strong dispersion near the absorption edge. In the infrared the refractive index is around 2.3.

For an explanation of an occasionally found inhomogeneity in ZnS films, a boundary layer of ZnO is assumed (42, 43). ZnS films show a high packing density. The stability of ZnS films, e.g. their adhesion, depends very much on the cleaning and pretreatment of the substrate. For use as an antireflection coating on Ge, e.g. it is recommended that one use a 150°C substrate temperature and an effective glow discharge just prior to evaporation. In this way films can be produced to

withstand several hours boiling in 5% salt water, repeated washing, and exposure to moisture without damage (59). ZnS evaporates at approximately 1200°C.

In many respects ZnSe is similar to ZnS. A disadvantage is the absorption in the short part of the visible up to 0.46 μ m, an advantage the higher refractive index of 2.65 at 550 nm. ZnSe is used for the production of laser mirrors (8, 9).

Sb₂S₃ is sometimes used as a high index material in the red part of the visible spectrum since it is absorbing at short wavelengths. Its refractive index is 2.35 at 600 nm (4).

Oxides represent a very important group of coating materials because of their mechanical and chemical stability as well as because of their wide range of useful refractive indices. [Their use at 10.6 μ m is severely restricted by high absorption in general. They may be important, of course, in the 2-6 μ m region.] The preparation of oxide films is generally not as easy as of fluoride or sulfide films since most oxides react with crucible materials or dissociate at the required high temperatures. Useful low index oxide films are SiO₂ and Si₂O₃. Medium index films are SiO, Al₂O₃, MgO, ThO₂, ZrO₂, and the rare earth oxides, whereas CeO₂ and TiO₂ represent high index materials. SiO₂ films are transparent from 200 nm up to 9 μ m. The infrared spectrum between 9 and 15 μ m shows some marked differences (34).

By evaporation of SiO without oxygen, films are produced which are absorbing in the visible range but transparent in the infrared up to approximately 8 μ m.

Al₂O₃ films are transparent from at least 200 nm up to 7 μ m if they are prepared correctly.

MgO films have not yet found wide application since their stability is limited. They are transparent from 220 nm to 8 μ m if evaporated with an electron beam.

The films are crystalline and show increasing crystal size with increasing substrate temperature. During extended exposure to air a hazy bluish scattering coating forms on the surface of MgO films. This limits their usefulness as an optical coating material if used as an outer layer (20).

The same safety provisions as with ThF_4 have to be taken since ThO_2 is also radioactive.

ZrO_2 films are transparent from 340 nm up to 12 μm . One difficulty encountered when using ZrO_2 is a marked tendency to form inhomogeneous films probably due to a structural effect. The mechanical and chemical behavior is excellent, and it can easily be combined with other oxides and with MgF_2 .

The rare earth oxides such as La_2O_3 , Pr_6O_{11} , and Nd_2O_3 (53), Sc_2O_3 (145, 146) and Y_2O_3 (145, 146) also form films with a refractive index in the range from 1.9-2.1.

CeO_2 films are transparent in the visible and infrared region up to 12 μm . Thick films of CeO_2 exhibit high scattering losses which limits their usability already in the near infrared. The films are cubic at all substrate temperatures and the difference in refractive index is due to a different content of grain boundaries since at higher temperature the crystal size increases and therefore the concentration of boundary layers decreases (14). CeO_2 films are very stable, hard, and well adherent.

TiO_2 is an important high index material. It forms hard and adherent films with good chemical stability. Thick TiO_2 films show scatter loss which limits the usefulness in the infrared to around 3 μm ; otherwise thin films can be used up to 10-12 μm .

Bi_2O_3 films have been prepared by evaporation (147).

Mentioned in the literature, but obviously rarely used, are the oxides of antimony Sb_2O_3 (147, 148), arsenic As_2O_3 (149), beryllium BeO , boron B_2O_3 , lead PbO (150), gallium Ga_2O_3 (149), germanium GeO_2 (149), and tellurium TeO_2 (147).

The II-VI and IV-VI compounds ZnTe , CdTe , GeTe , and PbTe are mostly evaporated from one crucible.

Silicon films are transparent at wavelengths larger than 1 up to $9\mu\text{m}$ where they normally show absorption due to some oxygen content. The films are hard and very resistant.

Ge films show high transmission from $2\mu\text{m}$ on toward longer wavelengths.

Te films are transparent from 4 to $8\mu\text{m}$. The refractive index is quite high (~ 5.5). The mechanical stability, however, is not too good.

Careful control of growth conditions was necessary for GaAs, InP, and InAs films to ensure that the evaporated films had an absorption-edge steepness approaching that of bulk single-crystal gallium arsenide of the same thickness.

The use of organosilicone compounds for light guides with extremely low losses (12) and of fluorocarbon films for moisture protection (192) have been discussed.

Examples of multilayer antireflection coatings for the visible and near infrared are a four-layer coating for glass with a refractive index of 1.52 in the visible range consisting of CeO_2 and MgF_2 (158), another four-layer coating consisting of MgF_2 , ZrO_2 , and SiO_2 (159), and a triple-layer coating for LiNbO_3 in the near infrared, using the materials ThF_4 , ZnS , and MgF_2 (160). For $1.06\mu\text{m}$ several double- and triple-layer coatings consisting of combinations of MgF_2 , MgO , SiO_2 , and ThF_4 are described (74).

Antireflection coatings for the typical infrared materials as silicon, germanium, indium arsenide, and indium antimonide have been investigated extensively by Cox and co-authors (59, 153, 161). Useful materials are SiO, ZnS, CeO₂, Si, Ge, and MgF₂.

For wavelengths up to 50 μm , CsI, AgCl, TlBr, and TlCl have been proposed by Sherman and Coleman (142).

Reflector stacks are used as laser mirrors, color beam splitters, cold mirrors, heat reflecting filters, edge filters, solar cell covers, and for many other applications. Reflector stacks normally consist of alternating films of high and low refractive index. For most applications, a high index contrast is desired. For laser-mirror reflector stacks in the visible and near infrared region, the following combinations have been used:

ZnS - MgF ₂ (162)	ZnSe - Na ₃ AlF ₆ (9)
ZnS - ThF ₄ (163-165)	ZnSe - ThF ₄ (8)
ZnS - Na ₃ AlF ₆ (163)	CeO ₂ - MgF ₂ (166)
	TiO ₂ - SiO ₂ (165, 167) .

For the CO₂ laser at 10 μm , the combinations Ge-BaF₂ (168) and CdTe-ThF₄ (16) are described.

TABLE I
FILM MATERIALS AND THIN FILM PROPERTIES

Starting material	Deposition method* and approximate evaporation temperature	Film composition	Film crystal structure and packing density η at substrate temperature T_s ; film stress S	Refractive index n at wavelength and substrate temperature T_s	Transmittance range (μm)
Na_3AlF_6	B (1000°C)	Depending on boat temperature	crystalline, $\eta = 0.88$ ($T_s = 30^\circ\text{C}$) $\eta = 0.92$ ($T_s = 190^\circ\text{C}$) S : low tensile	1.32-1.35 depending on film composition	0.2-14
MgF_2	B (1250°C)	MgF_2	crystalline $\eta = 0.72$ ($T_s = 30^\circ\text{C}$) $\eta = 0.96$ ($T_s = 300^\circ\text{C}$) S : high tensile	1.32-1.39 at 550 nm in vacuum, depending on T_s , 1.38-1.40 at 550 nm in air (depending on T_s)	0.11-4 (cracking)
SiO_2	E	SiO_2	amorphous $\eta = 0.9$ ($T_s = 30^\circ\text{C}$) $\eta = 0.98$ ($T_s = 150^\circ\text{C}$) S : compressive	1.45-1.46 at 550 nm	0.2-9
ThF_4 , ThOF_2	B (1100°C)	ThF_4	X-ray amorphous S : medium tensile	1.52 at 550 nm and $T_s = 35^\circ\text{C}$	0.2-15
SiO	B, R (1250-1350°C)	Si_2O_5	amorphous	1.55 at 550 nm ($T_s = 30^\circ\text{C}$)	0.4-9
Al_2O_3	E (2050°C)	Al_2O_3	amorphous	1.59 at 550 nm and $T_s = 40^\circ\text{C}$, 1.63 at $T_s = 300^\circ\text{C}$	0.2-7
CeF_3	B (1350°C)	CeF_3	crystalline S : high tensile	1.63 at 550 nm and $T_s = 300^\circ\text{C}$	0.3-5
MgO	J (2800°C)	MgO	crystalline	1.70 at 550 nm and $T_s = 50^\circ\text{C}$, 1.74 at $T_s = 300^\circ\text{C}$	0.2-8
SiO	B (1250-1350°C)	SiO	amorphous	2.0 at 550 nm and $T_s = 30^\circ\text{C}$	0.7-9
ThO_2	E (3050°C)	ThO_2		1.95 at 300 nm	0.3
PbF_2	B (850°C)	PbF_2	β - PbF_2 S : depending on thickness compressive or tensile	1.75 at 550 nm 1.98 at 300 nm ($T_s = 30^\circ\text{C}$)	0.3-17
ZrO_2	B or E (2700°C)	ZrO_2		1.97 at 550 nm ($T_s = 30^\circ\text{C}$) 2.05 ($T_s = 200^\circ\text{C}$)	0.31-12
CeO_2	B or E (1600°C)	CeO_2	crystalline		0.4-12
TiO	B, R (1750°C)	TiO_2	amorphous at room temperature, crystalline at higher T_s S : high tensile	1.9 at 550 nm ($T_s = 30^\circ\text{C}$) 2.3 at 550 nm ($T_s = 220^\circ\text{C}$) 2.55 at 550 nm ($T_s = 260^\circ\text{C}$)	0.4-3 (fouling)
ZnS	H (1200°C)	ZnS	crystalline S : medium compressive	2.3 at 550 nm ($T_s = 30^\circ\text{C}$)	0.4-14
Si	B or E (1500°C)	Si	amorphous up to $T_s = 300^\circ\text{C}$	3.4 at 3 μm	1-9
Ge	B or E (1600°C)	Ge	amorphous up to $T_s = 300^\circ\text{C}$	4.4 at 2 μm ($T_s = 30^\circ\text{C}$)	2-23
PbTe	B (850°C)	PbTe		5.6 at 5 μm	3.5-20

* B, boat; E, electron beam; R, reactive.

E. Ritter's References

1. G. Koppelman, *Ann. Phys. (Leipzig)* [7] 5, 388 (1960).
2. L. Young, *J. Opt. Soc. Amer.* 52, 753 (1962).
3. A. S. Valeev, *Opt. Spectrosc.* 18, 48 (1964).
4. H. Anders and R. Eichinger, *Optik* 25, 17 (1967).
5. R. Jacobsson, *Pap., Int. Vacuum Congr., 5th, 1971* Paper No. Q-1, p. 690 (1971).
6. H. Ahrens, H. Welling, and H. E. Scheel, *Appl. Phys.* 1, 69 (1973).
7. W. Brügel, "Einführung in die Ultrarotspektroskopie," p. 285. Steinkopff, Darmstadt, 1969.
8. W. Heitmann, *Z. Angew. Phys.* 21, 503 (1966).
9. W. Heitmann, *Z. Angew. Phys.* 19, 392 (1965).
10. J. E. Goell and R. D. Standley, *Proc. IEEE* 58, 1501 (1970).
11. D. H. Hensler, J. D. Cuthbert, R. J. Martin, and P. K. Tien, *Appl. Opt.* 10, 1037 (1971).
12. P. K. Tien, G. Smolinsky, and R. J. Martin, *Appl. Opt.* 11, 637 (1972).
13. P. H. Lissberger, *Rep. Progr. Phys.* 33, 197 (1970).
14. G. Hass, J. B. Ramsey, and R. Thüm, *J. Opt. Soc. Amer.* 48, 324 (1958).
15. W. P. Barr, *J. Sci. Instrum.* [2] 2, 1112 (1969).
16. A. I. Braunstein and M. Braunstein, *J. Vac. Sci. Technol.* B, 412 (1971).
17. O. W. Black and J. Wales, *Infrared Phys.* 8, 209 (1968).
18. B. Dudenhausen and G. Müllenstedt, *Z. Angew. Phys.* 27, 191 (1969).
19. J. T. Cox, G. Hass, and J. B. Ramsey, *J. Phys. (Paris)* 25, 250 (1961).
20. A. P. Bradford, G. Hass, and M. McFarland, *Appl. Opt.* 11, 2312 (1972).
21. H. Koch, *Phys. Status Solidi* 12, 533 (1965).
22. W. Heitmann and G. Koppelman, *Z. Angew. Phys.* 23, 221 (1967).
23. E. Ritter and R. Hoffmann, *J. Vac. Sci. Technol.* 6, 733 (1969).
24. D. Haeman, *Opt. Acta* 17, 639 (1970).
25. H. K. Pulker and E. Jung, *Thin Solid Films* 9, 57 (1971).
26. J. T. Gruyters and N. A. Krijzer, *Proc. Int. Conf. Thin Films, 1972* Vol. II, p. 299 (1972).
27. G. Koppelman, K. Krebs, and H. Leyendecker, *Z. Phys.* 163, 557 (1961).
28. M. Bourg, Thesis, Faculté des Sciences de l'Université D'Aix-Marseille (1963).
29. W. Heitmann, *Thin Solid Films* 5, 61 (1970).
30. E. Ritter, *Vak.-Tech.* 21, 42 (1972).
31. H. K. Pulker and C. Zanner, *Thin Solid Films* 5, 421 (1970).
32. G. Hass and C. D. Salzberg, *J. Opt. Soc. Amer.* 44, 181 (1954).
33. G. Siddal, *Vacuum* 9, 274 (1960).
34. E. Ritter, *Opt. Acta* 9, 197 (1962).
35. F. Vinckier, *Optik* 20, 43 (1963).
36. S. Fujiwara, *J. Opt. Soc. Amer.* 53, 1315 (1963).
37. S. Fujiwara, *J. Opt. Soc. Amer.* 53, 880 (1963).
38. J. F. Hall, Jr., *J. Opt. Soc. Amer.* 46, 1013 (1956).
39. K. Nagata, *Jap. J. Appl. Phys.* 7, 1181 (1968).
40. E. Bauer, in "Ergebnisse der Hochvakuumtechnik und der Physik dünner Schichten" (M. Auwärter, ed.) p. 39. Wiss. Verlagsges., Stuttgart, 1957.
41. A. Bourg, N. Barbanoux, and M. Bourg, *Opt. Acta* 12, 151 (1965).
42. W. R. Oliver, *Phil. Mag. [S]* 21, 1229 (1970).
43. W. R. Oliver, *Opt. Acta* 17, 591 (1970).
44. R. Jacobsson, *J. Phys. (Paris)* 25, 19 (1961).
45. R. Jacobsson and J. O. Martensson, *Appl. Opt.* 5, 29 (1966).
46. H. Anders and R. Eichinger, *Appl. Opt.* 4, 819 (1965).
47. H. Mayer, "Physik dünner Schichten," Vol. 1. Wiss. Verlagsges., Stuttgart, 1950.
48. O. S. Heavens, in "Physics of Thin Films" (G. Hass and R. E. Thüm, eds.), Vol. 2, p. 1963. Academic Press, New York, 1965.
49. F. Abelès, *Prog. Opt.* 2, 219 (1963).
50. O. S. Heavens, "Optical Properties of Thin Solid Films." Butterworth, London, 1955.

51. F. Abdels, *J. Phys. Radion* [8] 11, 310 (1950).
52. L. Huldt and T. Stallot, *Opt. Acta* 6, 27 (1959).
53. G. Hass, J. B. Ramsey, and R. Thun, *J. Opt. Soc. Amer.* 49, 116 (1959).
54. A. C. S. van Heel and W. van Vomm, *Appl. Opt.* 6, 793 (1967).
55. T. Krouse, Balzers Hochvakuum-Fachbericht No. 5 (1965) (Publication of Balzers AG).
56. M. Nishihori and K. Kinoshita, *Jap. J. Appl. Phys.* 11, 758 (1972).
57. K. Kinoshita, *Thin Solid Films* 12, 17 (1972).
58. R. Jacobsson and B. Kruse, *Thin Solid Films* 16, 71 (1973).
59. J. T. Fox and G. Hass, *J. Opt. Soc. Amer.* 48, 677 (1958).
60. R. C. Sundahl, *J. Vac. Sci. Technol.* 9, 181 (1972).
61. H. von Harrach and H. N. Chapman, *Proc. Int. Conf. Thin Films, 1972* Vol. II, p. 157 (1972).
62. A. E. Ennos, *Appl. Opt.* 5, 51 (1966).
63. R. W. Hoffmann, in "Physics of Thin Films" (G. Hass and R. Thun, eds.), Vol. 3, p. 211. Academic Press, New York, 1966.
64. T. J. Schenemann, *J. Vac. Sci. Technol.* 6, 115 (1969).
65. R. J. Schenemann, *J. Vac. Sci. Technol.* 7, 113 (1970).
66. H. Schröder and G. Schmidt, *Z. Angew. Phys.* 18, 121 (1964).
67. W. Heitmann, *Appl. Opt.* 10, 2685 (1971).
68. U.S.MIL-Spez. C-675 A (1964).
69. U.S.MIL-Spez. C-14806 A (1969).
70. Procurement Specification HAC NPS 30660-083 (1969).
71. A. J. Glass and A. H. Guenther, *Appl. Opt.* 12, 637 (1973).
72. L. I. De Sloover and H. E. Newman, "Laser Damage to Antireflection Coatings," USCEER Rep. No. 436, University of Southern California, Los Angeles, 1972.
73. E. S. Bliss, D. Milam, and R. A. Bradbury, *Appl. Opt.* 12, 677 (1973).
74. A. F. Turner, *Nat. Bur. Stand. (U.S.), Spec. Publ.* 356, (1971).
75. R. R. Austin and A. H. Guenther, *Appl. Opt.* 11, 605 (1972).
76. R. R. Austin, R. Michaud, A. H. Guenther, and J. Putman, *Appl. Opt.* 12, 665 (1973).
77. H. K. Pulker, *Proc. Int. Conf. Thin Films, 1972* Vol. II, p. 291 (1972).
78. G. Hass and W. R. Hunter, *Appl. Opt.* 9, 2101 (1970).
79. C. A. Nicoletta and A. G. Embanks, *Appl. Opt.* 11, 1365 (1972).
80. F. A. Koch and R. W. Vook, *J. Vac. Sci. Technol.* 10, 313 (1973).
81. E. Ritter and A. Ross, in "Ergebnisse der Hochvakuumtechnik und der Physik dünner Schichten" (M. Anwärter, ed.), Vol. II, p. 269. Wiss. Verlagsges., Stuttgart, 1971.
82. J. H. Blifford, Jr., *Appl. Opt.* 5, 105 (1966).
83. M. L. Baker and V. L. Yen, *Appl. Opt.* 6, 1313 (1967).
84. A. Peršin, B. Marković, H. Kunčarić, and M. Peršin, *Thin Solid Films* 3, 387 (1969).
85. D. H. McKenney and P. N. Slater, *Appl. Opt.* 9, 2135 (1970).
86. H. A. MacLeod, "Thin Film Optical Filters," Hilger & Watts, London, 1969.
87. H. Schröder, in "Physics of Thin Films" (G. Hass and R. Thun, eds.), Vol. 5, p. 87. Academic Press, New York, 1969.
88. Holland, "Vacuum Deposition of Thin Films," Chapman & Hall, London, 1961.
89. C. Powell, J. H. Oxley, and J. M. Blocher, Jr., eds., "Vapor Deposition," Wiley, New York, 1966.
90. K. L. Chopra, "Thin Film Phenomena," McGraw-Hill, New York, 1969.
91. G. Zinsmeiser, in "Mikroelektronik" (L. Steipe, ed.), p. 91. Oldenbourg, Munich, 1965.
92. P. B. Chapman, N. J. Downs, and H. J. King, *Appl. Opt.* 8, 1965 (1969).
93. H. Tanaka and H. Kuonura, *Jap. J. Appl. Phys.* 4, 633 (1965).
94. D. Poffmann and D. Leibowitz, *J. Vac. Sci. Technol.* 9, 326 (1972).
95. H. Lewis, *Microelectron. Rel.* 3, 109 (1961).
96. H. M. Smith and A. F. Turner, *Appl. Opt.* 4, 147 (1965).
97. J. A. R. Samson, J. P. Padur, and A. Sharma, *J. Opt. Soc. Amer.* 57, 966 (1967).
98. G. Grob, *J. Appl. Phys.* 39, 5804 (1968).
99. G. Hass and J. B. Ramsey, *Appl. Opt.* 8, 1115 (1969).
100. J. E. Johnson, *J. Appl. Phys.* 36, 3103 (1965).

101. J. L. Richards, P. B. Hart, and L. M. Callone, *J. Appl. Phys.* **34**, 3418 (1963).
 102. M. H. Francombe and J. E. Johnson, in "Physics of Thin Films" (G. Hass and R. E. Thun, eds.), Vol. 5, p. 443. Academic Press, New York, 1969.
 103. K. G. Günther and W. Hanlein, *Naturwissenschaften* **45**, 415 (1958).
 104. R. P. Howson, *J. Opt. Soc. Amer.* **55**, 271 (1965).
 105. J. E. Davey and T. Paulsey, *J. Appl. Phys.* **39**, 1911 (1968).
 106. E. Cremer, T. Kraus, and E. Ritter, *Z. Elektrochem.* **62**, 939 (1958).
 107. T. I. Putner, *Opt. Laser Technol.* **4**, 79 (1972).
 108. E. Ritter, *J. Vac. Sci. Technol.* **3**, 225 (1966).
 109. G. Hass, private communication (1973).
 110. W. Heitmann, *Appl. Opt.* **10**, 2111 (1971).
 111. W. Heitmann, *Vak.-Tech.* **21**, 1 (1972).
 112. P. Goldfinger and M. Jennehomme, *Advan. Mass Spectrom.* **1**, 531 (1959).
 113. J. Berkowitz, W. A. Chupka, and M. G. Ingram, *J. Chem. Phys.* **25**, 1569 (1957).
 114. H. K. Polker and E. Jung, *Thin Solid Films* **4**, 219 (1969).
 115. P. Gräber and K. G. Weil, *Ber. Bunsenges. Phys. Chem.* **76**, 410 (1972).
 116. E. Rutner, P. Goldfinger, and J. P. Hirth, eds., "Condensation and Evaporation of Solids." Gordon & Breach, New York, 1961.
 117. R. A. Leff, *Appl. Opt.* **10**, 968 (1971).
 118. W. J. Coleman, *J. Opt. Soc. Amer.* **63**, 29 (1973) (abstr.).
 119. C. Leja, *Acta Phys. Pol. A* **38**, 165 (1970).
 120. J. L. Vossen, *RCA Rev.* **32**, 289 (1971).
 121. D. B. Fraser and H. D. Cook, *J. Electrochem. Soc.* **119**, 1368 (1972).
 122. D. M. Mattox, *J. Appl. Phys.* **34**, 2493 (1963).
 123. H. R. Harker and R. J. Hill, *J. Vac. Sci. Technol.* **9**, 1395 (1972).
 124. W. Heitmann, *Appl. Opt.* **7**, 1511 (1968).
 125. J. M. Nieuwenhuizen and H. B. Haanstra, *Philips Tech. Rundsch.* **27**, 177 (1966).
 126. J. M. Pearson, *Thin Solid Films* **6**, 319 (1970).
 127. H. K. Polker and K. H. Günther, *Vak.-Tech.* **21**, 201 (1972).
 128. A. P. Bradford and G. Hass, *J. Opt. Soc. Amer.* **53**, 1086 (1963).
 129. A. P. Bradford, G. Hass, M. McFarland, and E. Ritter, *Appl. Opt.* **4**, 971 (1965).
 130. I. J. Hodgkinson, *Appl. Opt.* **9**, 1577 (1970).
 131. I. J. Hodgkinson, *Appl. Opt.* **11**, 1970 (1972).
 132. G. Hass and E. Ritter, *J. Vac. Sci. Technol.* **4**, 7 (1967).
 133. H. K. Polker and E. Ritter, in "Ergebnisse d. r. Hochvakuum-technik und der Physik dünner Schichten" (M. Auwaerter, ed.), Vol. II, p. 244. Wiss. Verlagsges., Stuttgart, 1971.
 134. G. Koppelman and K. Krebs, *Z. Phys.* **156**, 38 (1952).
 135. H. Anders, "Dünne Schichten für die Optik," Wiss. Verlagsges., Stuttgart, 1965.
 136. W. Heitmann and E. Ritter, *Appl. Opt.* **7**, 307 (1968).
 137. A. Heisen, *Optik* **19**, 59 (1961).
 138. J. T. Cox, G. Hass, and A. Thelen, *J. Opt. Soc. Amer.* **52**, 965 (1962).
 139. W. R. Hunter, J. F. Osantowski, and G. Hass, *Appl. Opt.* **10**, 510 (1971).
 140. M. R. Adriaens and B. Fenechalcher, *Appl. Opt.* **10**, 958 (1971).
 141. G. Honcia and K. Krebs, *Z. Phys.* **165**, 117 (1959).
 142. G. H. Sherman and P. D. Coleman, *Appl. Opt.* **10**, 2675 (1971).
 143. J. T. Cox, J. E. Waylonis, and W. R. Hunter, *J. Opt. Soc. Amer.* **49**, 807 (1959).
 144. J. H. Apfel, *J. Opt. Soc. Amer.* **56**, 553A (1966).
 145. W. Heitmann, *Appl. Opt.* **12**, 391 (1973).
 146. W. Heitmann, *Vak.-Tech.* **22**, 41 (1973).
 147. G. Honcia and K. Krebs, *Z. Phys.* **165**, 202 (1959).
 148. K. Heft, R. Kern, G. Nöldeke, and A. Steudel, *Z. Phys.* **175**, 391 (1963).
 149. G. Honcia and K. Krebs, *Z. Phys.* **165**, 213 (1961).
 150. A. E. Emes, *J. Opt. Soc. Amer.* **52**, 261 (1962).
 151. K. L. Chopra and S. K. Bahl, *J. Appl. Phys.* **40**, 4171 (1969).
 152. J. S. Seely, C. S. Evans, and R. Hunneman, *J. Vac. Sci. Technol.* **9**, 307 (1972).
 153. J. T. Cox, G. Hass, and G. F. Jacobus, *J. Opt. Soc. Amer.* **51**, 714 (1961).
 154. J. Wales, G. J. Lowitt, and R. A. Hill, *Thin Solid Films* **1**, 137 (1967).
 155. I. H. Pratt and S. Firestone, *J. Vac. Sci. Technol.* **8**, 256 (1971).

156. J. E. Goell, *Appl. Opt.* **12**, 737 (1973).
157. J. T. Cox and G. Hass, in "Physics of Thin Films" (G. Hass and R. E. Thun, eds.), Vol. 2, p. 239. Academic Press, New York, 1965.
158. A. J. Vermeulen, *Opt. Acta* **18**, 531 (1971).
159. J. Ward, *Vacuum* **22**, 369 (1972).
160. J. W. Barthold, *Appl. Opt.* **9**, 1190 (1970).
161. J. T. Cox, *J. Opt. Soc. Amer.* **51**, 1106 (1961).
162. D. B. Hennet, *J. Opt. Soc. Amer.* **52**, 31 (1962).
163. D. L. Perry, *Appl. Opt.* **4**, 987 (1965).
164. K. H. Behrndt and V. W. Doughty, *J. Vac. Sci. Technol.* **3**, 261 (1966).
165. D. W. Gregg and S. J. Thomas, *Appl. Phys. Lett.* **B**, 316 (1966).
166. D. S. Heavens, "Optical Masers." Methuen, London, 1964.
167. V. B. Costrell, *Laser Focus Nov.* p. 41 (1969).
168. C. T. Meneely, *Appl. Opt.* **6**, 1431 (1967).
169. D. K. Burge, H. E. Bennett, and E. J. Asley, *Appl. Opt.* **12**, 42 (1973).
170. L. F. Drummetter, Jr. and G. Hass, in "Physics of Thin Films" (G. Hass and R. E. Thun, eds.), Vol. 2, p. 305. Academic Press, New York, 1965.
171. A. P. Bradford, G. Hass, J. B. Heaney, and J. J. Triolo, *Appl. Opt.* **9**, 332 (1970).
172. G. Hass, J. B. Bansey, J. B. Heaney, and J. J. Triolo, *Appl. Opt.* **10**, 1296 (1971).
173. G. Smolinsky, *J. Vac. Sci. Technol.* **H**, 33 (1974).
174. L. L. Nichols, C. A. Ratcliffe, and B. L. Gordon, *Appl. Opt.* **12**, 2232 (1973).
175. E. Kerr, *Appl. Opt.* **12**, 2520 (1973).
176. R. A. Hoffmann, *Appl. Opt.* **13**, 1405 (1974).
177. H. P. Weber, P. A. Dunn, and W. N. Basilewitz, *Appl. Opt.* **12**, 755 (1973).
178. C. Weaver, *Vacuum* **35**, 171 (1965).
179. N. M. Polley and H. J. Whitaker, *J. Vac. Sci. Technol.* **H**, 114 (1974).
180. B. N. Chapman, *J. Vac. Sci. Technol.* **H**, 106 (1974).
181. H. P. Howson and A. Taylor, *Thin Solid Films* **9**, 109 (1971).
182. H. Schmeisser, *Vak.-Tech.* **21**, 165 (1972).
183. H. L. Claver and H. J. Seguin, *Rev. Sci. Instrum.* **41**, 427 (1970).
184. W. D. Westwood, B. J. Boynton, and S. J. Ingrey, *J. Vac. Sci. Technol.* **H**, 381 (1971).
185. R. H. Dratch, E. J. West, T. G. Giallorenzi, and J. F. Weller, *Appl. Opt.* **13**, 712 (1974).
186. J. G. Davy and J. J. Hanak, *J. Vac. Sci. Technol.* **H**, 43 (1974).
187. J. F. Hall, Jr. and W. F. C. Ferguson, *J. Opt. Soc. Amer.* **45**, 74 (1955).
188. J. F. Hall, Jr., *J. Opt. Soc. Amer.* **47**, 662 (1957).
189. E. T. Hutcheson, J. T. Cox, G. Hass, and W. H. Hunter, *Appl. Opt.* **11**, 1590 (1972).
190. E. T. Hutcheson, G. Hass, and J. T. Cox, *Appl. Opt.* **11**, 2245 (1972).
191. P. Baumeister, *Appl. Opt.* **12**, 923 (1973).
192. J. R. Hollahan, *J. Vac. Sci. Technol.* **H**, 167 (1974).

R. C. Pastor and M. Braunstein, Hughes Research Laboratories, "Advanced Mode Control and High-Power Optics Technology," Technical Report No. AFWL-TR-72-152, Vol. II, July 1973

An earlier study by other workers reported a large surface absorption at $10.6 \mu\text{m}$ (F. Horrigan, C. Klein, R. Rudko, and D. Wilson, Microwaves, pp. 68-76, Jan. 1969). For KCl the reported surface absorption was $> 80\%$ of the total absorption for a 1-cm thickness. The cause was thought to be hygroscopic behavior. However, our RAP treatment of the crystal surface, i.e., topochemical exchange, did not improve β . In addition, we showed that neither surface hydrolysis (exchange of OH^- for Cl^-) nor hygroscopic behavior (surface uptake of H_2O) contributed to the surface absorption of a KCl crystal with $\beta = 0.0042 \text{ cm}^{-1}$, with measurements well within a precision of $\pm 0.0004 \text{ cm}^{-1}$. Instead, our study indicated that fabrication damage (surface preparation) can contribute to bulk absorption in a manner which could be mistaken for surface absorption. The effect on absorptance of surface reworking indicates that the measured value may still have been affected by damage introduced by the polishing operation. Such damage is easily observed using polarized light on an annealed specimen, before and after polishing. [This important negative result for surface hydrolysis and hygroscopicity is not inconsistent with absorption by a few layers of water molecules as discussed in Sec. IV since the predicted value of $A_f = 10^{-4}$ is below the measurement precision of 4×10^{-4} .]

Two types of surface finish were given to KCl samples. They are designated as optical finish and window finish. Optical finish samples are worked until flat and parallel within one fringe of visible light. Window finish samples are flat within a few fringes, with no attempt made to achieve parallelism. The optical

finish is smoother and more uniform, with a characteristic size of the features a few tenths of a micrometer, similar to that of the Linde A abrasive used to prepare it. The window finished surface has some regions with the same characteristic size as the optical finish but also has some features greater than $1\mu\text{m}$ in size. The number and depth of scratches is also greater on the window finish surface. Optical finish samples showed a strong tendency to fog during the few minutes that they were exposed to the 50% relative humidity laboratory environment before placement in the desiccated calorimeter, even though placed in desiccators immediately after polishing was completed.

The most striking example of the effect of a fogged surface on the measured absorption was for a sample with both surface finishes. It was first found to have an absorption coefficient of 0.00048 cm^{-1} with a window finish. After return to the optical shop for application of an optical finish, the absorption coefficient was found to be 0.00185 cm^{-1} . The higher absorptions measured in the fogged optical finish samples may be a result of surface absorption caused by the fogging, but they are also partially due to the high scattering of these surfaces. Light scattered directly to the thermocouple in the calorimeter causes a temperature rise in the thermocouple which is then attributed to absorption in the sample. It is manifested as a component of the temperature signal, which does not have the normal time lag due to heat conduction when the laser is turned on or off.

Scanning electron microscope views of fogged surfaces showed that the fogging of the surface is caused by recrystallization of the surface region of the crystal; upward growing crystallites [which appeared to have typical heights and widths of $\sim 0.5\mu\text{m}$] scatter light and thus produce the fogged appearance.

The fogging problem was brought under control by heating the KC1 windows to $\approx 50^{\circ}\text{C}$ with an IR lamp immediately after polishing. Though it is believed this process removes water that was present on the surface as a result of the alcohol polish, it is not clear that this is the only process which leads to the increase in surface stability. The window can then be placed in a vacuum deposition chamber for coating or potted in carboline plastic for future use.

Morris Braunstein and J. Earl Rudisill, Hughes Research Laboratories,
"Protective-Antireflective Thin Films for Polycrystalline Zinc Selenide and
Alkali Halide Laser Windows," Contract No. F33615-73-C-5044, Final
Report, February 1975

It was found that the $10.6 \mu\text{m}$ refractive index of ThF_4 coatings on CdTe and
on ZnSe had the value $n_r = 1.35$, rather than the previously accepted value of
 $n_r = 1.50$.

Coating on ZnSe. Two-layer coatings of $\text{ThF}_4 / \text{ZnSe}$, of $\text{ThF}_4 / \text{ZnSe}$, and of $\text{BaF}_2 / \text{ZnS}$, where the notation indicates that the first material, ThF_4 , is deposited first, were deposited on ZnSe with a substrated temperature $T_S = 150^\circ\text{C}$ at a pressure of 10^{-6} to 10^{-7} torr and a deposition rate of 180 nm/min for ThF_4 , 50 - 60 nm/min for ZnS and ZnSe, and 200 nm/min for BaF_2 . The results are summarized in Tables IV and V [original report numbers]. The $\text{BaF}_2 / \text{ZnS}$ coating work was abandoned because this coating did not pass the environmental humidity test. The $\text{ThF}_4 / \text{ZnSe}$ coating had a value of $A_f = 3 \times 10^{-4}$ per surface, which is the lowest value for any $10.6 \mu\text{m}$ coating reported to date. Two windows coated with $\text{ThF}_4 / \text{ZnS}$ passed the military specification tests for adherence, humidity, salt spray, and abrasion (the most difficult test).

Coating on KCl. Two-layer coatings of ZnSe/ThF_4 were abandoned because they cracked and peeled upon removal from the vacuum system. The difficulty was attributed to strain induced through the large thickness requirement ($2 \mu\text{m}$) of the inner ZnSe layer. After many tries, one coating remained intact long enough to measure an absorptance of $A_f = 1.7 \times 10^{-3}$ per surface. For $\text{ThF}_4 / \text{ZnSe}$ coatings deposited on the KCl substrate at 150°C no apparent sticking or cracking and peeling difficulties were encountered. The ZnSe layer is thinner than in the ZnSe/ThF_4 coating. However, the thicker ThF_4 layer gave rise to a greater value of $A_f = 2.4 \times 10^{-3}$ to 4.0×10^{-3} per surface.

A difficulty with $\text{As}_2\text{S}_3/\text{ThF}_4$ coatings on KCl was anticipated since the sticking coefficient of As_2S_3 on KCl is practically zero for substrate temperatures greater than 75°C, while the substrate temperature must be at least 150°C for ThF_4 deposition in order to keep the absorptance of ThF_4 low. A layer of As_2S_3 baked at 175°C in vacuum for two hours apparently dissociated leaving an extremely thin layer whose absorption increased nearly an order of magnitude. Another KCl sample coated with As_2S_3 of optical thickness $0.457 \lambda_0$ yielded an absorption index of $\kappa = 7 \times 10^{-5}$ for As_2S_3 , which corresponds to $\beta_b = 0.8 \text{ cm}^{-1}$. [This is an important result that $\beta_f = \beta_b$ for As_2S_3 . This is the only case of $\beta_f = \beta_b$ found in the literature as of this writing. Also, the HRL value of $\beta_b = 0.8 \text{ cm}^{-1}$ is the lowest value found, and is believed to be the intrinsic $10.6 \mu\text{m}$ value.]

ThF_4 of optical thickness $0.168 \lambda_0$ was then deposited at 150°C to complete the AR coating. This system yielded reflectance values less than 0.03% per surface and an absorption value of 0.19% per surface. The amount of As_2S_3 that dissociated at 150°C, though apparently small, appears to be significant in that absorption values still exceed 0.1% per surface.

The coating performance of the coatings on KCl substrates are summarized in Table X.

TABLE IV. ANTIREFLECTION COATING RESULTS ON ZnSe WINDOWS

Coating Design	Optical Thicknesses λ	Absorption Per Surface, %			Reflectance Per Surface, %		
		Predicted	Goal	Achieved	Predicted	Goal	Achieved
ThF ₄	0.250	0.03	0.10	0.08	1.98	c. 1.0	2.20
BaF ₂ /ZnS	0.138/0.059	0.07	0.10	0.11	0	0.10	0.23
ThF ₄ /ZnSe	0.132/0.052	0.02	0.10	0.03	0	c. 1.0	0.03
ThF ₄ /ZnS	0.126/0.065	0.03	0.10	0.06	0	0.10	0.02

TABLE V. ENVIRONMENTAL RESULTS ON COATED ZnSe WINDOWS

Coating Design	Environmental Tests			
	Adherence	Humidity	Salt Spray	Abrasion
ThF_4	P	P	P	F
BaF_2/ZnS	P	F	-	-
ThF_4/ZnSe	P	F	P	F
ThF_4/ZnS	P	P ^(a)	P	P ^(b)

(a) Also passed an extended 28 day humidity test.

(b) Passed only on mechanical-chemical etched substrates.

TABLE X. ANTIREFLECTION COATING RESULTS ON KCl WINDOWS

Coating Design	Optical Thicknesses, λ	Absorption Per Surface, %			Reflectance Per Surface, %	
		Predicted	Goal	Achieved	Predicted	Goal
$ZnSe/ThF_4$	(a) 0.041/0.332	0.11	0.10	0.24	0	0.10
	(b) 0.459/0.168	0.07	0.10	0.17	0	0.10
As_2S_3/ThF_4	(b) 0.457/0.168	0.07	0.10	0.19	0	0.10

M. Braunstein, A. I. Braunstein, J. Earl Rudisill, and V. Wang, Hughes Research Laboratories, "Low Absorption Coating Technology," Final Technical Report, Contract No. F29601-72-C-0132, December 1973

[Although a portion of this report concerns coatings for metals to increase their reflectance, the thin-film work is applicable to window coatings. In considering the optical absorption by a contaminated surface, of adsorbed water for example, it is important to realize that the electric field at the surface of an antireflection coating is large, while the electric field at the surface of a reflection-enhancing coating is nearly zero for normal incidence. (For a highly reflecting coating the only power flow into the coating is that corresponding to the small absorption; thus $\underline{E} \times \underline{H} \cong 0$, which is consistent with $E = 0$.)]

An improvement in the absorptance of enhanced reflectivity multilayer dielectric mirrors from 0.005 at $10.6\mu\text{m}$ at the beginning of the study to a value as low as 0.0012 at $10.6\mu\text{m}$ for $^{84}\text{Ag}/(\text{ThF}_4/\text{CdTe})^3$ has been achieved. The absorptance improvement from 0.005 to 0.0012 has been shown to be due to improvements in the purity of the ThF_4 and CdTe dielectric materials; film deposition techniques are shown to be critical and must be carefully controlled. Further improvements in material purity or film deposition techniques can be expected to lower absorptance even more. New coatings with potential application at $10.6\mu\text{m}$ include the reflector $\text{Al}/(\text{KCl}/\text{As}_2\text{S}_3)^4$ which has shown 0.0016 absorptance and a high-energy density damage threshold of $\sim 50\text{ J/cm}^2$ for nsec pulses. The program goal, which was to produce reflectors having 99.9% reflectance at $10.6\mu\text{m}$, was almost met by achieving 99.88% for a $\text{Ag}/(\text{ThF}_4/\text{CdTe})^3$ reflector. For other coatings we have achieved reflectances of 99.78% for $\text{Cu}/(\text{ThF}_4/\text{CdTe})^2$, 99.82% for $\text{Al}/(\text{ZnS}/\text{Ge})^2$, and 99.84% for $\text{Al}/(\text{KCl}/\text{As}_2\text{S}_3)^4$. Rigorous control of

starting materials used for the coatings and the deposition techniques was found to be essential for the preparation of the high reflectance, low absorptance coatings.

Accurate single transverse mode damage threshold measurements have shown damage thresholds of around 35 J/cm^2 for simple metal mirrors. [The nominal 600 ns pulse consists of a ~ 230 ns pulse containing roughly one third of the total energy of the pulse, followed by a tail approximately $3 \mu\text{s}$ long containing the remaining two thirds of the energy.⁵⁴ On a finer time scale, 5-ns wide longitudinal mode-beating modulation was observed. Laser spot sizes were not reported, but most damage was reported to be at localized damage sites.] Damage resistance of dielectric enhanced reflectivity mirrors has progressed from 1 J/cm^2 to 65 J/cm^2 by careful selection of materials used for multilayer film fabrication. Several film and window materials have been found to exhibit good damage resistance, and are listed in approximate order of damage resistance: KCl, NaCl, As_2S_3 , ZnS, BaF_2 , ZnSe, CdTe.

[The report contains interesting microphotographs, scanning-electron microscope views, and X-ray microprobe views of film damage sites showing: randomly located microcraters whose density increases as the intensity of radiation increases (supposedly from inclusion damage); straight-line and square-matrix interference-fringe damage patterns for $\lambda/4$ CdTe films on CdTe (self films) resulting from the small wedge angle between the two surfaces of the high refractive index ($n_r = 3.0$) CdTe substrate; substrate separation of $\lambda/4$ ThF_4 films on a copper substrate; circular interference-fringe damage patterns produced by an incident plane wave whose intensity peak is to the side of a major inclusion, with scattering from the inclusion into the $\lambda/2$ thin film and interference between the incident wave, the scattered wave, and the reflected wave; and a fracture zone around an inclusion.]

Damage normally is accompanied by a small visible plasma or spark during these tests. In the case of As_2S_3 coatings, the observation of such a plasma caused the misleading termination of many tests. Microscopic examination of the surface after sparking revealed no microcratering or other sign of damage. After the sparking, what was apparent to the naked eye and the microscope was a decrease in visible light scattering similar to what might be expected of fire polishing of glass. Continuation of tests on these sites would reveal no additional sparking or marked changes as long as the energy density was gradually increased upon a given site. This conditioning of the test site could progress until values of as much as 65 J/cm^2 were reached, where damage in the form of darkening and film fracture was observed. This appearance of a plasma before real damage may be attributable to a cleaning process by the laser beam, where local absorption centers or inclusions are removed. [It is conceivable that high-power lasers could be brought up to power slowly in order to effect such cleaning action and thereby avoid damage.]

In general, film absorption indices at $10.6 \mu\text{m}$ must be 5×10^{-4} [$\beta = 6 \text{ cm}^{-1}$] or below in order to be able to reach the 99.9% reflectance [$A = 10^{-3}$] goal. It is desirable to be able to reach absorption index values near 1×10^{-4} [$\beta = 1.2 \text{ cm}^{-1}$] as this would allow some margin for error in the enhanced metallic reflector fabrication. [The required mirror-coating value of $\beta_f = 6 \text{ cm}^{-1}$ for $A_f = 10^{-3}$ is close to the window coating value of $\beta_f = 5 \text{ cm}^{-1}$ for $A_f = 10^{-3}$.]

[Two self films were grown.] A quarter-wave optical-thickness KC1 film on KC1 had $\beta_f < 0.6 \text{ cm}^{-1}$. A quarter-wave optical-thickness CdTe film on CdTe had $\beta_f \approx 2 \text{ cm}^{-1}$. The absorption coefficient of the uncoated CdTe substrate was $\beta_b = 3.4 \times 10^{-3} \text{ cm}^{-1}$. [It would be of interest to determine if extremely thick self films could be grown and if the absorption coefficient could be made to approach the bulk value.]

C. Willingham, D. Bua, H. Statz, and F. Horrigan, Raytheon Research Division, "Laser Window Studies," Final Technical Report, Contract No. DAAH01-74-C-0719, August 1975

The minimum detectable absorption coefficients measured by laser calorimetry at 5.25 and 10.6 micrometers for the films studied during this program were usually limited by the variability of the substrate absorptivities to approximately one reciprocal centimeter. Attenuated total reflection (ATR) spectra could not be quantitatively correlated with the laser calorimetry results, but the thorium fluoride and zinc sulfide spectra did contain characteristic absorptions which varied in intensity from supplier to supplier and could be qualitatively correlated with the calorimetric results. Hydrocarbon contamination of the specimens was generally observed in the form of characteristic absorptions in the 3.4-3.5 micrometer range. We point out that these absorptions have a tail which extends to the deuterium fluoride laser wavelengths near 3.8 micrometers.

[These hydrocarbon bands in the 3.4-3.5 μm range and to a considerably greater extent the water band at ~ 2.9 and $\sim 6.1 \mu\text{m}$ were the most prominent features of the spectra. Eighteen ATR plates, three each for ThF_4 , ZnS , and As_2S_3 on ZnSe substrates and ThF_4 , ZnSe , and As_2S_3 on BaF_2 substrates, were measured. All 18 spectra showed evidence of the water bands, ranging from barely detectable on one trace for ZnS on ZnSe and one for As_2S_3 on ZnSe to zero transmittance from 2.8 to 3.2 μm in the worst case.]

Indentation of arsenic trisulfide films frequently produced lifting of quantities of film from their substrates. In some cases, these films passed the cellophane tape test commonly used for adhesion evaluation.

Surface effects are major contributors to the absorptivity of alkaline earth fluorides at the deuterium and hydrogen fluoride laser frequencies.

Films obtained from commercial vendors have been studied and development of characterization techniques has begun. Films of ThF_4 , As_2S_3 , ZnS , and ZnSe on BaF_2 and ZnSe substrates were obtained from three commercial film producers: Broomer Laboratories, Plain View, New York; Optical Coating Laboratories, Inc., Santa Rosa, California; and Spectra-Physics, Inc., Mountain View, California.

The results of the calorimetric absorption measurements are as follows: First, with the exception of thorium fluoride films, all of the measurable film absorptivities exceed the corresponding measured or estimated bulk values significantly. Second, for As_2S_3 and ThF_4 films, which were deposited onto both substrate materials, the range and level of absorptivity is not influenced by the choice of substrate. Third, there is a significant variability in the level of absorptivity obtained by the three vendors. The largest variation occurs for the thorium fluoride films. There is also significant run-to-run variability of film absorptivity. Variations in film absorptivity may occur among consecutive deposition runs when all the deposition parameters normally associated with good thin film deposition practice are monitored and held constant.

While any attempts to explain the variations are pure speculation, it is interesting to note that in each of the first three deposition pairs, the second deposition had the lower absorptivity. Such behavior may be plausibly explained by assuming that the material from the first deposition acted as a getter for some absorbing species in the residual gas and that the gettering action was sufficiently strong that opening the chamber to change substrates and replenish the evaporant charge did not destroy it.

The sensitivity of any absorption spectroscopic technique may be increased by increasing the pathlength of the light through the absorbing medium. Attenuated total reflection (ATR) spectroscopy makes use of this approach by permitting the evanescent wave (that portion of the radiation which extends beyond the physical surface during total internal reflection) to interact with the absorbing medium as the primary beam is repeatedly reflected down a nominally lossless medium.

ATR spectra of thorium fluoride films deposited onto zinc selenide and barium fluoride substrates from Vendor No. 1 show strong absorption at 3400 cm^{-1} ($2.95\mu\text{m}$) and 1620 cm^{-1} ($6.17\mu\text{m}$) in spectrum, which are most likely caused by some interaction of the film material with water vapor. The similarity between this spectrum and the published spectrum of $\text{ThF}_4 \cdot 4\text{ H}_2\text{O}$ (R. A. Nyquist and R. O. Kagel, Infrared Spectra of Organic Compounds) is striking. Thorium fluoride depositions carried out at the Research Division determined that the major differences in the spectra from the three vendors were produced by substrate temperature variations during deposition. Room temperature substrates produce films having the absorptive, hydrated spectrum; substrate temperatures on the order of 150°C will produce films with little or only very weak $\{\text{H}_2\text{O}\}$ absorptions at 3400 and 1620 cm^{-1} . Recent results obtained at the Honeywell Research Center demonstrate that the deposition rate variations may also be used to produce variations in thorium fluoride film absorptivities. In a second experiment, one of the low absorption films supplied by Vendor No. 3 was held for two hours at 120°F in 95 percent humidity. This treatment essentially destroyed the adhesion of the thorium fluoride film but did not produce the water-associated absorptions in its ATR spectrum. The ATR spectra and calorimetry of thorium

fluoride films, taken together with the parallel deposition experiments and environmental testing, strongly suggest that water vapor which is present in the residual atmosphere of the deposition chamber plays a major role in the determination of the absorptivity of the film that showed great absorption.

[The results above are very important. They strongly support the recommendations that superclean depositions (ultrahigh vacuum, thorough baking of the deposition chamber and substrate, ultrahigh purity samples, supersmooth substrates) should be made and that films must have high densities.]

The spectra of the thorium fluoride films deposited onto barium fluoride substrates all appear to have stronger water-related absorptions. The "stronger" absorptions actually are produced by the close index of refraction match between the film and its substrate. More of the probe radiation is coupled into the thorium fluoride on the barium fluoride substrate than the film on the higher index zinc selenide substrate.

Absorptions at 2915 cm^{-1} and at 2845 cm^{-1} are caused by hydrocarbon contamination of the specimen surfaces. Organic compounds containing C-H bonds (effectively all organic surface contaminants) contain strong absorptions at approximately 2915 and 2845 cm^{-1} (3.43 and $3.51\mu\text{m}$) due to the C-H bond stretching. This hydrocarbon contamination is a significant feature of the surfaces for several reasons. First, a review of hydrocarbon absorption spectra reveals that their absorptivity at $3.8\mu\text{m}$ (the DF laser wavelength) is typically five percent of the maximum absorptivity at 2915 cm^{-1} . Second, if it is not removed prior to deposition of the antireflection coating, the trapped contamination layer may contribute to the degradation of the AR coating during high-power laser

illumination. While boiling Freon-113 will essentially remove these hydrocarbon absorptions from ATR spectra, indicating that they exist largely on the exposed surfaces of the specimens, lesser quantities trapped at the film-substrate interface cannot be precluded.

Finally, the absorption at 1500 cm^{-1} ($6.7\mu\text{m}$) is characteristic of the barium fluoride surface, probably a hydration product. The absorption may be seen in both the "substrate" and "film" spectra. Note that no information about the film-substrate interface may be drawn from this observation because half the reflections of the probe beam as it traverses the "film" side of the specimen take place at the uncoated back face.

For arsenic trisulfide films there is no obvious correlation between the laser calorimetry results and the spectra.

Professor J. Harrington, University of Alabama, Huntsville, has measured the absorptivity of strontium fluoride at the HF and DF chemical laser wavelengths (2.8 and 3.8 micrometers) to be $1-2 \times 10^{-3}$ for centimeter-thick pieces, an order of magnitude higher than our values which were taken as 5.25 micrometers. [Raytheon values of β_b are $4 \times 10^{-5}\text{ cm}^{-1}$ at $5.25\mu\text{m}$, $5 \times 10^{-4}\text{ cm}^{-1}$ at $3.8\mu\text{m}$, and $3.7 \times 10^{-4}\text{ cm}^{-1}$ at $2.8\mu\text{m}$.]

We believe the difference to be caused by the presence of a contaminating surface layer which is more absorbing at 2.8 and 3.8 micrometers than at 5.25. The difficulty of obtaining a surface which is non-absorbing at the fluoride laser wavelengths is illustrated by four ATR spectra of a specimen of barium fluoride. The first was taken immediately after it was removed from its polymer shipping bag, the second after a five-minute wash in trichloroethylene. Trichloroethylene

was chosen as the solvent because its infrared absorption spectrum contains no bands in the 3000-2500 cm^{-1} range. The trichloroethylene wash did not completely remove the hydrocarbon contamination so a second cleaning, a five-minute immersion in boiling trichloroethylene was evaluated. Finally, the specimen was allowed to remain in the spectrometer for 24 hours following the boiling treatment and a fourth spectrum was taken.

The ATR spectra demonstrate several points. First, storage of the ATR plate in a polymer container produced a significant absorption both at 2915 cm^{-1} and at 2630 cm^{-1} (3.8 μm). Second, trichloroethylene cleaning cannot completely remove the contamination, although the boiling solvent nearly removes all detectable traces of it. Third, the clean surface is very easily recontaminated. The surface absorptivity of the boiled specimen increased by nearly a factor of two during the 24 hour storage in what should have been the relatively clean environment of the infrared spectrometer. The sample holder touched the specimen only at the edges and was itself cleaned in trichloroethylene prior to the experiments. The sample chamber was flushed with tank nitrogen which either contained sufficient hydrocarbon impurities or was able to desorb them from the interior of the spectrometer and redeposit them on the specimen. Finally, the experiments demonstrate the necessity of evaluating surface cleaning procedures for laser optical components at the wavelengths at which they will ultimately be used. Since these components will, in general, receive antireflection coatings, the optimized cleaning procedure must additionally produce a surface upon which an adherent coating can be deposited.

T. F. Deutsch, "Research in Optical Materials and Structures for High Power Lasers," Raytheon Research Division Final Technical Report, Contract No. DAAH01-72-C-0194, December 1973

[Calorimetric and internal-reflection-spectroscopic measurements of surface absorptance A_s give a wealth of information on surface absorptance and its change by surface cleaning.] Values of A_s measured at $10.6\mu\text{m}$ range from 7.7×10^{-5} for a CdTe surface to 1.8×10^{-3} for a KBr surface. At $5.25\mu\text{m}$, $A_s = 10^{-6} \pm 2 \times 10^{-5}$ for the CdTe surface and $A_s = 9 \times 10^{-5}$ for a KCl surface. The surface absorption is generally a decade lower at the shorter wavelength. The $5.25\mu\text{m}$ A_s values of $1-3 \times 10^{-5}$ per surface obtained for some materials may be due to bulk or surface scatter and should be regarded as apparent surface absorptions or as an upper limit on the surface absorption.

In the alkali halides, the primary results of a number of plasma cleaning experiments was to show that, rather than cleaning the sample, it was relatively easy to contaminate it.

We found that while HCl chemical polishing can remove a number of bands, a new surface absorption band centered at $9.8\mu\text{m}$ and overlapping $10.6\mu\text{m}$ was often introduced. The magnitude of the normal incidence $10.6\mu\text{m}$ loss due to this absorption band was estimated to be $\sim 3 \times 10^{-4}$ per surface for a plate with a surface that was visually inferior to those obtained on our calorimeter samples. The $9.8\mu\text{m}$ band has been observed to increase in strength overnight on a plate kept in storage, suggesting it is due to a reaction of the surface with the atmosphere. This, together with the fact that a bulk absorption, possibly oxygen related, occurs in the same spectral region, suggested

that the surface absorption is due to oxygen compounds forming on the surface. However, when we deliberately attempted to increase the intensity of the $9.8\text{ }\mu\text{m}$ band by placing a KCl plate in a flowing oxygen atmosphere for one hour, we found no measurable change in band intensity. While the existence of a surface absorption band centered at $9.8\text{ }\mu\text{m}$ has certainly been established, the chemical group responsible has not been identified. [Kroger and Marburger^{*85} reported that NaCl exposed to atomic oxygen develops a surface layer which absorbs from ~ 930 to $\sim 1000\text{ cm}^{-1}$, with peaks at ~ 970 , ~ 990 , and $\sim 940\text{ cm}^{-1}$ (10.3 , $10.$, and $10.6\text{ }\mu\text{m}$) in order of decreasing intensity. The absorption was believed to be due to ClO_3 . We note further that the solar spectrum contains a strong absorption band with peaks at ~ 9.4 and $\sim 9.6\text{ }\mu\text{m}$ for absorption by ozone.³⁰ There are a number of materials containing O_3 that absorb near $10\text{ }\mu\text{m}$, including O_3 , ClO_3 , NO_3 , HCO_3 , and CO_3 . Materials containing O_2 tend to have the strongest absorption peaks away from $10.6\text{ }\mu\text{m}$. For example, CO_2 absorbs at ~ 2.8 and $\sim 4.3\text{ }\mu\text{m}$ and BO_2^- absorbs at 5.1 and $16.9\text{ }\mu\text{m}$. Thus it is likely that the $9.8\text{ }\mu\text{m}$ absorption is related to O_3 , possibly from atmospheric contamination, and the deliberate exposure to a flowing oxygen atmosphere did not form the O_3 compound, whereas the exposure to atomic oxygen did form the O_3 compound. Exposure to ozone would be of interest.]

The transmission of four KCl internal reflection plates was measured as received from the supplier; no HCl polish was used. Two plates were then stored in a desiccator while two others were stored in the laboratory, protected by cardboard boxes. After a month, the internal reflection spectra were remeasured. In contrast to the behavior of the HCl polished plates, no significant change was found in the $9.8\text{ }\mu\text{m}$ surface band for any of the samples. Surprisingly,

the strength of the $3.5\mu\text{m}$ band, often observed and attributed to C-H absorption, had increased for two of the plates, one from each storage condition. This casts doubt on our previous interpretation that this band is due to residual organic material from polishing operations. [Note that CH_4 , which is contained in the atmosphere, absorbs at $\sim 3.5\mu\text{m}^{30}$]

A Harrick Scientific, horizontal single-pass internal reflection attachment makes it possible to examine the same plate either in the internal reflection mode or in a simple transmission mode and to separate bulk and surface absorption using the two spectra obtained. Worthy of note is that this attachment also makes it possible to perform bulk transmission measurements with path lengths of about 5 cm on samples only one to two millimeters thick. Separation of surface and bulk absorptance was demonstrated by measuring $\beta_b(\lambda)$ and $A_s(\lambda)$, with values as low as $\beta_b = 10^{-3}\text{ cm}^{-1}$ and $A_s = 10^{-4}$ on a KBr internal reflection plate.

Auger-electron-spectroscopy measurements indicated a correlation between absorption coefficient and oxygen content. Spectra were taken of the specimens in the as-received condition and after ~ 500 and 1000 \AA had sputtered away from the surface. Surface oxygen concentrations as high as 3-1/2 percent and carbon concentrations ranging from 6-15 percent were found. The attempt to correlate the ion microprobe measurements with the Auger results was inconclusive. Two samples showing abnormally high $10.6\mu\text{m}$ absorption and the highest oxygen concentration by ion microprobe showed oxygen concentrations of the order of 1 percent at 1000 \AA below the surface and two low absorption samples showed no detectable oxygen at 1000 \AA . However, for some other

samples, the results of the two measurements did not correlate. Most striking is the fact that the Auger measurement gives oxygen concentrations of the order of 1 percent at 1000 Å below the surface, while the microprobe showed concentrations of only a few ppm at approximately 1 mm down. The fact that the Auger measurement detected carbon on all samples, including those with cleaved surfaces, suggests either that it is present in the bulk or it is picked up from atmospheric CO₂, rather than being introduced in the polishing process.

Chemical polishing of KCl produces the lowest surface absorption of the various polishing techniques examined, typically 10^{-4} per surface at 10.6 μm . The technique reduces, but does not eliminate, the surface absorption band centered at 9.8 μm . Considerable development will be necessary, however, to adapt this technique to the polishing of large windows rather than small test pieces for calorimetry.

TABLE A-1
PROPERTIES OF LASER WINDOW MATERIALS RELATED TO THERMAL FRACTURE
FIGURE OF MERIT

Semiconductors Material	K(W/cm°K)	σ (in $10^{-6} \cdot C^{-1}$)	E (in 10^6 psi)	σ_c (psi)	$\frac{\sigma_c K}{\sigma E}$ W/cm
Germanium (Ge) 80°K	0.59 (a) 5.5 (a)	5.7 (b) +1.05 (b)	14.9	13,500	94 4700
Silicon (Si) 80°K	1.48 (a) 15. (a)	2.33 (b) -0.77 (b)	19.0	9,000 (u)	300
Gallium Arsenide (GaAs) 80°K	0.48 (o) 2.8 (o)	5.7	12.3	20,000	137
Cadmium Telluride (CdTe)	0.06 (o)	5.9 (r)	3.4 (t)	4,500 (r)	13.4
Zinc Sulphide (ZnS)	0.167	7.8 (aa)	10.8 (aa)	11,000 (aa)	21.8
Zinc Selenide (ZnSe)	0.18 (aa)	8.5 (aa)	9.75 (aa)	8,000 (aa)	17.3
Diamond (synthetic Type IIb)	20 (s)	0.8 (s)	145. (s)	6×10^5 (s)	103,000
<hr/>					
Fluorides					
Lithium Fluoride (LiF)	0.11 (c) 0.025 (d)	37 (w)	9.4	2,000 (w)	0.63
Calcium Fluoride (CaF ₂)	0.092 (d)	19.7 (e)	11 (r)	5,300 (c)	2.2
Srontium Fluoride (SrF ₂) 80°K	0.1 (est.) 0.5 (z)	15.8 (t) 19.1 (v)	14.7 (x) (Calc. from elastic constant)	> 10,000 (cc) 6,100 (v)	2.6
Barium Fluoride (BaF ₂)	0.12 (d) 0.3 (to c-axis) (g)	20.2 (e)	7.7	3,900 (f)	3.0
Magnesium Fluoride (MgF ₂) 80°K	0.1 (1 to c-axis) 3.2 (g)	13.7 (to c-axis)(f) 9.6 (1 to c-axis)	24.5	7250-15, 130 (p) 7,670 (v)	

TAB. E A-1 (CONT'D)

Material	$K(W/cm^{\circ}K)$	α (in $10^{-6}\cdot C^{-1}$)	E (in 10^6 psi)	σ_c (psi)	$\frac{\sigma_c K}{\alpha E}$ (W/cm)
<u>Alkali Halides</u>					
Sodium Chloride (NaCl)	0.065 (c)	44 (c)	5.8 (c)	570 (c)	.14
Potassium Chloride (KC1)	0.065 (c)	36 (c)	4.3 (c)	> 640 (c)	.27
Potassium Bromide (KBr)	0.048	42	3.9	> 4000 (cc) 480	.13
<u>Oxides</u>					
Sapphire (Al_2O_3)	0.045 (h) 80°K	(\parallel to c-axis) 9.5 (h)	5.5 (c) (\perp to c-axis) 0.80 at 100°K (n) (polycrystalline)	50	65,000 (c) 106 15,400
Magnesium Oxide (MgO)	0.600 (l)	10.5 (j)	36.1 (c)	20,000 (k) (in bending)	32
	70°K	6.3	0.76		
<u>Glasses</u>					
Arsenic Trisulfide (As ₂ S ₃)	0.0036 (l)	22.4 (l)	1.16 (l)	85 (l)	0.0112
T.I. 1173 (Ge ₂₈ Sb ₁₂ Se ₆₀)	0.0030 (m)	15.0 (m)	3.1 (m)	2,500 (m) annealed	0.16
<u>Other</u>					
KRS-5	0.054 (c)	58 (c)	2.3 (l)	3,800 (b)	1.5
Thallium Bromoiodide (Tl(Br, I))					

Rev 12/73

REFERENCES FOR TABLE A-1

- (a) M. G. Holland, Phys. Rev. 132, 2461 (1963).
- (b) D. F. Gibbons, Phys. Rev. 112, 136 (1958).
- (c) S. Ballard, K. McCarthy and N. Wolfe, State-of-the-art Report, Optical Materials for Infrared Instrumentation, Willow Run Labs. University of Michigan (1959), Report No. 2389-11-S.
- (d) American Institute of Physics Handbook, pgs. 4-94 to 4-97.
- (e) D. B. Sirdeshmukh and V. T. Deshpande, Ind. J. Pure Appl. Phys. 2, 405 (1964).
- (f) S.S. Ballard, L.S. Combes, and K.A. McCarthy, J. Opt. Soc. Amer. 42, 684 (1952).
- (g) Extrapolated to 300°K from data of R.A. Kashnow and K.A. McCarthy, J. Phys. Chem. Solids 30, 813 (1969).
- (h) M.G. Holland, J. Appl. Phys. 33, 2910 (1962).
- (i) Y.S. Touloukian (ed.) Thermophysical Properties of High Temperature Materials 4, Pt. 1, p. 66, MacMillan (1967).
- (j) G.K. White and O.H. Anderson, J. Appl. Phys. 37, 430 (1966).
- (k) Norton Company Data Sheet.
- (l) American Optical Company Data Sheet.
- (m) Texas Instruments Company Data Sheet.
- (n) A. Schauer, Can. J. of Phys. 43, 523 (1965).
- (o) M.G. Holland, Phys. Rev. 134, A471 (1964).
- (p) W.D. Scott, J. Am. Ceram. Soc. 45, 586 (1962). Values are given for three crystal orientations.
- (q) K.V.K. Rao, S.V.N. Naidu, P.L. N. Setty, Acta. Cryst. 15, 528 (1962).
- (r) Eastman Kodak Data Sheet on Irtran Materials. Refers to polycrystalline CdTe.
- (s) H.M. Strong and R.H. Wentorf, Jr., Naturwissenschaften 59, 1 (1972).
- (t) Calculated from Elastic Constants of H.J. McSkimin and D.G. Thomas, J. Appl. Phys. 33, 56 (1962).

REFERENCES FOR TABLE A-1 (CONT'D)

- (u) J. T. Brown, Trans. AIME 215, 1068 (1959).
- (v) F.A. Horrigan and T.F. Deutsch, "Research in Optical Materials and Structures," Final Technical Report under Contract No. DAAH01-70-C-1251, Raytheon Research Division, Waltham, Mass. (Sept. 1971).
- (w) S.S. Ballard, L.S. Combes, K.A. McCarthy, J. Opt. Soc. Amer. 41, 772 (1951).
- (x) D. Gerlich, Phys. Rev. 136, 1366 (1964).
- (y) M. Neuberger, "II-IV Semiconducting Compounds Data Tables," EPIC Publication S-11 Hughes Aircraft Co., Culver City., Calif. (Oct. 1969).
- (z) J.A. Harrington and C.T. Walker, Phys. Rev. B1, 882 (1970).
- (aa) Data sheet for CVD ZnSe and ZnS, Raytheon Research Division, Advanced Materials Dept.
- (bb) L.S. Combes, S.S. Ballard, and K. A. McCarthy, J. Opt. Soc. Am. 41, 217 (1951).
- (cc) Harshaw Chemical Co., Solon, Ohio. Data sheet for PolytranTM KCl and CaF₂ (May 1973).

TABLE A-2

FIGURE OF MERIT FOR OPTICAL DISTORTION OF LASER WINDOWS

	n^*	α $10^{-6} \cdot C^{-1}$	$E < \pi > \sim \frac{1}{3} P_{11}^{**}$	$x_1 = \frac{dn}{dT}$ $10^{-6} \cdot C^{-1}$	$x_2 = (1+\nu)\alpha(n-1)$ $10^{-6} \cdot C^{-1}$	$x_3 = \frac{1}{k} n^3 E < \pi > \alpha$ $10^{-6} \cdot C^{-1}$
Ge	4.02	5.7	0.09 (mag)	277	23.1	16.7
Si	3.43	2.3	0.027	134	7.4	~0
GaAs	3.30	5.7	-0.055	149	17.5	-6
CdTe	2.69	5.9	0.05 (est.)	107	13.2	3
ZnS	2.20	7.8	0.03	52 (b)	12.5	1.2
ZnSe	2.40	8.5	0.05 (est.)	48 (c)	15.8	2.9
Diamond (synthetic Type IIb) μm	2.41 at 0.6	0.8 (e)	.04 (j)	8 vis. (e)	1.5	.22
LiF	1.35	37	0.007	-16	17.	.3
CaF ₂	1.41	19.7	0.019	-7.7	10.7	.5
SrF ₂	1.44	15.8	0.07 (est.)	-11.9	9.2	1.7
BaF ₂	1.45	20.3	0.07 (est.)	-17.	13.1	2.1
MgF ₂	1.38 ord. ray	13.7 c-axis	0.07 (est.)	+1.9 ord. ray at .7 μm	6.9	1.4
NaCl	1.52	44.	.046	-33 (d)	30	3.6
KCl	1.47	36.	.07	-32 (d)	23	4.0
KBr	1.54	42.	.07	-40	31	5.4
Al ₂ O ₃	1.67 ord. ray	5.5	.08	10	4.9	1
MgO	1.67	10.5	-0.08	18.9	9.4	-2
As ₂ S ₃	2.41	22.4	.10	1.9 -8.6 (c)	42	15
T.I. 1173 glass	2.60 at 10.6 μm	15.0		78.	37	
KRS-5	2.38	58	.07 (est.)	-237	106.7	27

TABLE A-2 (CONT'D)

$\chi = \sum_{i=1}^3 \chi_i$ $10^{-6} \cdot C^{-1}$	C J/cm ³ · C	K W/cm · C	
317	1.65	.59	Ge
141	1.63	1.43	Si
160	1.42	0.48	GaAs
117	1.3	0.06	CdTe
65	1.91	0.167	ZnS
67	1.87	0.18	ZnSe
9.7	1.8	20	Diamond (synthetic type IIb)
1.3	4.12	.11	LiF
3.5	2.71	.092	CaF ₂
-1	2.37 (h)	0.1 (est.)	SrF ₂
-1.8	1.96 (f)	.12	BaF ₂
10.2	3.14 (g)	0.1 - 0.3	MgF ₂
-.6	1.84	0.065	NaCl
-5	1.35	0.065	KCl
-3.6	.20	0.048	KBr
15.9	3.00	.45	Al ₂ O ₃
23.3	3.13	.6	MgO
58.9	1.46	.0036	As ₂ S ₃
	1.21	.0030	T.I. 1173
-103	--	.0054	KRS-5

Notes and References for Table A-2

* The refractive index values and dn/dT are taken from sources cited in Appendix A of Ref. a. The values of α and K are obtained from references given with Table III preceding. The values C are calculated from data given in Ref. c for Table III.

** Averaging the photoelastic coefficients π for the radial and azimuthal polarizations gives

$$\langle \pi \rangle \sim \frac{1}{2} (\pi_{11} + \pi_{12})$$

which in terms of the p coefficients⁽ⁱ⁾ becomes

$$\langle \pi \rangle \sim \frac{1}{2E} (1 - v) p_{11} + (1 - 3v) p_{12} \approx \frac{p_{11}}{3E}$$

where we have assumed $v = \frac{1}{3}$ as a typical value.

- (a) F. A. Horrigan and T. F. Deutsch, "Research in Optical Materials and Structures for High Power Lasers," Raytheon Research Division Final Technical Report on Contract DAAH01-70-C-1251, (Sept. 1971).
- (b) M. Neuberger II-VI "Semiconducting Compounds Data Tables," EPIC Publication S-11, Hughes Aircraft Co., Culver City, Calif. (Oct. 1969).
- (c) A. R. Hilton and C. E. Jones, *Appl. Optics* 6, 1513 (1967).
- (d) A. Smakula, "Physical Properties of Optical Crystals with Special Reference to Infrared," Report AD-206298, (1952).
- (e) Gmelin, *Handbook of Inorganic Chemistry*, No. 14, Carbon, Verlag Chemie, Weinheim.
- (f) K. S. Pitzer, W. V. Smith, and W. M. Latimer, *J. Amer. Chem. Soc.* 60, 1826 (1938).
- (g) Landolt-Bornstein, *Numerical Data and Functional Relationships in Science and Technology*, Vol. II, Part 4, Springer Verlag, Berlin (1961).
- (h) D. F. Smith, T. E. Gardner, B. B. Letson and A. R. Taylor, Jr., U. S. Bureau of Mines Report 6316 (1963).
- (i) J. F. Nye, "Physical Properties of Crystals," Clarendon Press, Oxford (1957).
- (j) Landolt-Bornstein, *Numerical Data and Functional Relationships in Science and Technology*, New Series Group III, Vol. 1, pg. 138, Springer Verlag, Berlin (1966).

TABLE A-3ABSORPTION COEFFICIENTS OF LASER WINDOW MATERIALS*

<u>Material</u>	$\beta_{10.6 \mu\text{m}}$ <u>cm⁻¹</u>	<u>Ref.</u>	$\beta_{5.25 \mu\text{m}}$ <u>cm⁻¹</u>	<u>Ref.</u>
Si	---		0.0059	b
Ge	0.012	b	0.0018 **	b
GaAs	0.008	c	0.0094 **	b
CdTe	2.5×10^{-4}	b	4.9×10^{-4}	b
ZnSe	9.5×10^{-4}	b	3.2×10^{-4}	b **
C (synthetic diamond)	0.06	b	---	
LiF	---		0.09	a
CaF ₂	3.5		5.0×10^{-4}	b
SrF ₂	0.7		4.1×10^{-5}	b
BaF ₂	0.19		1.2×10^{-5}	b
MgF ₂	---		0.014	a
NaCl	1.3×10^{-3}	b	---	
KCl	7×10^{-5}	b	0.4×10^{-5}	b
KBr	4.2×10^{-4}	b	2.1×10^{-4}	b
KRS-5	2.2×10^{-3}	b	---	
Al ₂ O ₃	---		1.4	a

* Lowest reported values are given.

** No surface absorption correction

(a) Raytheon ir spectrophotometer

(b) Raytheon CO₂/CO laser calorimeter

(c) A.G. Thompson, "Development of GaAs Infrared Window Material," Technical Summary Report on Contract N00014-70-C-0132, Bell and Howell Electronic Materials Div., Pasadena, Calif. (December 1970).

G. T. Johnston, D. A. Walsh, R. J. Harris, and J. A. Detrio, University of Dayton Research Institute, "Laboratory Characterization and Research on the Performance of Window Materials for High Power IR Lasers," Semiannual Progress Report No. 4, Contract No. F33615-74-C-5001, June 30, 1975

Sputtered ZnSe films with thickness greater than $1\text{ }\mu\text{m}$, deposited on etched KC1 substrates, passed the Scotch-tape test. [The value of $\beta_f \cong 5\text{ cm}^{-1}$ (considered tentative) is greater than the value of $\beta_f = 1-2\text{ cm}^{-1}$ obtained at other laboratories for evaporated films.] What is of more interest than the value of β_f is the fact that the value of A_f extrapolated to zero thickness is $A_f(0) = 3.3 \times 10^{-3}$, compared with $A_f \cong 4.3 \times 10^{-3}$ for a two-micron-thick film. The value of A_f was obtained by subtracting the absorptance after depositing the film from the value before the deposition. The (large) nonzero value of $A_f(0)$ implies a large value of absorptance from damage or contamination of the substrate-coating interface, or possibly from the coating surface. Preliminary results for evaporated ZnSe films gave $\beta_f \cong 5\text{ cm}^{-1}$, but $A_f(0) \ll 3.3 \times 10^{-3}$, in agreement with the assumption of interface absorption for sputtered films.

E. Bernal G., R. H. Anderson, J. H. Chaffin, B. G. Koepke, R. J. Stokes, and R. B. Maciolek, Honeywell, Inc., "Preparation and Characterization of Polycrystalline Halides for Use in High Power Laser Windows," Final Report, Contracts No. DAHC15-72-C-0227 and No. DAHC15-73-C-0464, 20 February 1974

Films of TiCl₃, TiBr₃, TlI, CuCl₂, and CuI have been prepared by standard evaporation techniques, with glass slides or cleaved single-crystal KCl as the substrate. Coatings of TiCl₃, TiBr₃, and CuCl₂ are not sufficiently stable in high humidity environments to serve as protective coatings for KCl. TlI and CuI films are stable in high humidity, and we have prepared TlI films (not alloyed with the KCl substrate) having an absorption coefficient of less than 1 cm⁻¹ at a wavelength of 10.6 μm. Recent experiments with R.F. sputtered CuI films have resulted in absorption coefficients near 100 cm⁻¹.

We have prepared TlI films that are alloyed with the KCl in the region of the film-substrate interface by co-depositing KCl and TlI from two independently heated crucibles. The absorption coefficient at 10.6 μm, measured with a laser calorimeter, averages near 25 cm⁻¹, which is higher than those for TlI films discretely deposited on KCl. The problem of higher optical absorption for TlI films alloyed with the KCl substrate has been identified and correlated with nonstoichiometry, specifically a halogen deficiency in the alloy region. A relatively hot (475°C) KCl vapor condensing at the same time as the relatively cool (250°C) TlI vapor, may be causing the TlI to decompose. By depositing in an inert gas atmosphere the effective temperature of each vapor species will be cooled by multiple collisions with the inert

gas, thereby reducing or eliminating the decomposition problem. If this is not the case, annealing the films in a halogen atmosphere may reduce the optical absorption. A 2000 Å thick TlI film on a glass substrate was unchanged after 450 hours in 100-percent relative humidity. We therefore conclude that TlI films will provide adequate moisture protection and optical transparency at $10.6 \mu\text{m}$ to serve as protective coatings for the alkali halides.¹¹³ [Repeating the humidity test for 200 nm thick TlI film on an alkali halide would be of interest. Young's^{*38} results suggest that the 200 nm TlI film may not protect the substrate from water attack. The positive glass-substrate result would not contradict a negative alkali-halide substrate result since the TlI film could be dense enough to be stable, but not dense enough to prevent attack of the substrate.]

H. E. Bennett, "High Energy Laser Mirrors and Windows," Michelson Laboratory, Naval Weapons Center, Semi-Annual Technical Report No. 5, March - September 1974

The two major influences leading to increased absorption in silver films have been shown to be (1) the presence of O_2 to pressure above 10^{-8} torr during deposition and (2) O_2 chemisorption on silver surfaces, both in situ and upon exposure to air. Exposure to air or even one atmosphere of dry nitrogen causes an increase in the absorption of silver films. This increase (at a wavelength of 5461 Å) is only 0.001 for the best films but may be as great as 0.017 for films deposited in an O_2 pressure of 2 by 10^{-5} torr.

An attempt was made to detect light-absorbing impurities in a $TaOF_2$ -coated $LiNbO_3$ sample by ion-beam profiling / Auger analysis. The initial turnon of the electron probe beam in the presence of Ar results in rapid removal of superficial C and an increase in signal from the coating constituents Th, O, and F. When the ion-profiling beam is turned on, the scan with both beams on provides a measurement of the relative concentration versus depth for each element monitored in the remaining portion of the coating. The profiling rate is estimated at approximately 35 Å/min.

A significant feature of the results for laser damage is the marked rise of the C peak at the coating-substrate interface, indicating C contamination of the $LiNbO_3$ surface. Another significant feature is contamination of the coating, as indicated by oscillations in the profiles.

The present program has succeeded in identifying several possible causes of laser-induced surface damage. These include (1) polishing defects,

(2) submicroscopic pitting, (3) stoichiometric deficiency which may provide electron trapping sites, (4) residual polishing particles and other forms of surface contamination, and (5) coating inhomogeneity. An in situ UHV facility to evaluate the relative importance of various possible damage sources has been designed and soon will be under construction.

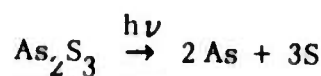
Two novel methods of measuring optical absorption are being investigated experimentally. In the first, the primary achievement has been the demonstration of the ability to separate bulk losses from surface losses in the visible spectrum. The most interesting result is the value, $A = 0.0163$, obtained for the absorption at a single surface of a dense-flint-glass prism from a Perkin-Elmer Model 99 monochromator. An optical-beam chopper directs a laser beam through thick and thin sections of a wedge-shaped sample in the alternate half cycles of the chopper. The square-wave signal is then proportional to the bulk absorption plus bulk scattering and is independent of surface absorption and scattering, assuming that the surface absorptance, scattering, and reflectance are spatially constant.

The second method of measuring β is by launching an acoustic surface wave and measuring the temperature dependence of its velocity (J. Parks, D. Rockwell, and T. Colbert, "IR Window Studies," USC Quarterly Technical Report No. 5, 15 Sept. 1973). We have encountered problems in insertion loss and reliability in devices employing this technique to date. In addition, RF feed-through signals of the same order of magnitude as the acoustic wave signals have been observed in these devices.

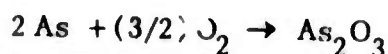
The value found for the bulk losses, $\beta + \tau = 4.4 \times 10^{-3} \text{ cm}^{-1}$, where τ is the bulk scattering coefficient, is comparable to the value obtained by others for good optical quality glass.

The major effort during the next reporting period will be devoted to extending the system's capabilities into the IR region.

A possible problem with As_2S_3 is the photodissociation of As_2S_3 followed by oxidation of the arsenic. It has been reported (J. S. Berkes, S. W. Ing, Jr., and W. J. Hillegas, J. Appl. Phys. 42, 4908, 1971) that As_2S_3 (or As_2Se_3) dissociates upon irradiation with visible light



with the subsequent oxidation of the arsenic



resulting in optical densification or additional absorption in the window region.
Photoemission and Auger spectroscopies, which we are now using to study the role of O_2 in Ce films, will be used to study the dissociation and oxidation of As_2S_3 , under controlled conditions. Photoemission spectroscopy provides a direct means for observing the density of electron states in the surface region.

H. E. Bennett, Michelson Laboratory, Naval Weapons Center, China Lake,
"High Energy Laser Mirrors and Windows," Semi-Annual Report No. 6,
September 1974 - March 1975

Surfaces with absorptance less than 1×10^{-4} , parallel to less than 3 sec
of arc and flat to better than a quarter wave in the visible, have been pro-
duced. This procedure, which employs a combination chemical-mechanical
polish, has been successfully applied to pure KC1 (single and polycrystalline),
KC1 alloys (single and polycrystalline), and NaCl windows.

Although we have demonstrated that it is possible to polish KC1 and NaCl surfaces using the pitch-lap, triacetin-polish technique to rms roughness values under 30 Å rms, we have not succeeded in producing surfaces with low surface absorption which are this smooth.

The first absorptance measurement on a triacetin-polished single crystal KC1 yielded total absorptance of 0.0062 to 0.014 (measurements at different spots) on a 5 mm-thick piece. Hope that the measurements were wrong was vanquished by measurements on a similar specimen polished by Harshaw which indicated total absorptance of 0.0011. Since the specimen with the high absorptance had been polished for weeks in order to try to optimize surface finish, the logical thing to assume was that extensive surface damage had resulted and the surface had been contaminated.

This theory was tested by etching the high absorptance specimen. After 3 minutes of etching the total absorptance was reduced to 0.00077, thus indicating surface absorptance in the polished piece on the order of 0.005 per surface in the polished surface. This high surface absorptance cast serious doubts

as to the usefulness of the polishing technique. However, as we were to discover, the technique could be used successfully if polishing time could be restricted to less than 8 hours and preferably 4 hours per surface.

After etch the specimen discussed above was polished until flat to one-half wave in the visible. The absorptance was measured after polish and found to be 0.00053. Since this value was less than that of the freshly etched piece, it seemed that all the surface contamination was not removed in the 3-minute etch. The specimen was etched again for 3 minutes and the absorptance went down to 0.00041. The specimen was polished again on both sides to a flatness of less than $\lambda/2$ in the visible on each surface. The specimen was polished a total of 8 hours using fresh feed and the total absorptance was 0.00066, indicating surface absorptance on the order of 1.2×10^{-4} per surface.

In general, NaCl was easier to polish than the KC1. Both figure and surface quality were easier to control; however, the problem of "coatability" discussed below is as serious for NaCl as for KC1. The absorptance of a polished specimen indicates no increase over value for the chemically etched surface; the total induced absorptance is less than 3×10^{-4} , i.e., less than 1.5×10^{-4} per surface.

Absorptance studies of thin films were initiated. One run was made with an As_2S_3 thin-film wedge, from which a bulk absorption coefficient of the film volume of $6.5 \times 10^4 \text{ cm}^{-1}$ is calculated for $\lambda = 0.4825 \mu\text{m}$. During the run certain time-dependent changes were observed; these are thought to be due to photo-decomposition of the material in the $\sim 0.15 \text{ watt/cm}^2$ cw laser radiation. More detailed studies of this effect are planned.

In previous reports we discussed the problems involved in coating KC1 windows with Ge films which are stable, uniform, and low absorbing. It is the presence of defects and contaminants in Ge films which causes the increased optical absorption and decreased optical stability. Since the number of defects and impurities in a film is influenced by deposition conditions, often one can find sample preparation techniques which produce improved coatings. For example, we have found that the most optically stable Ge films are formed with a deposition in UHV at 160°C followed by an anneal at 250°C after exposure of the film to air. This treatment produces a dense film with few defects, and a stable structure. The denseness of the film reduces oxygen uptake and optical absorption. Furthermore, the surface of KC1 is stoichiometric in the temperature range between 65°C and 300°C, whereas the surface contains excess potassium below 65°C. It is possible that coating at an elevated temperature can help stabilize the surface composition. Unfortunately a large thermal mismatch between Ge and KC1 prevents thermal cycling, and we have not been able to grow stable Ge films on KC1. On the other hand, we have been able to grow As_2S_3 coatings on KC1 with residual absorptions less than 10 cm^{-1} ; As_2S_3 has a closer thermal match to KC1 than does Ge. Therefore, we have shifted our effort during this period to amorphous or glassy As_2S_3 .

We report for the first time the deposit of Ge coatings (on quartz) which are simultaneously thick (half wave optical thickness at $10.6 \mu\text{m}$), optically uniform, low absorbing, and thermally stable. The recipe for producing high-quality Ge films is as follows: 1. During deposition the substrate and environment must be held at a uniform temperature of $160 \pm 10^\circ\text{C}$ (higher deposition temperatures, i.e., to $> 170^\circ\text{C}$ will result in crystallization of the film). To obtain the required

temperature uniformity, we heated the entire chamber; uniform Ge films could not be produced when the window was heated directly with a heater block.

2. The coated window is annealed in ultrahigh vacuum (1×10^{-10} torr) at 250°C for 2 hours after the coated window has been exposed to air. The entire system was heated to achieve a uniform anneal. 3. Germanium was evaporated from an E-gun; the bias of the gun was adjusted so that the evaporation always occurred from the center of the melt. 4. The window was separated from the evaporator by 20 inches. 5. The coating was deposited at 3 A/sec at a pressure of 2×10^{-9} torr.

Points 1 and 2 contain the improvements in coating technique which are required to produce high-quality Ge coatings on quartz or sapphire. As reported previously, the presence of oxygen is correlated with high residual absorption at $10.6\text{ }\mu\text{m}$. Ultraviolet photoemission spectra obtained with synchrotron radiation show that the oxygen is chemically bonded to the Ge, probably in the form of GeO . Since GeO has an absorption band which overlaps the $10.6\text{ }\mu\text{m}$ region, its presence certainly contributes to the increase of residual absorption at $10.6\text{ }\mu\text{m}$. Notice that all the improvements in technique for producing good Ge coatings on quartz involve treatment at elevated temperatures.

Unfortunately, thick (greater than quarter-wave) coatings on KCl do not tolerate cycling to high temperatures; we have found that the Ge coatings flake off after deposition at a uniform temperature of 160°C . In this connection, it is suggestive that ability to grow good coatings seems to be correlated with the thermal match between the coatings and the window. [Great thermal expansion mismatch is known to cause great film stress. In general, the "intrinsic"

stress is greater than the thermal-expansion mismatch stress.^{*2}] For example, we can produce good Ge coatings on quartz and sapphire, and the linear expansion coefficients of these materials at room temperature are 5.5, 4.1, and $5.8 \times 10^{-6}/^{\circ}\text{K}$, respectively. Similarly, we can produce good As_2S_3 coatings on KC1, and the linear expansion coefficient for these materials is 36 and $25 \times 10^{-6}/^{\circ}\text{K}$, respectively. Apparently the thermal mismatch between Ge and KC1, $20 \times 10^{-6}/^{\circ}\text{K}$, is so large that a 200°C temperature variation creates enough stress to destroy the coating. [The corresponding stress is of order $\sigma = \epsilon C_{e\ell} = 200 (20 \times 10^{-6}) (1.2 \times 10^7 \text{ psi}) = 4.8 \times 10^4 \text{ psi}$, which possibly could be great enough to destroy the coating.] This implies that the high temperature treatments, required to produce good Ge coatings on quartz or sapphire, will fail to produce good Ge coatings on KC1.

Previously we found As_2S_3 coatings on KC1 to be highly susceptible to damage by bombardment with high energy electrons during Auger analysis. The entire coating evaporated at one point. For this reason it appeared that thermal instability might be a serious limitation of As_2S_3 coatings. Bulk As_2S_3 is stable to temperatures well above 200°C . On the other hand, we found that As_2S_3 coatings evaporated at some temperatures less than 200°C . For some reason As_2S_3 is less stable in coating form than in bulk form.

The As_2S_3 coatings were deposited in an oil-pumped system at a vacuum of 4×10^{-6} torr. The evaporator, a molybdenum boat, was located 10 inches from the windows. With the boat at a temperature of 400°C , coatings were deposited at a rate of 10 A/sec.

A number of As_2S_3 coatings were deposited on polycrystalline Eu^{++} -doped KC1 window surfaces, and the absorption at $10.6 \mu\text{m}$ determined directly by

calorimetry. The range of coating absorption is practically within the limits
($2 \leq \beta \leq 10 \text{ cm}^{-1}$) previously reported. [It would be of interest to determine
if the value of β_f could be reduced to the lowest value $\beta_f = 0.8 \text{ cm}^{-1}$ observed
to date by thoroughly prebaking the system and depositing at 2×10^{-9} torr.]

The absorptance of coatings deposited on the polished surfaces is as much as a factor of 10 higher than that of chemically etched surfaces. Two possible mechanisms for the higher coating absorptance are: (1) inadequate cleaning of the polished surface, and (2) enhanced trapping of scattered light by the addition of a quarter-wave optical thickness, high index coating (As_2S_3). The value $\beta_f = 2.9 \text{ cm}^{-1}$ we feel can be obtained routinely and is within the limits needed for a usable protective coating on KC1. [Compare the HRL value of $\beta_f = 0.8 \text{ cm}^{-1}$.]

A possible problem with As_2S_3 involves the optical stability of the coatings.
It has been reported that As_2S_3 coatings become optically more dense and undergo a change in index of refraction when irradiated with high intensity visible light
with a photon energy greater than the band gap, i.e., for $h\nu > E_g$, where $E_g = 2 \text{ eV}$ or 6200 \AA . We have verified both the optical densification and increase in index of refraction in the visible and near IR regions, after irradiation with a high intensity xenon arc lamp. Further, in the IR ($2.5-10.6 \mu\text{m}$) we have observed no similar change in index; however, we have observed an increase in absorption $\sim 5 \text{ cm}^{-1}$ from transmission maxima. Calorimetric measurements show an increase of a factor of 2, from 2.9 cm^{-1} to about 6 cm^{-1} . Preliminary results suggest the increase in absorption can be reversed by annealing to a temperature of 150°C for 1-2 hours at a pressure of 10^{-3} torr. Further work is in progress to understand the effect of intense visible radiation on the stability of this material.

The condition of window surfaces during deposition profoundly influences the nature of the interface between the window and the coating. In an effort to better understand the relationship of surface conditions and optical absorption, we have initiated studies of electronic states at the surface of window and coating materials. In a recent publication, Rowe identified surface states on Ge using low energy electron loss spectroscopy (J. E. Rowe, Solid State Commun. 15, 1505, 1974). Here we report similar data which confirm his findings and show that a low density of carbon on the surface strongly affects electronic surface states.

D. L. Stierwalt and M. Hass, Proceedings of the Fourth Annual Conference on Infrared Laser Window Materials, Nov. 18-20, 1974, Tucson, Arizona, January 1975

The strength of the absorption band near $9.5 \mu\text{m}$ in KCl was observed to be reduced from $\sim 2.5 \times 10^{-4} \text{ cm}^{-1}$ [to $\sim 1.4 \times 10^{-4} \text{ cm}^{-1}$] by baking the sample at 250°C for 60 hours. After exposure to air for 30 hours the absorption coefficient increased to its original value of $\sim 2.5 \times 10^{-4} \text{ cm}^{-1}$.

[Also see Refs. *85 and *15. The most likely source of the $9.5 \mu\text{m}$ absorption band is a contaminant containing O_3 , such as NO_3 , ClO_3 , or KClO_3 . The contaminant could be adsorbed on the surface or absorbed in a damaged surface layer. Exposure of the sample to ozone in one case and to dry oxygen in another, rather than to air, would be of interest. Since molecules containing O_3 are strongly absorbing at $\sim 9.5 \mu\text{m}$, a monolayer on each surface of the sample would give an absorptance of $\sim 2 \times 10^{-4}$ (as shown in Sec. IV), which corresponds to an apparent value of $\beta = 2 \times 10^{-4} \text{ cm}^{-1}$ for a one-centimeter-thick sample.]

P. A. Young, "Thin Films for Use on Sodium Chloride Components of Carbon Dioxide Layers," Thin Solid Films 6, 423 (1970)

This paper is concerned with protective films to prevent attack of NaCl components by water vapor.

Sodium chloride is hygroscopic and a polished surface absorbs more water than a cleaved face, probably because it has a greater surface area as a result of the presence of a layer of crushed crystallites formed on the surface during the polishing process. The rate at which a polished crystal absorbs water has been measured as a function of relative humidity. The results, Fig. 1, indicate that the rate of absorption is slow for humidities less than about 80%, but rapidly increases at higher humidities. [Note that the value of 1 mg mass increase (for 90 percent relative humidity for 30 minutes) in the figure corresponds to a layer of water having the very great thickness $\sim 1 \text{ mg} (1 \text{ cm}^3/\text{g})/2\pi(2.5 \text{ cm}/2)^2 = 1 \mu\text{m}$! The theoretical $10.6 \mu\text{m}$ value of A_f is $\beta_f l_f = 950 \text{ cm}^{-1} (10^{-4}) = 9.5 \times 10^{-2}$. The experimental value was not reported. The theoretical value of A_f may be inaccurate as a result of using the value of β for water, whereas chemical interactions may convert the water to other chemical species (which would be expected to absorb rather strongly also since they contain oxygen). The greatest value of mass increase of approximately 3 mg in Fig. 1 corresponds to a layer of water approximately $3 \mu\text{m}$ thick. If the effect were purely a filling of pores between the crushed crystallites in the surface layer, a $12 \mu\text{m}$ -thick surface layer having 25 percent porosity would give this value of $3 \mu\text{m}$. However, in photographs and scanning electron microscope views of surfaces exposed to 100 percent relative humidity for one hour, it appears that the attack of the NaCl by water at the large scratches

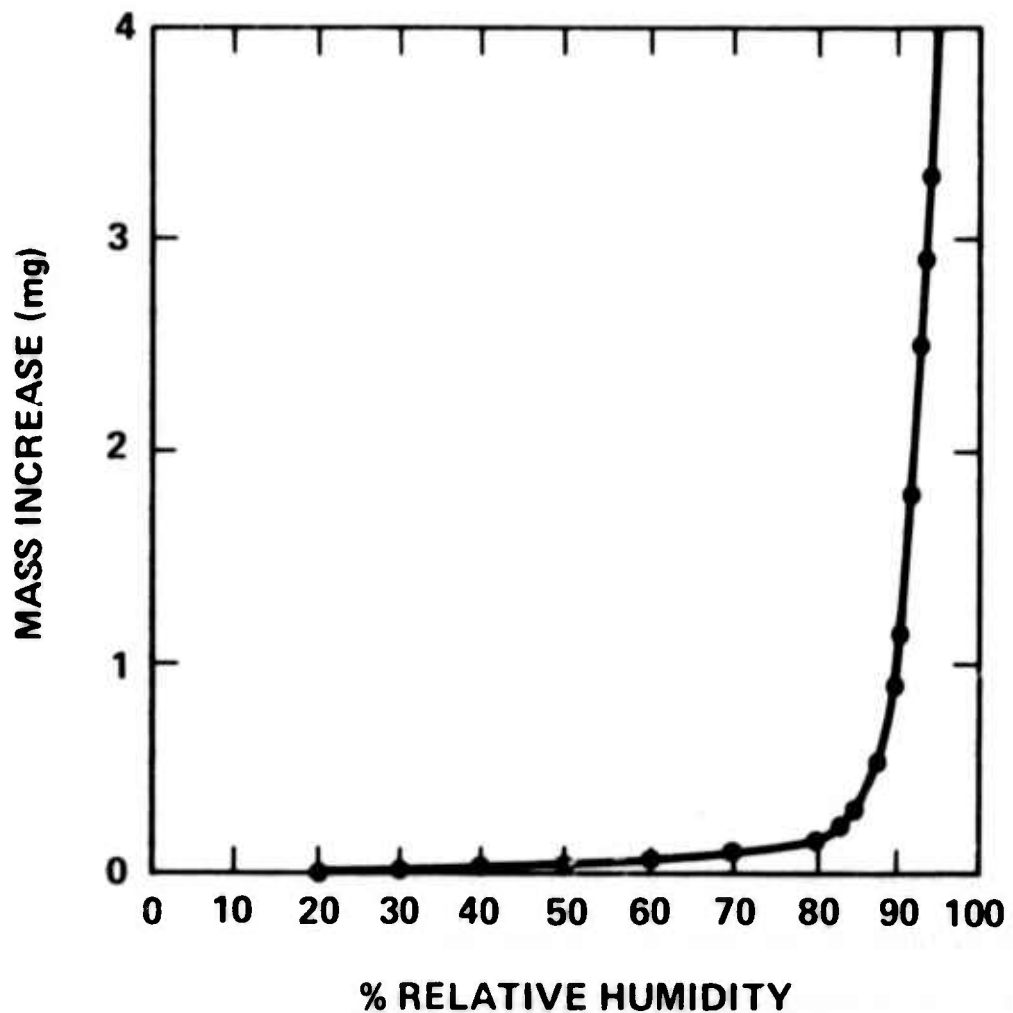


Fig. 1. Mass increase of a 2.5 cm diameter polished NaCl disc when exposed to water vapor at 300 K. Exposure time 30 min for each value of R. H.

($\sim 0.5\text{-}2 \mu\text{m}$) was quite heavy, the large scratches appearing to have increased to $\sim 20 \mu\text{m}$ size. It is difficult to extrapolate from 90 percent relative humidity (and 30 minute exposure) to 100 percent relative humidity (and one hour exposure) since the curve in Fig. 1 of mass increase vs percent relative humidity is so steep at high values of relative humidity. Nevertheless, it does not seem unreasonable that the mass increase corresponding to $3 \mu\text{m}$ of water could result from the water attack of the large scratches. This attack of the large scratches also affords a possible alternate explanation of the greater water absorption by polished NaCl than by cleaved NaCl.]

Prolonged exposure to water vapor saturates the surface and leads to recrystallization. When this occurs there is considerable absorption of laser radiation at the crystal surfaces, which can lead to the destruction of the crystal for sufficiently high laser powers. This damage frequently takes the form of extensive cleavages along crystal planes, as a result of the thermal gradients set up and of the high thermal expansion of NaCl.

It is difficult to prepare films of III-IV semiconductors by evaporation without some dissociation and consequent high optical absorption. This may be overcome by sputtering the films.

[It is of interest that Young measured a value of $\beta_b = 8 \times 10^{-4}$ at $11.6 \mu\text{m}$ and extrapolated $\beta_b = 3 \times 10^{-4} \text{ cm}^{-1}$ for NaCl. This value of $3 \times 10^{-4} \text{ cm}^{-1}$ is the lowest value of which the current authors are aware. The value of β_b at 10.6 cm^{-1} measured for BaF₂ agrees with the value measured by others.]

Five-centimeter diameter NaCl crystals were ground using $3 \mu\text{m}$ Al₂O₃ powder and then polished, parallel to one minute of arc and flat to two fringes,

using a soft pitch lap, glycerine and successive polishing sizes of 0.5 and 0.03 μm Al_2O_3 .

Films of As_2S_3 , BaF_2 , MgF_2 , and ZnS were prepared on NaCl substrates by vacuum evaporation of 99.99% pure material from a resistance heated boat under a vacuum of 10^{-5} torr. Ge films (using material with a resistivity of $50 \Omega \text{ cm}$) were prepared by electron beam gun evaporation under a vacuum of 10^{-6} torr. Film thicknesses ranged from 0.1-4 μm . In all cases the substrates were unheated and the deposition rates were: As_2S_3 , $2-6 \text{ nm s}^{-1}$; BaF_2 , $1-2 \text{ nm s}^{-1}$; Ge, $2-3 \text{ nm s}^{-1}$; MgF_2 , $3-5 \text{ nm s}^{-1}$; and ZnS , $0.5-1 \text{ nm s}^{-1}$. All the films adhered well to the substrates and showed no visible crazing.

Some multilayer stacks were deposited onto NaCl to give mirrors of different reflectivity at 10.6 μm ; As_2S_3 and BaF_2 were used as the high and low index films respectively. H-L-H and H-L-H-L-H stacks were prepared, each layer having an optical thickness of $\lambda/4$ at 10.6 μm .

Protection against water attack. The rate at which polished NaCl absorbs water rises very rapidly with increasing humidity above about 80% and the ability of a film to prevent this attack was tested under conditions of 100% relative humidity (R. H.). A film able to withstand these extreme conditions for a moderate time is expected to provide water protection under atmospheric conditions for a considerable period.

CO_2 laser measurements. Laser power was measured using a calibrated radiometer with an accuracy of $\pm 4\%$. The laser beam was then focused with a NaCl lens and a film on a substrate moved slowly along the laser axis towards this focus. In all cases a point was reached when the area of the film in the beam

would suddenly burn off and the laser power was then immediately cut off to prevent enlargement of this area. This process was repeated at a number of areas on the film. The minimum power density required to destroy the film corresponds to the holes in the film with the largest diameters and was obtained by dividing the laser output by their mean area.

RESULTS

Sodium chloride surfaces. It is difficult to obtain a scratch-free surface, since polishing materials are usually much harder. Also the surface heating during polishing leads to many dislocations and small cleavages in the NaCl surface because of its high coefficient of thermal expansion ($44 \times 10^{-6} \text{ K}^{-1}$).

Electron micrographs show the presence of large numbers of small scratches with widths in the range $0.05\text{-}0.2 \mu\text{m}$; these are attributed to the $0.03 \mu\text{m} \text{ Al}_2\text{O}_3$ particles used in the final polish. A smaller number of scratches in the range $0.2\text{-}0.5 \mu\text{m}$ wide probably remain from the first polish with $0.5 \mu\text{m} \text{ Al}_2\text{O}_3$. There are also occasional larger scratches up to $1.5 \mu\text{m}$ wide, which have sharp edges and present a problem in the deposition of a continuous film to be used as a water barrier. Some scratches are filled with a rubble of small NaCl particles broken off during polishing. In addition a small number of $2\text{-}4 \mu\text{m} \text{ Al}_2\text{O}_3$ grinding particles remained embedded in the soft NaCl surface.

Thin films of As_2S_3 have a vitreous structure, which is virtually independent of the nature of the substrate. At short wavelengths the optical absorption of thin films is the same as that of bulk material and there is very close agreement between the refractive indices of bulk and thin film As_2S_3 over the wavelength

range 0.49 to 16 μ m. As₂S₃ melts at 310°C and showed no measurable decomposition when evaporated.

BaF₂ films on NaCl substrates are expected to have a well defined crystalline structure because of the close unit cell matching. The BaF₂ films prepared were quite hard and showed good adhesion to the substrates.

The infrared absorption of the Ge crystals shows strong free carrier absorption, which increases approximately as λ^2 . At 10.6 μ m the absorption is entirely due to free carriers and the absorption coefficient is 0.07 cm⁻¹ at 300°K. The absorption at this wavelength shows a very rapid exponential increase with temperature. Ge films deposited onto single crystal or polycrystalline substrates show considerable crystallite growth.

MgF₂ films on amorphous substrates consist of small crystallites and the films have a high tensile stress, with some porosity. The crystallite size is increased when crystalline substrates are used but is likely to be restricted for NaCl substrates because of the mismatching between the unit cells.

ZnS can exist either in a cubic or hexagonal form. Evaporated ZnS films are polycrystalline and show high compressive or tensile stresses, depending on the dominant crystalline form. The films are normally slightly porous with a density about 1% less than that of crystals. The films are slightly hygroscopic and show a tendency to craze when exposed to high humidity.

Polished NaCl, with the distribution of scratches is rapidly damaged by water vapor, the attack being mainly at the scratches. Crystals with a very good polish

are not damaged as rapidly and the attack is mainly confined to the deeper scratches which are in the region of 0.2-0.5 μm wide.

Attempts to provide an effective water barrier using polycrystalline films of BaF₂ and MgF₂ were not successful. Films of both these materials consist of crystallites of varying orientations, with high strains at the crystallite boundaries. Since the films are formed by the growth and coalescing of crystallites, there is some degree of porosity and water vapor can penetrate the films. Water vapor caused rapid crazing of the film into islands, which were subsequently broken up still further. Water then easily penetrated through the cracks and attacked the NaCl in all directions under the film.

Good results were obtained with films of vitreous As₂S₃. These films have a continuous network structure and therefore have no weak spots at which water vapor can penetrate. NaCl coated with a relatively thin (0.58 μm) film of As₂S₃ was largely unaffected by short exposure at 100% R. H. but adequate protection was not possible at deep polishing scratches. Water penetrated through the film at these scratches and then spread under the film causing extensive damage. Increasing the film thickness to 0.92 μm prevented penetration at scratches less than about 0.5 μm wide and delayed attack at the deep scratches. However the coverage at the deep scratches was insufficient for long exposure and eventually water reached the NaCl and spread under the film. When a 1.85 μm As₂S₃ film was used water vapor, at 100% R. H., did not penetrate the film at any point over the period of observation. The deepest scratches are about 1.5 μm wide and have sharp edges; the film thickness required to give sufficient coverage at this type of scratch is therefore approximately the same as the scratch width. After a

long exposure to high humidity, water creeps under the film from the disc perimeter and eventually causes damage right across the disc, even though the film is intact.

Films of all five materials are able to withstand increasing power densities as the film thickness is reduced; this is expected since the laser energy absorbed in a film is approximately proportional to film thickness. Single crystal BaF₂ and polycrystalline bulk ZnS both have an absorption coefficient of approximately 0.2 cm^{-1} at $10.6\mu\text{m}$ and $1\mu\text{m}$ thick films of both materials are destroyed by 10^6 Wcm^{-2} . The bulk absorption coefficient of MgF₂ is 20 cm^{-1} at $10.6\mu\text{m}$ and $1\mu\text{m}$ films are burnt off by a power density of $1.5 \times 10^4 \text{ Wcm}^{-2}$. Ge crystals have a $10.6\mu\text{m}$ absorption coefficient of only 0.07 cm^{-1} , but a $1\mu\text{m}$ thick Ge film is destroyed by the comparatively low power density of $3 \times 10^3 \text{ Wcm}^{-2}$. The temperature dependences of the bulk absorption coefficients suggest that this anomaly results from the "thermal runaway" process that occurs in Ge crystals at high power densities.

As₂S₃ films can withstand higher power densities than any of the other materials examined. Films of As₂S₃ between 1 and $4\mu\text{m}$ thick are able to withstand power densities in excess of 10^6 Wcm^{-2} and thinner films can survive powers in the region of 10^7 Wcm^{-2} . The implication is therefore that the absorption coefficients, at $10.6\mu\text{m}$, of the polycrystalline films studied are higher than those of these materials in the bulk state, in order to account for the lower power densities required to burn these films off, compared with As₂S₃ films.

In conclusion, polycrystalline films do not appear to be very satisfactory as barriers against severe water vapor attack since they tend to disintegrate. Films of As₂S₃, however, have a network structure and provide an effective way of

preventing water damage. The film thickness required for this protection has to be sufficient to give adequate coverage over the entire NaCl surface and depends on the size of the largest surface damage present. Of the two low refractive index materials considered, BaF_2 is the more suitable than is MgF_2 for high power laser use.

[The value of the absorption coefficient of the films is difficult to obtain from the damage experiments of Young because the damage depends on the speed at which the sample approaches the focus and it depends on the unknown net energy that must be added to the film in order to cause the observed damage. However, a very rough approximation can be obtained by assuming that $\beta_f \cong 1 \text{ cm}^{-1}$ for the As_2S_3 films and scaling to other materials by using $T \sim IA \sim I\beta_f l_f$, which is expected to be valid if the two samples have the same speed with respect to the focus. The damage temperatures T surely will not be equal, but they probably will not differ by more than a factor of two or so. Thus, for MgF_2 ,

$$\begin{aligned}\beta_f &\cong 1 \text{ cm}^{-1} (1\ell)_{\text{As}_2\text{S}_3} / (1\ell)_{\text{MgF}_2} \\ &\cong 1 \text{ cm}^{-1} (10^6 \text{ W cm}^{-2} 4\mu\text{m}) / (1.5 \times 10^4 \text{ W cm}^{-2} 1\mu\text{m}) \\ &\cong 270 \text{ cm}^{-1}\end{aligned}$$

which must be considered as a very rough estimate (accuracy of a factor of 2 to 10). The corresponding values for BaF_2 and ZnS are somewhat (depending on the exact values of I , which are not given) greater than 4 cm^{-1} , which are reasonable in view of recently reported values of $1-2 \text{ cm}^{-1}$ and 2.4 cm^{-1} and the expected variation from film to film.]

[Finally, the theoretical conditions for failure are reasonable: The temperature rise for absorption in a layer of thickness $\ell_f \ll \ell_{th} = (\pi K t / 4C)^{1/2}$ and illuminated-spot diameter $D \gg \ell_{th}$ is^{48,49}

$$T = 2IA_f(t/\pi CK)^{1/2} . \quad (1)$$

For slow movement of the sample toward the focus a reasonable value of t is 1 sec (then $\ell_f = 1.7$ mm), and for As_2S_3 with $I = 10^6 W/cm^2$ and $A_f = 1 cm^{-1} (4 \times 10^{-4} cm) = 4 \times 10^{-4}$, with $C = 1.84 J/cm^3 K$ and $K = 0.065 W/cm K$ (both for KC1 since the thermal diffusion is into the KC1), (1) gives $T = 1,300 K$, which seems reasonable for damage.]

R. W. Hoffman, "The Mechanical Properties of Thin Condensed Films," Physics of Thin Films, 3, 211 (1966)

For the most part we shall be concerned with films of metals formed by evaporation techniques under various deposition conditions. Nonmetals will be considered when the corresponding information for metallic films is lacking.

The nucleation and growth of very thin films of Au, Ag, and Pb films have been examined under electron-microscope observation. The density of crystallization nuclei decreases, during deposition, by the coalescence of such nuclei. The nuclei are usually rounded, but exhibit sudden changes in shape when two join together in the early stages of growth. The mass-transport mechanism is believed to be surface diffusion. Reorientation of two crystallites has also been noted at this stage. As the growth continues, the nuclei become larger and grow together to form a network with many open areas. These holes ultimately fill in and may be the source of the large dislocation density found in most epitaxed films. The resulting grain size of the deposit is large compared with the initial separation of the nuclei, since as many as 100 initial nuclei may contribute to each grain. The grain size is thus determined primarily by the recrystallization process rather than the density of initial nuclei. The crystallite size increases as the substrate temperature is raised.

The stress in a thin film consists of two major components. One results from the different thermal-expansion coefficients of film and substrate combined with the difference between the deposition temperature and the temperature prevailing during the measurement; the other, sometimes referred to as

the "intrinsic" stress, arises from film contamination and the incomplete structural-ordering processes occurring during film growth.

Thermal stress can be calculated with good accuracy from the difference of the bulk expansion coefficients, and it does not exhibit any unusual behavior.

The coefficient of expansion is about 8 for glass, 10 to 20 for many metals, and 30 to 40 for the alkali halides, all in units of $10^{-6}/^{\circ}\text{C}$. A tension stress is found for metals on glass, but a compression stress for metals on alkali-halide substrates. For nickel films deposited at 75°C on soft glass and measured at 25°C , the differential expansion contributes about 5% to the total stress. As the substrate temperature is raised, the differential-expansion term increases and the intrinsic stress decreases, until the differential thermal expansion becomes at about 250°C the only contributor.

The intrinsic stress contribution to the total stress is more interesting since it reflects the growth of the film in a way not well understood at present. Even the experimental data published by different authors on the intrinsic stress are not very consistent. The average stress in thick films is relatively independent of the film thickness. The stress does not seem to depend strongly on the substrate material, even though such a dependence is expected.

Values for the intrinsic stress in dielectric films are summarized in Table III. Table III reveals two notable features. First, a relatively large number of dielectric films exhibit compressive stress even at low deposition temperatures, despite the relatively large film thickness, and second, the many instances where the absolute value of the stress is extremely small.

Films deposited at high partial pressures of water vapor or oxygen usually exhibit compression stress.

Dielectric films may show a marked mechanical instability when exposed to air after their formation. This effect is accentuated when the evaporation is at other than normal incidence (36), and it presents a serious limitation to the use of SiO in evaporated circuitry and optical coatings. These aging effects are caused by the partial pressure of water vapor, since no stress change was observed for exposure to dry nitrogen at atmospheric pressure.

Tensile stresses are definitely present before a LiF film becomes continuous at about 100 Å average thickness.

A satisfactory theory for the origin of intrinsic stresses has yet to be formulated. Murbach and Wilman (27) have advanced the hypothesis that the total film stress might be explained as thermal if one regards the film surface during deposition as having a high temperature. Hoffman et al. (63) question the validity of the hypothesis, because the thermal relaxation processes at the surface should be rapid enough to maintain the surface at approximately the substrate temperature. This contention is supported by Blackburn and Campbell (30), as well as by Pashley et al. (6), who showed experimentally that the condensing surface stays essentially at the substrate temperature. The thesis of a large temperature differential between condensing surface and substrates is also refuted by another observation.

There is no question that phase transitions in films should lead to corresponding changes in stress, since they are always accompanied by a change in volume.

The compressive stress in copper film increases with the growing thickness of a surface oxide layer, and decreases when the oxide is chemically thinned. This stress dependence on surface oxidation is not surprising and has been observed repeatedly.

Gimpl et al. (19a) finally suggest that amorphous layers might be found at both metal film surfaces, an assumption which is supposed to account for the high strength often measured on films. These amorphous layers are probably oxides which are responsible for most of the observed stress, since the body of the film should exhibit nearly the properties of the bulk metal and should thus relieve higher stresses by plastic flow.

Van der Merwe (68-71) has shown that epitaxial films can reduce their total energy by forming interfacial dislocations which decrease the lattice misfits at the expense of introducing an elastic strain into the film. As a consequence of Van der Merwe's theory, dislocation-free films can only exist when their thickness and substrate-lattice misfit stay below given threshold values. Thus, for a given misfit below the critical or threshold value, a relatively thick deposit might be obtained which is strained to match the substrate lattice without interfacial dislocations, but for misfits greater than the misfit threshold, interfacial dislocations always occur for even a monolayer film. The critical misfit values can be as large as 13% for a "soft" film with "strong" bonding to the substrate. "Hard" films with a "weak" bond, on the other hand, may have a critical misfit value of only 0.04%. Only Matthews (72) has so far checked experimentally the theory of Van der Merwe on epitaxial films. His observations on 450-thick PbS films grown on PbSe and PbS crystals not only

show the predicted dislocations by diffraction contrast, but an elastic strain of 0.06%, which agrees precisely with the theoretical value. There is, unfortunately, little agreement between the large body of experimental stress and strain data obtained on polycrystalline films and the theory. For one, experimental evidence does not verify the prediction that the homogeneous strain should vary inversely with film thickness. Second, tension or compression should be observed depending on the condition of a positive or negative misfit, whereas most experiments show tension film stress regardless of the sign of the misfit. Finally, there is little quantitative agreement between predicted and measured stress values. It is probably not surprising that the theory of Van der Merwe breaks down for polycrystalline films, since the fine structure of the substrate surface has in this case little influence on the film growth.

Surface tension can be an important contribution to the stress of thin films. However, surface tension is only a minor factor in the stress behavior of films of typical thickness of a few hundred angstroms or greater.

TABLE III
INTRINSIC STRESSES IN DIELECTRIC FILMS APPROXIMATELY 5000-A THICK

Material	Substrate temp., °C*	Substrate material	Stress, 10^8 dyne/cm ² *	Sign†	Method‡	Ref.
ZnS	110	Glass	1.0	C	C	30
	A	Glass	(0.022)	C	C	28
	A	Mica		C	C	60
SiO	110	Glass	1.2	C	C	30
	A	Nickel	4	T	C	33
	75	Glass	2.0	T	C	30
MgF ₂	110	Mica	2.2	T	B	38
	A	Glass	(0.11)	T	C	28
	A	Mica	(0.11)	T	C	60
	A	Glass	1	T		57
LiF	110	Glass	0.4	T	C	30
	A	Cellulose	2.0	T	ED	47
	A	Glass	0.28	T		57
	A	Mica	(0.023)	T	C	60
CaF ₂	110	Glass	(0.023)	T	C	28
	A	Glass	0.2	T	C	30
	A	Mica	(<0.0003)	T	C	60
Cryolite	A	Glass	(None)		C	28
	A	Glass	(0.061)	T	C	28
	A	Glass	(0.06)	T	C	60
PbCl ₂	50	Glass	0.5	T		57
	A	Glass	0.18	T	C	30
PbF ₂	110	Glass	(0.014)	T	C	28
AgCl	A	Glass	0.8	T	C	30
AgF	A	Glass	(None)		C	28
AgI	A	Glass	(None)		C	28
BaF ₂	A	Glass	(None)		C	28
BaO	50	Glass	(0.006)	T	C	28
Sb ₂ O ₃	A	Glass	0.15	C	C	30
Sb ₂ S ₃	A	Glass	(0.004)	C	C	28
Ce ₂ O ₃	50	Glass	(0.007)	T	C	28
CeF ₃	40	Glass	1.6	C	C	30
CdS	110	Glass	0.8	C	C	30
SnO ₂	A	Glass	(0.008)	T	C	30
C	A	Glass	4.0	C	C	28
NaF	A	Glass	0.1	T		57
B ₂ O ₃	90	Glass	0.1	T	C	30
Chiolite	A	Glass	(0.029)	T	C	28
AlPh'	40	Glass	0.6	C	C	30
MgPh'	40	Glass	0.6	C	C	30
MoO ₃	A	Glass	(0.013)	T	C	28
CuI	A	Glass	(None)		C	28
AlF ₃	A	Glass	(None)		C	28
SrSO ₄	A	Glass	(None)		C	28

* A, thermally floating at ambient temperature. † Values in parentheses are relative.

‡ C and T, compression or tension.

§ B, end-supported beam; C, cantilever beam; and ED, electron-diffraction technique.

¶ Al and Mg thalocyanine.

Anthony E. Ennos, "Stresses Developed in Optical Film Coatings," *Appl. Opt.* 5, 51 (1966)

The development of stress in evaporated dielectric and metal films, used as optical coatings, has been investigated experimentally by observing the bending of a thin silica strip as it becomes coated. The substrate temperature in all cases was close to ambient. Chamber pressure was in the region 5×10^{-6} torr to 5×10^{-5} torr.

In ZnS films there is always an initial stage of tensile stress, which reverses to compressive after the first 50-100 Å have been deposited. For both fast and slow evaporation, the stress has reached a near maximum value by the time a quarter-wave optical thickness [visible] has been deposited, and the stress thereafter remains sensibly constant at the same value for both cases. The values of maximum stress obtained ($\sim 2000 \text{ kg/cm}^2 = 3 \times 10^4 \text{ psi} = 1.96 \times 10^8 \text{ Pa}$) are rather higher than those quoted by Campbell (D. S. Campbell, *Electron Reliability and Microminiaturization* 2, 207, 1963). No relief or stress takes place after deposition ceases.

Magnesium fluoride develops a very high tensile stress both for slow and for fast evaporation. The stress builds up to a substantially constant value ($\sim 5000 \text{ kg/cm}^2 = 7 \times 10^4 \text{ psi}$) in the first quarter-wave. There is a slight increase in stress at the end of the deposition; considerable stress relief takes place when the layer is exposed to air, the final value lying around 3400 kg/cm^2 . The measured value of stress is higher than that previously published, but the substrate temperature in the present experiments was lower.

The effect of exposing thorium oxyfluoride layers to the atmosphere is interesting. The stress decreases appreciably, and the apparent refractive index rises from 1.51 to a value of about 1.52. The effect occurred only when gases containing water vapor were introduced.

Cryolite is somewhat hygroscopic. It develops a tensile stress which increases continually with thickness. There is a considerable aging effect after stopping deposition. The resultant stress is fairly low for quarter- and half-wave layers ($\sim 300 \text{ kg/cm}^2$).

Thallium chloride deposits with very little stress (maximum 30 kg/cm^2).
It is water soluble, and the film scatters visible light.

Thallium iodide develops a significant compressive stress ($\sim 300 \text{ kg/cm}^2$) which falls to a small value for very thick layers. Stress relief occurs after deposition ends.

KRS5 films are water soluble with composition similar to the bulk material. Its stress behavior is similar to thallium iodide, but yields lower values of stress.

The refractive index of evaporated films of cadmium telluride is about 3.05 in the near infrared, as opposed to 2.6 for the bulk material. This is most probably due to partial decomposition, the evaporated film being composed of a mixture of telluride and tellurium.

Other films investigated include CaF_2 , PbF_2 , CeF_3 , SiO , PbCl_2 , and Ge.

Resultant stress of multilayer stacks was not necessarily that to be expected from a combination of stresses of the individual layers.

Significant stress appears in films as little as 30-50 Å thick. It is known that at this thickness most films are discontinuous, i. e., the crystals growing on individual nuclei are not large enough to join up. Most material's investigated develop a tensile stress. This is what is to be expected from a film material which, when it is first condensed, must be considerably hotter than the substrate. On cooling, thermal contraction will cause a tensile stress. The compressive stress of the cadmium telluride reported here is probably due to dissociation of the material and partial recombination on the surface. The reduction in tensile stress of thorium oxyfluoride films exposed to damp air is also due to the same effect.

For those materials which develop a constant stress shortly after growth (e.g., ZnS, MgF₂, ThOF₂), one supposes that a stable equilibrium stress is built up within the film. There is no reason for these films to break internally as the thickness increases, and any failure that occurs will be initiated at the film substrate interface, where there is, of course, a large reversal of stress. It is interesting to note that, for zinc sulfide, and to a lesser extent, thorium oxyfluoride, the stress builds up slowly with thickness for fast evaporation and rapidly for slow evaporation. One can conclude that the crystal growth process is continuing in the sublayers at a finite rate, while at the same time fresh material is being deposited on top.

These materials are hard, do not show great stress relief in the vacuum after the end of deposition, and, combined in multilayers, give a net stress not greatly different from that to be expected by summation.

Materials in which the values of stress vary strongly with thickness must have considerable inhomogeneity of structure. That atomic rearrangement in the crystallites is taking place all the time is borne out by the fact that the stress changes considerably after the end of deposition (e.g., cryolite, chiolite, lead fluoride, thallium salts). These materials can be classed as soft in that they do not exert the same stresses in multilayers as to be expected from single-film values.

Some remarks can be made regarding the failure of films by cracking, peeling, etc. It is obvious from these measurements that the fact that a high stress exists in a film does not necessarily mean that it will break. Compressive stresses can be borne more easily than tensile ones, for instance, since a large area of film will have to become detached if it fails in compression. In fact, three factors are involved in the process of failure: (a) the stress in the film and its direction, (b) the rupture strength of the film material alone, and (c) the bond strength between film and substrate. The latter can exert a great influence. For example, a film having very great rupture strength will only break when the shearing force between substrate and film becomes greater than the adhesive force. On the other hand, a film having weak rupture strength may break internally before the adhesive forces are overcome. This can manifest itself as a cludging of the film rather than as a complete break.

Stanley K. Dickinson, "Infrared Laser Window Materials Property Data for ZnSe, KC₁, NaCl, CaF₂, SrF₂, BaF₂," Air Force Cambridge Research Laboratories Report AFCRL-TR-75-0318, 6 June 1975

This reference contains a valuable collection of coatings information. The present report grew to such great size that the excerpts from this reference were removed in the final draft. The relative information on coatings is contained in the following pages:

Coatings on ZnSe	35-47
Coatings on KC ₁	86-100
Coatings on NaCl	144-146
Coatings on CaF ₂	160-169
Coatings on SrF ₂	180-181
Coatings on BaF ₂	193-194

E. Bernal G., J. H. Chaffin, B. G. Koepke, R. B. Maciolek, and R. J. Stokes, "A Study of Polycrystalline Halides for High Power Laser Applications," Honeywell Inc. Semi-annual Technical Report #4, Contract No. DAHC15-73-C-0464, 15 January 1976

The previous problems of obtaining clear, $2 \mu\text{m}$ -thick TlI coatings on KCl have now been solved by adding an intermediate rinsing operation in the chemical polish sequence and raising the substrate temperature to $\sim 170^\circ\text{C}$ and increasing the deposition rate to $\sim 250 \text{ nm/min}$. [The crystallite grain size in the films appeared to be $\sim 10\text{-}20 \mu\text{m}$ in Fig. 35b.] The film absorption coefficient was $\beta_f < 1 \text{ cm}^{-1}$.

Small particles about $0.4 \mu\text{m}$ in diameter, believed to be potassium acetate ($\text{KC}_2\text{H}_3\text{O}_2$), on the KCl substrate were identified as the cause of the hazy TlI coatings. The intermediate rinse removed this precipitate.

TlI grows in a loosely packed columnar structure on room temperature substrates unless growth conditions are very favorable to epitaxy.

Chemical polishing appears to be the best method of removing mechanical imperfections in the KCl surface. Pure chemicals and a dry atmosphere are used to avoid fogging the KCl during removal from the polishing and rinsing solutions. Foreign material on the substrate such as dust and oily residues is a problem encountered in all thin film preparations.

B. E. Knox, J. Geneczko, L. Gilbert, R. Howard, G. Mariner, and K. Vedam,
Proceedings of the Fourth Annual Conference on Infrared Laser Window Ma-
terials, Nov. 18-20, 1974, Tucson, Arizona, January 1975

For Ge films on KCl, Ge was found to penetrate tens of nanometers into the substrate beyond the KCl-Ge interface. The Ge film readily oxidized throughout its bulk on exposure to normal atmosphere, with concomitant pronounced absorption at $10.6 \mu\text{m}$. Sputtered CdTe films had tellurium-rich surfaces, and small amounts of oxygen are incorporated in the surface layers of the film. [These results suggest that the values of β_f for sputtered Ge and CdTe films are expected to be too great for these films to be useful for high-power use.]

John R. Kurdock and Edward A. Strouse, Perkin-Elmer Corporation, "Optical Processing of Alkali Halides and Polycrystalline Zinc Selenide for High-Power Laser Applications," Technical Report AFML-TR-74-166 Part II, July 1975

Samples of KC1 and ZnSe were machined using a single-point diamond tool. Recent work on copper metal mirrors using this technique gave good results in the fabrication of samples, with reflectivities of 99.2% at 10.6 μm and surface roughness of less than 70 Å peak-to-peak. However, after machining the KC1 and ZnSe sample surfaces contained tool grooves. There is, at the top of each tool groove, a ridge of material that is apparently displaced from the tool track. The overall surface resembles that of a finely ground sample. Variation of tool speed and spindle speed have not resulted in surfaces significantly different from those ground with a 5 μm abrasive. This failure of the single-point-diamond micromachining process to produce acceptable surfaces was disappointing.

At face value the results of a chemical-mechanical polishing technique show that surface absorption was reduced 0.025% per surface by etching, indicating that residual absorption due to polishing damage, however small, is certainly not insignificant.

In all of the previous work in AR coatings on ZnSe and in all other development work on multilayer thin film devices at Perkin-Elmer, the experimenters have been able to rely on an extensive library of stress data taken from measurements on the Ennos interferometer using fused silica and BK-7 substrates. In past experiments these data have been applied without significant error to systems deposited on CerVit, germanium, silicon, Irtran II, Irtran IV, sapphire, and a number

of different optical glasses. In these instances, the difference in stress in the film due to the difference in expansion coefficient between the actual substrate and the substrate on which the initial stress measurement was made was obviously only a small fraction of the residual stress in the film, which is due primarily to condensation phenomena. Thus the biggest surprise in the present program and the factor that created the bulk of the initial problems in applying antireflection coatings to KCl was the inability to predict the film residual stresses due to the modification of these values by the difference in expansion coefficients between KCl and the film materials.

The influence on stress due to the high expansion coefficient of KCl was manifest in the failure in the compression mode of coatings in which both the high (ZnSe) and low (ThF_4) film materials were deposited at the high substrate temperature (150°-250°C) that had been used for the ZnSe AR coating designs. Samples deposited at lower temperatures (30°-80°C) were more durable but showed absorption in excess of 0.1%, a value that increased with time because of hydration of the ThF_4 film. Experiments performed later in the program indicate that this dilemma could be resolved by applying the thorium fluoride films at 150°C and the zinc selenide films at a lower temperature (80°C). The results of three runs that represent attempts to refine the six-layer ZnSe (80°C)/ ThF_4 (150°C) design to match its theoretically predicted performance are that the total film absorption was measured at less than 0.1 percent. It is evident however, that some difficulty was experienced in controlling both the minimum reflectivity value and the center wavelength location.

When KRS-5 is deposited on a substrate with a low coefficient of expansion, it forms a film with a low tensile stress. It has a low value of bulk absorption coefficient and, while not as hard as zinc selenide (Knoop number 40 compared with Knoop number 100), it is harder than the component materials, thallium bromide and thallium iodide (Knoop number ~10).

In this investigation only single discrete films of KRS-5 were evaluated. The thickness was chosen to represent the thickness that would be employed in a six-film design. The results indicated excellent adhesion to KC1. The first two runs produced erratic absorption measurements, presumably because of the poor quality substrates, but a later run on substrates of better quality indicated that the $1.1\mu\text{m}$ -thick film had less than 0.05% absorption. The KRS-5 vapor would not condense on substrates held at 150°C which means that in a multilayer combination with thorium fluoride it would be necessary to cycle the substrate temperature between alternate film depositions. Another negative factor was an index homogeneity in the film thickness direction. This took the form of a refractive index increasing with thickness, which is indicative of preferential evaporation or condensation of the iodide component at the initial stages of the evaporation. It is probable that, in practice, what we have is a thin layer of the pure iodide material or a layer very rich in the iodide material at the substrate surface. It might be avoided by forming the films from a vapor phase mixture (coevaporation) of the two components.

Because of the aberrations of compressive stress enhancement in zinc selenide films and tensile stress relief in thorium fluoride films deposited on KC1 substrates, it could be postulated that this same mechanism might permit

the deposition of thick films of highly tensile material such as cerium fluoride, which cannot normally be deposited in the form of thick film on low expansion substrates.

In the only experimental deposition of cerium fluoride, a film deposited on a KCl substrate held at 250°C failed in compression on removal from the vacuum chamber. A film condensed on a BK-7 substrate in the same cycle remained intact.

The results indicate that the flexibility afforded by the Herpin design approach can be exploited to yield an antireflection coating for KCl using ZnSe and ThF_4 which has less than 0.1 percent absorption. However, the lowest value of reflection achieved in practice was 0.2 percent, and the design in its present configuration will not pass the MIL-M-13508B tape test.

Walter Heitmann, "Vacuum Evaporated Films of Aluminum Fluoride," *Thin Solid Films*, 5, 61 (1970)

[It appears that β_f is too great at $10.6 \mu\text{m}$ for AlF_3 to be a useful antireflection coating at this wavelength. The transmittance of a $0.8 \mu\text{m}$ -thick AlF_3 layer on a KBr substrate starts to decrease at $10 \mu\text{m}$. The absorptance at $10.6 \mu\text{m}$ appears to be $A_f \approx 0.02$, corresponding to $\beta_f \approx 250 \text{ cm}^{-1}$, but this value may be highly inaccurate since it is obtained from a transmittance curve. This value of $A_f = 0.02$ is two orders of magnitude greater than the desired value of 10^{-4} .]

Evaporated aluminum fluoride forms porous films in vacuum with a refractive index of 1.23 and a tensile stress of about $1.6 \times 10^9 \text{ dyne/cm}^2$. Exposed to air, refractive index and optical thickness of the film increase about 13% while the stress is considerably reduced. These changes are probably caused by chemisorption of water. The refractive index of the coatings in air is 1.385 with no perceptible dispersion between 0.25 and $1 \mu\text{m}$. AlF_3 films are practically free of absorption for wavelengths from 0.2 to $10 \mu\text{m}$ with the exception of two absorption bands at 3 and $6 \mu\text{m}$. The coatings are not affected by water and show good mechanical stability. Evaporated AlF_3 films are amorphous and have a very smooth uniform surface.

Only a few compounds and some elements fulfill the practical requirements for optical film materials. Even these materials are not totally satisfying. This is illustrated by considering some properties of the low-index fluorides: cryolite forms soft moisture-sensitive and sometimes inhomogeneous layers. Magnesium fluoride films exhibit large internal stresses. They tend to crack from

a certain thickness and in multilayers they often destroy the whole stack. Thorium fluoride, however, while having nearly perfect properties, is somewhat radioactive. The application of large quantities of ThF_4 requires expensive protective measures.

In the literature we found only some short notes on AlF_3 films, stating a refractive index of 1.38-1.39. For the water solubility of the material a value of 0.559 g/100 cm³ is reported. Therefore a certain water sensitivity of these films is to be expected.

We obtained as the average value of numerous measurements a refractive index of $n = 1.385 \pm 0.5\%$ for the wavelength region from 250 to 1000 nm. In vacuum the refractive index of the films was considerably lower. From changes in the transmittance, which were measured for film thickness control during deposition, a refractive index of $n = 1.23$ was calculated. When air was admitted into the bell jar, the transmittance of the film changed. From subsequent measurements in air in the spectrophotometer, $n = 1.385$ was determined which means an increase of 13%. Since bulk aluminum fluoride has a refractive index of $n_m = 1.3767$, the films show a packing density of $P = 0.64$ in vacuum. When exposed to air the refractive index of the film rises to a value which exceeds that of the bulk material. This is probably caused by hydrate formation. Fluellite ($\text{AlF}_3 \cdot \text{H}_2\text{O}$), for instance, has a refractive index of $n = 1.49$. Chemisorption of water is probably also the reason for the decrease of stress in the films already mentioned. The formation of porous layers is not only observed for AlF_3 . As we have shown in a previous publication, nearly all commonly used fluorides for thin film production form more or less porous films.

The infrared transmittance of a $0.8\mu\text{m}$ -thick AlF_3 layer on a KBr substrate shows a broad absorption band between 2.7 and $3.8\mu\text{m}$ and a weaker band between 5.8 and $6.7\mu\text{m}$. The absorption bands in the AlF_3 films are also probably caused by water. At $10\mu\text{m}$ the inherent absorption of the aluminum fluoride begins.

To test the water resistance, one quartz glass and one plate glass with a $0.8\mu\text{m}$ -thick AlF_3 layer were put into tap water for one hour. The films did not show any visible changes. From transmittance measurements it was also found that the refractive index was not altered. In spite of the water solubility of the bulk AlF_3 mentioned earlier, the films were found to be stable in water.^{*114}
This is also likely to be due to the hydrate formation.

The films were strongly rubbed with a wet cotton plug wrapped around a wooden stick. Even this test did not cause any damage. Evaporation of relatively thick AlF_3 coatings showed that film thicknesses of at least $2\mu\text{m}$ can be produced on suitably prepared surfaces without formation of cracks.

X-ray analysis revealed that aluminum fluoride forms amorphous films.

Trouble may be caused by the large difference of the refractive index and the optical thickness of the film in air and in vacuum.

Air Force Cambridge Research Laboratories LQ Technical Memorandum #30,
"High Power Infrared Laser Window Materials," edited by Normantas Klausutis,
Semi-annual Report No. 1, July 1, 1975

Crack-free CeF_3 coatings adhered strongly to KCl substrates and were immune to atmospheric humidity. Values of β_f were not reported, but transmission measurements on a Beckman IR7 spectrometer showed "100 percent transparency in the 3-14 μm region." [This probably implies that the film absorptance A_f satisfies $A_f < 10^{-2}$, compared with the desired value of 10^{-4} cm^{-1} . Calorimetric measurements are needed to determine if A_f approaches the 10^{-4} value. As discussed in Sec. XI, there is weak evidence ("good to 14 μm ")⁶⁸ that previous CeF_3 films had A_f considerably greater than 10^{-4} .] These CeF_3 films were deposited at 0.13 to 0.23 nm/sec, 1.1×10^{-5} to $1.2 \times 10^{-5} \text{ Pa}$ (8×10^{-8} to 9×10^{-8} torr), and a substrate temperature of 150°C. They were 1-2 μm thick and nearly invisible to the eye. They passed the Scotch-tape test, and showed no visible deterioration after exposure to atmospheric humidity for one week.

Sputtered MgF_2 , LaF_3 , BiF_3 films and high-vacuum, thermally deposited films of PbF_2 and LaF_3 were found to be unsatisfactory. [Thermally deposited MgF_2 is of course one of the standard coating materials.] The PbF_2 films were soft and milky and showed optical absorption characteristics of OH^- or H_2O . Carbon and sulfur were found as surface contaminants.

J. H. Chaffin, "Protective Coatings for Alkali Halide Optical Components," Third Conference on High Power Infrared Laser Window Materials, Nov. 12-14, 1973, AFCRL-TR-74-0085(III), 14 February 1974

Copper chloride, TlCl, and TlBr films on KCl substrates are not stable in the presence of humidity. Cul films are stable in humidity, but we have been unable to reduce β_f below 10^3 cm^{-1} at $10.6 \mu\text{m}$, even though $\beta_b = 1 \text{ cm}^{-1}$ has been reported. A long diffusion tail of Cu into the KCl substrate is probably related to the great value of β_f .

We have fabricated TlI films on KCl substrates with $\beta_f < 1 \text{ cm}^{-1}$. It is essential to deposit these films very slowly (3 nm/min) to achieve this degree of transparency. TlI films on glass substrates are very stable in humid environments. [In a later report, Ref. *64 which is also excerpted, clear 2 μm -thick TlI films on KCl were obtained by adding a rinse step to the chemical polish procedure and depositing at the high substrate temperature 170 C at the high rate 250 nm/min.]

H. Winston, R. Pastor, R. Turk, A. I. Braunstein, and R. F. Scholl, Hughes Research Laboratories, "Fluoride Window Materials for Use as Laser Windows in the 2 to 6 μm Spectral Region," Technical Report AFML-TR-75-73, Contract No. F33615-73-C-5075, Final Report for period 15 March 1973 through 15 December 1974

It was pointed out that the band over which the laser energy is emitted is approximately 0.5 μm wide for all three chemical lasers (CO at 5.3 μm , DF at 3.8 μm , and HF at 2.8 μm). Thus coatings with low reflectance over this width of $\sim 0.5 \mu\text{m}$ are desired. Two-layer coatings, which are called 1/4-1/4 coatings, consisting of quarter wavelength optical thickness layers of two materials, and three-layer coatings, called 1/4-1/2-1/4 coatings, consisting of a first layer of quarter wavelength optical thickness, a second layer of half wavelength optical thickness, and a third layer of quarter wavelength optical thickness were designed and fabricated.

individual layers of CeF_3 and MgF_2 prepared on CaF_2 substrates showed absorption bands at 6 μm and 2.9 μm . [Water absorbs at these two frequencies. At AFCRL, CeF_3 films on KCl showed "100 percent transparency in the 3-14 μm region."¹⁰⁶]

In prior work, it was found that similar absorption bands at 2.9 and 6.1 μm in ThF_4 films were only present when the films were deposited at temperatures below 120°C. The first attempts to eliminate the absorption bands in MgF_2 and CeF_3 films, therefore, aimed at determination of a substrate temperature which would eliminate the bands. This has thus far been unsuccessful at temperatures up to 300°C.

The next series of experiments was aimed at the determination of the effect of source material purity on the absorption bands in the films. MgF_2 films were

prepared from Harshaw MgF_2 crystals, and CeF_3 films were prepared from HRL RAP CeF_3 at substrate temperatures up to 300°C. No change in the film absorption bands was observed.

The fluoride film absorption bands are believed to be caused by the incorporation of residual gases (particularly water) into the growing films. Directions for further work are to increase the evaporation rate to reduce the effects of residual gases, and to reduce the residual water in the system by baking and prolonged pumping. [Water absorption and adsorption after deposition could also be responsible for these optical absorption bands, as discussed in Sec. IV.]

Attenuated-total-reflection (ATR) spectroscopy with the Beckman IR-12 and the RIIC TR-25 attachment yields only qualitative information about the intensity of absorption. However, characteristic absorption bands stand out prominently, and changes in them with surface treatment are easy to monitor. Typical absorption bands in CaF_2 ATR plates are at 2.9, 3.4, 3.5, 5.7, 6.2, and 6.8 μm . After Freon vapor degreasing, one ATR spectrum showed a dramatic reduction in the absorption of the bands, indicating that they are indeed surface-related. A further reduction in the bands followed firm rubbing with tissues moistened with methanol.

It was found that the apparent calorimetric absorption depends strongly on the water vapor content of the atmosphere in the calorimeter chamber. A striking example of this effect is a series of measurements on a forged CaF_2 specimen. When the calorimeter head contained room air, the absorption constant was 0.0027 cm^{-1} , typical of many earlier measurements. After 15 minutes in a desiccated calorimeter chamber, the apparent absorption decreased to 0.0014 cm^{-1} , and after an hour it decreased further to 0.0012 cm^{-1} . It appears that there is a close coincidence between one of the sharp output lines of the CO laser and one of the sharp

water vapor absorption lines, and that energy absorbed by the water vapor is transferred by convection to the calorimetric sample. In fact, we now believe that this has been the major source of temperature rise in our calorimetric measurements, rather than the absorption of the sample itself. Of course, the problem can best be handled by employing a vacuum calorimeter.

M. Braunstein, J. E. Rudisill, and A. I. Braunstein, "Optical Coatings for High Energy ZnSe Laser Windows," Third Conference on High Power Infrared Laser Window Materials, Nov. 12-14, 1973, AFCRL-TR-74-0085(III), 14 February 1974

The value of n_r of ThF_4 was found to be 1.35, rather than 1.5. Coatings of $\text{BaF}_2 / \text{ZnS}$, $\text{ThF}_4 / \text{ZnSe}$, and $\text{ThF}_4 / \text{ZnS}$ were deposited on ZnSe substrates. The value of A_f was $A_f = 3 \times 10^{-4}$ at $10.6 \mu\text{m}$ for a $\text{ThF}_4 / \text{ZnSe}$ coating on ZnSe. This coating passed the MIL Spec. adherence, humidity, and salt spray tests, but failed the abrasion test. No coating passed the abrasion test. [In a later report,^{*9} two $\text{ThF}_4 / \text{ZnS}$ coatings on ZnSe passed the abrasion test.]

E. Bernal G., R. H. Anderson, J. H. Chaffin, B. G. Koepke, R. J. Stokes, and R. B. Macioiek, Honeywell, Inc., "Preparation and Characterization of Poly-crystalline Halides for Use in High Power Laser Windows," Quarterly Technical Report No. 6, Contract No. DAHC15-72-C-0227 and DAHC15-73-C-0464, 1 July to 30 September 1973

Thallium bromide (TlBr) powder was obtained from the Ventron Corporation with a heavy metal impurity level of less than 10 ppm. This powder was sublimed from a boron nitride crucible with a bell jar pressure of 2×10^{-5} torr and condensed on glass and cleaved single crystal KCl substrates held at room temperature. The deposition rate was 7.5 Å/sec and the total film thickness was 10,586 Å.

The optical absorption coefficient at 10.6 μm of the TlBr film on KCl was determined by laser calorimetry to be 11.8 cm^{-1} . One of the films on glass was placed in a 100 percent relative humidity environment and turned cloudy in less than one minute. The other film on glass was left in the ambient environment over a weekend, and it also turned cloudy. This extreme sensitivity to humidity is somewhat surprising since TlBr has a bulk solubility of only 0.05 g/100 ml of water. In an effort to find out what causes the cloudiness, we took a series of SEM and Nomarski micrographs. An SEM view at 15,000 \times of a TlBr film on glass which had been overcoated with a thin layer of gold immediately upon removal from the TlBr deposition facility shows that the surface of the as-deposited film appears to be smooth, with no structure visible. Another film, made at the same time as the first and exposed to 100 percent humidity for five minutes and photographed by the SEM with no overcoating shows that the surface seems to be covered with large crystallites. It is safe to assume that these crystallites can scatter enough light to cause the cloudy

appearance. A Nomarski micrograph of the same specimen reveals the same surface condition.

We made another TlBr film in which the substrate temperature was held at 100°C during deposition. This film displayed the same extreme sensitivity to humidity as described above, and we are therefore forced to conclude that thallium bromide films are not suitable as protective coatings for the alkali halides. [Since ThF₄ films also are unstable unless deposited at >150 C, a substrate temperature even greater than 100 C possibly could give stable TlBr films.]

We have tried several completely different methods of fabricating CuI films including reactive thermal evaporation, reactive RF sputtering, and iodinating sputtered copper films. The only method which consistently yields clear, highly adherent films is the standard thermal evaporation process. Despite the fact that deposition rates and substrate temperatures have been varied over very wide ranges, the lowest 10.6 μm absorption coefficient attained to date is approximately 1000 cm⁻¹¹¹⁵. Our initial suspicion as to the source of the high absorption was that the films were growing off - stoichiometry, and since Gudden and Schottky (Physik. Z. 36, 717, 1935) have characterized CuI as a stoichiometric imbalance conductor, this could lead to high electrical conductivity with high absorption at 10.6 μm. We began to question this hypothesis because variations in deposition rate, substrate temperature, and annealing treatments in both iodine vapor and vacuum conditions were not efficacious in lowering the absorption coefficient.

Searching for other possible causes, one film was analyzed at Physical Electronics, Inc., by a combination Auger spectroscopy/sputtering operation to obtain the profile of the concentration of various elements through the film thickness and down into the KCl substrate. Very small concentrations of carbon and oxygen were detected. We feel that it is likely that the high absorption of our Cul films is related to the long copper diffusion tail that extends approximately two film thicknesses into the KCl substrate.

Kraemer (J. Chem. Phys. 33, 991, 1960) has studied the uv properties of cuprous halide films on alkali halide crystals. He has observed spectra suggesting the interstitial diffusion of Cu⁺ ions into KCl and KBr from films of CuCl and CuBr, but not from Cul films. We found that this does, in fact, occur for Cul films on KCl substrates. Kraemer points out that Cu⁺ ions should diffuse most rapidly into KCl, less rapidly in KBr, and perhaps not at all in KI because of decreasing interstitial distances between halide ions. We plan to deposit Cul films on KI single crystals and repeat some of the above measurements. If we are able to prepare sufficiently transparent films on KI substrates, we will consider the possibilities of a "double-alloy" coating, i.e., KCl → KI → Cul, in which the KI serves the function of a copper diffusion barrier.

Ferdinand A. Kroger and John H. Marburger, "IR Window Studies," University of Southern California Semiannual Technical Report No. 1, Contract No. F19628-75-C-0080, 15 March 1975

[See our notes in the excerpt of Ref.*15 relating the work in this to the $9.8\text{ }\mu\text{m}$ absorption band in KCl.]

Sodium chloride exposed to atomic oxygen develops a surface layer which absorbs from ~ 930 to 1000 cm^{-1} , with peaks at ~ 970 , ~ 990 , and $\sim 940\text{ cm}^{-1}$ (10.3, 10.1, and $10.6\text{ }\mu\text{m}$), in order of decreasing intensity. The absorption, which was believed to be due to ClO_3 , continued to increase without signs of saturation for periods of exposure to the atomic oxygen up to nine hours, at which time the transmittance at the strong 970 cm^{-1} peak was reduced by ~ 17 percent. This value of absorptance corresponds to an effective thickness of pure NaClO_3 of 10-100 nm.
The lack of saturation implies that more than one or two monolayers of absorbing ions are involved. The role of diffusion of atomic oxygen in the bulk and through the antireflection or protective coatings were expected to be important and were hoped to be investigated in the future.

The effects of atomic oxygen on KCl and KBr were much weaker than on NaCl, the absorption bands being wider and at least an order of magnitude weaker.

E. Bernal G., J. H. Chaffin, B. G. Koepke, R. B. Maciolek, and R. J. Stokes, Honeywell, Inc. Semiannual Technical Report #1, Contract No. DAHC15-73-C-0464, 1 January 1975 to 15 July 1975

A two-layer T11 ($2.1 \mu\text{m}$ thick)/ ThF_4 ($1.2 \mu\text{m}$ thick) coating⁸⁴ on KCl showed a reflectance of 9×10^{-4} at $9.5 \mu\text{m}$. The calorimetric absorption coefficient of the composite coating was 8 cm^{-1} [corresponding to an absorptance $A_f = 8(2.1 + 1.2) 10^{-4} = 2.6 \times 10^{-3}$, supposedly], most of which was attributed to the ThF_4 . [The interpretation of most of the absorptance coming from $1.2 \mu\text{m}$ of ThF_4 gives $\beta_f = 22 \text{ cm}^{-1}$, which is reasonable but greater than the lowest reported value of $< 1.2 \text{ cm}^{-1}$. The value of $\beta_f < 1 \text{ cm}^{-1}$ for T11 was given in later publications.]^{*86,*109}

Films of T11 grown on glass, cleaved KCl, and mechanically polished KCl are clear until a critical thickness of ~ 3 to $0.5 \mu\text{m}$ is reached. [The problem of obtaining clear, $2 \mu\text{m}$ -thick T11 coating on KCl was solved in a later report. See Ref. 95, which is excerpted in this section.] Then the films turn uniformly hazy as a result of scattering in the coating itself. By contrast, films grown on chemically polished KCl substrates exhibited cloudy streaks at small thicknesses as a result of scattering at the coating-substrate interface. The haze was not believed to be due to coating surface roughness in either case. Edge views (obtained by cleaving the substrates) of cloudy coating by the scanning electron microscope indicate that the films begin to grow in a "pancake" morphology, then abruptly switch to a loosely packed columnar growth pattern. The unclouded coatings had the appearance of cleaved surfaces.

The difficulty in growing clear, thick T11 films dramatically increased with a second purchase of T11 powder. It was found that the second purchase was purer than the first and that the first powder contained a small trace of sulfur. Intentionally adding 0.3 wt percent sulfur to the purer T11 powder resulted in a large

value of $\beta_f = 100 \text{ cm}^{-1}$ at $10.6 \mu\text{m}$ and severely cracked and crazed films.

[Adding a smaller amount, say a few parts per million, of sulfur or somehow exposing a clean, fresh substrate to sulfur before the deposition of the coating would be of interest for T1I and other coatings. The relation of the sulfur results here to the final solution to the hazing problem reported in Ref.*95, which is also excerpted, is not known.] By varying the deposition rate from 50 nm/min to 500 nm/min it was found that two-micron-thick T1I films that were only slightly hazy could be grown consistently at 100 nm/min. The films were, however, epitaxial. [Concern was expressed over the birefringence of the epitaxial films.]

X-ray diffraction, X-ray oscillation camera, and scanning electron microscope studies indicated that the T1I films are single crystal and in some cases grow epitaxially on KCl.

The good T1I coatings were deposited at room temperature. Coatings deposited at 100 C were cloudy and had rough surfaces.

John R. Kurdock, Perkin-Elmer Corporation, "Optical Processing of Alkali Halides and Polycrystalline Zinc Selenide for High-Power Laser Applications," Quarterly Progress Report No. 2, Contract No. F33615-73-C-5127, October 1973

Thorium fluoride is known to be reactive with residual water vapor in a coating chamber atmosphere, and the hydrated ThF_4 films so produced have more absorption on hydrous films. It is fairly well known in optical coating practice that if the condensation rates are reduced, the grain or particle size of the films will be increased due to the fact that fewer nucleating points are formed on the substrate during the initial deposition. It seems that the absorption mechanism for ThF_4 films is primarily concerned with chamber residual atmospheres reacting with the ThF_4 vapor.

John R. Kurdock, Perkin-Elmer Corporation, "Optical Processing of Alkali Halides and Polycrystalline Zinc Selenide for High-Power Laser Applications," Quarterly Progress Report No. 3, Contract No. F33615-73-C-5127, January 1974

Thin ($\approx 1000 \text{ \AA}$) PrF_3 protective films deposited on ZnSe (at 250°C)

did not pass the MIL-C-675A requirements for abrasion and humidity.

Using the three-film Herpin Section, antireflection coatings (ZnSe- ThF_4 -ZnSe) have been produced that meet all the design goals except durability.

[Thin films of PrF_3 and CeF_3 applied over ZnSe- ThF_4 -ZnSe did provide some increase in abrasion resistance.¹¹⁶ It was not known whether or not the resistance to humidity attack was increased.¹¹⁶

John K. Kurdock, Perkin-Elmer Corporation, "Optical Processing of Alkali Halides and Polycrystalline Zinc Selenide for High-Power Laser Applications," Quarterly Progress Report No. 4, Contract No. F33615-73-C-5127, April 1974

An unspecified substrate and antireflection coating that was overcoated with 50-60 nm-thick CeF_3 or ThO_2 films had $A_f < 0.1\%$ [apparently a measured value at $10.6 \mu\text{m}$] and passed the MIL-C-675 eraser and humidity tests and the MIL-M-13508B Scotch-Tape tests.

E. Bernal G., R. H. Anderson, J. H. Chaffin, B. G. Koepke, R. B. Maciolek, and R. J. Stokes, Honeywell, Inc., "A Study of Polycrystalline Halides," Semi-annual Technical Report #1, Contract DAHC15-73-C-0464, 15 July 1974

We have extensively investigated the properties of KC1 and T1I coatings evaporated in a tenuous argon atmosphere prepared by first evacuating the bell jar to $\sim 5 \times 10^{-7}$ torr and then admitting argon through a needle valve until the pressure reached 1×10^{-4} torr. The substrate temperature was 60°C, and the crucible-substrate distance was 40 cm.

We observed that the films are clear and adherent up to pressures of 7×10^{-4} torr, but at 8×10^{-4} torr the T1I films become very cloudy. The absorption at $10.6\mu\text{m}$ for these films, as measured calorimetrically, was found to be unaffected by the argon at pressures up to 6×10^{-4} torr. Two six-inch long glass substrates were coated with T1I, one in a hard vacuum (1×10^{-6} torr) and the other in an argon atmosphere of 4×10^{-4} torr. A comparison of the interference colors of the two films showed that the film evaporated in argon had a much more uniform thickness than the vacuum-prepared film; the scattering due to the argon is responsible. Alloy coatings of T1I and KC1 $\sim 1500\text{ \AA}$ thick on KC1 substrates survive the "Scotch-tape test," but inasmuch as T1I is an extremely soft material, the coatings do not resist abrasion to any degree. This will not be a serious drawback provided the remaining anti-reflection coatings can be deposited onto the T1I coating and providing that these "exterior" coatings have good mechanical stability.

Micrographs of a 2000\text{ \AA} thick discrete T1I film on a cleaved and on a mechanically polished KC1 surface, as-deposited, after exposure to 100 percent relative humidity, show that moisture attack is through as-deposited

pinholes in the T11 film, and that the pinhole size and/or density is smaller for the mechanically polished surface than for the cleaved surface.

Scanning Auger micrographs have been taken of chemically polished surfaces. The most useful are those measuring the carbon distribution of the surface, since all of our polishes and rinses are carbon-containing compounds. Carbon is uniformly distributed over the surfaces. An Auger profile showed that the carbon-containing residue was about 50 Å thick. A layer this thin would probably not produce measurable optical effects, but it could certainly interface with good coating adhesion and integrity. We plan to try to remove this thin residue with R. F. -induced low energy ion bombardment, without degrading the surface optical properties. [The absorptance from a 5 nm (50 Å) thick carbon-containing residue may not be negligible. At an absorption peak (perhaps C-H at 3-4 μ m or CO₂ at 4.3 μ m) a typical value of β is 10^5 cm^{-1} . Thus, the resonance absorptance of the 5 nm thick carbon residue is expected to be of order $A_f = \beta d = 5 \times 10^{-2}$, which is quite large. Such absorptance could be mistaken for $\beta_f = 2.5 \times 10^3 \text{ cm}^{-1}$ in a 200 nm thick film.]

E. Bernal G., J. H. Chaffin, B. G. Koepke, R. B. Maciolek, and R. J. Stokes, Honeywell, Inc., "A Study of Polycrystalline Halides for High Power Laser Applications," Semiannual Technical Report #2, Contract DAHC15-73-C-0464, 15 January 1975

Chemical polishing of (110) and (111) surfaces was successfully performed in a low-humidity environment on stress-free surfaces of samples that were carefully polished with light pressure. We found that chemical treatment in high humidity of any crystallographic face that had been heavily burnished during mechanical polishing produced disastrous results. The enhancement of the scratches and very non-uniform surface is the result of the stress-dependent solubility of KCl in the polish and in the water that condenses on the surface upon evaporation of the isopropyl alcohol in high humidity.

The rate of moisture attack on alkali halide surfaces is a strong function of the condition of the surface, i.e., surface stress and smoothness. Nomarski interference micrographs show the effect of moisture on a severely scratched single potassium chloride blank. Breathing on the sample, which is a severe test because of the warm temperature of the water vapor exhaled, results in enhancement of all the scratches in the original surface. But the overwhelming features of the surface attacked by moisture is the exposure of the damage produced by mechanical polishing which had been covered by a smoothly smeared layer during the final mechanical step. This is what we call burnishing, and it is responsible for the familiar surfaces of alkali halides that look good but are severely etched by moisture.

These tests prove conclusively the importance of very careful mechanical polish to minimize burnishing and avoid imbedded particles of grinding compound.

They also explain why chemical polishing should be done in low humidity environments to avoid water etching when solvents evaporate before the chemical polishing is completed. Finally, they give clear evidence of the moisture resistance of chemically polished surfaces. The problems presented by chemical polishing of polycrystalline halides are certainly more complex than is the case for single crystals. However, results to date suggest that by careful mechanical polishing and proper annealing it should be possible to produce high quality surfaces by chemical polishing.

Evaporated TlI films on KCl or glass substrates are occasionally observed to be cloudy due to a very rough film surface, with large-scale roughness of order of the film thickness of 2000 Å. This cloudiness is sometimes not uniform over the entire film area, but instead is in the form of streaks; in this case, we attribute the cloudiness to gross chemical residue left on the substrate by the cleaning or polishing procedure. It was found that only the substrate temperature during the film deposition directly affected the optical clarity of the coatings. It was found that at 25°C substrate temperature, the coatings are always clear except under a bizarre set of circumstances. At $T_s = 60^{\circ}\text{C}$, roughly 10 percent of the films grow cloudy; at $T_s = 100^{\circ}\text{C}$, all of the films are cloudy. At $T_s = 125^{\circ}\text{C}$, no films grow on KCl, i.e., the sticking coefficient has dropped to zero; however, a cloudy film grows on glass at this temperature. We conclude that during deposition the substrate temperature should be kept below 45°C to ensure clear TlI coatings; however, the coatings may subsequently be annealed at higher temperatures as described below.

After preparing a large number of T1I films on 25°C KC1 substrates, we observed that a few, for no apparent reason, grew cloudy. We finally speculated that there might be a correlation between the installation of "new" aluminum foil (which is used as a shield to reduce deposits on the sides of the bell jar) and cloudy films. Subsequent experimentation has shown this to be a well-founded speculation. A deposition performed with new aluminum foil in the vacuum system results in a cloudy film; a second deposition using the same aluminum foil results in a clear film. We do not understand what could be causing this effect at present. [This is perhaps additional evidence for the need for thorough baking.]

It is possible to anneal samples at 100°C for at least 24 hours with no deterioration of the coatings, but clear films annealed at 125°C for 24 hours become cloudy due to the formation of a heavily faceted surface. It may be possible to safely raise the temperature to a higher value for a shorter period of time for the purpose of applying another coating, but the absolute temperature limit is somewhere around 175°C. Beyond 175°C the vapor pressure of T1I begins to rise rapidly, and the coating begins to evaporate.

Pinholes in the T1I coating have never been observed by us prior to exposing the sample to humidity. After exposure they can then be located because the humidity brings KC1 to the surface through the pinhole and the KC1 subsequently crystallizes near the pinhole upon removal of the sample from the humidity. It is felt that the pinholes are almost entirely due to mechanical surface imperfections. [The fact that 200 nm-thick T1I films on KC1 do not prevent

moisture attack as a result of pin holes in the film is in agreement with Young's^{*38} findings that crystalline films did not prevent moisture attack on NaCl.]

We would like to warn that the problems of producing a surface for coating are subtly different, and in many ways more severe, than the problems of producing good quality infrared optical surfaces.

F. A. Horrigan and T. F. Deutsch, "Research in Optical Materials and Structures for High-Power Lasers," Raytheon Research Division Quarterly Technical Report No. 3, Contract No. DAAH01-72-C-0194, July 1972

The OH concentration of a series of KCl samples was determined using UV spectroscopy, and found to be of the order of 1-2 molar ppm. No correlation between OH concentration and $10.6\mu\text{m}$ loss could be established for samples with $\beta = 3 \times 10^{-3} \text{ cm}^{-1}$. [The lack of a measurable effect of OH⁻ on β_b at $10.6\mu\text{m}$ is as expected¹⁸ since the tail of the OH⁻ infrared-absorption line, center near $3\mu\text{m}$, is very small at $10.6\mu\text{m}$.]

In the measurement of low absorptance ($A \sim 10^{-4}$), any small pickup by the sample thermocouple can become appreciable compared to the temperature rise due to material's absorption. Stray pickup can come from scatter or reflection of the laser beam or reradiation from the power cone. The following experiment was performed to determine the amount of stray pickup occurring in our apparatus.

A 1/2 inch diameter hole was drilled through a 1 in. square sample of zinc selenide, and the sample was mounted in the standard measurement position. Under ideal conditions there should be no temperature rise indicated by the sample thermocouple, since the hole in the sample is larger than the laser beam and the 9 mm input irises. However, the sample temperature rose about 0.05°C , which corresponds to a Power Absorbed/Power Transmitted of 2.7×10^{-4} . This absorbed power was coming from either reflection or reradiation by the power cone or scatter from the edge of the irises.

The experiment was then repeated with the sample moved closer to the input irises, keeping it as far away as possible from the power cone in an attempt to try to minimize small-angle scatter from the edge of the irises. The pickup in this case has been reduced by about a factor of two. Also, the shape of the curve indicates that direct reflection and scatter have been eliminated, and that the remaining pickup is due to reradiation, probably from the power cone. It is expected that the installation of the bulk-absorbing power absorber will reduce this effect considerably. In addition, another iris will be placed on the other side of the sample to further reduce the spurious pickup.

G. Hass, J. B. Ramsey, and R. Thun, "Optical Properties of Various Evaporated Rare Earth Oxides and Fluorides," J. Opt. Soc. Am. 49, 116 (1959)

The optical properties of evaporated rare earth compounds such as Y_2O_3 , La_2O_3 , Pr_6O_{11} , Sm_2O_3 , Gd_2O_3 , LaF_3 , NdF_3 , and CF_3 were studied in the wavelength region from 0.22 micron to 2 microns. The materials were evaporated from tungsten boats and condensed on glass and fused quartz substrates at various temperatures. The oxides condensed as almost amorphous films, whereas the fluorides developed fairly large grains as indicated by their sharp electron diffraction rings. All films were hard and showed excellent chemical and mechanical durability. An increase in n and k at $\lambda = 0.22$ micron is evidently caused by an increase of the film density concurring with a sintering process.

The fluorides exhibited a simpler behavior than the oxides for two reasons. First, the fluorides are chemically more stable and show, therefore, no decomposition during the evaporation. Secondly, the fluorides are deposited as relatively large crystals as indicated by their sharp electron diffraction rings which show the pattern of the regular fluoride structure. In contrast, La_2O_3 as an example for the oxides, has an almost amorphous film structure. Such amorphous film structures are frequently more influenced by a small change of the deposition conditions than well crystallized forms, and they show, therefore, properties less consistent from coating to coating.

Reinhard Glang, John G. Kren, and William J. Patrick, "Vacuum Evaporation of Cadmium Telluride," *J. Electrochem. Soc.* 110, 407 (1963)

Cadmium telluride films 0.1-1 μ thick were deposited on glass substrates between 25° and 250°C at ambient pressures below 10^{-6} Torr. The vapors, although dissociated into the constituents, form stoichiometric, crystalline CdTe films with zincblende structure. The films are continuous, uniform, and adhere well to glass surfaces if deposited at or above 100°C. To avoid condensation of free tellurium, substrate temperatures above 150°C are required. At these condensation temperatures, films about 0.5 μ thick have grain sizes of 1000-2500 Å, and their (111) crystal faces are oriented parallel to the substrate surface. Regardless of deposition temperature, all films have resistivities of 10^7 ohm-cm or higher, even if impurities are added to the source material.

[Cadmium vacancies, resulting from excess tellurium, give rise to p-type conductivity with 0.15 eV activation energy. Is it known if there is a corresponding infrared absorption extending from ~8.3 μ m longer wavelengths?]

Richard J. Scheuerman, "Deformation of Optical Surfaces by Film Stress,"
J. Vac. Sci. Technol. 6, 145 (1969)

In general, stress in a thin film is most easily detected by measuring the bending of the substrate upon which it is deposited. A Laser Stress Interferometer (A. E. Ennos, Appl. Opt. 5, 51, 1966) mounted in the vacuum chamber was utilized to measure the bending of a thin fused-silica strip which formed one mirror of the interferometer. This method has an inherently high sensitivity and is capable of detecting a stress of 5.7 kg/cm^2 ($= 5.6 \times 10^5 \text{ Pa} = 81 \text{ psi}$) in a film 1000 \AA thick. Films of ZnS, ThF_4 , and SiO_2 $\sim 110 \text{ nm}$ thick had stresses ranging from 1100 to 2800 kg/cm^2 (1.6×10^4 to $4.0 \times 10^4 \text{ psi}$).

A. K. Jonscher and P. A. Walley, "Electrical Conduction in Non-Metallic Amorphous Films," J. Vac. Sci. Technol. 6, 662 (1969)

A distinction is made between simple amorphous films such as silicon germanium and other semiconductors, glassy films, and finally, noncrystalline polymers, both conducting and insulating.

Glasses contain microscopic regions of short-range order which define their physical properties, such as energy band structure, while the long-range order is absent because adjacent microscopic regions are randomly oriented. The glassy state is a metastable state. Glasses are characterized by the presence of more than one type of bond and by a relative insensitivity to the magnitude of bond angles in the structure.

Such materials as amorphous silicon or germanium may be characterized by only one type of strongly oriented covalent bond with approximately tetrahedral coordination, which determines the short range order and, therefore, the electronic properties.

For our purposes we shall define a polymer as a solid possessing some relatively strong bonds, typically covalent, which define extended macromolecules in the form of linear chains, rings, or planar lattices, and other much weaker bonds providing intermolecular links. Amorphous polymers retain a definite periodic order within the macromolecules, while the mutual arrangement of the latter remains random. According to this definition, plastic sulphur, amorphous selenium, and tellurium, as well as crystalline graphite, are all polymers.

On comparing glasses with amorphous germanium and silicon, it can be seen that glasses are more stable. Where there is only one type of atom and the bonding arrangement as in germanium and silicon, more strain is involved in deviating from the crystalline structure. It is well known in silicon oxide that the ratio of silicon atoms to oxygen atoms is not a constant, but depends on deposition conditions. We can infer that the short range structure of silicon oxide need not be the same in various regions of the film. In order to relieve stress, there may be regions where there are more Si-Si bonds than Si-O bonds or vice versa. This random variation in the bonding arrangements in compounds or materials like carbon or selenium, may be what gives rise to what we call glassy structures (as opposed to amorphous structures) in which more continuously bonded extended networks occur.

Our own evidence suggests a model in which initial more or less uniform amorphous material undergoes a continuous process of nucleation and growth of microscopic regions of progressively increasing order. As these relatively more ordered regions increase in size, one has to accept the possibility that the surrounding disordered or amorphous matrix becomes depleted of atoms, and thus has a larger number of vacancies than the original material. We leave open the question of the extent of ordering in the more ordered regions; this could be anything between the dodecahedra model and completely crystalline grains.

Theoretical conclusions based on Gubanov's theory (A. I. Gubanov, Quantum Electron Theory of Amorphous Conductors, 1965) are as follows: (a) the allowed energy bands of crystalline materials retain their basic identities, but they become distorted near the band edges by the presence of deep "tail states" which

correspond to progressively more and more localized levels; (b) the forbidden gap between the free band edges, to the extent to which it may be defined, is larger than in the corresponding crystal; (c) the states due to donor and acceptor impurities tend to disappear in the allowed bands or, in the case of glasses, these impurities become ineffective by slight adjustment of local bonding. Thus the material becomes less sensitive to impurities than its crystalline counterpart; (d) the mobility in the quasi-localized deep levels is much less than in the free bands of the crystal, typically by some orders of magnitude.

Conclusions

A. dc Conduction at Low Fields. This may be hopping or very narrow band. If the former, the principal contribution to resistance must come from "bottlenecks" or regions of difficult hops.

B. dc Conduction at High Fields. Poole-Frenkel mechanism, i.e., some form of field-assisted hopping is very typical of amorphous materials.

C. dc Conduction at Very Low Temperature. When thermal activation becomes insufficient, a new mechanism frequently sets in showing $I \propto V^n$ where n is greater than 3 and may be as high as 15 to 20. There is vanishing activation energy, typical of amorphous materials.

D. ac Losses at Low Frequencies. There is ionic or electronic polarization of interfacial or bulk type, not leading to dc conduction.

E. ac Losses at Low and Intermediate Frequencies. These could be due to Maxwell-Wagner mechanism, in which conducting regions are presently in a relatively less conducting matrix.

F. ac Conduction at High Frequencies. It is almost certain there is electronic hopping, decreasing activation energy with increasing frequency. All these mechanisms may be different and may have different activation energies.

A. Vecht, 'Methods of Activating and Recrystallizing Thin Films of II-VI Compounds,' Physics of Thin Films, 3, 165 (1966)

When a II-VI compound is evaporated onto a cold substrate, it does not exhibit the required crystallinity, but is cryptocrystalline -- i. e., its crystal structure cannot be resolved optically and can only be determined by X-ray analysis. To increase the crystallite size, the substrate temperature can be raised during deposition, or a postevaporation heat treatment can be employed. When evaporated films of II-VI compounds are heated, their cryptocrystalline structure gradually gives way to a mosaic crystallite structure. Crystal boundaries can be more readily detected under reflected than under transmitted light. In hexagonal compounds, crystalline areas can best be distinguished from the amorphous regions under polarized transmitted light.

Z. H. Meiksin, "Discontinuous and Cermet Films," Physics of Thin Films, Vol. 8, 99 (1975)

In general, when a film is deposited on a glasslike substrate in vacuum by evaporation or sputtering, the nucleation of the deposited film begins at many different nucleation sites, usually at imperfections in the substrate surface as a result of the loss of the high mobility of arriving particles at such sites. Additional particles arriving from the source agglomerate about the nuclei, and an island structured film is formed. As the deposition continues, islands coalesce decreasing the island density. The islands then grow until contact is made with neighbors, and gradually the voids between the agglomerates are filled producing a filamentlike network. Eventually, a macroscopically uniform thin film is obtained.

The sheet resistance of a metallic thin film decreases by several orders of magnitude as the film structure changes from the discontinuous to the uniform continuous film structure. Similarly, there is a pronounced change in the optical absorption spectrum. The resistivity of discontinuous films is governed by quantum tunneling. The same tunneling process is also responsible for a high strain coefficient of resistance. Two factors that yield discontinuous films impractical for general use are poor reproducibility and instability. Cermet and low density tantalum films can be made thicker than discontinuous films. They can be considered physically continuous, but electrically discontinuous or quasicontinuous.

The average thickness of gold films in this range is typically below 100 Å. The linear dimensions of the islands and of the interisland spacings can vary from a few angstroms to several tens of angstroms. It is generally agreed that conduction in such films is by quantum tunneling.

Films of average thickness of the order of 100 Å (typical for gold films) consist of agglomerates which just make contact with their neighbors. The contact diameter is typically between 10 and 50 Å.

Filament like thin films. Films in the range of average thickness between 100 and 200 Å (typical for gold films) can be considered to consist of fine filaments or capillaries.

Cermet films are composites of a metallic component and a dielectric component. Such films were developed to obtain films with higher values of resistance per square than are possible with continuous metallic thin films. Cermet films consist essentially of conductive phases similar in structure to discontinuous and quasi-continuous films as presented in the previous sections, but the vacuum or air in the voids of the metallic film is replaced with a solid dielectric phase. This results in more resistive films. Most work has been done with chromium-silicon monoxide and with gold-silicon monoxide films.

Low density tantalum films are obtained by sputtering at relatively low voltages between 1000 and 3000 V. Diffusion along grain boundaries is several orders of magnitude faster than in the bulk. Thus, oxidation at grain boundaries can occur both internally because of migration of trapped oxygen, and externally from the surface. The oxidation process becomes even faster at higher temperatures. Eventually the films become electrically discontinuous even though they are physically continuous.

A careful study of low density tantalum films ranging from 100 to 500 Å thickness has shown that the film growth does not follow the classical pattern of film growth of metal films. Films of 100 Å thickness consist of aggregates that

are linked by metallic bridges, and each aggregate contains many crystallites. As the thickness of the film increases, the average size of the aggregate increases until it reaches approximately 350 Å. Simultaneously, however, the size of the voids, or channels, increases from approximately 20 to 50 Å.

A. K. Jonscher and R. M. Hill, "Electrical Conduction in Disordered Nonmetallic Films," Physics of Thin Films, Vol. 8, 169 (1975)

The effect of the lack of structure on the electronic properties of liquid semiconductors has been the subject of extensive studies from which the principal conclusion has been that the electronic properties are primarily a function of the short-range order in a material, whether liquid or solid (1). It is believed that the crystalline band structure model remains substantially unchanged so long as the environment and coordination of individual atoms in the system under investigation remains substantially unchanged. The disappearance of crystalline long-range order has important consequences for transport and other physical properties but does not affect the basic nature of the solid, e.g., the broad features of the optical absorption spectrum.

A definition of an amorphous solid would be that it is a material lacking any form of order. The arrangement of nearest neighbors, in typical amorphous solids, is subject to severe constraints and departs only slightly from the disposition in a perfect lattice. This is a direct consequence of the fact that chemical bonds, especially covalent ones, are relatively rigid both in direction and in length, and their distortion beyond certain limits requires excessive energy.

Glasses have a multiplicity of flexible bonds and therefore remain vitreous over a wide range of temperatures. These materials have the ability to form more than one type of bond.

The amorphous state is to some extent unstable, or metastable, and frequently exhibits a gradual or even rapid transition to an ordered crystalline state. One obvious consequence of this fact is that amorphous samples often show irreversible

"drift" in their electrical properties, especially at elevated temperatures and also under the "catalytic" action of metallic contacts. A particular example of metastability is afforded by reversible switching, which can be observed in a wide range of glassy materials.

There are three types of disorder which may be found in any amorphous material (2). The first may be described as a continuously connected long-range disorder which retains the topological perfection of a single crystal, i.e., no bonds are broken and no foreign impurities are present. The second type of disorder arises in relatively "rigidly" bonded materials and is characterized by a large density of broken bonds forming "grain boundaries" separating relatively well-ordered small "crystallites" giving a discontinuous structure with a rather lower density than a single crystal. It is interesting to note that both the continuously disordered material and the "microcrystalline" material would give similar radial distribution curves, which at present form the principal tool of structure analysis; this means that it is very difficult to distinguish experimentally between these two alternatives. Finally, the third type of disorder is due to foreign impurities incorporated interstitially or substitutionally in the disordered "lattice" of either of the first two types.

By far the most important source of experimental data on amorphous materials is the measurement of electrical conduction as a function of temperature, electric field, and frequency, with drift mobility and photoconduction added as a bonus in certain cases.

There is broad agreement (13) in the results that the conduction and valence bands of allowed levels in which electrons may move in crystalline insulators are

basically preserved, but the forbidden energy gap of the crystal is replaced by a "pseudo-gap" in which the density of states remains finite, if low, throughout its width. It has long been recognized that one condition for the validity of the "free-electron" theory is that the resulting mean free path λ should be greater than the interatomic spacing a . Experimental measurements on a range of disordered solids indicate mobilities significantly below this value, and this has led to the concept of hopping as an alternative conduction mechanism.

Hopping can be defined quite generally as thermally assisted transitions between localized sites which in the electronic case may involve an element of tunneling. It was first recognized in crystalline germanium and silicon containing partially compensating donors and acceptors (14-17). At sufficiently low temperatures, for which thermal excitation of carriers into the relevant free band may be neglected, the residual conductivity is due to thermally assisted hopping of carriers between occupied and empty shallow levels.

The concept of hopping fitted in very well with the idea of deep localized levels in the forbidden gap of amorphous solids and it is generally agreed that the low-field conduction in these materials is of the hopping type (8, 13, 18-23). What is much less definite is the precise nature of the hopping transitions involved, i.e., the types of levels between which hopping takes place and the quantitative laws governing these transitions.

It is generally agreed that the deep levels are strongly localized, which means that the transition probabilities between them are small. We may distinguish the following four types of transport: hopping conduction in the region of strong localization, percolation paths of easy transitions between selected

sites as the ratio approaches unity, impurity band formation where the ratio is larger than unity, and the limit of free band conduction where localization does not occur at all.

On the important question of the distribution in energy of the density of the localized levels we have little reliable experimental information and very little theoretical guidance. We do not even know whether the density of states should always show a monotonic decrease away from the free band edges and whether enhanced densities may or may not exist in specific energy ranges.

A continuous long-range disorder without any broken bonds might be expected to lead to a wide distribution of localized levels in the "forbidden gap" of the material. This form of disorder would be expected intuitively to lead to decreasing density of states with distance from the band edges. This may lead to a measure of overlap between the states derived from the conduction band and those derived from the valence band. On the other hand, a single well-defined type of short-range disorder, for example, a broken bond or an interstitial atom, may be expected to lead to localized levels more clearly restricted in energy since the nearest-neighbor interactions are relatively well defined, regardless of the absence of long-range order (24).

We adopt the convention, advocated by Allgaier (25) that the only physically meaningful carriers are electrons and no useful purpose is served by introducing the concept of holes. This convention is applicable only to transport within the "forbidden gap."

Denoting an occupied state by a solid symbol and an empty state by a light contour, we may envisage the following two basic charging reactions:



and



The state denoted by \square is electrically neutral when full and becomes positively charged when empty, the state \circlearrowleft is electrically neutral when empty and becomes negatively charged when full.

In the case of donorlike centers in which the interaction between the electron and its positively charged center is coulombic, it is possible to estimate the binding energy from the "hydrogenic" model, taking into account a suitable value of the dielectric constant of the material and assuming a free electron mass for the carrier. No such estimate is generally possible for traplike levels which depend on short-range interactions whose nature is not so well understood.

Any long-range disorder arising from a loss of perfect periodicity but not involving broken bonds or electron numbers in excess of those required to satisfy bonding conditions may be expected to lead to the splitting off of localized levels from both the conduction and valence bands. All levels deriving from the conduction band would be neutral when empty and would therefore represent electron traps defined by Eq. (3). There is a widely held opinion, for example, that amorphous germanium is p-type because vacancies in crystalline germanium behave like acceptors (26), although there is no firm experimental proof of p-type behavior in amorphous germanium.

If the Fermi level falls in a region of energy in which there is a finite density of localized states, hopping conduction, with a small activation of energy, is possible.

Our discussion of the effects of disorder on the formation of various localized levels would be incomplete without some reference to the important differences that may arise between materials of different bond types, viz. covalent versus ionic. There is evidence, mainly from photo-injection studies in metal-insulator-semiconductor structures (28-30), suggesting that some ionically bonded solids show remarkably few, if any, deep levels. Covalently bonded crystalline solids show both a high density of surface states, resulting in effective pinning of the Fermi level at the surface independent of the metal work function, and also a rigid conservation of k vector in optical transitions. One would expect that the covalently bonded materials, such as amorphous Ge, Si, and C, some chalcogenide glasses, and probably silicon "monoxide," would give the behavior characteristic of deep levels, mainly hopping conductivity. It would be wrong, however, to expect similar behavior of the more strongly ionic disordered solids, in particular silicon dioxide. In our opinion it is grossly misleading in many real systems which may be very inhomogeneous. We have to distinguish two types of inhomogeneity: local or microscopic inhomogeneities arising out of local fluctuation of short-range order, and gross inhomogeneities due to macroscopic discontinuities in the material. The result is that the microscopic path of a carrier is not straight along the electric field but follows a random pattern.

Gross inhomogeneities may arise in amorphous materials as a result of the inherent instability of the vitreous state and its tendency to crystallize. Any tendency for nucleation of crystallites in the amorphous solid will result in the formation of regions of locally lower density elsewhere since the amorphous solid normally contains more vacancies than the crystal.

An ohmic contact is defined as one that is capable of supplying and removing charge carriers from the bulk material at exactly the required rate, without either producing an accumulation of excess carriers or blocking their passage. In the case of crystalline insulators and semiconductors in which conduction occurs effectively only in a free band, the requirement for an ohmic contact is seen to be the "flat band" situation. A barrier is due to a mismatch between the work functions of the metal and the semiconductor which forces the Fermi level at the surface to fall at an energy ϕ below the edge of the conduction band. Typical surface state densities in crystalline semiconductors are in the range 10^{11} - 10^{12} cm⁻² and the total density of surface atoms in a solid is typically 1.5×10^{15} cm⁻².

The method of thermally stimulated currents (TSC) has been used widely in crystalline large-gap materials, such as photoconductors and phosphors, to study the energy level structure in the forbidden gap. Its principal advantage lies in its simplicity, the main disadvantage in the difficulty of interpreting the results unambiguously.

In the context of thin films, the most common method of excitation is the application of a bias voltage V_b to the films, at a certain bias temperature T_b , followed by lowering of temperature, with the bias applied to a temperature at which the flow of current effectively ceases. The voltage is then changed to a collecting voltage $V_c \neq V_b$, including the possibility $V_c = 0$, and the temperature is gradually increased at a steady rate $R = dT/dt$. Under suitable conditions, one or more current peaks appear.

It is unfortunate that the other "classic" amorphous semiconductor materials, Si and Ge, have such low activation energies that any investigations of these by TSC techniques would require extremely low temperatures.

Conclusions: The essential concept that distinguishes a disordered solid from its perfectly crystalline and ordered counterpart is that of the localization of allowable energy states within what would in the latter case be the forbidden gap. Optical absorption experiments show that the broad characteristic of the absorption in a crystalline solid is retained, but that the fine structure, both within the bands and at the band edges, is smeared out. We have little knowledge of the optical cross sections to be expected of a localized defect, or even how such cross sections would vary with energy. The mean free path of the carrier is much less than that expected from normal crystalline scattering processes. Strictly applying the mean free path analysis leads to values of the mean free path of the order of, or less than, interatomic spacings. In crystalline semiconductors, with an empty forbidden gap, non-isoelectronic doping has a large effect on the properties of the material because the Fermi level is free to move within the range of the forbidden gap. However, once one allows that the gap may contain a finite density of states, then the Fermi energy may become pinned, making the material insensitive to doping. All theoretical approaches to the analysis of conduction in amorphous solids assume a homogeneous model. There is plenty of evidence that most real systems contain microscopic inhomogeneities - whether due to phase separation in glasses, regions of variable density in amorphous materials, or fluctuations in composition in compounds.

To some degree conduction experiments can be used for the characterization. There is no doubt that observation of Poole-Frenkel or Poole's behavior requires the presence of ionizable neutral centers, i. e. donor/acceptor sites. Unfortunately, the Mott $T^{-1/4}$ behavior can be expected either from the neutral traplike centers, or from a highly interactive dense impurity band where the coulombic potentials of the single charged centers interact to give a randomly perturbed local potential and hence a finite energy spectrum for the band.

J. A. Bruce, J. J. Comer, C. V. Collins, and H. G. Lipson, "Effects of Ion Beam Polishing on Alkali Halide Laser Window Materials," Third Conference on High Power Infrared Laser Window Materials, Nov. 12-14, 1973, AFCRL-TR-74-0085(III), 14 February 1974

[This paper reports successful argon-ion beam polishings of single-crystal KCl and KCl-KBr.]

B. L. Weigand, "The Potential of Thin Organic Polymeric Films as Protective Coatings for Alkali Halide Crystals," Third Conference on High Power Infrared Laser Window Materials, Nov. 12-14, 1973, AFCRL-TR-74-0085(III), 14 February 1974

The author is encouraged by the possibility of protecting alkali halides with organic polymeric fluorocarbon films that do not show the characteristic hydrocarbon absorption bands at $10\text{-}11 \mu\text{m}$ and $3\text{-}4.5 \mu\text{m}$. [In Sec. VI it is argued that the great values of the moisture-vapor transmission rates of presently known polymer films precludes their use as protective films for high-power alkali-halide windows or coatings. The suggested films have too great absorption, even though there are no bands peaked near the laser frequencies, for use as high-power antireflection coatings. The absorptance probably is too great even for thin protective coatings. (As an example of strong absorption without bands, water has no absorption bands near $10.6 \mu\text{m}$, but $\beta_{10.6} = 10^3 \text{ cm}^{-1}$.) For example, the absorptance of 1,1-difluoroethane in Fig. 2 of the reference appears to be ~ 40 percent. The thicknesses of the films in the figures, which were from previous Autonetics reports, were not known, but were believed to be several hundred nanometers thick on 25 bounce attenuated-total-reflection (ATR) plates,¹¹⁷ for a total effective thickness of $\sim 5 \mu\text{m}$, very roughly. The absorption coefficient would then have the value $\beta_f \approx 0.4/5 \times 10^{-4} = 800 \text{ cm}^{-1}$, and the absorptance of a $0.1 \mu\text{m}$ -thick protective coating would then be $A_p \approx (0.1 \mu\text{m})(800 \text{ cm}^{-1}) = 8 \times 10^{-3}$, which is a factor of 80 greater than the desired value of 10^{-4} .]

[Such previous difficulties as those of Young^{*38} and Chaffin and coworkers^{*109} in protecting alkali halides suggest that complete coverage of large areas by thin films ($\ell_f \gtrless 0.1 \mu\text{m}$) may be difficult. Polycrystalline films would not protect large areas, and the thickness of glassy films had to be of the order of the largest

scratches and imperfections on the substrates.^{*38} Even though polymeric films could possibly give better protection than glassy films, it is questionable that very thin films would give complete pin-hole-free coverage of large areas.

Weigand¹¹⁷ estimated that at least 100 nm thicknesses would be required to obtain pin-hole-free coatings and that obtaining such coatings over large areas of the order of 10 cm diameter would be a difficult engineering project.]

[Hexachlorobutadiene should be one of the better materials considered in this paper.¹¹⁷ A 0.65 μm -thick sample on a 30-bounce ATR plate of KRS-5 showed a 9 percent transmittance reduction at 10.6 μm from the value at a large flat peak from 8.5-10 μm .¹¹⁷ Thus, $\beta_f = 0.09/30(0.65 \mu\text{m}) = 46 \text{ cm}^{-1}$, and the absorptance of a single, 0.1 μm -thick protective coating should be $A_p = (46 \text{ cm}^{-1})(10^{-5} \text{ cm}) = 5 \times 10^{-4}$, very roughly. Since this is an approximate value and it is only a factor of five greater than the desired value of 10^{-4} (assuming that two more factors of 10^{-4} could be tolerated for the protective coating on the two antireflection coatings), it is conceivable that a sufficiently small value of β could be obtained. However, a program to protect alkali halides with thin polymeric films would be highly speculative in view of the questions of obtaining a sufficiently small value of absorptance and of obtaining complete pin-hole-free coverage with very thin films.]

B. E. Knox and K. Vedam, "Coating Science and Technology," Third Conference on High Power Infrared Laser Window Materials, Nov. 12-14, 1973, AFCRL-TR-74-0085(III), 14 February 1974

It is pointed out that the strong adhesion of metal films to glass can be attributed to an intermediate oxide layer which produces chemically bound films and that tetrahedral carbon films, or so-called "diamond films," have been observed by mass spectrometrists for many years and appear inside their ionization chambers. Attempts to laser evaporate graphite and allow the plume of evaporated species (mainly C₃ and C₁) to pass through a microwave cavity in an attempt to predominantly form atomic carbon which we hoped might form diamond structure carbon were unsuccessful. Calculations after the failure showed that the laser flux was too small.

T. M. Donovan, L. E. Jenkins, R. C. O'Handley, and D. J. White, "Thin Film Coatings for Alkali Halide Windows," Third Conference on High Power Infrared Laser Window Materials, Nov. 12-14, 1973, AFCRL-TR-74-0085(III), 14 February 1974

Amorphous Ge of one-half-wave optical thickness at $10.6 \mu\text{m}$ had $\beta_f = 40 \text{ cm}^{-1} \pm 30 \text{ cm}^{-1}$. Film thickness ranged from 0.1 to $2 \mu\text{m}$, deposition rates were 0.2 - 0.3 nm/sec , and both ultrahigh (uhv) and standard vacuums were used. Under uhv conditions, crystallization occurred for $T_s \leq 200 \text{ C}$. Air-exposed or standard-vacuum-deposited films crystallize at $T_s \geq 300 \text{ C}$. [The absorption coefficient of amorphous Ge on a KCl substrate increased monotonically from 40 cm^{-1} at $h\omega = 0.1 \text{ eV}$ ($10.6 \mu\text{m}$) to 10^5 cm^{-1} at 1.3 eV ($0.9 \mu\text{m}$), believed to be a result of absorption from "states in the gap" of the amorphous semiconductor.] Amorphous Ge on fused quartz had lower values of β_f , by a factor of ~ 10 at $2.5 \mu\text{m}$ (where $\beta_f = 100 \text{ cm}^{-1}$) [again showing the possible great effect of the substrate on β_f]. [Improved results for amorphous Ge films are reported by Bennett in Ref. *19, which is also abstracted in this section.]

M. Braunstein, "Laser Window Surface Finishing and Coating Technology," Third Conference on High Power Infrared Laser Window Materials, Nov. 12-14, 1973, AFCRL-TR-74-0085(III), 14 February 1974

The Ge film with the lowest absorption, $\beta_f = 10 \text{ cm}^{-1}$, was produced on a ZnSe substrate using ion-beam sputtering. A comparable absorption of 12 cm^{-1} for a film produced on KCl in uhv was obtained at the highest deposition rate of 7 nm/sec. T. Donovan obtained 77 cm^{-1} for 0.1 to 0.3 nm/sec under uhv conditions. There is evidence for K and Cl impurity migration into the Ge film. Mechanically polished ZnSe surface layers are softer than the underlying crystalline substrate. The surface layer is caused by smearing of the surface during lapping in the near-final polishing stages, since scratches are positioned within the layer and result from finer abrasives. We have estimated that the surface layer is about 500 nm thick and is amorphous, since no structure is seen in the layer itself. Ion polishing of ZnSe first reduced β , then increased β and scattering.

P. Kraatz, S. J. Holmes, and A. Klugman, "Window Surfaces and Coatings for Lasers Operating in the 3-5 μm Region," Third Conference on High Power Infrared Laser Window Materials, Nov. 12-14, 1973, AFCRL-TR-74-0085(III), 14 February 1974

Coatings of $\text{MgF}_2 / \text{MgO}$, $\text{ThF}_4 / \text{PbF}_2$, and $\text{ThF}_4 / \text{PbF}_2$ were deposited on CaF_2 . [Absorptance was not measured.]

Air Force Cambridge Research Laboratories LQ Technical Memorandum No. 35, Part 1, Semi-Annual Report No. 2, edited by B. Bendow and P. D. Gianino, Dec. 31, 1975

LaF_3 , CeF_3 , NdF_3 , GdF_3 , and HoF_3 coatings of thickness 1-2 μm on KCl on ZnSe at high substrate temperatures and low deposition rates all showed very high absorption at ~ 3 and $\sim 6 \mu\text{m}$ [probably water, possibly absorbed in porous films after deposition], which was not removed by deposition at $\sim 10^{-11}$ torr. Values of β_f at 10.6 μm ranged from 32 to 106 cm^{-1} . [Since $\beta_f > 0.5 \text{ cm}^{-1}$, these films are not satisfactory for high-power, 10.6 μm use.]

Perry A. Miles, D. W. Readey, and R. T. Newberg, "Research on Halide Super-alloy Windows," Raytheon Research Division Final Report, Contract No. F19628-72-C-0307, 20 April 1972 to 30 October 1973

Coatings of As_2S_3 with thickness ranging from $\sim 2 \mu\text{m}$ to $20 \mu\text{m}$ were deposited on cleaved and on polished KCl substrates. The background pressure immediately before evaporation was 8×10^{-7} torr. During the evaporation the pressure rose to between 10^{-5} and 6×10^{-5} torr. Evaporation times ranged from 10 to 35 minutes. Substrate temperatures ranged from 35 C to 67 C in some cases and were maintained near 35 C in later runs. Values of β_f at $10.6 \mu\text{m}$ ranged from 3 to 7 cm^{-1} in early runs, and a value of $\beta_f = 1.5 \text{ cm}^{-1}$, which is near the bulk value [of $\beta_b \approx 0.8 \text{ cm}^{-1}$], was obtained in a late run. [The Hughes Research Laboratories^{*9} also achieved $\beta_f \approx \beta_b$.] The decrease in β_f resulted from repetition rather than change of technique. [Repetition apparently cleans the system in this case.] It is highly significant that a repeat of two measurements after a three-day interval showed an increase in the film absorptance (by $\sim 7 \times 10^{-4}$ for a seven-micron-thick coating and by $\sim 8 \times 10^{-4}$ for a $12 \mu\text{m}$ -thick film). [It would be of interest to perform such time-dependent measurements for all of the coatings of the various thicknesses, since this should distinguish between surface effects, such as adsorbed layers of water, and such bulk-coating effects as filling of pores with water. The results for the two thicknesses measured are inconclusive, but they do suggest that the additional absorptance was from the surface since a bulk effect should have shown an absorptance increase at $12 \mu\text{m}$ of 7×10^{-4} ($12/7$) $= 1.2 \times 10^{-3}$, compared with the measured value of 8×10^{-4} .]

J. H. Chaffin and R. A. Skogman, "Thallium Iodide Protective Coatings for Alkali Halide Optical Components," Proceedings of the Fourth Annual Conference on Infrared Laser Window Materials, Nov. 18-20, 1974, Tucson, Arizona, January 1975

Thallium iodide films on KCl had $\beta_f < 1 \text{ cm}^{-1}$ and $n_r = 2.1$ at $10.6 \mu\text{m}$.

Pin holes in the coating allowed moisture attack of the KCl substrates. The value of β_f increased rapidly for deposition rates exceeding 6 nm/min . [A later Honeywell publication⁸⁶ reports deposition rates of $50-500 \text{ nm/min}$.] For substrate temperatures greater than 60°C the films were cloudy and had rough surfaces. Graded TlI-KCl coatings had $\beta_f = 50 \text{ cm}^{-1}$.

M. Braunstein and J. E. Rudisill, "Polishing and Coating for Large Diameter (15 cm) High Energy ZnSe Laser Windows and Coatings for Alkali Halide Windows," Proceedings of the Fourth Annual Conference on Infrared Laser Window Materials, Nov. 18-20, 1974, Tucson, Arizona, January 1975

A ThF_4/ZnSe coating on ZnSe had $A_f = 8 \times 10^{-4}$, a ZnSe/ThF_4 coating on KCl had $A_f = 1.7 \times 10^{-3}$, and an $\text{As}_2\text{S}_3/\text{ThF}_4$ coating on KCl had 1.9×10^{-3} . Coatings of ZnSe/ThF_4 on KCl cracked and peeled upon removal from the vacuum system (as a result of the strain in the $2 \mu\text{m}$ thick inner ZnSe layer). One ZnSe/ThF_4 film remained intact for a period of time, but then crazed.

M. Braunstein, A. I. Braunstein, D. Zuccaro, and R. R. Hart, "Ge and ThF₄ Films for High Energy Laser Components," Proceedings of the Fourth Annual Conference on Infrared Laser Window Materials, Nov. 18-20, 1974, Tucson, Arizona, January 1975

Germanium and ThF₄ films on KCl and ZnSe substrates were prepared by ultrahigh vacuum and ion-sputtering techniques. The lowest 10.6 μ m-absorption coefficient obtained was $\beta_f \cong 10 \text{ cm}^{-1}$ for both the Ge and ThF₄ films.

P. Kraatz and P. J. Mendoza, "CO Laser Calorimetry for Surface and Coating Evaluation," Proceedings of the Fourth Annual Conference on Infrared Laser Window Materials, Nov. 18-20, 1974, Tucson, Arizona, January 1975

At the CO laser wavelengths (near $5.2 \mu\text{m}$) for CaF_2 substrates, the values of film absorptance were $\beta_f = 2.1 \text{ cm}^{-1}$ for ThF_4 and $\beta_f = 2.3 \text{ cm}^{-1}$ for PbF_2 .

XIV. ACKNOWLEDGEMENTS

In preparing this report, I have solicited comments from a representative sample of active workers in the field of coatings for high-power infrared optics. I am indebted to a number of people for a great amount of assistance, and I deeply appreciate the time and effort that they have contributed. At the beginning of the program the current status of coatings for high-power infrared materials was discussed with the following investigators: Dr. R. R. Austin, Dr. H. E. Bennett, Dr. E. Bernal G., Mr. A. Braunstein, Mr. M. Braunstein, Dr. T. F. Deutsch, Dr. T. M. Donovan, Dr. C. J. Duthler, Dr. S. Geller, Dr. A. J. Glass, Dr. M. Hass, Dr. A. R. Hilton, Dr. T. D. Holstein, Dr. J. Kershenstein, Dr. G. E. Kuhl, Dr. J. R. Kurdock, Dr. J. Lehman, Dr. J. H. Marburger, Dr. D. Milam, Dr. P. A. Miles, Dr. T. Norwood, Dr. H. Posen, Dr. G. Ruse, Mr. C. S. Sahagian, Dr. M. Shen, Maj. J. L. Stapp, Dr. C. M. Stickley, Lt. L. Van Uitert, Dr. B. L. Weigand, Dr. R. W. White, and Capt. H. V. Winsor.

A preliminary draft of the report was circulated for comments. I want to thank the following for their response: Dr. R. R. Austin, Dr. E. Bernal G., Mr. A. Braunstein, Dr. T. M. Donovan, Dr. M. Hass, Dr. L. P. Mott, and Dr. H. Posen. Dr. G. Ruse, University of Colorado, stressed the importance of thorough baking of the entire system and pointed out that this was essential in attaining stable films of certain compounds.

XIV. REFERENCES [†]

[†] Research supported by the Defense Advanced Research Projects Agency and monitored by the Defense Supply Service, Washington, D. C.

1. A glossary of terms particular to this report is given at the end of Sec. III.
- *2. E. Ritter, Physics of Thin Films 8, 1 (1975).
- *3. R. C. Pastor and M. Braunstein, Hughes Research Laboratories Technical Report No. AFWL-TR-72-152, Vol. II, July 1973.
4. G. Ruse, University of Colorado, private communication (1976).
5. F. A. Horrigan and R. I. Rudko, Raytheon Research Division Final Technical Report, Contract DAAH01-69-C-0038, 1969; F. A. Horrigan, C. Klein, R. Rudko, and D. Wilson, Microwaves 8, 68 (1969); F. A. Horrigan and T. F. Deutsch, Raytheon Research Division Final Technical Report, Contract DAAH01-70-C-1251, 1971; T. F. Deutsch and R. I. Rudko, Raytheon Research Division Final Technical Report, Contract DAAH01-72-C-0194, 1973.
6. M. Sparks, J. Appl. Phys. 42, 5029 (1971).
7. M. Sparks and M. Cottis, J. Appl. Phys. 44, 787 (1973).
8. M. Sparks and H. C. Chow, J. Appl. Phys. 45, 1510 (1974); M. Sparks and H. C. Chow, Third Conference on High Power Infrared Laser Window Materials, ed. by C. A. Pitha, H. Posen, and A. Armington, AFCRL-TR-74-0085, Vol. III, 1083 (Air Force Cambridge Research Laboratories, 1974).
- *9. M. Braunstein and J. E. Rudisill, Hughes Research Laboratories Final Report, Contract F33615-73-C-5044, February 1975.
- *10. M. Braunstein, A. I. Braunstein, J. E. Rudisill, and V. Wang, Hughes Research Laboratories Final Technical Report, Contract F29601-72-C-0132, Dec. 1973.
11. H. Posen, Air Force Cambridge Research Laboratories, comments on a preliminary draft of the present report, unpublished (1976).

[†] References marked * are excerpted in Sec. XIII.

12. R. R. Austin, Perkin-Elmer Corporation, private communication (1976).
13. C. Weaver, Vacuum 15, 171 (1965).
- *14. C. Willingham, D. Bua, H. Statz, and F. Horrigan, Raytheon Research Division Final Technical Report, Contract DAAH01-74-C-0719, August 1975.
- *15. T. F. Deutsch, Raytheon Research Division Final Technical Report, Contract DAAH01-72-C-0194, December 1973.
16. T. F. Deutsch, J. Electronic Matls. 4, 663 (1975).
- *17. G. T. Johnston, D. A. Walsh, R. J. Harris, and J. A. Detrio, University of Dayton Research Institute Semiannual Progress Report No. 4, Contract F33615-74-C-5001, 30 June 1975.
18. C. J. Duthler, J. Appl. Phys. 45, 2668 (1974); Proceedings of Fourth Annual Conference on Infrared Laser Window Materials, Tucson, Arizona, Nov. 18-20, 1974 (January, 1975).
- *19. E. Bernal G., R. H. Anderson, J. H. Cnaffin, B. G. Koepke, R. J. Stokes, and R. B. Maciolek, Honeywell, Inc. Final Report, Contracts DAHC15-72-C-0227 and DAHC15-73-C-0464, February 1974.
20. T. J. Magee, Stanford Research Institute Technical Report No. 2266-1 (1972).
21. H. G. Lipson, A. Kahan, P. Ligor, and J. J. Martin, Proc. Fourth Conference on Infrared Laser Windows, ed. by C. R. Andrews and C. L. Strecker, U.S. Air Force Materials Laboratory Special Report, Wright-Patterson AFB, Ohio (1975), p. 589.
22. T. J. Magee, N. M. Johnson, and J. Peng, Phys. Stat. Sol. A (to be published, 1976).
23. T. J. Magee, N. M. Johnson, M. Lehmann, J. Peng, and J. Hannigan, Rev. Sci. Instr. (to be published).
24. M. Sparks and C. J. Duthler, J. Appl. Phys. 44, 3038 (1973).
25. A. J. Sievers, Cornell University, private communication (1976).
26. Capt. H. Winsor, private communication (1976).

27. M. Hass, Naval Research Laboratories, comments on a preliminary draft of the present report, unpublished (1976).
28. P. Benjamin and C. Weaver, Proc. Roy. Soc. (London) A 274, 267 (1963).
29. "26 Frequently Used Spectra for the Infrared Spectroscopic," Sadler Research Labs, Inc., 3316 Spring Garden St., Philadelphia, Pa. 19104.
30. Handbook of Military Infrared Technology, ed. by W. L. Wolfe (U.S. Government Printing Office, 1965).
31. M. Hass, J. W. Davisson, H. B. Rosenstock, and J. Babiskin, Proceedings of the Fourth Annual Conference on Infrared Laser Window Materials, Tucson, Ariz., Nov. 18-20, 1974 (January 1975).
- *32. H. E. Bennett, U.S. Naval Weapons Center Semi-Annual Technical Report No. 5, "High Energy Laser Mirrors and Windows," March-September 1974.
- *32a. H. E. Bennett, U.S. Naval Weapons Center Semi-Annual Technical Report No. 6, "High Energy Laser Mirrors and Windows," September 1974-March 1975.
33. A. Braunstein, Hughes Research Laboratories, private communication (1976).
34. H. E. Bennett, private communication (1976).
35. M. Sparks, Rand Corporation Report WN-7243-PR, June 1971.
36. J. H. Parks, D. A. Rockwell, T. S. Colbert, K. M. Lakin, and D. Mih, Appl. Phys. Lett. 25, 537 (1974).
- *37. D. L. Stierwalt and M. Hass, Proceedings of Fourth Annual Conference on Infrared Laser Window Materials, Tucson, Ariz., Nov. 18-20, 1974 (January 1975).
- 37a. L. P. Mott, Optical Coating Laboratories, comments on a preliminary draft of the present report, unpublished (1976).
- *38. P. A. Young, Thin Solid Films 6, 423 (1970).
39. V. Vang, C. R. Giuliano, and B. Garcia, Proceedings of Fifth Annual Conference on Infrared Laser Window Materials, Las Vegas, Nevada, Dec. 1-4, 1975, ed. by C. R. Andrews and C. L. Strecker (February 1976).
- 39a. D. S. Campbell in Handbook of Thin Film Technology, ed. by L. I. Maissel and R. Glang (McGraw-Hill, New York, 1970).

40. L. Van Uitert, H. J. Guggenheim, H. M. O'Brien, A. W. Warner, Jr., D. Brownlow, J. L. Bernstein, G. A. Pasteur, and L. F. Johnson, "Physical Properties of Thorium Fluoride," (to be published in *Matls. Res. Bulletin*, June 1976).
41. Handbook of Thin Film Technology, ed. by L. I. Maissel and R. Glang (McGraw-Hill, New York, 1970).
42. B. N. Chapman, *J. Vac. Sci. Technol.* 11, 106 (1974).
- *43. R. W. Hoffman, *Physics of Thin Films* 3, 211 (1966).
- *44. A. E. Ennos, *Appl. Opt.* 5, 51 (1966).
45. A. F. Turner, "Thick Thin Films," Bausch & Lomb Technical Report (1951).
46. The numerical values given throughout are for the values of parameters listed in Eq. (3.3) unless specified otherwise.
47. M. Sparks, *J. Appl. Phys.* 42, 5029 (1971).
48. M. Sparks, *J. Appl. Phys.* 47, 837 (1976).
49. M. Sparks, "Temperature and Stress Analysis for Bulk- and Surface-Heated Slabs," Parke Mathematical Laboratories, Inc. Report TM-2 (1971).
50. M. Sparks and H. C. Chow, *J. Appl. Phys.* 45, 1510 (1974).
51. W. Ewing, A. Golubovic, I. Berman, R. Bradbury, J. Fitzgerald, J. Bruce, and J. Comer, Proceedings of the Fifth Conference on Infrared Laser Window Materials, 1-4 Dec. 1975, ed. by C. R. Andrews and C. L. Strecker (Febr. 1976).
52. C. J. Duthler, *Appl. Phys. Lett.* 24, 5 (1974).
53. N. L. Boling, private communication (1976).
54. N. L. Boling and G. Dube, *Appl. Phys. Lett.* 23, 658 (1973).
- 54a. Damage thresholds quoted as energy densities (J/cm^2) have little significance unless the pulse duration, pulse shape, focal spot size, and in some cases the focal volume are known. As discussed in Sec. VIII, changing the values of these parameters can change the energy density by many orders of magnitude.
- 54b. A. J. Glass, Lawrence Livermore Laboratory, private communication (1976).

55. D. W. Fradin, E. Yablonovitch, and M. Bass, *Appl. Opt.* **12**, 700 (1973).
56. M. Sparks, 7th NBS-ONR-ASTM Symposium on Damage in Laser Materials, Boulder, Colo., July 1975 (to be published by National Bureau of Standards).
57. C. Kittel, Introduction to Solid State Physics, Fourth Edition (Wiley & Sons, New York, 1971), p. 462.
58. M. Sparks, Rand Corporation Report R-545-PR, September (1971); M. Sparks, Rand Corporation Report R-863-PR, September (1973).
59. Such symbols as Na(F, Cl) denote the set of materials NaF and NaCl.
60. C. S. Sahagian and C. A. Pitha, "Compendium on High Power Infrared Laser Window Materials (LQ-10 Program)," Air Force Cambridge Research Laboratories Report No. AFCRL-72-0170, 9 March 1972.
- *61. S. K. Dickinson, Air Force Cambridge Research Laboratories Report No. AFCRL-TR-75-0318, 6 June 1975.
62. American Institute of Physics Handbook, 3rd edition, ed. by F. E. Gray (McGraw-Hill, New York, 1972).
63. A. Braunstein, private communication.
- *64. E. Bernal G., J. H. Chaffin, B. G. Koepke, R. B. Maciolek, and R. J. Stokes, Honeywell, Inc. Semiannual Technical Report #4, Contract DAHC15-73-C-0464, 15 January 1976.
- *65. B. E. Knox, J. Genczko, L. Gilbert, R. Howard, G. Mariner, and K. Vedara, Proceedings of the Fourth Annual Conference on Infrared Laser Window Materials, Tucson, Ariz., Nov. 18-20, 1974 (January 1975).
- *66. J. R. Kerdock and E. A. Strouse, Perkin-Elmer Corporation Technical Report No. AFML-TR-74-166, Part II, July (1975).
67. A. R. Hilton, private communication (1976).
68. It is assumed that materials listed by Ritter in Ref. *2 as useful "to 15 μm " or to a lower wavelength probably will have too great absorption to be useful at 10.6 μm , as discussed in Sec. VII.

69. F. A. Horrigan and T. F. Deutsch, Raytheon Research Division Final Technical Report, Contract DAAH01-70-C-1251, September 1971.
- *70. W. Heitmann, Thin Solid Films 5, 61 (1970).
- *71. Air Force Cambridge Research Laboratories LQ Technical Memorandum No. 30, ed. by N. Klausutis, Semiannual Report No. 1, 1 July 1975.
- *72. J. H. Chaffin, Third Conference on High Power Infrared Laser Window Materials, Nov. 12-14, 1973, AFCRL-TR-74-0085(III), 14 February 1974.
73. T. M. Donovan, private communication (1976).
74. M. Sparks and C. J. Duthler, Xonics, Inc. Third Technical Report, Contract DAHC15-73-C-0127, 30 June 1974.
- *75. H. Winston, R. Pastor, R. Turk, A. I. Braunstein, and R. F. Scholl, Hughes Research Laboratories Technical Report AFML-TR-75-73, Contract F33615-73-C-5075, Final Report for period 15 March 1973 through 15 December 1974.
76. Rough estimate obtained from transmittance curve. See note in the excerpt of Ref. *70.
77. P. A. Miles, private communication (December 1974).
78. J. Harrington, as reported in Ref. *14.
79. E. Bernal G., private communication.
- *80. M. Braunstein, J. E. Rudisill, and A. I. Braunstein, Third Conference on High Power Infrared Laser Window Materials, Vol. III, ed. by C. A. Pitha and B. Bendow, AFCRL-TR-74-0085, 14 February 1974.
- *81. E. Bernal G., R. H. Anderson, J. H. Chaffin, B. G. Koepke, R. J. Stokes, and R. B. Maciolek, Honeywell, Inc. Quarterly Technical Report No. 6, Contracts DAHC15-72-C-0227 and DAHC15-73-C-0464, 1 July to 30 September 1973.
82. C. T. Moynihan, P. B. Macedo, M. Maklad, and R. Mohr, Conference on High Power Infrared Laser Window Materials, ed. by C. A. Pitha, AFCRL-TR-73-0372, 19 June 1973.
83. F. A. Horrigan and T. F. Deutsch, Raytheon Research Division Quarterly Technical Report No. 3, Contract DAAH01-72-C-0194, July 1972.

84. For multiple coatings, such symbols as ThF₄/ZnSe mean that ThF₄ is deposited first, then ZnSe is deposited.
- *85. F. A. Kroger and J. I. Marburger, University of Southern California Semi-annual Technical Report No. 1, Contract F19628-75-C-0080, 15 March 1975.
- *86. E. Bernal G., J. H. Chaffin, B. G. Koepke, R. B. Maciolek, and R. J. Stokes, Honeywell, Inc. Semiannual Technical Report No. 1, Contract DAHC15-73-C-0464, 1 January to 15 July 1975.
- *87. J. R. Kurdock, Perkin-Elmer Corporation Quarterly Progress Report No. 2, Contract F33615-73-C-5127, October 1973.
- *88. J. R. Kurdock, Perkin-Elmer Corporation Quarterly Progress Report No. 3, Contract F33615-73-C-5127, January 1974.
- *89. J. R. Kurdock, Perkin-Elmer Corporation Quarterly Progress Report No. 4, Contract F33615-73-C-5127, April 1974.
- *90. E. Bernal G., R. H. Anderson, J. H. Chaffin, B. G. Koepke, R. B. Maciolek, and R. J. Stokes, Honeywell, Inc. Semiannual Technical Report No. 1, Contract DAHC15-73-C-0464, 15 July 1974.
- *91. E. Bernal G., J. H. Chaffin, B. G. Koepke, R. B. Maciolek, and R. J. Stokes, Honeywell, Inc. Semiannual Technical Report No. 2, Contract DAHC15-73-C-0464, 15 January 1975.
- *92. F. A. Horrigan and T. F. Deutsch, Raytheon Research Division Quarterly Technical Report No. 3, Contract DAAH01-72-C-0194, July 1972.
- *93. G. Hass, J. B. Ramsey, and R. Thun, *J. Opt. Soc. Am.* 49, 116 (1959).
- *94. R. Glang, J. G. Kren, and W. J. Patrick, *J. Electrochem. Soc.* 110, 407 (1963).
- *95. R. J. Scheuerman, *J. Vac. Sci. Technol.* 6, 145 (1969).
- *96. A. K. Jonscher and P. A. Walley, *J. Vac. Sci. Technol.* 6, 662 (1969).
- *97. A. Vecht, *Physics of Thin Films* 3, 165 (1966).
- *98. Z. H. Meiksin, *Physics of Thin Films* 8, 99 (1975).
- *99. A. K. Jonscher and R. M. Hill, *Physics of Thin Films* 8, 169 (1975).

- *100. J. A. Bruce, J. J. Comer, C. V. Collins, and H. G. Lipson, Third Conference on High Power Infrared Laser Window Materials, Nov. 12-14, 1973, AFCRL-TR-74-0085(III), 14 February 1974.
- *101. B. L. Weigand, Third Conference on High Power Infrared Laser Window Materials, Nov. 12-14, 1973, AFCRL-TR-74-0085(III), 14 February 1974.
- *102. B. E. Knox and K. Vedam, Third Conference on High Power Infrared Laser Window Materials, Nov. 12-14, 1973, AFCRL-TR-74-0085(III), 14 February 1974.
- *103. T. M. Donovan, L. E. Jenkins, R. C. O'Handley, and D. J. White, Third Conference on High Power Infrared Laser Window Materials, Nov. 12-14, 1973, AFCRL-TR-74-0085(III), 14 February 1974.
- *104. M. Braunstein, Third Conference on High Power Infrared Laser Window Materials, Nov. 12-14, 1973, AFCRL-TR-74-0085(III), 14 February 1974.
- *105. P. Kraatz, S. J. Holmes, and A. Klugman, Third Conference on High Power Infrared Laser Window Materials, Nov. 12-14, 1973, AFCRL-TR-74-0085(III) 14 February 1974.
- *106. Air Force Cambridge Research Laboratories LQ Technical Memorandum No. 35, Part 1, Semi-Annual Report No. 2, ed. by B. Bendow and P. D. Gianino, December 31, 1975.
- *107. P. A. Miles, D. W. Readey, and R. T. Newberg, Raytheon Research Division Final Report, Contract F19628-72-C-0307, 20 April 1972 to 30 October 1973.
- *108. J. A. Chaffin and R. A. Skogman, Proceedings of Fourth Annual Conference on Infrared Laser Window Materials, Nov. 18-20, 1974, Tucson, Arizona (January 1975).
- *109. M. Braunstein and J. E. Rudisill, Proceedings of Fourth Annual Conference on Infrared Laser Window Materials, Nov. 13-20, 1974, Tucson, Arizona (January 1975).
- *110. M. Braunstein, A. I. Braunstein, D. Zuccaro, and R. R. Hart, Proceedings of Fourth Annual Conference on Infrared Laser Window Materials, Nov. 18-20, 1974, Tucson, Arizona (January 1975).

Sec. XV

- *111. P. Kraatz and P. J. Mendoza, Proceedings of Fourth Annual Conference on Infrared Laser Window Materials, Nov. 18-20, 1974, Tucson, Arizona (January 1975).
- 112. In Sec. XIII our comments are enclosed in brackets.
- 113. In a later report, Ref. *91, it was found that 200 nm of T1I did not protect a KC1 substrate.
- 114. This is an interesting result that the large effect of water saturates in the sense that there are great changes in the films on exposure to water vapor and little further changes even when immersed in tap water.
- 115. Spectroscopic transmittance measurements, which could detect $A_f = 10^3 \text{ cm}^{-1}$ $10^4 \text{ cm} = 0.1$, would be useful in determining the source of the great absorption.
- 116. J. R. Kurdock, private communication (1976).
- 117. B. L. Weigand, private communication (1976).